

University of Southampton Research Repository

Copyright © and Moral Rights for this thesis and, where applicable, any accompanying data are retained by the author and/or other copyright owners. A copy can be downloaded for personal non-commercial research or study, without prior permission or charge. This thesis and the accompanying data cannot be reproduced or quoted extensively from without first obtaining permission in writing from the copyright holder/s. The content of the thesis and accompanying research data (where applicable) must not be changed in any way or sold commercially in any format or medium without the formal permission of the copyright holder/s.

When referring to this thesis and any accompanying data, full bibliographic details must be given, e.g.

Thesis: Author (Year of Submission) "Full thesis title", University of Southampton, name of the University Faculty or School or Department, PhD Thesis, pagination.

Data: Author (Year) Title. URI [dataset]

University of Southampton

Faculty of Environmental and Life Sciences

School of Health Sciences

**Sensorial and Physiological Response in the Skin Device
Interaction for Personal Care/Devices**

by

Pakhi Chaturvedi

Supervised by: Dr P. R. Worsley

Professor D. L. Bader

Dr. W. Kroon (Philips, NL)

Dr. G. Zanelli (Philips, NL)

Thesis for the degree of Doctor of Philosophy

May 2023

University of Southampton

Abstract

Faculty of Environmental and Life Sciences

School of Health Sciences

Doctor of Philosophy

Sensorial and Physiological Response in the Skin Device Interaction for Personal Care/Devices

by

Pakhi Chaturvedi

Skin sensitivity (SS) is a commonly occurring response to a range of stimuli, including environmental conditions, chemical irritants, and mechanical forces. Factors affecting whether an individual reports SS has been a topic of interest for many years, with studies ranging from questionnaire screening tools to objective measurements of skin characteristics. Despite these studies, there is no consensus regarding a definition of SS. Furthermore, as differences in individual tolerance to stimuli has led to a demand for personalised products, SS continues to be an emerging clinical and social challenge. Consequently, the present research aimed to investigate the variability in skin sensitivity using an array of skin assessment tools. Specifically, mechanical loading in the form of consumer devices were considered, such as electrical shavers where a dynamic combination of pressure and shear is exerted on the skin surface. The bearded area of the cheek and neck in males were selected as regions of interest in context of electrical shaving, enabling examination of inter- and intra-subject variability in perception of enhanced skin sensitivity.

Parameters for characterising skin health were identified following a review of the scientific literature. Findings revealed that the structure and function of the stratum corneum (SC) and its effective barrier properties were closely associated with perception of sensitivity, assessed through parameters such as TEWL, SC thickness, and surface redness. As such, the need for a multifactorial array of skin tissue responses was proposed for understanding the complex pathological mechanisms underlying SS. Furthermore, Optical Coherence Tomography (OCT) was identified as a potential imaging tool to characterise structural and physiological difference in skin sites before and after mechanical stimulation. Consequently, OCT-derived skin parameters were defined and algorithms were developed for estimating values from the cheek and neck. Study I was designed to investigate the short-term effects of several mechanical insults in a consumer panel with a range of self-assessed SS. Study II was designed to investigate the short- and long-term effects of electric shaving where a new stimulus model was developed by introducing repetitive loading, reflecting the real-world scenario where consumers follow a daily shaving routine.

The results presented in this thesis revealed significant spatial differences in the skin tissue, e.g., higher baseline TEWL and temperature was observed on the neck, indicating a weaker skin barrier than the cheek. OCT-derived skin parameters revealed higher basal roughness on the neck. The shaving insult resulted in a decrease in the barrier function accompanied by hyperaemia and inflammation, with the magnitude of the result corresponding to the anatomical site and beard length. Additionally, participants with higher self-reported sensitivity to mechanical stimuli

demonstrated higher force values while shaving and higher discomfort post shaving. Remarkably, an increase in the perception of SS and the force of stimulus application correlated with a decrease in the SC integrity, decrease in optical density of the tissue, and a change in the skin reflectivity.

The combination of techniques e.g., OCT imaging, biophysical measures of SC function, and inflammatory biomarkers provided a comprehensive set of parameters critical in strengthening our understanding of skin sensitivity and its associations with mechanical loading. The presented thesis addresses the difficulty in quantifying the skin-device interaction and provides a direction for selection of suitable skin measurement tools. This is particularly relevant for device manufacturers interested in developing skin-friendly products, accounting for the increasing demands for personalised solutions.

Table of Contents

Table of Contents	i
Table of Tables.....	v
Table of Figures	ix
Research Thesis: Declaration of Authorship	xvii
Dissemination.....	xix
Dedication	xxi
Acknowledgements	xxiii
Definitions and Abbreviation	xxv
Chapter 1 Introduction.....	1
1.1 Research Context.....	1
1.2 Research Motivation.....	2
1.3 Background on the Research Topic.....	2
1.4 Research Scope and Goals	4
Chapter 2 Literature Review.....	7
2.1 Skin Structure and Function.....	7
2.2 Genesis of Skin Sensitivity.....	9
2.2.1 Types of stimuli.....	9
2.2.2 Origin of responses	10
2.2.3 Intrinsic factors	11
2.2.4 Extrinsic factors.....	11
2.3 State-of-the-art Objective Methods for Assessing Skin Sensitivity	12
2.3.1 Stratum corneum water content and permeability	12
2.3.2 Skin structure.....	14
2.3.3 Erythema / Skin Colour	14
2.3.4 Microcirculation / Blood Perfusion	15
2.3.5 Skin temperature and microclimate.....	16
2.3.6 Pruritus & Inflammation	17
2.3.7 Skin pH	17

Table of Contents

2.3.8	Sebum content / oiliness.....	18
2.3.9	Discussion	20
2.4	Secondary Analysis of Biophysical Data in a SS/NSS cohort	23
2.4.1	Methods.....	24
2.4.2	Results.....	25
2.4.3	Discussion	32
2.5	Aims and Objectives.....	34
Chapter 3 Protocol Development for quantifying skin sensitivity using OCT ...		37
3.1	Experimental setup	37
3.2	OCT parameters to assess skin structure and morphology	41
3.3	Development of OCT Parameters.....	45
3.3.1	Skin surface detection – Version 1	47
3.3.2	Skin surface detection – Version 2	49
3.3.3	Epidermal Thickness calculation.....	52
3.3.4	Scaled Intensity Drop (SID) calculation.....	54
3.3.5	Surface roughness.....	56
3.4	Protocol Development Summary	59
Chapter 4 A consumer study to evaluate the skin’s biophysical response to mechanical challenges		63
4.1	Introduction	63
4.2	Methods.....	64
4.2.1	Skin sensitivity questionnaire.....	64
4.2.2	Participant Selection and Recruitment.....	65
4.2.3	Skin Sensitivity label assignment.....	66
4.2.4	Measurement Protocol	67
4.2.5	Mechanical stimuli: Tape stripping, friction, and shaving	70
4.2.6	Statistical analysis	74
4.3	Results.....	76
4.3.1	Baseline skin characteristics.....	76
4.3.2	Temporal responses of the mechanical insults	80

4.3.3	Comparison of the skin responses between the cheek and neck.....	90
4.3.4	Comparison of skin responses between participants categorised with different skin sensitivity	96
4.4	Discussion	105
Chapter 5 Characterisation of OCT parameters following mechanical challenges in the consumer cohort		111
5.1	Introduction	111
5.2	Methods.....	111
5.2.1	Area under the Curve (AuC) estimation	113
5.2.2	Statistical Analysis	114
5.3	Results	115
5.3.1	Baseline characteristics.....	115
5.3.2	Temporal responses to mechanical stimuli	119
5.3.3	Correlation between the OCT-skin parameters on the cheek and neck.....	123
5.3.4	Relationship between OCT-skin parameters and biophysical parameters ...	125
5.3.5	Relationship between OCT-skin parameters and SS categories	126
5.4	Discussion	128
Chapter 6 Assessment of skin integrity at different anatomical locations in response to shaving		133
6.1	Introduction	133
6.2	Methods.....	134
6.2.1	Participant recruitment and preparation	134
6.2.2	Protocol.....	136
6.2.3	Imaging parameters selection and optimization	140
6.2.4	Redness estimation	150
6.2.5	Biochemical analysis	151
6.2.6	Statistical analysis	152
6.3	Results	153
6.3.1	Comparison of baseline characteristics for each anatomical site.....	153
6.3.2	Temporal response for each anatomical site	156

Table of Contents

6.3.3 Biochemical markers	172
6.4 Discussion	179
Chapter 7 Perceived and observed changes in skin response following shaving	187
7.1 Introduction	187
7.2 Methods.....	187
7.2.1 Perceived sensitivity and intrinsic factors	188
7.2.2 Estimation of Extrinsic factors.....	188
7.2.3 Statistical Analysis	189
7.3 Results.....	190
7.3.1 Case study	192
7.3.2 Intrinsic and Extrinsic factors associated with shaving.....	196
7.3.3 Selecting an optimised array of skin parameters	198
7.3.4 Associations between Intrinsic and Extrinsic factors, and the skin tissue responses	202
7.4 Discussion	205
Chapter 8 General Discussion and Future Work	211
8.1 Meeting the research objectives.....	211
8.2 Research novelty.....	214
8.3 General limitations.....	218
8.4 Translation of research to industry	219
8.5 Future Work.....	220
Appendix A Skin Sensitivity Questionnaire	223
Appendix B Study-II Participant Information Sheet.....	225
Appendix C Additional figures from Chapter 4.....	231
Appendix D Additional figures from Chapter 5.....	239
Appendix E Additional figures from Chapter 6.....	247
Appendix F Additional figures from Chapter 7.....	251
Bibliography.....	253

Table of Tables

Table 1.1 Overview of research topics within the STINTS consortium with the current research highlighted.	1
Table 2.1 Advantages and limitations of measurements methods and the skin properties quantified.	19
Table 2.2 Participant details from Retrospective Analysis dataset in ascending order of the number of tape strips.	25
Table 3.1 OCT scan pattern and image acquisition times tested.	40
Table 3.2 Demographic details of participants from preliminary experiments.	45
Table 3.3 Comparison of image processing parameters in the skin surface detection algorithms.	50
Table 3.4 Summary of OCT parameters from the preliminary dataset, listed in ascending order by the participant's age. SID is represented by the magnitude of the result.	60
Table 4.1 Coding values for the responses from the SS Questionnaire.	65
Table 4.2 Sequence of biophysical measurements of skin and acquisition times for each site.	68
Table 4.3 Participant details from the study. Where blank, the data was not available.	76
Table 4.4 Summary of the baseline values of the biophysical parameters at the three test sessions.	77
Table 4.5 Analysis of the fold changes in the biophysical parameters post stimulus for each test session on the cheek. Within each session for each biophysical parameter, the values have been shaded from white to blue in ascending order.	83
Table 4.6 Analysis of the fold changes in the biophysical parameters post stimulus for each test session on the neck. Within each session for each biophysical parameter, the values have been shaded from white to blue in ascending order.	88
Table 4.7 Summary of responses from SS questionnaire in July and December. Only 18 participants completed both assessments. Where blank, the response stayed the same. The corresponding S-scores and SS labels are stated.	106

Table of Tables

Table 5.1 Summary of the baseline values of the OCT-skin parameters for the three test sessions. Statistically significant differences between the sites and sessions have been noted using the Mann-Whitney test @.....	116
Table 5.2 Ranks for participants from Session 1 at baseline for all the skin parameters, sorted by the SS category.	127
Table 5.3 Roughness values obtained from OCT images for various anatomical sites reported in literature. Results have been included for healthy skin at baseline.	130
Table 6.1 Sequence of measurements of skin and acquisition times for each site.....	137
Table 6.2 Overview of imaging parameters that can be extracted in the present study, including previously developed OCT-skin parameters and Vivosight parameters.	141
Table 6.3 Participant details from the study with the calculated S-score and SS Label.....	153
Table 6.4 P-values from the Friedman Test investigating the influence of time on each location for the selected parameters. $p < 0.05$ has been highlighted in yellow.	156
Table 6.5 Median ratio in values from baseline. Highlighted cells represent a ratio greater than 1.3 (this threshold was arbitrarily selected).....	182
Table 7.1 Participant details including calculated S-scores, self reported Mech SS, and estimated load characteristics.....	191
Table 7.2 Spearman correlation values, p-values, and sample size for all Intrinsic and Extrinsic factors. Pairs with $p < 0.05$ have been highlighted in bold with shades of light to dark blue for ascending positive r values.	198
Table 7.3 Spearman correlation values, p-values, and sample size for the biophysical, structural, and biochemical parameters. Pairs with $p < 0.05$ have been highlighted in bold with shades of light to dark blue for ascending positive r values and shades of light to dark red for descending negative r values.	200
Table 7.4 Decision matrix to reduce the number of variables, minimising the array of skin tissue responses. Spatial and temporal differences have been summarized considering the observations from Chapter 6.	201
Table 7.5 Spearman correlation values, p-values, and sample size between Intrinsic and Extrinsic factors, and the skin tissue responses. Pairs with $p < 0.05$ have been highlighted	

in bold with shades of light to dark blue for ascending positive r values and shades of light to dark red for descending negative r values.202

Table 7.6 Participant ranks for each parameter in the Short Beard session. Where data is missing, the cells have been filled black.204

Table of Figures

Figure 1.1 Flow chart of inter-subject variability. Adapted from “Sensitive Skin Syndrome”, 2006 (“Sensitive Ski. Syndr.,” 2006).	4
Figure 1.2 Scope of the research project.	5
Figure 1.3 Illustration of the conceptual relationship between skin sensitivity and objectifiable skin responses. Enhanced SS may be due to a lower threshold and/or a heightened/prolonged response or combination of responses.....	5
Figure 2.1 Three-dimensional sketch of the skin layers and their thickness. Adapted from Geerligs, 2009 (Geerligs, 2009).....	8
Figure 2.2 The relationship between resolution and penetration depth for different skin imaging modalities. Adapted from “Handbook of Optical Coherence Tomography”, 2001 (“Handbook of Optical Coherence Tomography,” 2001).	21
Figure 2.3 Comparison of biophysical values at baseline for SS and NSS groups. Adapted from (Richters et al., 2016).....	24
Figure 2.4 Temporal Δ Response of the skin for the SS and NSS groups for (a) TEWL, (b) SC Hydration, and (c) Redness.....	27
Figure 2.5 Δ Response with individual Q-scores for (a) TEWL, (b) SC Hydration, and (c) Redness. The Q-score is plotted on the second Y axis.....	29
Figure 2.6 Scatterplots at 30 minutes and 72 hours for (a) TEWL, (b) SC Hydration, and (c) Redness with R_s and p values from the Spearman Correlation test.	31
Figure 3.1 OCT system with different camera orientations. (a) Camera positioned vertically for forearm imaging; (b) camera position horizontally for facial imaging.	38
Figure 3.2 Accessories to maintain the required focal distance for facial OCT imaging. (a) Mount with smaller aperture used for the neck; (b) Mount with larger aperture used for the cheek.	39
Figure 3.3 Typical position of a participant when imaging the (a) cheek and (b) neck, using the OCT system.....	39
Figure 3.4 Schematic of a 3D-OCT Scan with a stack of exemplar B-scans and a single A-scan. .	41

Table of Figures

Figure 3.5 Example of a 3D-OCT Averaged A-scan, representing the depth of the signal penetration on the x-axis and the Intensity of the signal on the y-axis. Each of the thin coloured lines represents the average of the A-scan in a single B-scan, i.e., 2D averaged A-scan. The 3D averaged A-scan (thick black line) is the average of the 2D averaged A-scans.	42
Figure 3.6 Annotated 2D-OCT scan of the cheek.	42
Figure 3.7 Illustration of epidermal thickness calculation.....	43
Figure 3.8 Illustration of Scaled Intensity Drop calculation from 5% to 90% cumulative intensity.....	44
Figure 3.9 Examples of 2D-OCT scans with visibly different surface roughness between the (a) cheek and (b) neck for the same healthy individual.....	45
Figure 3.10 Camera images and B-mode images for the cheek.	46
Figure 3.11 Camera images and B-mode images for the neck.	46
Figure 3.12 Flow diagram illustrating the processing stages of Skin surface detection - Version 1.	47
Figure 3.13 Individual A-scans and averaged A-scans (overlaid in bold) at different stages of the image processing.	48
Figure 3.14 Exemplar B-mode images where hair has been wrongly detected as skin, highlighting the limitation in the version 1 skin surface detection algorithm.	48
Figure 3.15 Examples of gaussian filtered images with different the kernel sizes (σ).	49
Figure 3.16 Flowchart of Skin surface detection - Version 2.	51
Figure 3.17 Comparing the skin surface detection algorithm versions 1 and 2 on a B-mode image with hair. The blue line indicates detected skin surface from each version...	52
Figure 3.18 A-scans from the 3D-OCT scans highlighting the thickness of the epidermis on the cheek for (a) D11, (c) D12, (e) D13, (g) D14, (i) D15 and on the neck for (b) D11, (d) D12, (f) D13, (h) D14, (j) D15.	53
Figure 3.19 Comparison of SID at 60%, 70%, 80%, and 90% of the normalised intensity points for two exemplar A-scans.	54

Figure 3.20 A-scans from the 3D-OCT scans highlighting the SID on the cheek for (a) D11, (c) D12, (e) D13, (g) D14, (i) D15 and on the neck for (b) D11, (d) D12, (f) D13, (h) D14, (j) D15.....	55
Figure 3.21 Example of participant D13 surface roughness calculation. (a) For the Cheek; $R_q = 11.5 \mu\text{m}$; (b) For the neck; $R_q = 22.7 \mu\text{m}$	57
Figure 3.22 Estimated roughness on the cheek and neck for each participant.	58
Figure 4.1 Participant selection criteria flowchart.....	66
Figure 4.2 Stencil placement to identify skin area for measurements on the (a) cheek and (b) neck.	68
Figure 4.3 Example of a participants position when measured with the OCT system.	69
Figure 4.4 Tape stripping equipment used in session 1.....	70
Figure 4.5 Annotated image of the Philips S9000 shaver used in the study.	71
Figure 4.6 Colour feedback options of the S9000 shaving handle.....	71
Figure 4.7 Shaving handle and mounts used in sessions 2 and 3.	73
Figure 4.8 Protocol for Mechanical response study at Philips.....	74
Figure 4.9 Baseline values for all three sessions for (a) TEWL at cheek, (b) TEWL at neck, (c) Hydration at cheek, (d) Hydration at neck, (e) Redness at cheek, (f) Redness at neck, (g) Temperature at cheek, (h) Temperature at neck.	79
Figure 4.10 Temporal responses to the mechanical stimuli on the cheek for (a) TEWL, (b) Hydration, (c) Redness, (d) Temperature. Outlier values for individual participants are also indicated, as are statistically significant differences from baseline.	81
Figure 4.11 Temporal responses to the mechanical stimuli on the neck for (a) TEWL, (b) Hydration, (c) Redness, (d) Temperature. Outlier values for individual participants are also indicated, as are statistically significant differences from baseline.	86
Figure 4.12 Relationship between the TEWL on the cheek and the neck for Session 1 at (a) Time = -1, (b) Time = 0, (c) Time = 10, (d) Time = 20, (e) Time = 30.	90
Figure 4.13 Relationship between the skin hydration on the cheek and the neck for Session 1 at (a) Time = -1, (b) Time = 0, (c) Time = 10, (d) Time = 20, (e) Time = 30.	91

Table of Figures

Figure 4.14 Relationship between the redness on the cheek and the neck for Session 1 at (a) Time = -1, (b) Time = 0, (c) Time = 10, (d) Time = 20, (e) Time = 30.....	92
Figure 4.15 Relationship between the temperature on the cheek and the neck for Session 1 at (a) Time = -1, (b) Time = 0, (c) Time = 10, (d) Time = 20, (e) Time = 30.....	93
Figure 4.16 Relationship between the TEWL on the cheek and the neck for Session 2 at (a) Time = -1, (b) Time = 0, (c) Time = 10, (d) Time = 20, (e) Time = 30.....	94
Figure 4.17 Relationship between the TEWL on the cheek and the neck for Session 3 at (a) Time = -1, (b) Time = 0, (c) Time = 10, (d) Time = 20, (e) Time = 30.....	95
Figure 4.18 TEWL values for each SS category for the three sessions involving separate mechanical insults on the (a) cheek and (b) neck. Outlier values for individual participants are also indicated, as are significant differences ($p < 0.05$) between the SS categories.	97
Figure 4.19 Hydration values for each SS category for the three sessions involving separate mechanical insults on the (a) cheek and (b) neck. Outlier values for individual participants are also indicated, as are significant differences ($p < 0.05$) between the SS categories.....	99
Figure 4.20 Redness values for each SS category for the three sessions involving separate mechanical insults on the (a) cheek and (b) neck. Outlier values for individual participants are also indicated, as are significant differences ($p < 0.05$) between the SS categories.....	101
Figure 4.21 Temperature values for each SS category for the three sessions involving separate mechanical insults on the (a) cheek and (b) neck. Outlier values for individual participants are also indicated, as are significant differences ($p < 0.05$) between the SS categories.....	103
Figure 5.1 OCT scans from the cheek and neck for one participant at baseline. The skin surface detected from the MATLAB algorithm has been highlighted in blue. Additionally, detected artefacts have been highlighted in red.	112
Figure 5.2 Temporal A-scans for the cheek and neck for one participant.	112
Figure 5.3 Exemplar A-lines for two individuals. (a) Individual 1 reveals missing second peaks for the A-lines mostly on the cheek. (b) Individual 2 reveal missing second peaks for several A-lines on the cheek and neck.	113

Figure 5.4 Illustration of Area under the curve calculation from an Averaged A-line.....	114
Figure 5.5 Baseline values for SID, AuC, and Rq for the three sessions for (a) SID on the cheek, (b) SID on the neck, (c) AuC on the cheek, (d) AuC on the neck, (e) Rq on the cheek, (f) Rq on the neck.	118
Figure 5.6 Temporal response to mechanical insults on the cheek for (a) SID, (b) AuC, (c) Rq. Outlier values for individual participants are also indicated, as are statistically significant differences from baseline using the Mann Whitney test.	120
Figure 5.7 Temporal response to mechanical insults on the neck for (a) SID, (b) AuC, (c) Rq. Outlier values for individual participants are also indicated, as are statistically significant differences from baseline using the Mann Whitney test.	122
Figure 5.8 Relationship between the cheek and neck at baseline for SID in (a) Session 1, (b) Session 2, (c) Session 3; for AuC in (d) Session 1, (e) Session 2, (f) Session 3; for Rq in (g) Session 1, (h) Session 2, (i) Session 3.....	124
Figure 5.9 Spearman correlation scatterplots between OCT-skin parameters and biophysical parameters on the neck at baseline for Session 2. Where $p < 0.05$, the plots have been highlighted in yellow.....	125
Figure 5.10 Spearman correlation between the roughness and hydration on the neck for Sessions 1, 2, and 3 at baseline.....	126
Figure 5.11 Exemplar OCT scans and A-scans for P3 and P21 at baseline in session 1 on the cheek. * AuC is calculated from the non-normalized A-scans as this parameter is standardised with respect to the depth <i>in vivo</i> . However, the estimation method has been plotted on the normalised A-scan for visual comparison with the SID estimation.....	129
Figure 6.1 Region of interest highlighted on the forearms, cheek, and neck by drawing a square.	135
Figure 6.2 Protocol for assessing the structural and functional response of the skin to shaving.	136
Figure 6.3 Placement of the Sebutape on the arm.....	137
Figure 6.4 Example of the shaving stimulus on the forearm, cheek, and neck.	138
Figure 6.5 Labels for the timepoints of the data collection on the forearms: BL → Baseline; S1+0.3hr → 20 minutes post first stimulus; S1+24hr → 24 hours post first stimulus;	

Table of Figures

S2+0.3hr → 20 minutes post second stimulus; S2+24hr → 24 hours post second stimulus.	138
Figure 6.6 Exemplar dermatitis response on the neck in the preliminary test.	139
Figure 6.7 Labels for the timepoints of the data collection on the cheek and neck: BL → Baseline; S+0.3hr → 20 minutes post stimulus; S+24hr → 24 hours post stimulus. It is noted that Session 1 is referred to as “Long Beard” and Session 2 as “Short Beard”.139	
Figure 6.8 Annotated Dynamic OCT image with parameters from the Vivosight OCT system as follows: 1. Plexus depth (μm), 2. Vessel diameter (μm), 3. Vessel density (%), 4. Optical attenuation coefficient (mm^{-1}), 5. Surface reflectivity ratio, 6. Epidermal thickness (μm), 7. Epidermal thickness variation (μm), 8. Epidermal contrast (%), 9. Mean variation of surface height, Ra, 10. RMS variation of surface height, Rq, 11. Peak-to-trough difference of the surface height, Rz.	140
Figure 6.9 Exemplar A-line for an OCT scan of the cheek at baseline. The plot was created using the average Intensity values from the OCT images stack using the VivoTools software.	143
Figure 6.10 Scatterplot of SID vs OAC for all OCT scans in the present study.	144
Figure 6.11 Dynamic OCT scan of the cheek at baseline. (a) En-face image of the stack at a depth of 0.3 mm, (b) exemplar 2D-OCT scan from the stack, (c) plot of depth versus vascular density for the OCT scan.	145
Figure 6.12 Scatterplot of Plexus Depth versus Vessel Diameter from all the OCT scans from the present study.	145
Figure 6.13 Exemplar Vascular Densities plots for OCT scans of the cheek corresponding to the Short Beard from the present study. Statistically significant differences between measurement times are calculated using Wilcoxon Signed Rank test.	146
Figure 6.14 Exemplar Intensity profile for OCT scan of the cheek. (a) 2D-OCT scan; (b) A-scan from the VivoTools software where Epidermal thickness is not detected; (c) A-scan from the MATLAB algorithm with estimation of the Epidermal thickness. ..	147
Figure 6.15 Comparison of RMS Roughness estimation from the VivoTools software and the MATLAB algorithm. a) Exemplar DSLR image of the cheek; (b) Post-processed surface rendering from VivoTools; (c) Surface rendering from MATLAB algorithm.	148

Figure 6.16 Scatterplot of Roughness values from MATLAB and VivoTools from all the OCT scans from the present study.....	149
Figure 6.17 CIELAB colour sphere (Tang et al., 2015) with exemplar images from the present study.	150
Figure 6.18 Schematic for redness estimation highlighting the region of interest in the original RGB image, skin mask generation, and the resulting a* image.	151
Figure 6.19 Baseline characteristics for all anatomical locations for (a) TEWL, (b) Hydration, (c) Redness, (d) SID, (e) AuC, (f) Rq, (g) Plexus depth, (h) Vessel diameter, (i) Vessel Density, (j) SRR. Outlier values are indicated, as are statistically significant differences between groups using the Wilcoxon test (* $p < 0.05$).....	155
Figure 6.20 Temporal response following shaving on the arm for (a) TEWL, (b) Hydration, (c) Redness, (d) SID, (e) AuC, (f) Rq, (g) Plexus depth, (h) Vessel diameter, (i) Vessel Density, (j) SRR. Outlier values are indicated, as are statistically significant differences from baseline and statistically significant recovery from stimulus using the Wilcoxon test.....	159
Figure 6.21 Temporal response following tape stripping on the arm for (a) TEWL, (b) Hydration, (c) Redness, (d) SID, (e) AuC, (f) Rq, (g) Plexus depth, (h) Vessel diameter, (i) Vessel Density, (j) SRR. Outlier values are indicated, as are statistically significant differences from baseline and statistically significant recovery from stimulus using the Wilcoxon test.....	163
Figure 6.22 Temporal response following shaving on the cheek for (a) TEWL, (b) Hydration, (c) Redness, (d) SID, (e) AuC, (f) Rq, (g) Plexus depth, (h) Vessel diameter, (i) Vessel Density, (j) SRR.. Outlier values are indicated, as are statistically significant differences from baseline and statistically significant recovery from stimulus using the Wilcoxon test.....	167
Figure 6.23 Temporal response following shaving on the neck for (a) TEWL, (b) Hydration, (c) Redness, (d) SID, (e) AuC, (f) Rq, (g) Plexus depth, (h) Vessel diameter, (i) Vessel Density, (j) SRR. Outlier values are indicated, as are statistically significant differences from baseline and statistically significant recovery from stimulus using the Wilcoxon test.....	170
Figure 6.24 Temporal response following shaving on the cheek for the Short Beard for (a) IL-1 α , (b) IL-1RA, (c) IL-6, (d) IL-8, (e) IFN- γ , (f) TNF- α . Sample sizes and outlier values are	

Table of Figures

indicated, as are statistically significant differences from baseline and statistically significant recovery from stimulus using the Wilcoxon test.	175
Figure 6.25 Temporal response following shaving on the neck for the Short Beard for (a) IL-1 α , (b) IL-1RA, (c) IL-6, (d) IL-8, (e) IFN- γ , (f) TNF- α . Sample sizes and outlier values are indicated, as are statistically significant differences from baseline and statistically significant recovery from stimulus using the Wilcoxon test.	178
Figure 7.1 Exemplar image of the neck with estimation of the count of detected hair.	188
Figure 7.2 Exemplar Force vs Time plots from the shaving stimulus on the cheek and neck for one participant.	189
Figure 7.3 S-scores for all participants, sorted in ascending order. Associated Q-scores and Mech SS have also been plotted. Furthermore, axis labels have been formatted to represent the shaving device and frequency reported by the participants.	190
Figure 7.4 Case study for P7 from the Long Beard session (does not include biochemical parameters).	194
Figure 7.5 Case study for P7 from the Short Beard session.	195
Figure 7.6 Scatterplots of values on the cheek and neck for the Long and Short Beard sessions for (a) F_{rms} , (b) f_{stroke} , (c) N_{max} , (d) N_{hair}	197
Figure 7.7 Conceptualization of the skin responses to shaving, and the intrinsic and extrinsic factors influencing skin sensitivity.....	207
Figure 8.1 Revisiting the illustration of the conceptual relationship between shaving and skin sensitivity.....	216
Figure 8.2 P-values and pareto chart of an exemplar regression model.	221

Research Thesis: Declaration of Authorship

Print name: Pakhi Chaturvedi

Title of thesis: Sensorial and Physiological Response in the Skin Device Interaction for Personal Care/Devices

I declare that this thesis and the work presented in it are my own and has been generated by me as the result of my own original research.

I confirm that:

1. This work was done wholly or mainly while in candidature for a research degree at this University;
2. Where any part of this thesis has previously been submitted for a degree or any other qualification at this University or any other institution, this has been clearly stated;
3. Where I have consulted the published work of others, this is always clearly attributed;
4. Where I have quoted from the work of others, the source is always given. With the exception of such quotations, this thesis is entirely my own work;
5. I have acknowledged all main sources of help;
6. Where the thesis is based on work done by myself jointly with others, I have made clear exactly what was done by others and what I have contributed myself;
7. Parts of this work have been published as:-
Chaturvedi, P, Worsley, PR, Zanelli, G, Kroon, W, Bader, DL. Quantifying skin sensitivity caused by mechanical insults: a review. *Skin Res Technol.* 2021; 28: 187– 199.

Signature: Date: 12/05/2023

Dissemination

Publications

Chaturvedi, P, Worsley, PR, Zanelli, G, Kroon, W, Bader, DL. Quantifying skin sensitivity caused by mechanical insults: a review. *Skin Res Technol.* 2021; 28: 187– 199. <https://doi.org/10.1111/srt.13104>

Conference abstracts

Pakhi C. (2021) The effects of perceived skin sensitivity on the physiological response to mechanical loading. European Pressure Ulcers Advisory Panel (EPUAP), 18 - 19 October, 2021, Virtual meeting.

Public Engagement Event poster

Pakhi C. (2022) Understanding “Sensitive Skin” in response to shaving. Public Engagement Event, 28 June, 2022, University of Southampton.

This thesis is dedicated to Niharika Chaturvedi – my sister and closest confidante.

I am grateful for your rigid and relentless encouragement.

I am here because of you (quite literally!).

Thanks, Di.

Acknowledgements

I am deeply grateful to my supervisors. Their guidance, encouragement, and support throughout my Ph.D. program were instrumental in shaping my research and helped me to develop as a scholar. In particular,

Dr. Wilco Kroon, thank you for the hours spent brainstorming and troubleshooting concepts with me as a peer. You reminded me to have fun and led by example to work with enthusiasm. Your passion motivates me to follow in your footsteps. *Dank je wel!*

Dr. Peter Worsley, thank you for creating a collaborative environment through the nuances of digital communication. I am grateful for your attention to detail, teaching me elevate the quality of my work at present and in the future.

Dr. Giulia Zanelli, thank you for always supporting me. Your leadership made my journey comfortable, personally and professionally. I am grateful for your efforts in building this innovative project and feel honoured to have been a part of your team.

Professor Dan Bader, thank you for sharing your immense expertise. Your insights challenged me to refine my arguments. I am saddened by your passing away, and hope you have found eternal peace.

I would like to express my appreciation to the participants who generously gave me their time (sitting through intensive and occasionally painful experiments, and returning to do it all over again!). Their contributions are crucial to my study and founds the back-bone of my research.

I am grateful to my colleagues at Philips, University of Southampton, and within the STINTS consortium for helping me contextualise the importance of my research.

I would also like to thank my friend, Lisanne Hameleers. Your companionship carried me through the ups and downs of my Ph.D. journey (and the global pandemic). I am inspired by your work ethic and your energy for living life to the fullest. I cherish the memories of living together as one functioning adult!

A special thanks to my fiancé, Dr. Ishaan Sood. Thank you for being flexible in the face of logic. Your partnership has taught me to be confident and bold. I truly admire your inherent curiosity and ability to continually learn. I am excited for our future together.

Finally, thank you to my family for their love. Specifically to my mother, whose unwavering presence gave me the strength to persevere through challenging times and helped me achieve this milestone. I've said it before and I say it again - I owe you all of my success.

Definitions and Abbreviation

a.u.	arbitrary units
AuC.....	Area under the Curve
CBF	Cutaneous Blood Flow
CRS	Confocal Raman Spectroscopy
DEJ.....	Dermal Epidermal Junction
Doppler OMAG.....	Doppler Optical Microangiography
IFN- γ	Interferon-gamma
IL.....	Interleukin
LDF	Laser Doppler Flowmetry
LDI	Laser Doppler Imaging
LDPI	Laser Doppler Perfusion Imaging
LDV	Laser Doppler Velocimetry
LSCI.....	Laser Speckle Contrast Imaging
MSCA.....	Marie Skłodowska-Curie Actions
NSS	Non-Sensitive Skin
OAC	Optical Attenuation Coefficient
OCT.....	Optical Coherence Tomography
OCTA	Optical Coherence Tomography Angiography
PCL.....	Philips Consumer Lifestyle
RCM.....	Reflectance Confocal Microscopy
SC	Stratum Corneum
SFDI	Spatial Frequency Domain Imaging
SID	Scaled Intensity Drop
SRR	Skin Reflectivity Ratio
SS.....	Sensitive Skin
STINTS	Skin Tissue Integrity under Shear

TEWL..... Transepidermal Water Loss

TNF..... Tumour Necrosis Factor

TRP..... Transient Receptor Potential

TS Tape Strips

US..... Ultrasonography

VAS..... Visual Analogue Scale

Chapter 1 Introduction

1.1 Research Context

This work is carried out as part of the project “Skin Tissue Integrity under Shear” (STINTS) that is funded from the European Union’s Horizon 2020 research and innovation programme under the Marie Skłodowska-Curie Actions (MSCA) grant agreement no. 811965. The main scientific aim of STINTS is to understand the complex biomechanical and biochemical pathways leading to loss of skin integrity, following exposure of the skin to prolonged pressure and shear forces that ultimately result in damage at the cellular level. The STINTS project constitutes of 13 early-stage researchers (Table 1.1) in collaboration with 8 academic/private beneficiaries and 6 partners worldwide.

Table 1.1 Overview of research topics within the STINTS consortium with the current research highlighted.

Researcher	Host	Project title
1	Univ. Birmingham, UK	Skin material models and boundary conditions of Stratum Corneum and biomarkers.
2	Univ. Southampton, UK	Identifying early changes in skin integrity using biomarkers and physical sensors.
3	Univ. Southampton, UK	Testing medical interventions in clinical practice using biomarkers and physical sensors.
4	Unilever Research, UK	Multi-scale multi-physics modelling and measurement of skin permeation and boundary conditions of Stratum Corneum.
5	Eindhoven Univ. Tech., NL	Multi-scale, multi-physics modelling of the upper layers of the skin.
6	Eindhoven Univ. Tech., NL	Skin material models (ex vivo shear and compression) for skin device interaction.
7	Philips Consumer Lifestyle, NL	Sensorial and physiological response in the skin-device interaction for personal care/devices.
8	Univ. Grenoble Alpes, FR	Custom-mechanical biomechanical multi-scale multi-physics modelling for simulation-driven support surface optimization.
9	Univ. Grenoble Alpes, FR	Personalized multi-scale, multi-physics modelling of the interactions between soft tissues and support surfaces.
10	Tel Aviv Univ., IL	Multi-scale, multi-physics modelling of structure-function relations in subcutaneous fat.
11	Tel Aviv Univ., IL	Model protective efficacy of smart materials for support surfaces.
12	Univ. Lille, FR	Low frequency ultrasound diagnostics sensor and therapy device for Pressure Ulcers.
13	Univ. Lille, FR	Portable diagnostics sensor to rapidly assess mechanical and sensorial properties of skin.

The following thesis is being submitted through a collaborative project between Philips Consumer Lifestyle (PCL; a division of Royal Philips) and the University of Southampton. The research is based within the Male Grooming Innovation and Development department at PCL, which pioneers innovation for electric shavers.

1.2 Research Motivation

It is known that extreme cases of skin loading can lead to tissue damage in the form of acute injuries i.e., cuts or grazes, or wounds that occur due to prolonged mechanical insults e.g., pressure ulcers (Bouten et al. 2003). Such skin damage could be exacerbated in individuals who have a reduced tolerance to loading, which may be evident in those with enhanced skin sensitivity. Clinical examples include those individuals who spend lengthy periods in sitting or lying postures, and those who require medical devices which are attached to the skin for diagnostic or therapeutic purposes (Gefen 2020). A recent example of the latter is the use of respiratory personal equipment used by healthcare professionals to manage Covid-19 patients in hospitals during the pandemic (Abiakam et al. 2021). In addition, consumer products such as electrical shavers interact with the skin while exerting a combination of dynamic loading in the form of pressure and shear. Indeed, it has long been established that in certain users, shaving can cause redness, inflammation, acne, and other symptoms associated with skin sensitivity (Shellow 1938). To meet the demands for personalised products and interventions to promote skin health, there is a need to establish individual thresholds of tolerance to external mechanical stimuli, and work towards personalised solutions to promote skin health.

1.3 Background on the Research Topic

Sensitive Skin (SS) is a widely occurring phenomenon, with self-reported prevalence approximated at 60-70% for women and 50-60% for men, regardless of factors like living environment or socio-economic status (Farage 2019). Furthermore, individuals reporting SS is on the rise as indicated by the increasing number of people consulting dermatologists with specific SS-related concerns (Loffler et al. 2001; Halvorsen et al. 2008; Berardesca et al. 2013). In addition, there is an increase in prevalence of adverse reactions to cosmetics (Re et al. 2001). This could be attributed to greater recognition/evidence of symptoms or even increased interest in cosmetics and the general

maintenance of healthy skin (Farage and Maibach 2010). As such, SS continues to be an active area of interest in both industry and medicine/dermatology research fields.

However, the study of SS is hindered by the lack of a quantifiable definition, which can be assessed using objective measurement approaches. Many efforts have been taken to quantify the severity of SS in a standardized manner beyond that of a self-report. Researchers have attempted to define “Sensitive Skin” but there is still a lack of consensus. A recent paper considers SS

“A syndrome defined by the occurrence of unpleasant sensations (stinging, burning, pain, pruritus, and tingling sensations) in response to stimuli that normally should not provoke such sensations. These unpleasant sensations cannot be explained by lesions attributable to any skin disease. The skin can appear normal or be accompanied by erythema. Sensitive skin can affect all body locations, especially the face” (Misery et al. 2017).

While this definition addresses the varied nature of stimuli and responses associated with SS, its qualitative and generic nature limits the potential for it to be measured objectively and further the understanding of the underlying physiological mechanisms such as enhanced immune response or hyper-reactive neural pathways. Additionally, the individual variability of clinical manifestations makes standardization and quantification of SS challenging, further indicating the need to quantify skin status with more robust objective parameters (Slodownik et al. 2007; Do et al. 2020).

It has been reported that the prevalence of self-assessed SS are higher than those determined by dermatologists during clinical examinations (Halvorsen et al. 2008). As such, there seems to be more to sensitive skin than that studied in the confines of dermatology from which much of our current understanding originates. This may be explained by the inter-subject variability in the triggers and the magnitude of the perceived tissue response (Figure 1.1). While different individuals could be considered to have sensitive skin, their responses might have arisen from different physiological pathways and therefore require different solutions to mitigate the skin reaction.

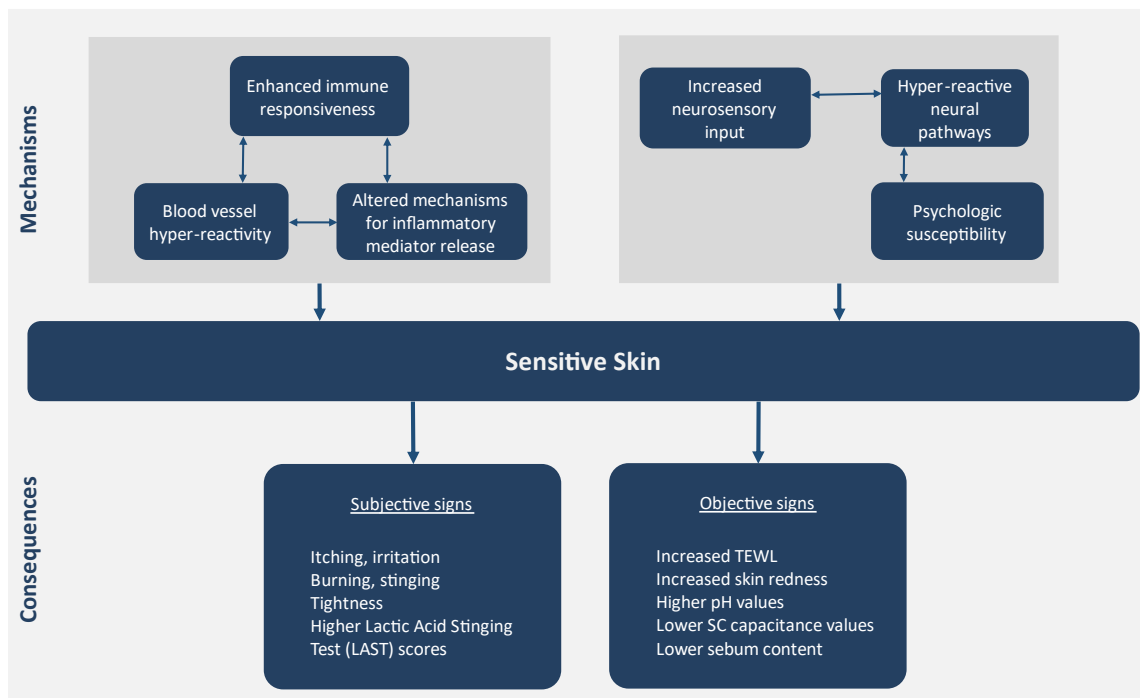


Figure 1.1 Flow chart of inter-subject variability. Adapted from “Sensitive Skin Syndrome”, 2006 (Enzo Berardesca, Maibach, and Fluhr 2006).

Such inter-subject differences in occurrence and perception of sensitive skin raises the issue around identifying the commonality in the underlying pathways. Arguably, the next step to improve our understanding of the genesis of skin sensitivity is to avoid ambiguity by 1) limiting the scope to a specific stimulus-response relationship and 2) focusing on objective methods to quantify the response irrespective of the associated pathways. Consequently, this research is motivated by the impact of characterizing inter-subject variability in skin parameters and its influence on the design and development of skin-contacting devices.

1.4 Research Scope and Goals

This research focuses on non-invasive measurement tools that are objective, reliable, and validated for use when evaluating skin responses to a range of stimuli. To limit the scope, the focus is on the pathways associated with mechanically induced skin sensitivity, e.g., pressure and shear forces elicited when rubbing something against facial skin such as while shaving. Considering the vastness of the topic, the specific scope of this research has been illustrated in [Figure 1.2](#).

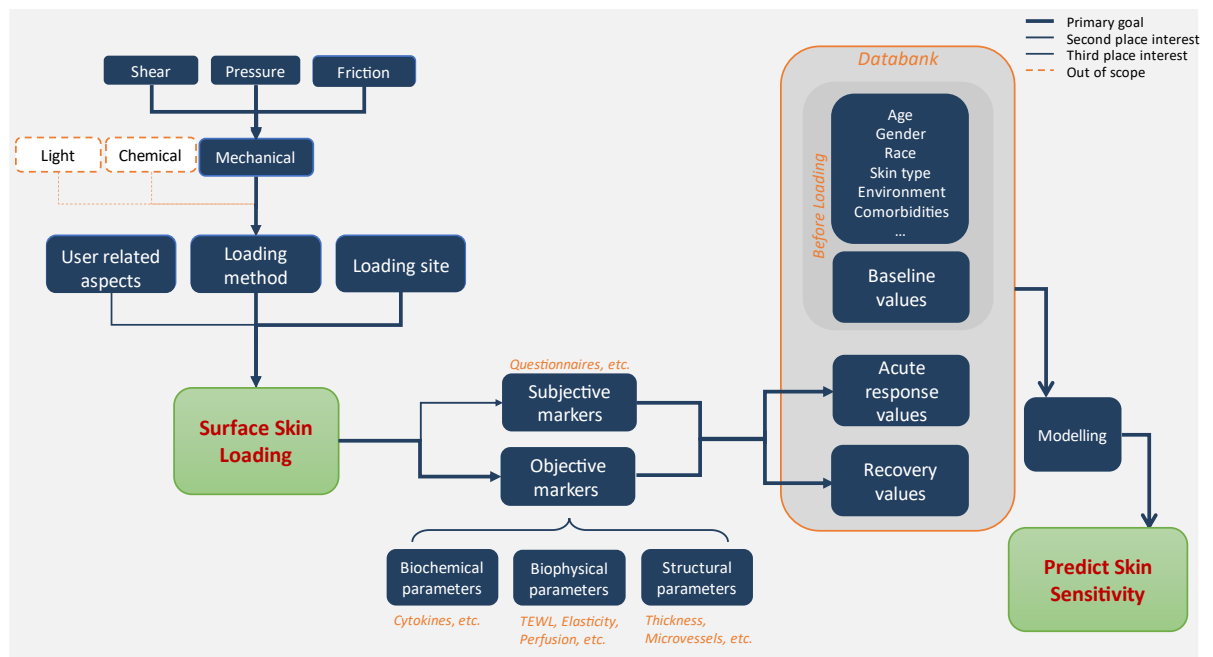


Figure 1.2 Scope of the research project.

The overall goal of this research is to define skin sensitivity as a function of skin parameters, illustrated in Figure 1.3. Furthermore, this research aims to be able to predict the occurrence of skin sensitivity in individuals in response to mechanical loading by correlating the physiological (objectively measured) and the sensorial (subjectively quantified) responses of skin following stimulus interaction (e.g., skin-contacting consumer products), and investigating the trends in baseline physiological parameters and subsequent skin recovery.

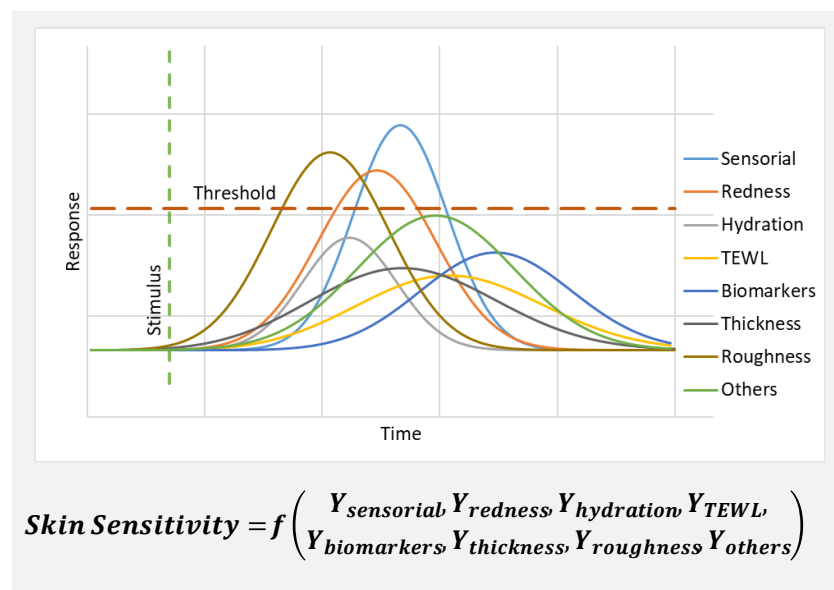


Figure 1.3 Illustration of the conceptual relationship between skin sensitivity and objectifiable skin responses. Enhanced SS may be due to a lower threshold and/or a heightened/prolonged response or combination of responses.

Chapter 2 Literature Review

Publication: Chaturvedi, P, Worsley, PR, Zanelli, G, Kroon, W, Bader, DL. Quantifying skin sensitivity caused by mechanical insults: a review. Skin Res Technol. 2021; 28: 187– 199. <https://doi.org/10.1111/srt.13104>

A literature review was conducted with an aim to understand the structure and function of the skin, the factors implicated in genesis of skin sensitivity, and to identify state-of-the-art techniques to quantify skin integrity in response to mechanical loading. This chapter presents a combination of a narrative literature review (Sections 2.1 – 2.3) and a secondary analysis (Section 2.4) to achieve the following specific objectives:

- Summarise the structure and function of the skin.
- Identify factors (intrinsic and extrinsic) which affect skin sensitivity.
- Gain an understanding of the existing techniques used to estimate skin health parameters.
- Critically evaluate the reliability of these methods with respect to mechanical loading.
- Identify skin parameters of interest and the protocols for prospective *in vivo* experiments.

2.1 Skin Structure and Function

Skin is the largest organ of the body (Geerligs 2009). It is a multi-layered, viscoelastic, complex living tissue consisting of three distinct layers: the epidermis (~ 100 µm thick), the dermis (~ 1000 µm thick), and the hypodermis (>1000 µm thick), as illustrated in Figure 2.1. The epidermis can be further divided into the Stratum Corneum (SC; ~ 20µm thick) and the viable epidermis (~ 80µm thick). SC is the horny upper layer of the epidermis, made up of about 15-20 layers of dead cells called corneocytes, which are held together by lipids and desmosomes. This is commonly referred to as a “brick-and-mortar” structure and plays a key role in the barrier function of the skin. The viable epidermis is largely made up of cells called keratinocytes, which migrate outwards to the skin surface where they become non-viable. This layer also contains other cell types including melanocytes which produce the colour pigment called melanin, Langerhan cells which are responsible for immune response, and Merckel cells which provide tactile sensation.

The dermis contains microvessels such as hair follicles, sebaceous glands, sweat glands, and nerve endings. The hypodermis, also known as the subcutaneous layer, contains adipose tissue (fat cells),

connective tissue, larger nerves and blood vessels, and macrophages (cells which are part of the immune system). Subjacent to this layer can be a muscle layer, which overlies either bony prominences or internal tissues and organs.

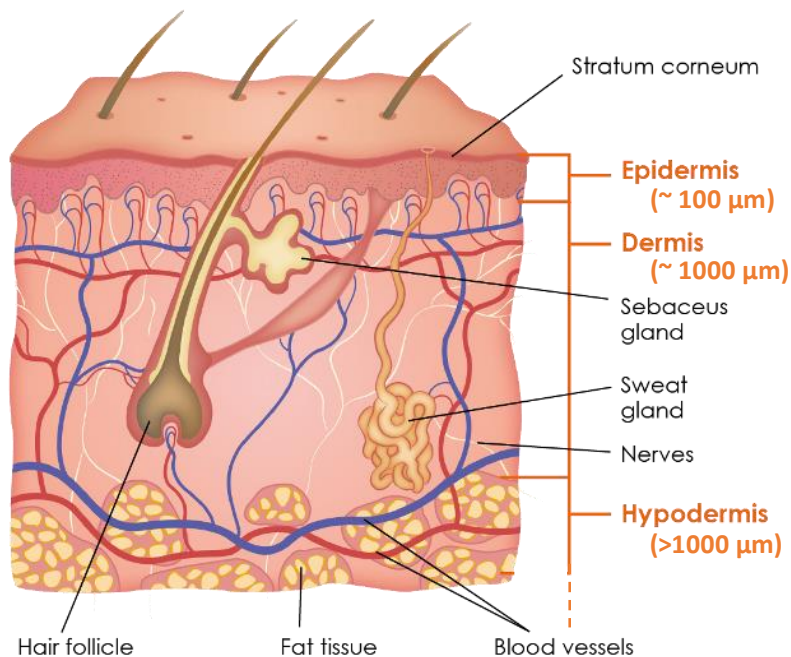


Figure 2.1 Three-dimensional sketch of the skin layers and their thickness. Adapted from Geerligs, 2009 (Geerligs 2009).

As an organ, the skin has several functions. Skin homeostasis aims to maintain tissue integrity in response to chemical, mechanical or environmental insults. The skin's unique structure and function enable it to respond to insults and protect the underlying soft tissues. Distinct responses and signalling pathways include changes in local perfusion, inflammation, and remodelling. These support the skin's primary functions which are listed below:

- i) **Barrier/protective function** – The major function of the skin is to form a barrier between the internal structures and the hostile external environment, protecting against physical, chemical and microbial insults, as well as against the loss of water and electrolytes (Feingold and Elias 2014).
- ii) **Immunological function** – In addition to its barrier function, the skin combats attacks from a host of toxins, pathogenic organisms, and physical stresses. Depending on the cytokine milieu, certain skin cells promote or attenuate the inflammatory response, supporting the early detection of environmental threats (Bangert et al. 2011).
- iii) **Sensory function** – The skin contains an extensive network of nerve cells that detect and relay changes in the environment. There are separate receptors for heat, cold, touch, pain, and itch.

Damage to these nerve cells is known as neuropathy, which results in a change in sensation (hyper or hyposensitivity) in the affected areas.

- iv) **Secretory function** – Secretion refers to the process of producing and releasing substances by specialized cells or glands. E.g., the sebaceous glands are responsible for secreting an oily substance called sebum, released through the shafts of the hair follicle. Sebum serves to lubricate the skin's surface protecting it against friction and enhancing its resistance to moisture.
- v) **Excretory function** – Excretion refers to the removal of waste products from the body. While the skin is not a primary excretory organ, the sweat glands support clearing of excess micronutrients, metabolic waste, and toxins from the body. These glands are influenced by the sympathetic nervous system, the primary goal of which is to stimulate the body's fight-or-flight response, otherwise utilised in maintaining the body's homeostasis.
- vi) **Thermoregulatory function** – This function of the skin involves regulation of body temperature via insulation, changes in peripheral circulation, and fluid balance via sweat.

The structural and physiological properties of the skin make it an important sensory organ to protect the human body from external insults and to communicate environmental factors to other organ systems. In some individuals, the ability of the skin tissue to respond to specific external factors can differ significantly, indicating differences in perceived skin sensitivity.

2.2 Genesis of Skin Sensitivity

Many researchers have relied exclusively on questionnaires for benchmarking skin sensitivity, with typical factors listed in [Figure 1.1](#). These cover a plethora of stimuli and responses a person can encounter, collating them into a sensitivity index. Consequently, predisposing factors can be found, e.g., individuals with SS were shown to have a higher risk of developing allergies when compared to those without SS (Loffler et al. 2001; Re et al. 2001). However, there remains a gap in objective measurements to identify the underlying mechanism associated with SS.

2.2.1 Types of stimuli

The difficulty in understanding SS is linked to the numerous variables complicating the “cause and effect” relationship. The stimuli are often unspecified, and the responses are ambiguous and undefined, questioning what aspect of the latter makes the tissue/individual “sensitive”. Some of the commonly known stimuli for SS can be classified as:

i) **Biochemical stimuli** – These could be the ingredients of cosmetics, soaps, detergents, and other similar topical products used by consumers such as sodium lauryl sulphate or lactic acid (Berardesca et al. 1991). Such ingredients trigger neurological and/or immunological responses perceived as SS, e.g., itching, inflammation, redness, rashes, and ulcers.

ii) **Mechanical stimuli** – An example of this type of stimulus is observed in amputees. The combination of pressure and shear forces acting on the skin at the socket interface during daily activities can compromise skin health, causing “stump ulcers” and abrasions. These loads can be static (during standing) or dynamic (during gait) in nature, which can result in breakdown of skin integrity (Swanson et al. 2020).

iii) **Environmental stimuli** – Different environmental factors (hot/cold temperatures, humid/dry weather, UV rays) have emerged as strongly associated with perceived SS. For example, a study questioning over 1000 individuals reported more than 50% individuals responding with some degree of irritation to most environmental conditions (Farage 2008).

iv) **Psychosomatic stimuli** – Emotional stress plays a substantial role in the skin health and its general status. As an example, there is clear evidence that the symptom of itch can be triggered by negative emotions, e.g. after watching a threatening movie (Verhoeven et al. 2008).

In the real-world scenario, one needs to consider a combination of multiple stimuli, which could be acting simultaneously. For example, moisture has been shown to increase the interfacial friction, which can prove damaging to the skin surface (Gerhardt et al. 2008). Consumers using electrical shavers to groom facial hair experience such combination stimuli regularly. Depending on a wet or dry shave, the handling of the device needs to be modified to adjust the pressure and shear forces for the desired outcome.

2.2.2 Origin of responses

Researchers have tried to identify the physiological pathways through which skin symptoms are displayed. Factors that have been implicated can be classified as originating from the following sources:

i) **Neurological** – Sensory receptors such as Transient Receptor Potential channels (TRP channels) play a central role in the perception of sensitivity. Certain TRPs are stimulated by chemicals, heat/cold, mechanical changes in the lipid layer, etc, acting as cellular sensors, influencing pain perception and inflammation (Duarte et al. 2017).

ii) **Immunological** – The immune system can be triggered to release pro-inflammatory cytokines, such as interleukins and tumour necrosis factor (TNF). These inflammatory proteins are related to the itching and burning sensations characteristic of SS (Guerra-Tapia 2019).

2.2.3 Intrinsic factors

Physiological systems of the human body, interacting through complex signalling pathways, are predisposing factors that need to be considered while studying SS. These intrinsic factors account for the interpersonal variability observed in the population. Individual thresholds, which can be influenced by genetics, diet, lifestyle etc., lead to differences in perception of sensitivity even though the stimulating triggers and response pathways might be the same. For example, SS was found to be twice as common in people with irritable bowel syndrome (Misery et al. 2019). This has created the hypothesis that other comorbidities might contribute to skin related issues and be clustered under the umbrella term “Sensitive Skin”.

User-behaviour associated with medical or consumer devices is another intrinsic factor that governs the sensitivity of skin. In the example of electric shaving, over-use of the device to achieve a clean shave might induce redness and inflammation of the patch of skin due to the mechanical stimuli exceeding the intrinsic threshold. These “sensitive skin” symptoms could be further aggravated by other intrinsic features like age, genetic predisposition, sex, or hormonal activities. This implies that general user-behaviour guidelines for consumer devices that contact skin may not mitigate all skin sensitivity issues, creating a demand for modular solutions that suit the individual’s needs. The increase in demand for personalized products is reflected in consumer care in general. For the issue of SS, this emphasizes the need for objective methods to quantify parameters of skin health, allowing individuals to receive customizable solutions for their routines.

2.2.4 Extrinsic factors

The relationship between stimuli and skin response is further complicated by extrinsic factors, such as the site of insult on the body. For example, studies have reported that the face is largely regarded as the most common site for enhanced skin sensitivity (Farage and Maibach 2010). Additionally, extrinsic factors, like the magnitude, frequency, and duration of stimuli, also influence the skin tissue response. A small stimulus over a long interval (for example, wearing a face mask for respiratory support) can cause modest deformations to the underlying skin and sub-dermal tissues, which over a period of hours can cause cell damage. By contrast, a large stimulus over a short interval (for example mechanical indentation) damages cells through direct deformation, where tissue strain values exceed 50%. This damage is usually visible within a few minutes (Bouten et al.

2003). Ideally, the measurement of skin sensitivity would account for these extrinsic factors, when determining the skin response.

2.3 State-of-the-art Objective Methods for Assessing Skin Sensitivity

There is no “gold standard” for identification of Sensitive Skin from either the medical community or the cosmetic industry (Slodownik et al. 2007). Several non-invasive biophysical and imaging tools have been employed, each of which have examined different parameters that characterise skin integrity (Table 2.1) and are discussed separately.

2.3.1 Stratum corneum water content and permeability

Water content of the stratum corneum (SC) directly affects the barrier function of the skin, as measured through a change in permeability (Fluhr et al. 2006). Failure of the SC to retain water induces dryness and increases the susceptibility to irritants (Tupker et al. 1990). Conversely, it is well established that prolonged exposure to moisture decreases the mechanical integrity of the epidermis and hence increases its susceptibility to localized damage at skin and device interface (Gerhardt et al. 2008; Dąbrowska et al. 2016; Bostan et al. 2019).

Transepidermal water loss (TEWL) –

A cornerstone measurement of skin response are changes in TEWL which is estimated locally by the physiological process allowing the transport of water through the SC into the external environment. This transport process is, in part, dependent on the orderly arrangement of the intercellular lipids in the SC to form a barrier, which can represent an intrinsic factor in skin sensitivity (Verdier-Sévrain and Bonté 2007). TEWL systems have been used for *in vivo* measurements of the rate of evaporation of water through the skin surface in order to detect changes in SC permeability (Fluhr et al. 2006). Two different principles are employed for TEWL measurements, involving either the unventilated (closed) chamber method or the ventilated (open) chamber method, whose performances are not directly comparable. Each have limitations, for example, the closed chamber method interferes with the skin surface microclimate during measurement, while the open chamber method is intrinsically prone to influences from surrounding environmental conditions (Seidenari et al. 1998; Kleesz et al. 2011; van Erp et al. 2018).

Many studies have reported higher TEWL values following mechanical insults to individuals reported to present with enhanced skin sensitivity (Loffler et al. 2001; Pinto et al. 2011; Richters et al. 2016). In a separate study involving tape stripping of skin in healthy volunteers, rapid increases in TEWL values were evident with prolonged tape contact and higher contact pressures (Loffler et

al. 2004). However, this approach was unable to differentiate between TEWL values in the baseline or unloaded state for SS and NSS cohorts. Such findings clearly raise questions about both the nature of the relationship between sensory irritation and the baseline skin barrier function, and the use of TEWL as an impartial method to quantify skin sensitivity.

Electrical Impedance Systems –

The measurement of the water content or hydration of the SC can involve either electrical capacitance or conductance principles (Rawlings and Harding 2004). Both systems yield relative changes of the dielectric constant between the SC and a surface electrode (measured in arbitrary units) but are strongly influenced by the nature of the skin contact and local surface roughness. The Corneometer (Courage & Khazaka, Germany) is a frequently used commercial capacitance measurement system. However, it has limited reproducibility and measurement errors are easily introduced by features at the skin surface, including hair, sweat and dirt particles (Richters et al. 2015; van Erp et al. 2018).

Many studies have reported lower capacitance values for individuals with clinically diagnosed dry skin (Sparavigna et al. 2006). In addition, lower values were measured on facial areas of individuals with sensitive skin compared to a non-sensitive control group (Roussaki-Schulze et al. 2005). These findings imply that dehydration is associated with enhanced skin sensitivity, as water is rapidly transported from the SC into the atmosphere. However, mechanical challenges, in the form of tape stripping, were not reported to influence SC hydration levels (Loffler et al. 2004; Kottner et al. 2015). More research is needed to identify the role of hydration in the occurrence of mechanically induced skin sensitivity.

Imaging Systems –

In order to detect the spatial distribution of water in the SC, imaging techniques such as Confocal Raman Spectroscopy (CRS) have been proposed. CRS exploits the inelastic scattering of light to measure the biochemical composition of the skin (Darlenski et al. 2009). This *in vivo* technique is well suited for clinical applications but requires trained personnel for measurement and interpretation of images. Regardless, there are conflicting reports with respect to the link between SC hydration and SS using imaging. One study using CRS demonstrated significantly different composition between hydrated and dry skin samples (Dąbrowska et al. 2016). By contrast, an examination of the molecular composition of the skin barrier, using both CRS and the SC water content methods (Richters et al. 2017), revealed no differences between cohorts of SS and non-SS individuals, noting that those SS subjects also reported dry facial and body skin as compared with non-SS.

2.3.2 Skin structure

Differences in skin sensitivity may reflect variations in skin structure and/or morphology. For example, a thinner SC might imply a more fragile skin barrier, which might be associated with enhanced skin sensitivity (Berardesca et al. 2013). In addition, changes in skin structure following a stimulus might indicate physiological responses, such as oedema, which could serve as a proxy for skin sensitivity.

Common *in vivo* techniques for skin structure assessment, such as capillaroscopy, dermoscopy, and infrared photography, provide rapid and inexpensive results, although expertise is needed for robust interpretation. Alternative technologies, such as reflectance confocal microscopy (RCM), laser speckle contrast imaging (LSCI), optical coherence tomography (OCT), and ultrasound imaging, provide expensive options with a range of depth resolutions, to examine the structure of skin and sub-dermal tissues. In particular, they have been used to quantify the presence of oedema in the dermal and deeper sub-dermal layers following loading (Welzel et al. 2003; Bader and Worsley 2018). These techniques have also been used to investigate the appropriateness of SC thickness in predicting skin sensitivity (Agner and Serup 1989; Ma et al. 2017; Richters et al. 2017). None of these studies, however, reported consistency in correlating changes in SC thickness following mechanical loading and skin sensitivity. Nonetheless, one study reported that fewer tape strips were required to remove the SC in sensitive skin (Richters et al. 2016), suggesting that enhanced skin sensitivity is associated with impaired cell adhesion. A mechanistic link might be found in the role of cell shape and size in cell adhesion. Indeed, using RCM, the depth at which cells still form a "honeycomb" structure is reportedly indicative of high skin sensitivity (Ma et al. 2017).

Other factors such as tissue stiffness and surface roughness represent parameters implicated in the assessment of skin sensitivity (Maurer et al. 2016) although, to date, they have not been studied in-depth. In addition, an assessment of vascular density may reflect skin sensitivity (Chen and Zheng, 2020). Indeed, in related investigations a decreased microvascular density has been reported to be associated with cardiovascular and metabolic diseases, such as hypertension, diabetes, obesity and metabolic syndrome (Deegan and Wang 2019).

2.3.3 Erythema / Skin Colour

Erythema or redness of skin has regularly been recognized as a key indicator in the clinical presentation of sensitive skin (Seidenari et al. 1998), as well as with mechanical irritation of skin, such as shaving (Maurer et al. 2016; Rietzler et al. 2016). However, the perception of skin colour and redness is highly subjective in nature (Farage 2008). This has motivated the development of

reliable and reproducible methods to provide an objective evaluation of skin colour (Fullerton et al. 1996).

Tristimulus colorimetry represents such a measurement method that is used to analyse light reflected from skin structures in the blue, green and red spectrum. Based on the light source, commercial devices such as the Chromameter (Minolta, Japan) have been used and increased values for redness have been reported in SS subjects (Diogo and Papoila 2010). Moreover, erythema has been closely associated with modified blood perfusion following chemical stimulation (Richters et al. 2015). However, the relationship between the light absorbance values and the extent of erythema is highly dependent on the pigmentation of the skin (Clarys et al. 2000). Subsequently, its relationship to skin sensitivity remains unclear.

An alternative measurement principle, termed reflectance spectrophotometry, involves analyses of light spectrum reflected from the skin. Depending on the wavelengths of the light, several commercial systems are available, for example, DermaSpectrometer (Cortex Technology, Denmark), Mexameter (Courage-Khazaka Electronic, Germany) or Dermacatch (Colorix, Switzerland). Multi- and hyperspectral imaging systems can be considered extensions to these, where 2D photos involving reflections of multiple wavelengths are analysed, similar to RCM, to assess changes in relative composition of the skin (Paul et al. 2015).

Interestingly, OCT has also been used to identify objective parameters relating to erythema. For example, one study measured the light attenuation coefficient of the skin layers, reporting that erythema/pigmentation decreased the signal intensity in the dermis (Welzel et al. 2004). In clinical studies, the light attenuation coefficient of skin layers has been associated with dermatological conditions, such as psoriasis and contact dermatitis (Welzel et al. 2003). Such a distinction was not possible with clinical ultrasound scanners due to its inferior resolution when compared to OCT.

2.3.4 Microcirculation / Blood Perfusion

Skin microcirculation, often termed cutaneous blood flow (CBF), is represented by the process of blood flow through small blood vessels. It is important for thermoregulation, skin metabolism and transcutaneous transportation. Assessment of skin microcirculation has proved a common objective measure in both dermatology and cosmetology, for instance microcirculation impairment is known to increase with age and its associated comorbidities (Bentov and Reed 2015).

Laser Doppler Flowmetry (LDF) and Laser Doppler Velocimetry (LDV) are the most widely used methods for CBF assessment (Berardesca et al. 2002). They produce an output signal that is proportional to the local blood perfusion, measured in arbitrary units. Although LDV can be used to

quantify the magnitude of allergic and irritant skin reactions, it cannot discriminate between the two (Primavera and Berardesca 2005). Technological developments, such as laser doppler imaging (LDI), laser doppler perfusion imaging (LDPI), and LSCI additionally provide 2D images of the spatial change in blood flow.

Only a few studies exist on the effects of mechanical loading on changes in microcirculation. Of the few, LDI was reported to provide an objective tool for blood flow assessment and that reactive hyperaemia was linearly related to the magnitude of peel force resulting from adhesive tapes (Mayrovitz and Carta 1996). By contrast, many studies have used LDV/LDPI to examine skin changes following chemical stimulation (Lammintausta et al. 1988; Issachar et al. 1998; Diogo and Papoila 2010). These studies report a markedly higher value for SS subjects following stimulation, despite minimal difference in baseline values. Thus, the changes in blood perfusion evoked in individuals with enhanced skin sensitivity could be a direct result of increased penetration of chemicals indicating an impaired SC barrier function. However, the relationship between CBF and enhanced skin sensitivity to mechanical loading remains poorly understood.

Extension to ultrasound imaging and OCT also provide information on spatial profiles of blood perfusion (Deegan and Wang 2019). For example, Doppler Optical Microangiography (Doppler OMAG) has been implemented to quantify changes in blood flow (Wang et al. 2015). This study demonstrated that tape stripping results in a transient increase in CBF, which was significant at the dermal epidermal junction.

2.3.5 Skin temperature and microclimate

Body temperature regulation is maintained, in part, by outward heat flow from skin through underlying micro vessels and physiological processes. Conversely, skin temperature can affect the local tissue physiology, providing additional risk to vulnerable tissues already compromised by external stimuli (Bader and Worsley 2018).

Several researchers have evaluated the relationship between changes in skin temperature and the development of mechanically induced pressure damage. One study revealed that patients subjected to prolonged sacral loading had an increased risk of damage, as the relative skin temperature started to decrease by 0.1°C (Jiang et al. 2020). These results were consistent with other studies evaluating the role of skin temperature as an early indicator of pressure damage (Kanazawa et al. 2016). Researchers have also reported a correlation between skin surface temperature and intrinsic factors, such as emotional state when exposed to cognitive tasks, expanding the triggers associated with SS (Rimm-Kaufman and Kagan 1996).

There are a number of methods to monitor the skin microclimate, including thermocouples, infrared thermography and hygrometers (Bader and Worsley 2018). These have demonstrated, for example, that temperatures exceeding 35°C have a detrimental effect on the barrier function of the SC by reducing its mechanical stiffness and strength (Bader and Worsley 2018). Furthermore, a reduced reactive hyperaemic response was reported when local cooling was simultaneously applied with pressure in healthy subjects (Tzen et al. 2010). However, researchers have suggested that analyses of skin blood flow is more effective than local skin temperature measurements to monitor development of pressure-induced damage (Jan et al. 2012). Likewise, studies have reported that susceptible patients have prolonged recovery times of blood flow during pressure relief (Meijer et al. 1994). Thus, assessment and management of skin temperature plays an important role in the health status of mechanically loaded skin tissues, thereby highlighting possible solutions for maintaining skin health. Further research examining the relationship between skin temperature, emotional state, and microcirculation would provide insight into the inter-subject differences in the perception of skin sensitivity.

2.3.6 Pruritus & Inflammation

Skin inflammatory disorders represent a high proportion of cases in dermatology (Wang et al. 2015). Specifically, physical irritation of the skin is known to induce an inflammatory response with local hyperaemia (Maurer et al. 2016). Historically, the assessment of inflammatory skin reactions has largely relied on invasive techniques, such as biopsies, and visual assessment methods. An alternative approach is to sample biomarkers associated with inflammatory processes in fluids excreted from skin, such as sebum or sweat (Perkins et al. 2001). As an example, the expression of the pro-inflammatory cytokine, IL-1 α , was shown to be significantly increased following periods of continuous and intermittent loading of the sacral skin (Soetens et al. 2019). Furthermore, this study also suggested that a normalized IL-1 α ratio provided an early indicator of skin status, thereby highlighting its potential to identify individuals at risk of loss of skin integrity. Biomarker sampling and analysis falls outside the scope of the current review, although perspectives on its use in future research have been included in the discussion.

2.3.7 Skin pH

The 'acid mantle' of the SC plays an important role in the barrier function of skin (Schmid-Wendtner and Korting 2006). Indeed, elevation in skin pH results in an increased basal TEWL and an impairment in the epidermal barrier function (Hachem et al. 2005; Fluhr et al. 2008). For example, daily use of water or a mild detergent on the skin can result in an immediate increase in pH that remains elevated up to 6 hours after washing in some individuals (Lambers et al. 2006).

Skin pH can be measured by electrochemical methods involving contacting the skin surface with a glass electrode, which represents a simple, rapid, and reproducible method (Darlenski et al. 2009). Skin pH is known to increase after 50 years of age, and in cutaneous ailments, such as atopic dermatitis, psoriasis, rosacea, dry skin, and sensitive skin (Lambers et al. 2006). By contrast, other studies have reported no significant differences in skin pH for SS individuals (Seidenari et al. 1998; Roussaki-Schulze et al. 2005). While the influence of mechanical stimuli on the skin surface is still to be associated with effects on its pH, the imbalance in skin pH could influence mechanisms (e.g., barrier function) that typically evoke responses following mechanical insults.

2.3.8 Sebum content / oiliness

Several studies have reported a general decrease in sebum levels in individuals with SS (Seidenari et al. 1998; Roussaki-Schulze et al. 2005). Sebum, secreted by the sebaceous glands, lubricates the skin, minimizes frictional forces, and as such might reduce the skin's reaction to mechanical loading. However, direct evidence describing the effects of sebum on the skin response to mechanical loading is lacking.

Objective measures of skin surface sebum can be performed using several non-invasive methods. For example, Sebumetry measures the lipid content by transmitting light through an opaque plastic film in after it has been in contact with the skin surface for approximately 30 seconds. Transparency of the film correlates to lipid adherence. This method has been reported to be both highly reproducible and efficient (Darlenski et al. 2009). However, its reliability is highly dependent on the estimation of total sebum amount on the skin surface (Andreassi and Andreassi 2007; Bader and Worsley 2018).

Table 2.1 Advantages and limitations of measurements methods and the skin properties quantified.

References	Measurement techniques	SC hydration	Skin structure	Erythema	Microcirculation	Temperature	pH	Sebum	Advantages	Limitations
Deegan, 2019; Roustit & Cracowski, 2012	Capillaroscopy								Rapid; inexpensive; high repeatability and reliability; more detailed vascular evaluation than dermoscopy.	Vessel irregularities difficult to quantify (subjective); susceptible to pressure artefacts.
Richters, 2017; Piet E. J. van Erp, 2018	Confocal Raman Spectroscopy								High spatial and temporal resolution; high biochemical specificity.	Expensive; requires training; bulky set-up.
Deegan, 2019	Dermoscopy								Real-time; inexpensive; easy to use; can detect vascular changes.	Training needed for image interpretation (subjective); poor specificity; low resolution.
Logger et al., 2020; Piet E. J. van Erp, 2018	Diffuse reflectance spectroscopy								Easy to use; small/ medium- sized probes makes it easily applicable.	Influenced by environment; no information on extent of erythema.
Piet E. J. van Erp, 2018	Impedance systems (capacitance and conductance)								Easy to use; inexpensive.	Indirect measurement; Influenced by environment; poor reproducibility.
Logger, 2020	Infrared photography								Rapid; inexpensive.	No differentiation between arterial and venous structures; post-processing required; less accurate than contact methods.
Logger, 2020	Infrared thermography								Real-time; easy to use.	Influenced by intrinsic and extrinsic factors; less accurate than contact methods
Berardesca, 2002; Deegan, 2019	Laser Doppler Velocimetry (LDV) - Laser Doppler Flowmetry (LDF) - Laser Doppler Perfusion Imaging (LDPI)								Inexpensive; portable. LDF provides continuous, real-time flow information. LDPI has low variability between measurements.	Influenced by intrinsic and extrinsic factors; no information about depth. LDF has higher variability between measurements. LDPI is not real-time and has lower temporal resolution.
Deegan, 2019; Roustit, 2012	Laser Speckle Contrast Imaging (LSCI)								Real-time imaging with perfusion mapping.	Lacks the resolution required for microvessel morphological analyses.
Deegan, 2019; Thilo Gambichler et al., 2011; Swanson et al., 2020b; Welzel, 2001	Optical Coherence Tomography (OCT) - Doppler OCT - OCT Angiography (OCTA)								Rapid; real time; high penetration depth; resolution comparable with histology. Doppler OCT has high sensitivity. OCTA allows capillary-level resolution.	Expensive; no cellular and subcellular details visible; post-processing required; susceptible to motion artefact. Doppler OCT is susceptible to operator-dependent variations.
Logger, 2020	pH-metry								Easy to use; rapid.	Small skin areas measured; questionable reliability due to short a measurement time.
Swanson, 2020b	Photoacoustic Imaging								Highly sensitive.	Questionable utility due to size and usability of physical prototype system; long acquisition time.
Logger, 2020; Yafeng Ma et al., 2020; Rodijk et al., 2016	Reflectance Confocal Microscopy								Real-time; resolution comparable with histology.	Expensive; limited penetration depth; training needed for image interpretation; susceptible to motion artefacts.
Piérard, 1998; Piet E. J. van Erp, 2018	Reflectance Spectrophotometry								Easy to use; small- sized probes for measurement in recessed body parts; inexpensive.	Influenced by environment; no information on extent of erythema or on perceived skin colour.
Logger, 2020; Piet E. J. van Erp, 2018	Sebumetry								Easy to use; inexpensive.	Influenced by intrinsic and extrinsic factors.
Deegan, 2019	Spatial Frequency Domain Imaging (SFDI)								Simultaneous superficial structural imaging and perfusion.	Long acquisition time; sensitive to ambient light.
Kleesz, 2011; Seidenari, 1998; Piet E. J. van Erp, 2018	Transepidermal Water Loss (TEWL)								Easy to use; inexpensive.	Indirect measurement; climate-controlled environment needed.
Richters, 2015; Piet E. J. van Erp, 2018	Tristimulus Colorimetry								Easy to use; small/ medium- sized probes for measurement in recessed body parts; inexpensive.	Influenced by environment; no information on extent of erythema or on molecular origin of skin colour.
Agner, 1989; Deegan, 2019	Ultrasonography (US) - Doppler Sonography (Colour Doppler)								Real-time; widely available; clear visualization of dermis and subcutis. Doppler Sonography provides vascular and perfusion information.	Training needed; low resolution; no visualization of epidermis. Doppler sonography is susceptible to aliasing.

2.3.9 Discussion

The above sections detail skin parameters that have been investigated with reference to the aetiology of enhanced skin sensitivity. They highlight that “Sensitive Skin” represents a multifactorial issue, which despite attempts by both researchers and clinicians is difficult to define objectively. There are a number of commercially available biophysical methods with the potential to quantify skin parameters (Antonov et al. 2016; Bader and Worsley 2018), only a few have been associated with the assessment of SS. Indeed most studies which have evaluated these tools have employed able-bodied cohorts and have not addressed the predefined characteristics of SS (Farage and Maibach 2010). Furthermore, studies on SS has been largely undertaken within the cosmetic industry, and often unreported, with an emphasis on chemical products designed to elicit a specific tissue response (Seidenari et al. 1998; Sun et al. 2016; Balsam and E. 2009). It is evident, however, that interest in the topic also encompasses the medical and consumer devices due to its implications in identifying individuals at higher risk of compromising skin integrity. For example, the physical interaction of a therapeutic or diagnostic device with skin tissue. This review also highlights the importance of comparing the skin response to mechanical loading in cohorts of individuals with and without SS. In the few such studies, the integrity of the SC and its effective barrier function appears to be closely associated with SS (Seidenari et al. 1998). This was evident with parameters derived from a range of techniques, including TEWL, SC hydration, SC thickness, layer adhesion, erythema, inflammation, and surface temperature. Further research exploring the relationship between such parameters would help quantify inter-subject differences within distinct cohorts with varying degrees of skin sensitivity.

According to some researchers, the skin can be considered as sensitive when its integrity is compromised and its primary function of protecting the body from external insults is affected (Proksch et al. 2008). Following this logic, researchers have attempted to quantify the barrier function by evaluating the anatomy and physiology linked with the epidermis. Structurally, at baseline, skin tissue of individuals reporting enhanced sensitivity has been associated with a thinner stratum corneum, reduced number of corneocytes, increased nerve fibre density, and a higher number of sweat glands (Berardesca et al. 1991; Chan 2018; Farage 2019). Functionally, it has been associated with an increased penetration of water-soluble chemicals, heightened inflammatory or vascular responsiveness, decreased hydration, decreased alkali resistance and less sebum production (Roussaki-Schulze et al. 2005; Farage and Maibach 2010; Inamadar and Palit 2013; Falcone et al. 2017; Guerra-Tapia 2019). This review presents a table of biophysical and imaging measurement techniques available for characterization of such skin parameters ([Table 2.1](#)). Some of these techniques quantify only one specific skin parameter. For example, TEWL measurements

result in the flux density of water vapour across the SC in $\text{g/m}^2\text{h}$ and laser Doppler velocimetry quantifies the microcirculation through small blood vessels in arbitrary units. These techniques are widely popular and offer advantages for clinical use, although their use in isolation could limit the understanding of both structural and physiological changes to skin following mechanical insults.

With respect to the multifactorial nature of SS, a multimodal measurement method is required to identify the range of features in a robust manner present at different skin depths, which characterise the symptoms associated with SS. Use of existing tools provide both advantages and disadvantages. For example, popular clinical tools such as dermoscopy provide detailed information of the skin structure and highlight the presence of erythema, although the inevitable differences in interpretations between clinician's results in poor reliability. By contrast, Confocal Raman Spectroscopy is highly specific in identifying structural skin characteristics and has been associated with quantifying SC hydration. However, the equipment cost and requirement of trained personnel for interpretation of results limits its widespread use in clinical practice. Other imaging modalities such as ultrasonography provide an increased imaging depth, thus allowing visualization of the subsurface dermal and subcutaneous layers, and the underlying blood perfusion patterns. This has enabled identification of oedema and related pathologies. However, individual imaging modalities are optimised at different resolutions and penetration depths, as indicated in [Figure 2.2](#), offering advantages to each for *in vivo* imaging depending on the depth of penetration required for the skin and subdermal tissue assessment.

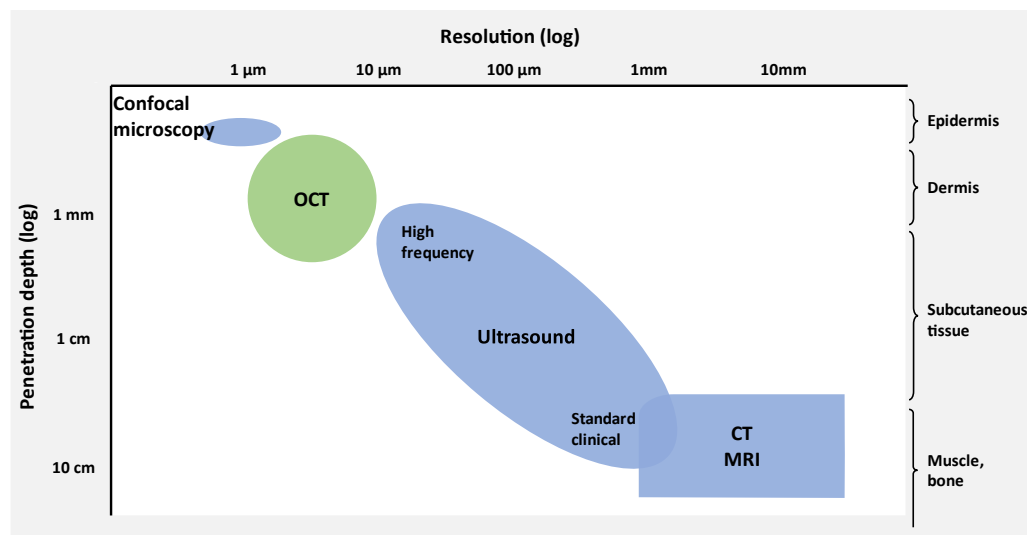


Figure 2.2 The relationship between resolution and penetration depth for different skin imaging modalities. Adapted from “Handbook of Optical Coherence Tomography”, 2001 (“Handbook of Optical Coherence Tomography,” 2001).

The review identifies Optical Coherence Tomography (OCT) as a potential tool for assessing a range of structural and physiological skin parameters. This non-invasive technique has gained popularity in clinical research in ophthalmology and cardiology, which requirements match OCT's inherent resolution and depth of penetration (Figure 2.2), and in dermatology where it has been used to differentiate between different skin pathologies (Welzel 2001; Thilo et al. 2011; Olsen et al. 2018). Indeed, its examination of skin anatomy as well as local physiology, including blood perfusion, make it an ideal candidate to provide a robust means to objectively assess skin health in both unloaded and loaded states (Deegan and Wang 2019; Swanson et al. 2020; Maiti et al. 2020). Appropriate algorithms have been developed to process OCT data to extract information, such as skin layer thickness, roughness, and local tissue stiffness (Josse et al. 2011; Hu et al. 2016; Maiti et al. 2016; Taghavikhalilbad et al. 2017; Askaruly et al. 2019; Maiti et al. 2020) and to quantify vasculature, blood perfusion, and erythema (Welzel et al. 2004; Wang et al. 2015; Swanson et al. 2020). OCT has been shown to detect physiological changes in a variety of skin conditions such as contact dermatitis, psoriasis, and scleroderma (Abignano et al. 2013; Welzel et al. 2003; Welzel et al. 2004), linking the parametric output of this technique with clinical applications in dermatology. However, the resolution of OCT is limited in terms of its potential to visualise cellular details and differentiate between microvessels. Moreover, this technique does not provide information regarding SC hydration, pH levels, sebum content, or temperature of skin, each of which have been highlighted as important parameters in detecting changes in skin health status. Furthermore, motion artefacts associated with OCT imaging, require post processing for noise reduction. Nevertheless, with its functional modifications involving Doppler imaging (Jiang et al. 2020), angiographic spectroscopy (Wang et al. 2015; Zaveri 2016), and Elastography (Kennedy et al. 2011; Wang and Larin 2016), OCT offers potential for promising applications in research and clinical practice.

There is also emerging evidence regarding the role of non-invasive collection and analysis of selected biomarkers as an early identification of skin inflammation and metabolic compromise. For example, production of signalling molecules, such as cytokines, are known to be triggered during inflammatory processes. These proteins can be obtained from biofluids such as sebum, which can be collected using commercially available absorbent tapes (Sebutapes). Several researchers have reported a significant upregulation in the level of cytokines following various loading procedures (Bronneberg et al. 2007; De Wert et al. 2015; Bostan et al. 2019; Soetens et al. 2019). Others have shown similar results after treating the skin with chemical irritants (Ulfgren et al. 2000; de Jongh et al. 2007). For example, one study analysed the cytokines obtained from sampling sebum in skin sites treated with irritants, such as sodium lauryl sulphate. Even in the absence of visible erythema, they reported an upregulation of these molecules, stating possibilities of identifying at-risk patients (Perkins et al. 2001). Studies exploring characteristics of sensitive skin have reported differences in

post-insult biochemistry of SS individuals as compared to non-SS individuals (Richters et al. 2016; Raj et al. 2017; Yatagai et al. 2018). Developing our understanding of how different biomarkers are expressed in sensitive skin and their subsequent upregulation to mechanical loading could provide critical insight into the management of this clinical issue.

The combination of multimodal imaging techniques e.g., OCT, biophysical measures of SC function, and biomarkers of skin health could provide the array of parameters critical in unlocking our understanding of skin sensitivity and its associations with mechanical loading. Consequently, prospective studies could be designed to include evaluations of both perceived and measured skin symptoms, establishing differences in sensitivity before, during, and after mechanical insults. The results of such studies would allow for quantification of differences between cohorts who have differing perceptions of skin sensitivity with respect to a specified stimulus, further allowing researchers to define SS indicators. With improved understanding, personalised solutions could be adopted e.g., medical devices or shavers, to accommodate the needs of varying skin types and sensitivities.

2.4 Secondary Analysis of Biophysical Data in a SS/NSS cohort

To inform a new protocol, biophysical skin responses linked with self-assessed skin sensitivity were analysed from an established database (Richters et al. 2016). In their study, SS and non-SS (NSS) groups were assigned via a “Q-score” obtained from a novel self-assessment questionnaire covering the occurrence and extent of tissue responses following different stimuli interactions (Richters et al. 2017). The *in vivo* biophysical measurements included redness, TEWL, and SC hydration (SCH).

The authors reported no significant differences in median baseline values of the biophysical parameters for the SS and NSS groups (Figure 2.3). Following tape stripping to mechanically stimulate the skin, they reported that the number of tapes required to completely remove the SC was significantly lower in the SS group than that of the NSS group (Table 2.2), while the thickness of the SC was comparable. The authors also reported that maximum values for redness and SCH were reached at 30 minutes after stimulus, and for TEWL at either 30 minutes or 8 hours after stimulus. Also, erythema responses peaked at either 30 minutes or 8 hours after stimulus.

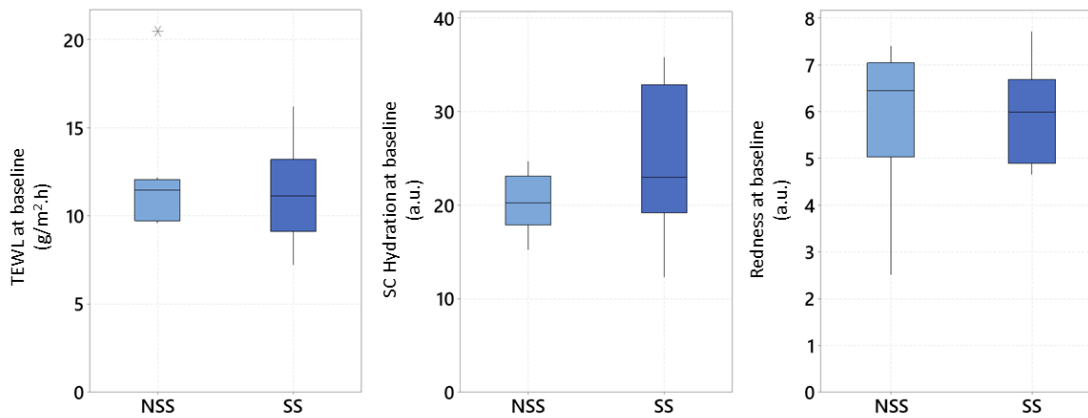


Figure 2.3 Comparison of biophysical values at baseline for SS and NSS groups. Adapted from (Richters et al. 2016).

The aim of the secondary analysis is to critically evaluate trends in biophysical parameters for SS and NSS individuals following a standard mechanical load (i.e., biophysical responses per tape strip). This approach differs from that by Richters et al., where the mechanical load differed between participants based on the total number of tape strips needed to remove the SC entirely. Thus, this research reanalysed the data¹ with the following objectives:

- Identify the optimal time frame for biophysical measurements of the tissue response linked to normalized stimulus rather than the absolute stimulus; and
- Identify possible new patterns in normalised biophysical responses with respect to Q-scores of skin sensitivity.

2.4.1 Methods

In the original study, 16 participants were selected based on criteria including Q-scores, Fitz-Patrick skin type (either type 2 or type 3), and to exclude participants with any skin disease. Thereafter, the groups with SS and NSS skin were matched for gender. Mechanical stimulation was performed using sequential tape stripping on the upper side of the intergluteal cleft and stopped when the skin became homogeneously refulgent. As such, the number of tapes used per participant varied.

As we are interested in a standardized mechanical load, we normalised the skin responses with respect to the number of tapes, as follows:

¹ Courtesy of Dr. Piet van Erp, Radboud University, The Netherlands.

$$\text{Normalized value} = \frac{\text{Value}}{\text{\#tape strips}} \quad (\text{Equation 2.1})$$

Furthermore, the normalised biophysical responses were adjusted by subtracting the baseline values as follows:

$$\Delta \text{ Response} = \text{Normalised value} - \frac{\text{Baseline value}}{\text{\#tape strips}} \quad (\text{Equation 2.2})$$

The data were non-normally distributed and boxplots of the Δ Response were plotted for the NSS and SS groups. Differences in the groups were evaluated for statistical significance using the Mann Whitney U test. Correlations of Δ TEWL, Δ SCH, Δ Redness values with respect to the Q-score were determined at each time point. Correlations were determined through Spearman's Rank tests.

2.4.2 Results

Details of the participants from the dataset are summarised in [Table 2.2](#). This includes the participant ID, demographic details (gender, age, Fitz-Patrick skin type), self-assessed responses of dryness on face and body, calculated Q-score and subsequent SS/NSS label, and number of tape strips used during the study.

Table 2.2 Participant details from Retrospective Analysis dataset in ascending order of the number of tape strips.

ID	Gender	Age	Skin type	Dry Face	Dry Body	Q-Score	SS / NSS	Number of tape strips
118	Female	28	2	Normal	Dry	126	SS	17
15	Female	20	2	Normal	Normal	175	SS	18
49	Male	21	2	Combined	Normal	68	SS	22
78	Male	24	2	Combined	Combined	103	SS	24
122	Female	20	3	Combined	Dry	219	SS	25
7	Female	24	3	Normal	Normal	43	NSS	25
23	Male	19	3	Normal	Normal	37	NSS	26
106	Female	24	2	Dry	Dry	363	SS	26
34	Female	20	2	Combined	Normal	44	NSS	27
82	Male	21	2	Oily	Normal	98	SS	31
109	Male	24	2	Combined	Dry	204	SS	33
18	Male	20	3	Normal	Normal	32	NSS	36
65	Female	22	3	Dry	Normal	11	NSS	37
44	Male	21	2	Combined	Normal	30	NSS	49
22	Male	19	3	Dry	Normal	13	NSS	52
25	Female	19	3	Combined	Normal	12	NSS	58

Results of the normalized biophysical parameters are shown in [Figure 2.4](#). It is noted that for each parameter there was a high degree of variability in the response post-tape stripping, as observed by the quartile and range values. The $\Delta TEWL$ ([Figure 2.4a](#)) increased from basal values at 30 minutes post-tape stripping for both the NSS and SS groups and remained elevated at up to 24 hours. However, the SS group revealed higher values at $t=30$ min, $t=8$ hrs, and $t=24$ hrs ($p<0.05$). A partial recovery relative to baseline was observed at 72 hours post-tape stripping for both SS and NSS groups ([Figure 2.4a](#)).

By contrast, ΔSCH ([Figure 2.4b](#)) provided limited differentiation between SS and NSS groups. Temporal trends in SC hydration post-tape stripping revealed that for both groups there was an increase in values at 30 minutes. This response then declined at 8 and 24 hours, where values returned to basal (median ΔSCH at 24 hours = 0.14, for NSS and SS groups). It is of note that at 72 hours post-tape stripping both NSS and SS groups had negative values i.e., ΔSCH values were lower than baseline. This was most pronounced in the SS group with a value of -0.74 (interquartile range -1.21 to -0.62) such that the SS and NSS group medians were statistically different ($p<0.05$).

$\Delta Redness$ ([Figure 2.4c](#)) had high degree of variability in the values post-tape stripping. Some differences in the median $\Delta Redness$ between SS and NSS groups were observed at 8 and 24 hours post-tape stripping ($p>0.05$). $\Delta Redness$ remained elevated throughout the test period, with only a partial recovery noted at 72 hours.

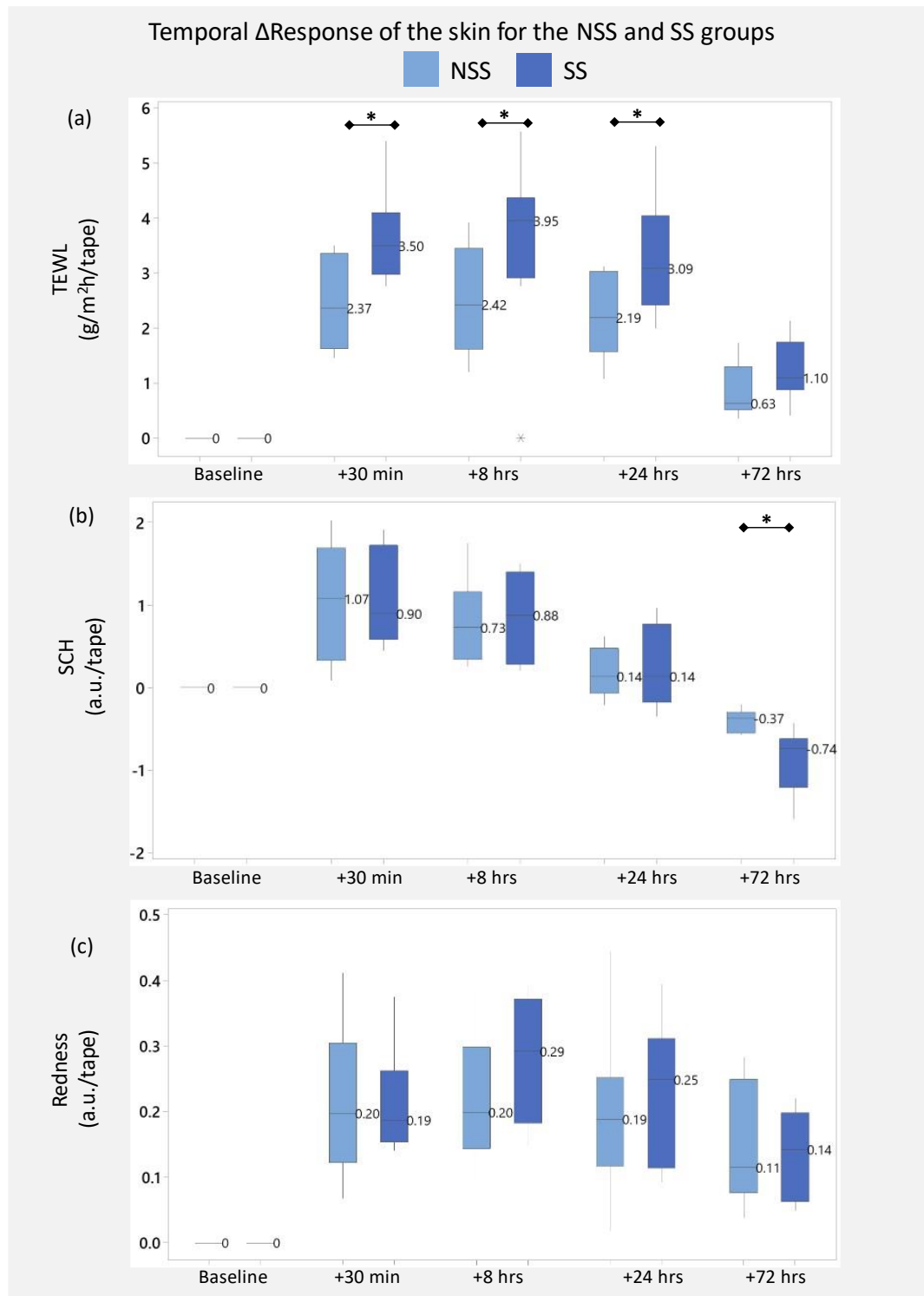


Figure 2.4 Temporal Δ Response of the skin for the SS and NSS groups for (a) TEWL, (b) SC Hydration, and (c) Redness.

The analysis illustrated in [Figure 2.4](#) does not consider possible clusters within the groups, i.e., in following the approach by Richters et al. and clustering them into NSS and SS groups based on Q-score, more subtle relations between the Q-score and biophysical response might have been overlooked. Accordingly, the separate responses for each of the biophysical parameter could be analysed and presented against the individual Q-scores in ranked order, as presented in [Figure 2.5](#).

From [Figure 2.5a](#), it is evident that for 75% (n=6/8) of the NSS group at 72 hours the normalised TEWL values are similar to those observed at baseline. Within this NSS cohort, those with a Q-score >30 revealed an elevated Δ TEWL response (2-4 g/m²/hr/TS) compared to those with Q-score <30 (1-2 g/m²/hr/TS), with the values elevated from basal up till 8 hours post-tape stripping. Indeed, there were consistent changes within each individual for Δ TEWL at 30-minute, 8-hour, and 24-hour (values 1.45-5.40 g/m²/hr/TS, 1.20-5.57 g/m²/hr/TS, 1.08-5.30 g/m²/hr/TS, respectively). For the SS cohort, there was variability in the magnitude of the Δ TEWL between individuals, with increases observed in all participants between 30 minutes to 24 hours post-tape stripping. The relative difference in Δ TEWL between SS participant did not appear to correlate with the corresponding Q-score.

The Δ SCH demonstrated a high degree of variability between participants of both NSS and SS groups ([Figure 2.5b](#)). In addition, there was a clear temporal trend with Δ SCH highest at 30 minutes post-tape stripping and corresponding decreases at 8, 24, and 72 hours. In the latter case, the values reach baseline at 24 hours and negative values at 72 hours, indicative of skin drying effect. As with the Δ TEWL, the magnitude of Δ SCH did not correspond with the Q-score.

Similar to Δ TEWL, for the Δ Redness within the NSS cohort ([Figure 2.5c](#)), those with a Q-score >30 revealed an elevated value as compared to those with Q-score <30, with values continuing to be elevated in most participants up to 24 hours post-tape stripping.

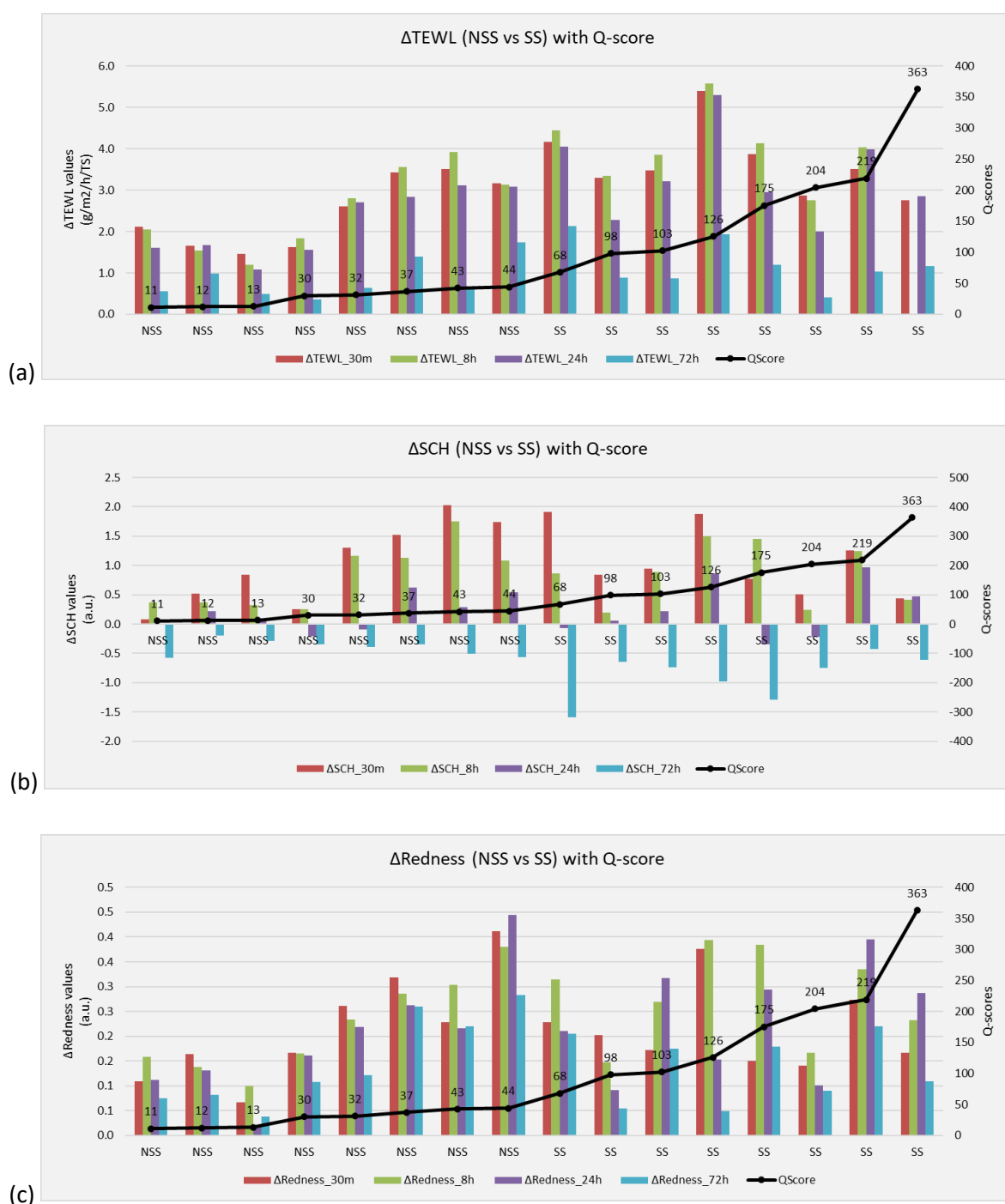


Figure 2.5 Δ Response with individual Q-scores for (a) TEWL, (b) SC Hydration, and (c) Redness. The Q-score is plotted on the second Y axis.

For all the biophysical parameters at 30 minutes post-tape stripping it was observed that below a Q-score of approximately 100, the values of the Δ Response increased monotonically. This is evidenced by the significant correlations for the NSS group and positive correlation coefficients (Figure 2.6). For values >100 , representing SS individuals, there was a less apparent trend, with most values decreasing with a higher level of variability (no significant trends). By contrast, the

Chapter 2

associations between Q-score and the Δ Response at 72 hours was limited, with redness being the only significant parameter. It is of note that TEWL and redness demonstrated similar trends between Q-scores and Δ Response, such that for both parameters the lower Q-scores (0-100) revealed a positive association while the higher Q-scores (>100) revealed a negative association. There may have been a ceiling effect on these associations whereby the range of the values at 72 hours was less than that observed at 30 minutes.

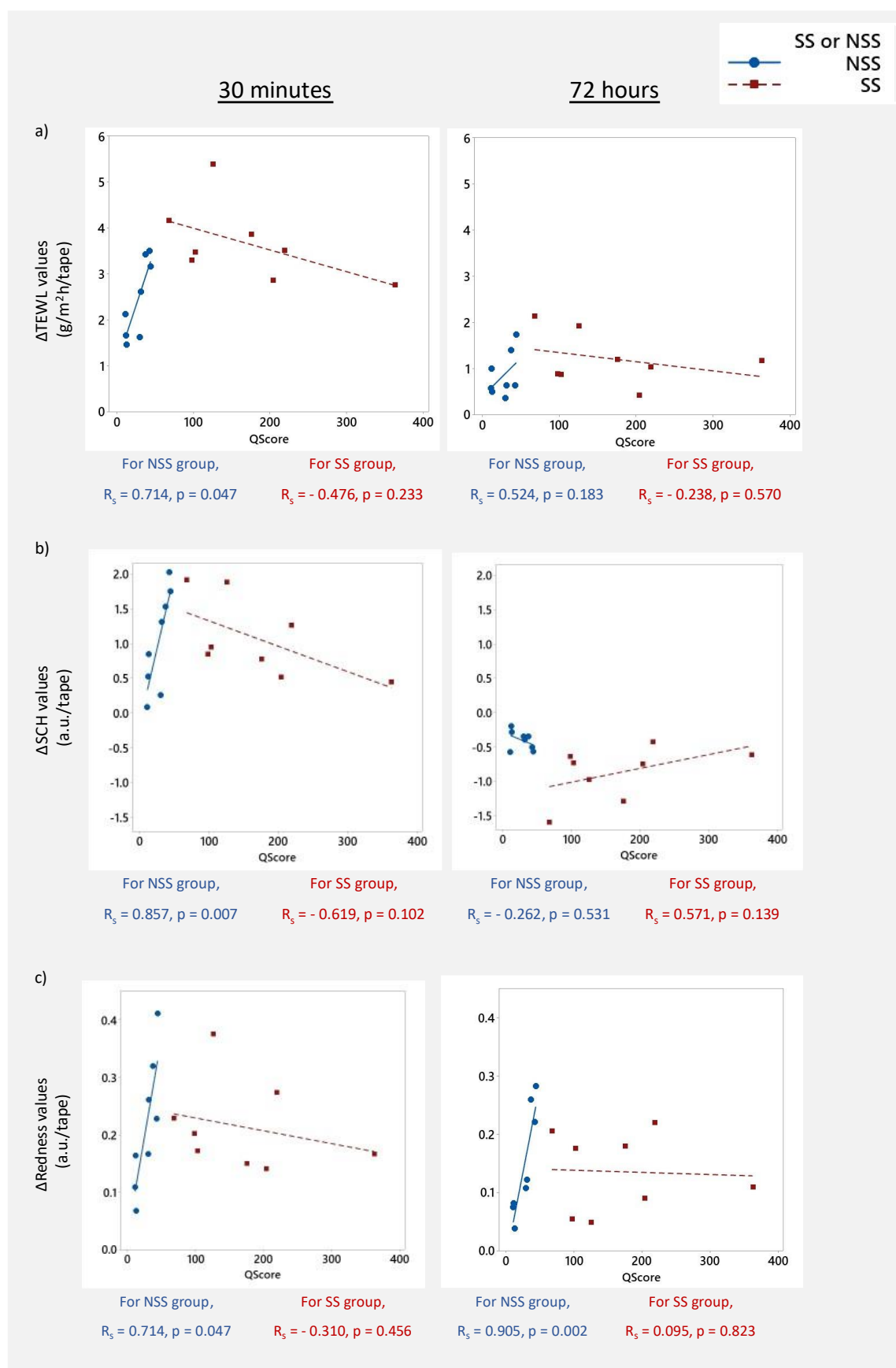


Figure 2.6 Scatterplots at 30 minutes and 72 hours for (a) TEWL, (b) SC Hydration, and (c) Redness with R_s and p values from the Spearman Correlation test.

2.4.3 Discussion

Retrospective analysis was conducted using the dataset published by Richters (Richters et al. 2016) where the effects of tape stripping from 30 minutes up to 72 hours after stimulus interaction were studied. Temporal changes for each of the Δ Response were reported. It is evident that with tape stripping the trends for both, sensitivity groups and each parameter, are similar with a significant increase in Δ Response at 30 minutes and 8 hours, and a subsequent decrease thereafter. Indeed, Δ SCH returns to baseline value by 24 hours, whereas Δ TEWL and Δ Redness remain elevated at 72 hours. It is also noted that Δ SCH was lower than baseline at 72 hours, implying a general drying out of the skin at this time following tape stripping. When comparing data between the sensitivity groups, the SS group demonstrated higher values for Δ TEWL and Δ SCH compared to the values associated with the NSS group (Figure 2.4 a, b). By contrast, elevated values for Δ Redness were only evident in the SS group at 8 hours and 24 hours, respectively (Figure 2.4c). Close examination revealed that the differences between groups for each of the three parameters at consecutive time intervals for Δ TEWL and Δ Redness were most marked at 8 hours following tape stripping.

Tape stripping is a well-recognized method when investigating skin responses due to, amongst others, mechanical stimulus (Lademann et al. 2009; Surber et al. 2001). Indeed, it has been utilised in few studies aiming to quantify the differences in SS and non-SS individuals (Seidenari et al. 1998; Ota 2002), including the original study referred to in this chapter. Additionally, it has also been used for characterising facial skin parameters (Gorcea et al. 2013), which is the anatomical region of interest in the present research. Furthermore, tape stripping has been compared to shaving in terms of the biophysical response of the skin tissue (Rodijk et al. 2016), where between 8-12 tapes appeared to be a suitable model to mimic the mechanical impact of shaving for roughly 30 seconds. This comparison was critical in receiving approval from the ethics committee for introducing tape stripping on facial skin of consumers for future studies.

Changes in skin parameters at 30 minutes appear to be indicative of the 24-hour response, with recovery only observed in the 72-hour time point. As such, a shorter protocol including up to 30 minutes time-point is sufficient to evaluate the skin response. However, as the earliest time point was 30 minutes post-stimulus, the immediate effect within 30 minutes of tape stripping on biophysical parameters remains to be explored. Moreover, for discriminating SS from NSS, Richters developed the Q-score, but the level of detail underlying the questionnaire (total 32 questions with 8 general questions, and 4 specific questions on 6 stimuli each) poses at least two major practical difficulties when applied outside the clinical realm to generate new data: they demand perseverance of the study subject, hampering a sufficiently high response rate needed for screening; and more importantly, they involve clinically sensitive information, or information

otherwise restricted by GDPR. As an alternative, to be used in the prospective study, a short version of the questionnaire was developed ([Appendix A](#)) for a consumer-friendly environment, consisting of the 4 non-medical questions that best predicted the categorisation into NSS and SS by the Q-score. However, future analysis remains to be conducted to establish the correlation between the biophysical values and combinations thereof with respect to the Q-score to find experimental proof for the response curves as conceptualised in [Figure 1.3](#).

2.5 Aims and Objectives

Following the review of the current state of the art and relevant data sets of individuals with and without SS, the subsequent research aims and objectives were defined for the PhD. It is noted that OCT imaging is particularly included in the project given the availability of a system at the facility and it's aforementioned potential in dermatological applications.

Aim 1: Investigate the use of robust objective parameters from OCT and biophysical approaches to evaluate the status of skin pre- and post-mechanical insult.

Objectives:

- 1.a) Evaluate trends in biophysical parameters from retrospective data taken from individuals with sensitive skin following mechanical insults.
- 1.b) Evaluate feasibility of OCT imaging in key skin sites to monitor skin status.
- 1.c) Optimise OCT image processing techniques to extract skin parameters indicative of mechanically induced changes in integrity.

Aim 2: Study the link between perceived skin sensitivity and the variability of skin response to simple mechanical loading using objective skin parameters.

Objectives:

- 2.a) Develop a means to apply simple mechanical load to the skin of the face and neck.
- 2.b) Recruit volunteers with varying degrees of SS to study the relationship between parameters contributing to skin sensitivity (e.g., layer thickness and local physiology).
- 2.c) Employ a range of non-invasive approaches (including OCT imaging and biophysical measurements) to assess the skin status pre- and post-mechanical insult.
- 2.d) Examine the long-term effects of singular and repetitive mechanical loading.
- 2.e) Explore correlations between perceived and objectively defined skin parameters following mechanical insults.

Aim 3: Study the influence of perceived skin sensitivity and the variability of skin response to complex mechanical loading using objective skin parameters.

Objectives:

- 3.a) Develop a means to apply complex mechanical load to the cheek and neck skin using a shaving handle integrated with force sensors.
- 3.b) Recruit volunteers with varying degrees of SS to study the relationship between parameters contributing to skin sensitivity (e.g., skin layer stiffness and local physiology).

- 3.c) Use an optimal set of non-invasive approaches including OCT, biophysical and biomarkers to assess skin status pre- and post-complex mechanical loading.
- 3.d) Examine the relationships between complex loads (magnitude and duration of loading) and the skin's response using the pre-defined skin parameters.
- 3.e) Explore the correlations between perceived and objectively defined skin parameters following mechanical insults.

Aim 4: Inform device design for optimal skin-device interaction, addressing personalized solutions.

Objectives:

- 4.a) Develop temporal profiles of skin responses and adaptability to mechanical loading.
- 4.b) Employ analytical techniques to predict levels of skin sensitivity in individuals (at a specified site, with a specified load).
- 4.c) Suggest guidelines for optimal personalized skin-device interaction.

Chapter 3 Protocol Development for quantifying skin sensitivity using OCT

The investigation of skin sensitivity has been hindered by a lack of consensus as to the objective definitions of stimuli as well as the overall skin response ([Chapter 2](#)). This was addressed in the present study by adopting an array of subjective and objective parameters of skin integrity. These included biophysical, biomarker, and imaging tools to investigate the effects of distinct mechanical stimuli, in the form of tape stripping, friction, and electric shaving. It was proposed to examine the changes in skin structure at relevant body sites e.g., cheek and neck. Changes were monitored using Optical Coherence Tomography (OCT), which required the development of a protocol to analyse its feasibility.

Several studies have reported the differences in skin morphology at different anatomical locations (Gambichler et al. 2006; Mogensen et al. 2008; Tsugita et al. 2013; Maiti et al. 2020; Monnier et al. 2020). While many of these studies have reported data for the cheek, data for the neck is scarce. As such, the general aim of the present research is to extract a series of parameters derived from OCT images that quantify the unloaded skin and the changes following mechanical loading. Specifically, the aim is to establish the value of these parameters in delineating sensitivity between individuals, as well as characterising differences between cheek and neck within individuals.

Objectives:

- Establish a protocol to acquire OCT skin images of the cheek and neck.
- Develop processing algorithms to extract relevant parameters for characterising the skin.
- Explore the feasibility of these parameters to differentiate between and within individuals.

3.1 Experimental setup

Preliminary experiments were conducted with the Thorlabs Telesto Spectral Domain OCT system (TEL221, imaging depth 1.5 mm, axial resolution 5.5 μm , centre wavelength 930nm) at the Phillips Laboratories in Drachten, The Netherlands. The system had been previously set up for imaging the forearm, with the camera mounted onto a robotic arm and facing vertically downwards ([Figure 3.1](#)). To prepare the system for facial imaging, accessories were conceptualized, and 3D printed to change the orientation of the camera probe.

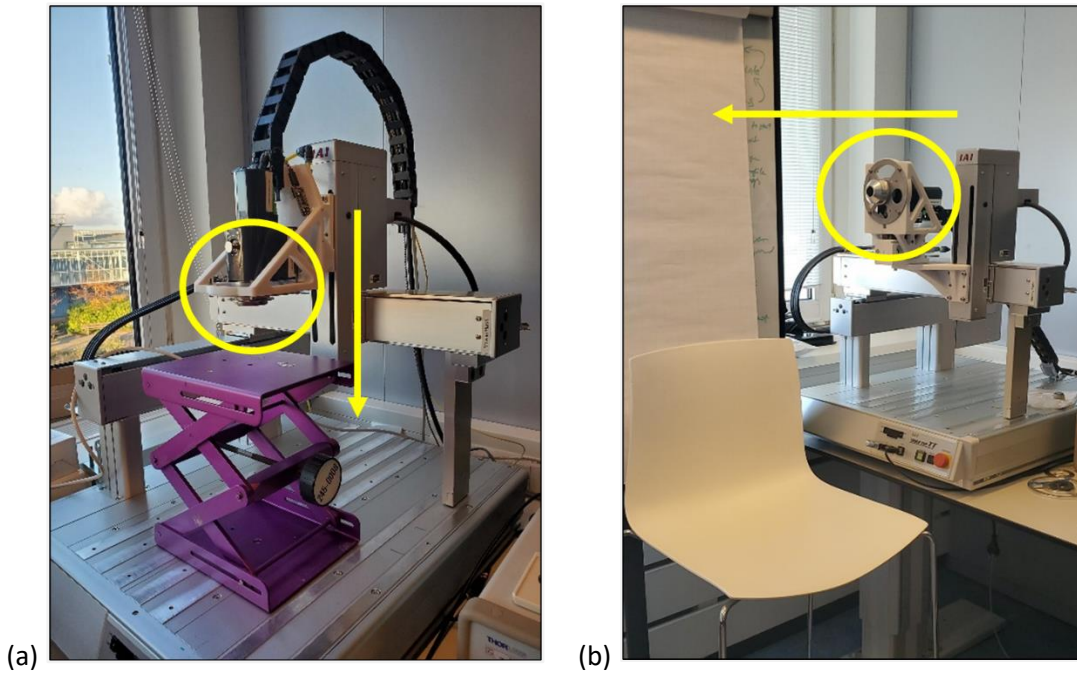


Figure 3.1 OCT system with different camera orientations. (a) Camera positioned vertically for forearm imaging; (b) camera position horizontally for facial imaging.

Furthermore, accessories were developed in-house so that the skin was in focus during image acquisition. The mount shown in [Figure 3.2a](#) was already available with the equipment. However, it was observed that due to flexibility of the facial tissue on the cheek, the skin would protrude into this mount causing a doming effect. Accordingly, a solution was needed to maintain contact pressure with the camera mount, thereby reducing motion artefacts while avoiding local pressure peaks resulting in excessive skin protrusion through the aperture. To mitigate the protrusion effect, a mount with a larger aperture was preferred to lower the contact pressure and capture images further away from any unnatural boundary condition imposed by it. Thus, a new mount was designed, and 3D printed ([Figure 3.2b](#)). Although, this newly developed prototype was suitable for imaging the cheek, it was found to be unsuitable on the neck as the large aperture was not stable due to the neck curvature. A compromise was reached where the two separate accessories were selected for imaging the cheek and neck using OCT. Thus, the participant could be seated with their cheek/neck resting against the camera, as indicated in [Figure 3.3](#).

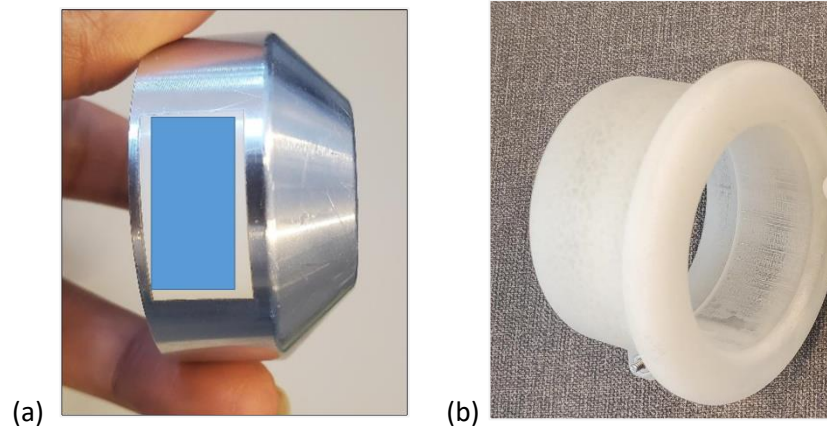


Figure 3.2 Accessories to maintain the required focal distance for facial OCT imaging. (a) Mount with smaller aperture used for the neck; (b) Mount with larger aperture used for the cheek.

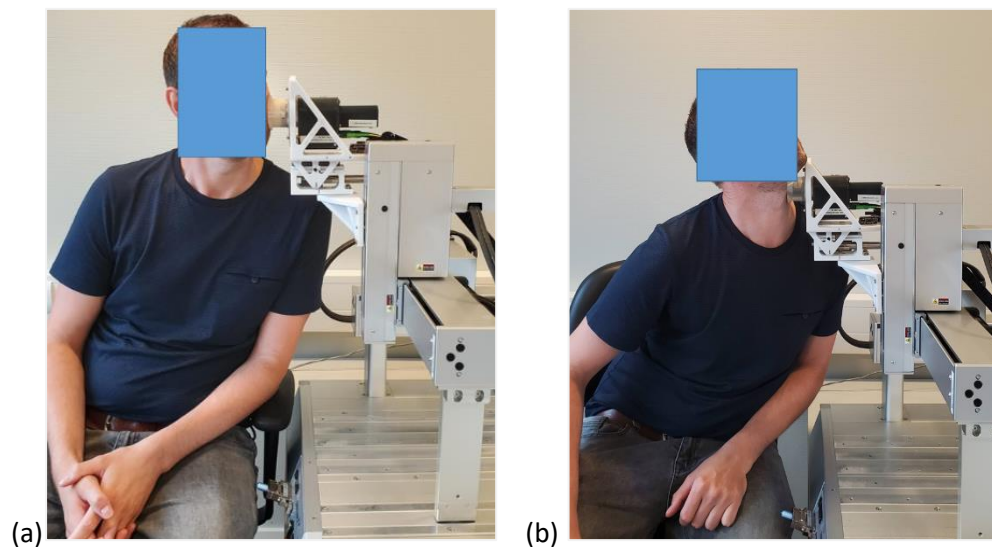


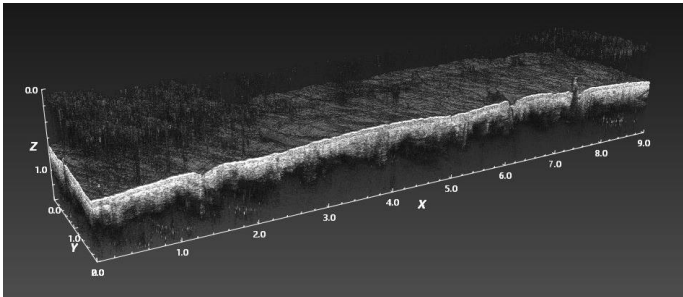
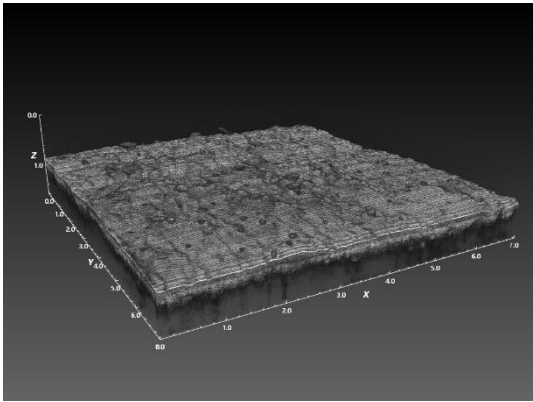
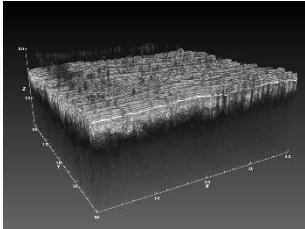
Figure 3.3 Typical position of a participant when imaging the (a) cheek and (b) neck, using the OCT system.

Furthermore, the OCT system included an associated software, ThorImage (version 5.4.2), where scanning parameters could be prescribed. Different combinations of pixel sizes and field of views (FOV) were tested to select suitable balance between image quality and acquisition times, as illustrated in

Table 3.1. A preferably large field of view and/or high resolution yielded long acquisition times, that increased risks of motion artefacts in the scans. Initially, a combination of $10 \times 6 \mu\text{m}$ pixel size and $9 \times 2 \text{ mm}$ FOV was selected as this rendered an acquisition time of 12 seconds. The results from these scans are included in this chapter. As participants were comfortable to hold a stable position for up to 20 seconds, ultimately $6 \times 6 \mu\text{m}$ pixel size and $4 \times 4 \text{ mm}$ FOV was used for future studies.

Nonetheless, particularly while taking sequential B-scans in the neck, motion artifacts due to heart beats were present.

Table 3.1 OCT scan pattern and image acquisition times tested.

Pixel Size, Field of View	Acquisition time	Example 3D-OCT Scan
10 x 6 μm , 9 x 2 mm	12 seconds	
6 x 6 μm , 7 x 7 mm	56 seconds	
6 x 6 μm , 4 x 4 mm	20 seconds	

3.2 OCT parameters to assess skin structure and morphology

OCT uses infrared light to create a grey-value reflection intensity profile across the depth of a tissue (Welzel 2001; Thilo et al. 2011; Deegan and Wang 2019), expressed in a logarithmic scale. By projecting the light beam in a plane perpendicular to the skin, a 3D depth profile of the skin is obtained. Typically, there is a fast and a slow axis in the scanning plane. The reflection profiles, or A-lines, acquired along the fast axis form a B-scan (2D-image), and a stack of B-scans along the slow axis forms the 3D depth profile. A schematic of an *in vivo* 3D-OCT scan of the cheek with B-scans and A-lines is shown in Figure 3.4.

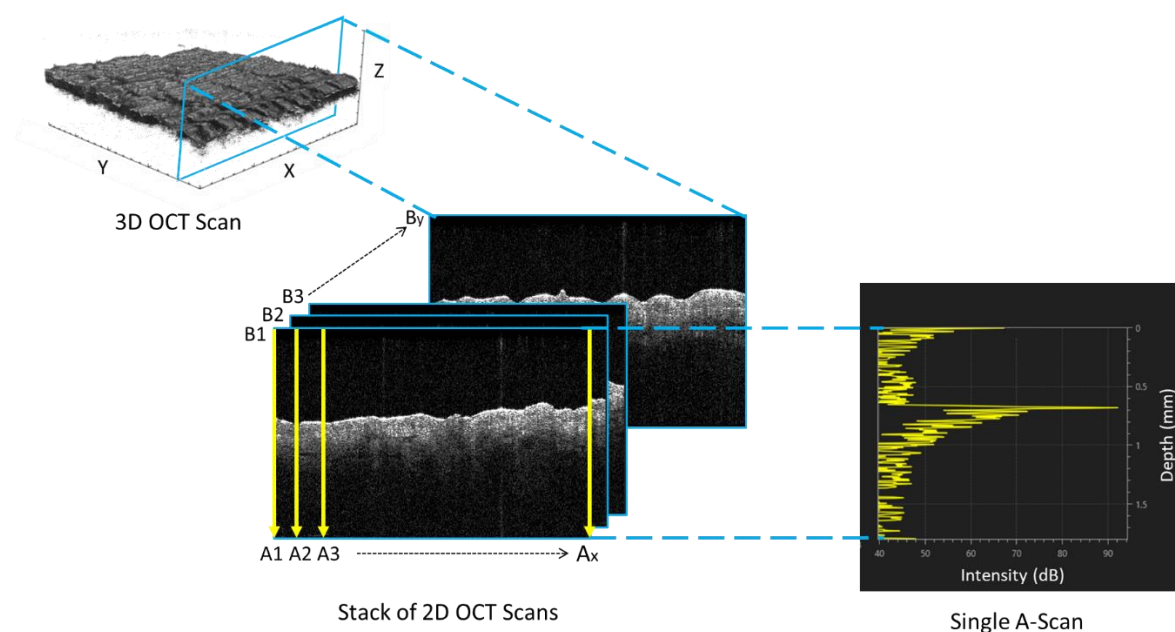


Figure 3.4 Schematic of a 3D-OCT Scan with a stack of exemplar B-scans and a single A-scan.

It is noted that individual A-scans contains considerable noise and do not represent the entire 2D or 3D stack. Consequently, averaging is needed before reliable parameters can be extracted. Thus, averaged A-scans can be generated for each 2D-OCT image, which can be further averaged along the Y-direction to generate an average A-scan representing the entire 3D-OCT scan (Figure 3.5). The “Averaged A-scan” of the 3D-OCT scans is further used to estimate skin parameters as discussed in the following paragraphs.

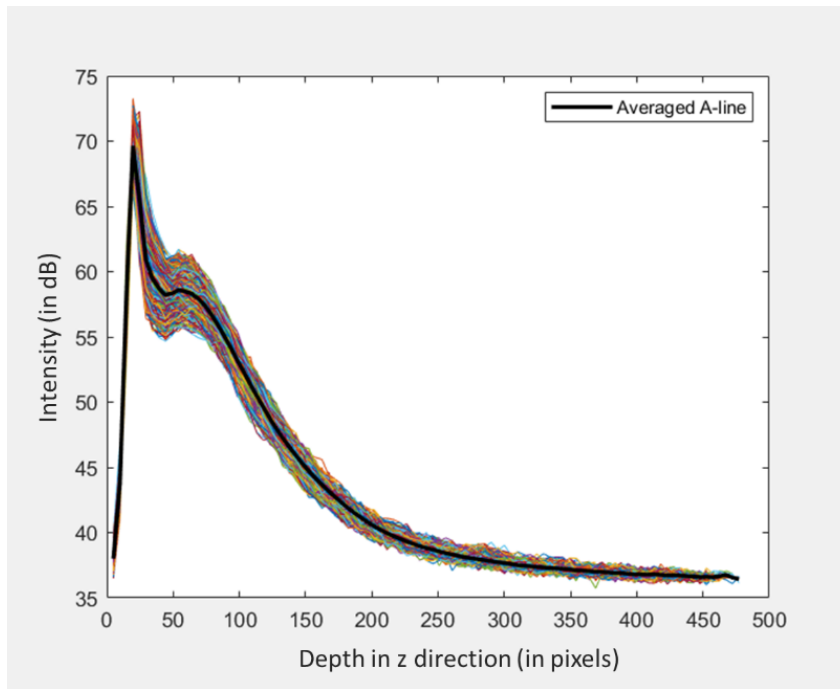


Figure 3.5 Example of a 3D-OCT Averaged A-scan, representing the depth of the signal penetration on the x-axis and the Intensity of the signal on the y-axis. Each of the thin coloured lines represents the average of the A-scan in a single B-scan, i.e., 2D averaged A-scan. The 3D averaged A-scan (thick black line) is the average of the 2D averaged A-scans.

In Figure 3.6, a B-scan of the skin on the cheek is shown in which several structures are annotated. Clearly visible are features such as hair and the two layers of skin, namely, the epidermis and dermis, which have previously been identified in OCT studies when comparing with histological reports (Gambichler et al. 2007).

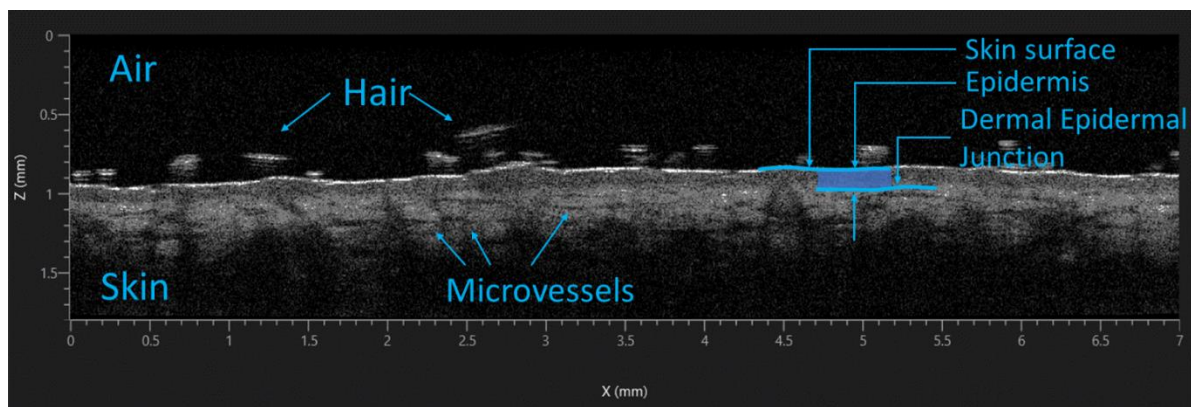


Figure 3.6 Annotated 2D-OCT scan of the cheek.

Several parameters can be extracted from these OCT scans to characterise the skin objectively. The present research focuses on the following:

1. Epidermal thickness –

Skin thickness can be influenced by factors such as gender, age, skin type, and anatomic site (Gambichler et al. 2006). Furthermore, researchers have investigated the effects of surface interactions such as application of topical products that cause irritation or mechanical stimulus such as tape stripping of the epidermal structure (Lademann et al. 2009; Qin et al. 2018), generally reporting a decrease in thickness due to the intervention. Epidermal thickness changes have also been investigated for SS/non-SS individuals (Richters et al. 2016), reporting that fewer tapes were required to strip off the SC in SS individuals as compared to non-SS. Thus, this parameter was considered relevant in the present research.

For OCT scans, the epidermal thickness is characterised by the difference in depth values of the two peaks in the Averaged A-scan plot (Welzel et al. 2004). The first peak corresponds to the surface of the skin and the second peak has been associated with the dermal-epidermal junction (Figure 3.7), as such the layer between these peaks corresponds to the epidermis (Mogensen et al. 2008; Josse et al. 2011; Taghavikhalilbad et al. 2017).

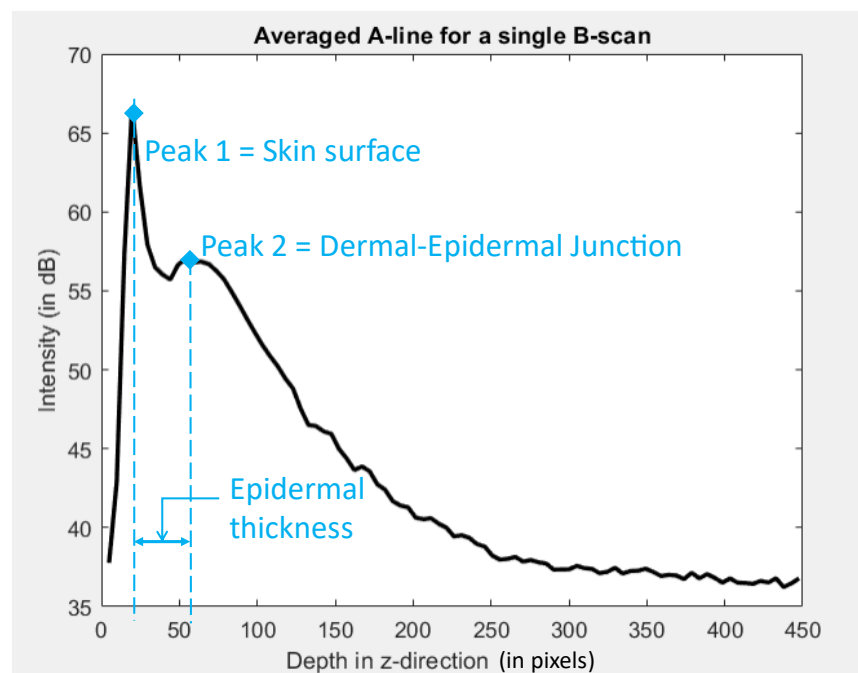


Figure 3.7 Illustration of epidermal thickness calculation.

2. Signal attenuation –

OCT signal attenuation is influenced by the presence of structures such as sebaceous glands, blood vessels, and collagen and/or other compositions (Welzel et al. 2003). With variation in structure, the attenuation of the signal varies accordingly. Thus, this parameter highlights the composition and its density in the skin tissue.

With reference to a previously reported algorithm (Adegun et al. 2013), the Scaled Intensity Drop (SID) has been introduced as a metric for this OCT signal attenuation (Figure 3.8). It is computed as the ratio of the difference in intensity values corresponding to two points on the cumulative intensity curve and the depth of the signal at both points (Equation 3.1). These authors calculated the SID between the 5% and 90% backscatter points (Adegun et al. 2013).

$$\text{Scaled Intensity Drop (SID)} = \text{Intensity Drop} / \text{Attenuation Depth} \quad (\text{Equation 3.1})$$

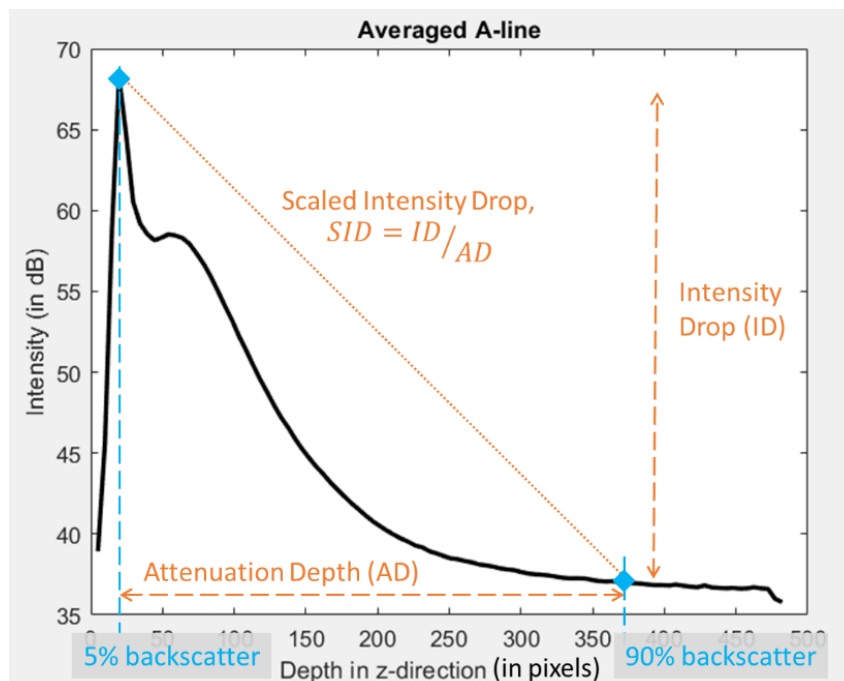


Figure 3.8 Illustration of Scaled Intensity Drop calculation from 5% to 90% cumulative intensity.

3. Surface roughness –

Skin roughness is often monitored as an indicator of the effect of topical treatments, e.g., when examining facial wrinkles (Ferreira et al. 2010). Additionally, this parameter has been also used to distinguish healthy skin and diseased skin for conditions such as psoriasis (Welzel

et al. 2003). For devices interacting with the skin surface, the mechanical forces at the interface are influenced by the roughness of interacting surfaces. Thus, this parameter could prove opportune in the present research.

Figure 3.9 illustrates the evident difference in the roughness of the skin surface between the cheek and neck for one healthy individual. The roughness of the skin surface can be estimated from such 2D-OCT scans by calculating the root mean square of the deviation of the peaks/troughs from the mean line of the skin surface (Maiti et al. 2016; Askaruly et al. 2019).

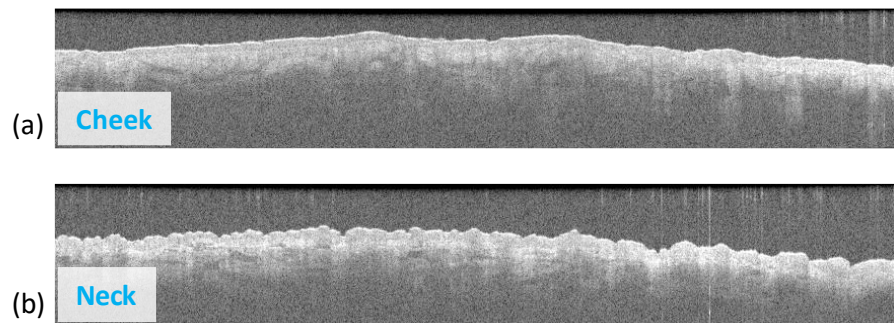


Figure 3.9 Examples of 2D-OCT scans with visibly different surface roughness between the (a) cheek and (b) neck for the same healthy individual.

3.3 Development of OCT Parameters

Preliminary experiments were conducted as input for the development of image processing algorithms that characterised basal skin using OCT. The scan pattern for this dataset was $10 \times 6 \mu\text{m}$ pixel size and $9 \times 2 \text{ mm}$ field of view. The demographic details of five healthy participants, each identified with an ID, are included in Table 3.2.

Table 3.2 Demographic details of participants from preliminary experiments.

Participant ID	Gender	Ethnicity	Age
D11	Male	Caucasian	49
D12	Male	Caucasian	26
D13	Male	Caucasian	44
D14	Female	Indian	27
D15	Male	Caucasian	39

Exemplar B-mode images acquired from this preliminary dataset are shown on the cheek and neck in [Figure 3.10](#) and [Figure 3.11](#), respectively. For each participant, the camera image highlights the macroscopic skin area that was sampled by the OCT probe. The B-modes reveal the different layers of the skin tissue represented by varying intensities of the optical signal.

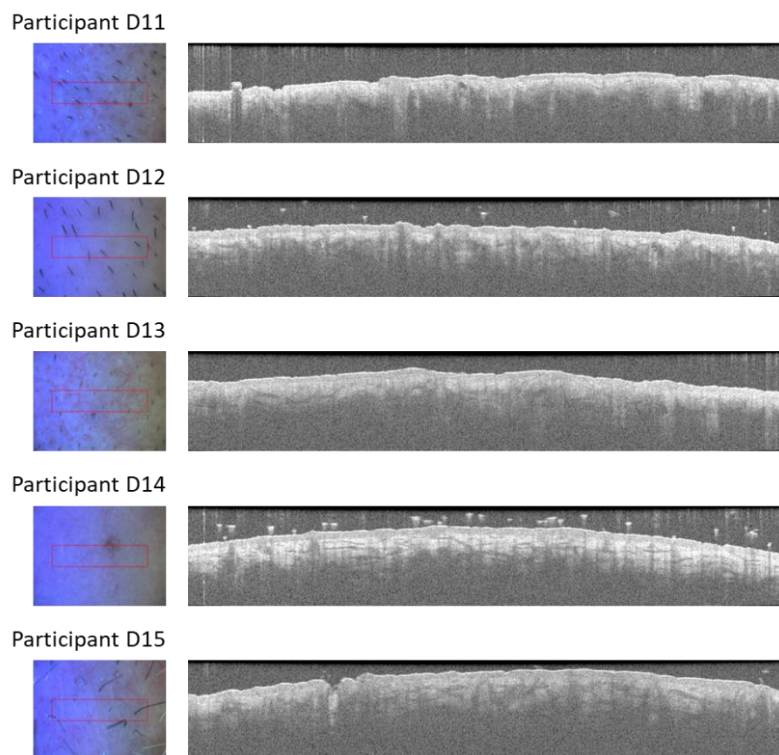


Figure 3.10 Camera images and B-mode images for the cheek.

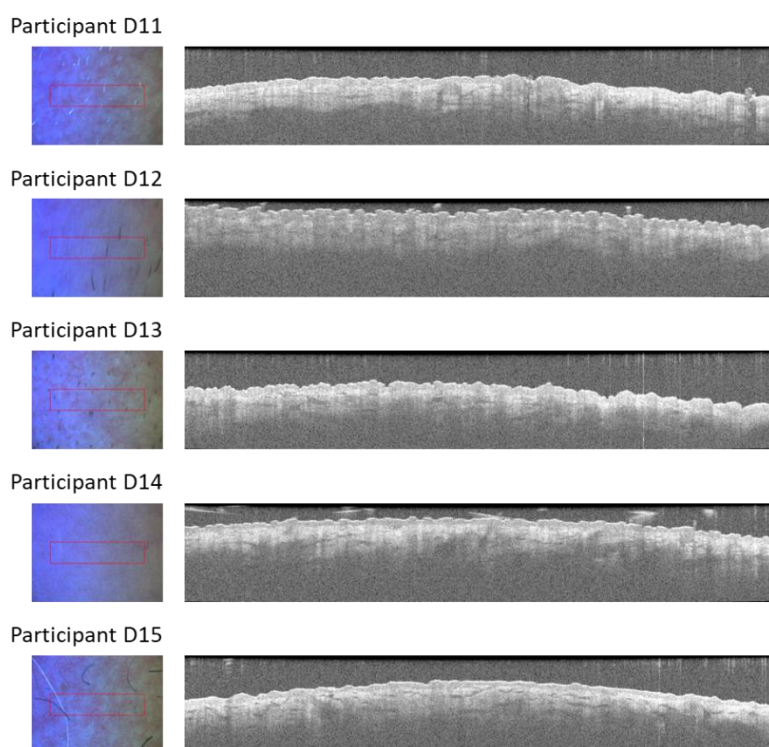


Figure 3.11 Camera images and B-mode images for the neck.

To estimate the epidermal thickness, intensity gradient, and surface roughness from such OCT scans, it is critical to accurately detect the skin surface and distinguish it from noise, in the form of hair follicles or background features. Thus, a MATLAB script was developed to estimate the skin surface in the raw OCT images, which is detailed in the following paragraphs.

3.3.1 Skin surface detection – Version 1

A script was developed based on the algorithm previously reported (Askaruly et al. 2019). The processing stages are depicted in Figure 3.12. First, a Gaussian filter is used on the original OCT image in the depth direction to reduce the effect of signal to noise. Next, a median filter is used in the lateral direction to create a smoothed image while preserving the edges of the original image. Then, a differential filter is applied to highlight the surface boundary. Finally, the skin surface is rendered by finding the minimal intensity values from the previous stage.

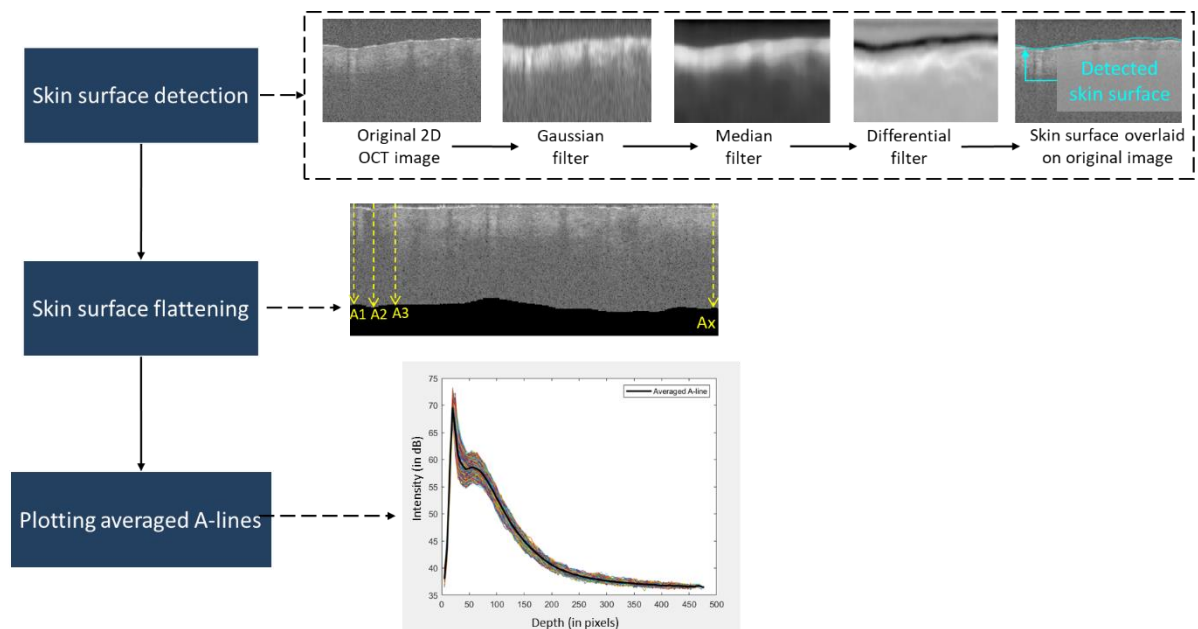


Figure 3.12 Flow diagram illustrating the processing stages of Skin surface detection - Version 1.

After the skin surface is detected, the A-scans can be plotted for estimation of the skin parameters. However, due to the variation in level of the skin surface within and across each B-scan, averaging the A-scans at this stage may lead to loss of features in the results (Figure 3.13). Thus, surface-flattened B-scans are generated by setting the detected skin surface at the same level. The subsequent A-scans plotted are now aligned at the first peak and a corresponding averaged A-scan can be plotted to represent the stack.

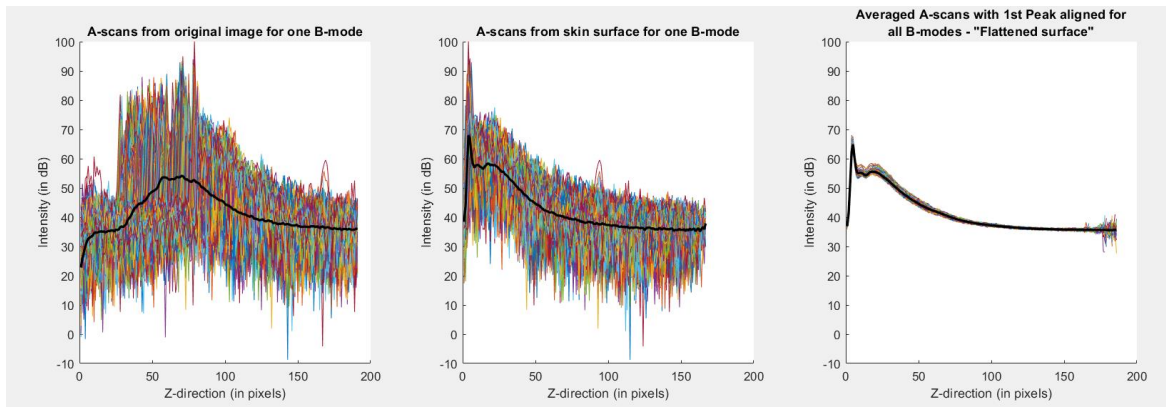


Figure 3.13 Individual A-scans and averaged A-scans (overlaid in bold) at different stages of the image processing.

However, it is noted that this algorithm was not able to distinguish hair from the skin surface, as illustrated in Figure 3.14. This is considered an important limitation as the OCT images are captured on the skin areas with beard growth, i.e., presence of hair in the scan may impede the OCT signal from reaching the skin surface, thereby casting a shadow in the Z-direction. Thus, the version 1 algorithm needed to be improved.

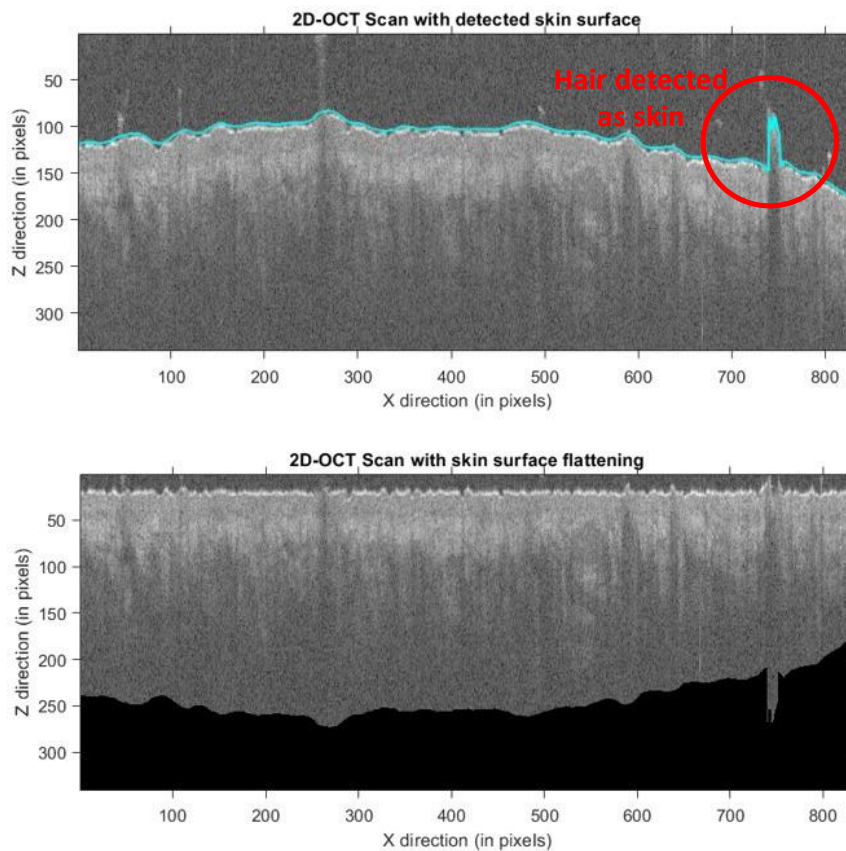


Figure 3.14 Exemplar B-mode images where hair has been wrongly detected as skin, highlighting the limitation in the version 1 skin surface detection algorithm.

3.3.2 Skin surface detection – Version 2

The version 1 algorithm was modified as detailed in Table 3.3 and illustrated in Figure 3.16. First, a scaled-space filter (Witkin 1984) is used rather than a fixed-kernel gaussian filter to smooth the image in the depth direction. Then, the mean of the different scaled spaces is taken to combine the features of the individually filtered images (Figure 3.15), where the smaller kernel sizes closely follow the skin surface but are influenced by noise, whereas the larger kernel sizes are less prone to noise but introduce excessive blurring.

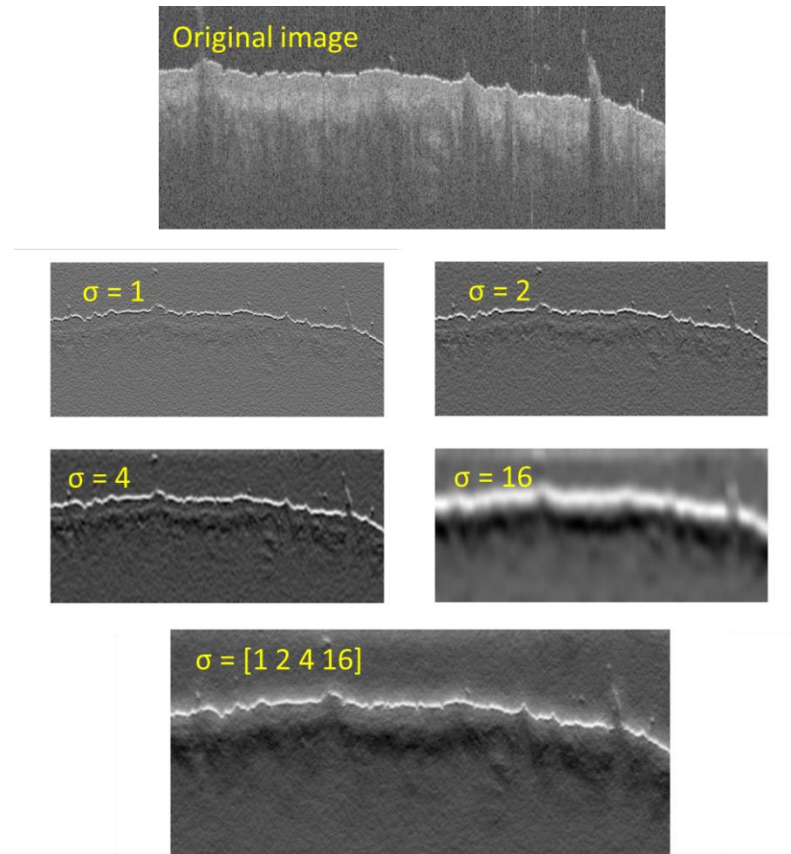


Figure 3.15 Examples of gaussian filtered images with different the kernel sizes (σ).

This is followed by a median filter with a range of 3 pixels only. The reduced median filter range prevents excessive filtering in the lateral direction, retaining the features contributing to the peaks in the A-scans. However, this stage does not filter out hairs at the skin surface. Thus, the B-scans are then evaluated for noise along the temporary skin surface using an envelope which has been created using a “rolling ball” (Huang et al. 2016). This method is combines morphological image filtering techniques of erosion followed by dilation, where a “ball” of a predetermined radius follows the skin surface creating an envelope above and below the surface. Any features outside this envelope are then considered as noise and discarded. The pixels below the surface noise are also discarded. Thus, the skin surface is clearly determined. This is followed by surface flattening as detailed in the previous version of the algorithm. Finally, the Averaged A-scan can be extracted for

estimation of the skin parameter. Here, the Averaged A-scans from each B-mode are normalised with respect to the first peak, further reducing the spread in the 3D-OCT Averaged A-scan.

Table 3.3 Comparison of image processing parameters in the skin surface detection algorithms.

Image processing step	Skin surface detection Version 1	Skin surface detection Version 2	Reason
Depth filtering	Gaussian filter, $\sigma = 3$	Scaled-space filter, $f = [1\ 2\ 4\ 16]$	Scaled-space filtering allows flexible blurring of the image.
Lateral filtering	Median filter, $m = 6 \cdot \sigma = 18$	Median filter, $m = 3$	Reducing the median filter retains the finer characteristics of the image.
Artefact detection	N/A	“Rolling ball” method	Artefacts can be discarded from the scans along with the shadows cast in the Z-direction.
A-scan averaging	Absolute values	Normalised values	Reduces the spread between the averaged A-scans from each B-mode in the 3D stack.

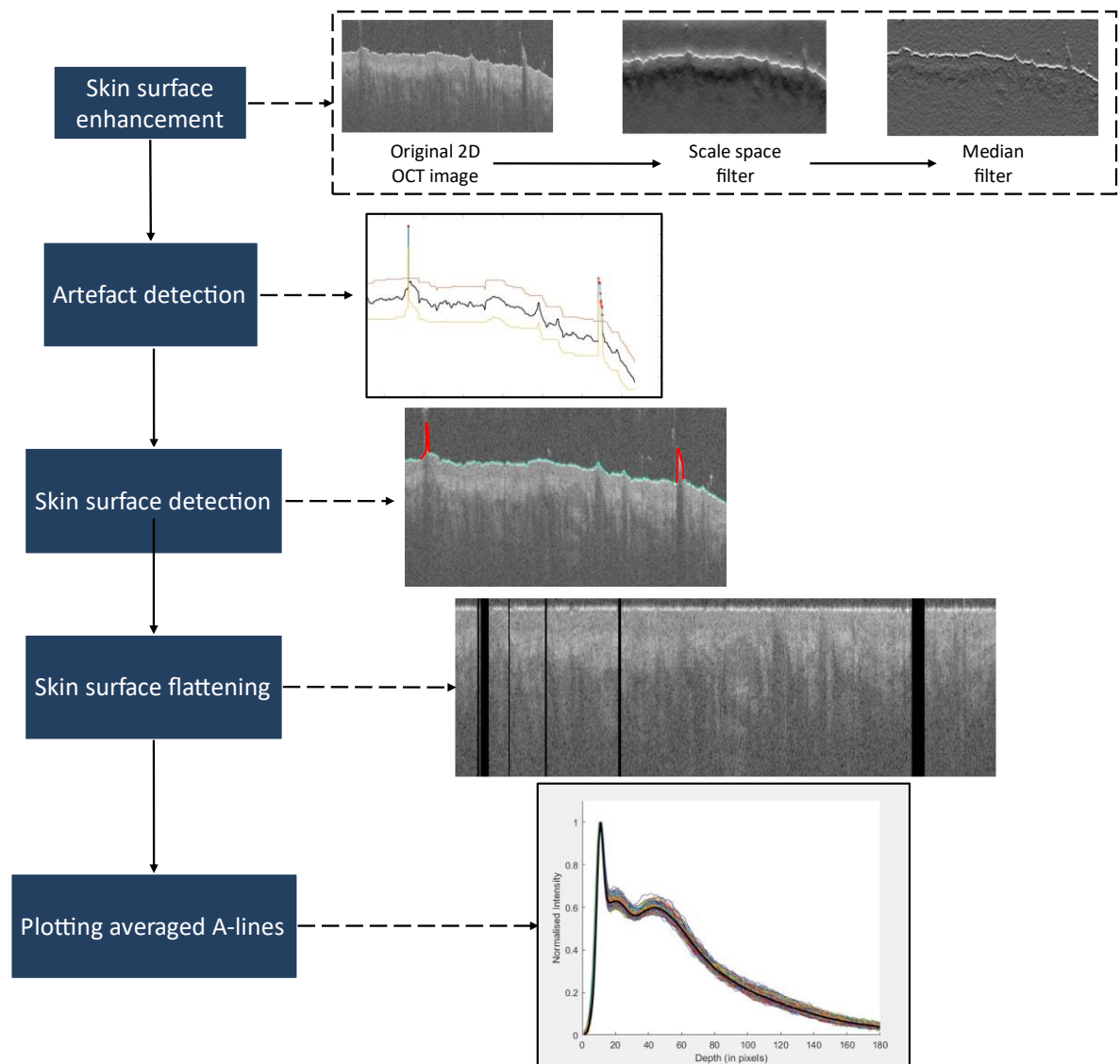


Figure 3.16 Flowchart of Skin surface detection - Version 2.

Version 2 of the algorithm provided two distinct improvements in the skin surface detection when compared to version 1, as highlighted from the same image in [Figure 3.16](#). In particular, the former followed the skin surface more closely as the image was not excessively smoothed in the depth direction. Furthermore, it was able to detect artefacts such as hair and discard them from the stack. Accordingly, the skin parameter estimation for the preliminary dataset was conducted using the Version 2 algorithm.

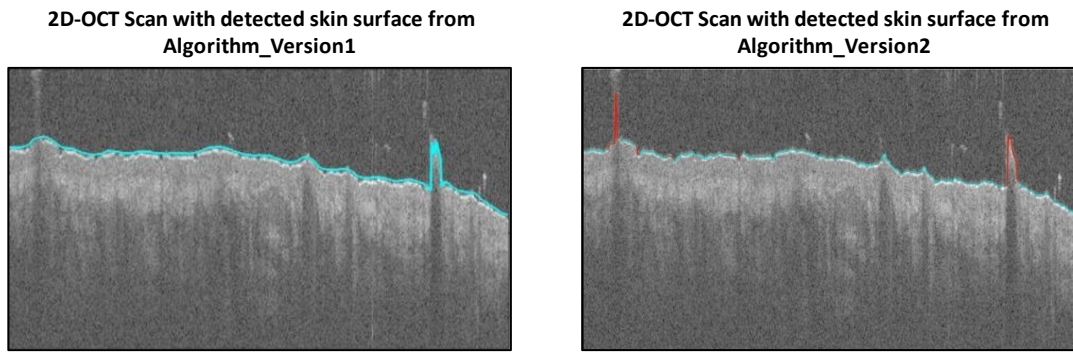


Figure 3.17 Comparing the skin surface detection algorithm versions 1 and 2 on a B-mode image with hair. The blue line indicates detected skin surface from each version.

3.3.3 Epidermal Thickness calculation

To calculate the epidermal thickness, the A-line intensity profiles were plotted as illustrated in [Figure 3.7](#). The resulting Averaged A-scans for each participant are shown below in [Figure 3.18](#).

These individual profiles demonstrate a degree of variability between the A-scan profiles, although the trend in waveform features is consistent across the imaging area. As the epidermal thickness on the face has been reported to range from 0.030mm to 0.063mm (Chopra et al. 2015), the current algorithm was prescribed to distinguish the first two peaks that are at least 0.025mm apart. However, close examination of the Averaged A-scans has revealed a third peak, generally associated with the images on the cheek ([Figure 3.18](#)). This may be attributed to the wavy nature of the dermal-epidermal junction irrespective of the flattening of the skin surface. Where present, two thickness values are reported, with respect to both Peak 2 and Peak 3.

The median thickness on the cheek with respect to Peak 2 was 0.035mm and with respect to Peak 3 was 0.105mm (n=5). From the literature, thickness of the cheek has contrasting values with one researcher stating it as 0.045 mm (Chopra et al. 2015) and another as 0.094 mm (Firooz et al. 2016). Further analysis with a larger sample size may help us identify the suitable parameters regarding which peak to select for epidermal thickness calculation.

With respect to the Averaged A-scans on the neck, only participant (D11) demonstrated a distinct third peak. In addition, there were clear differences between the nature of the second peak as detected by the algorithm with, for example, participant D13 only demonstrating a small peak while D14 demonstrated a large second peak. Overall, the median thickness on the neck was estimated to be 0.102mm, which should be compared to contrasting reported values of 0.040 mm (Chopra et al. 2015) and 0.10 mm (Firooz et al. 2016). The values on the neck are generally lower than the corresponding values on the cheek, although there is no consistent trend in the thickness values at each facial site across the small cohort.

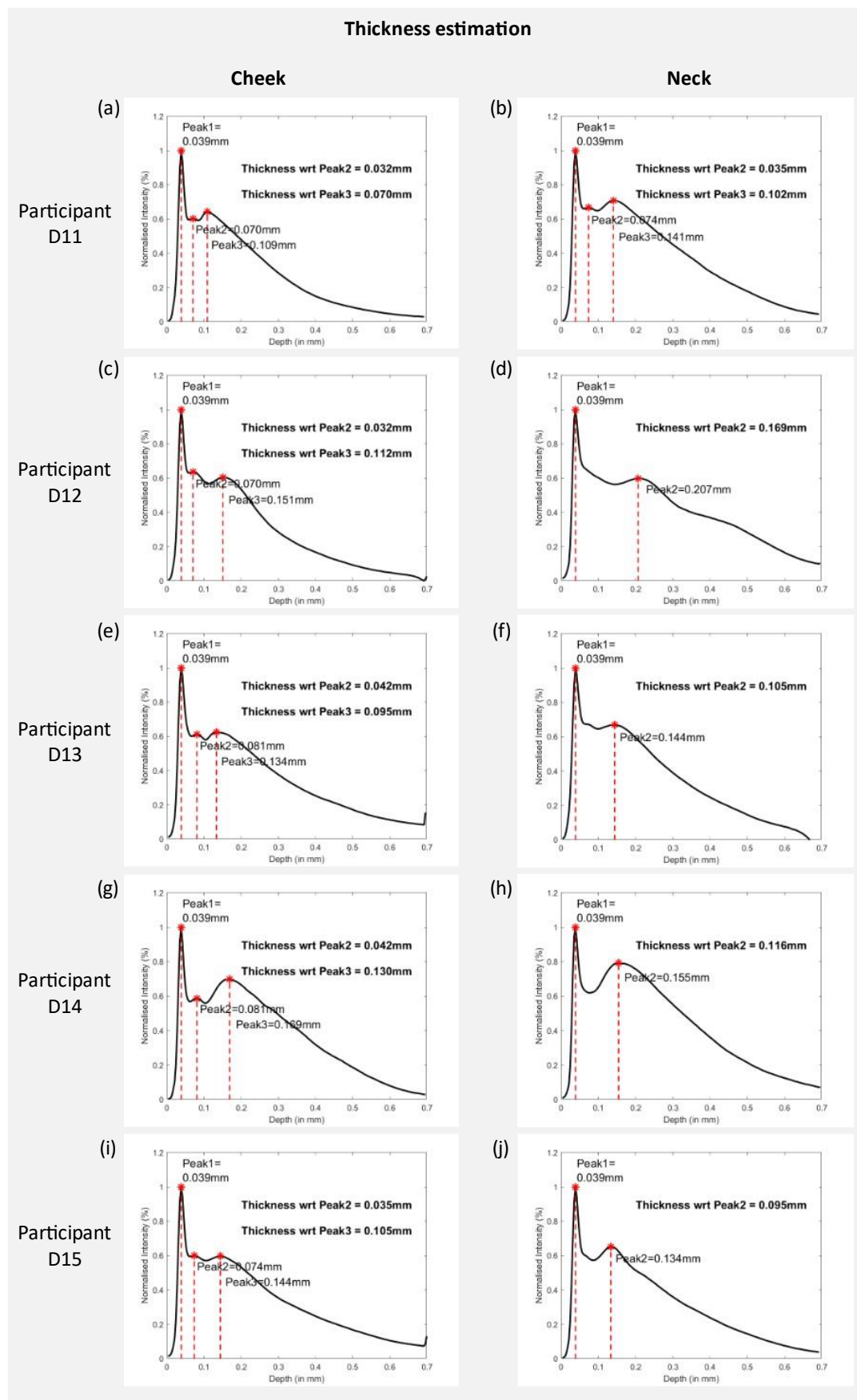


Figure 3.18 A-scans from the 3D-OCT scans highlighting the thickness of the epidermis on the cheek for (a) D11, (c) D12, (e) D13, (g) D14, (i) D15 and on the neck for (b) D11, (d) D12, (f) D13, (h) D14, (j) D15.

3.3.4 Scaled Intensity Drop (SID) calculation

The initial intention was to calculate the SID between the 5% and 90% cumulative intensity points, as illustrated in Figure 3.8. However, close analysis of the previous study (Adegun et al. 2013) indicated that these authors selected the initial point on the intensity curve based on the depth of the 1st peak in the A-scan. Thus, the present algorithm was modified for this dataset to calculate the relative intensity from the Peak 1 in the A-scan plots. Furthermore, to optimise the parameter to find maximal differences between independent scans, the SID was examined at different depths corresponding to the 60%, 70%, 80%, and 90% of the normalised intensity points in the A-scans, as indicated in Figure 3.19.

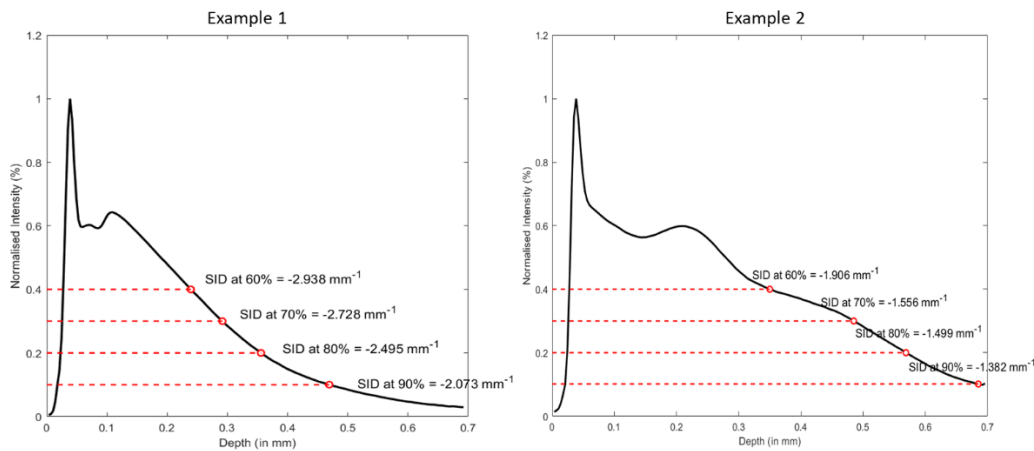


Figure 3.19 Comparison of SID at 60%, 70%, 80%, and 90% of the normalised intensity points for two exemplar A-scans.

From these preliminary results, it was observed that the OCT signal continued to scatter beyond the 60% and 70% normalised intensity points, demonstrated by the non-linear decrease in intensity of the A-scans. Additionally, the 90% normalised intensity point was observed to coincide with the tail of the curve which, in some cases, may not represent a reliable OCT signal. Thus, in the present study a lower threshold of 80% of the maximum intensity was selected and the SID was defined as the coefficient of the slope from Peak 1 to 80% of the maximum intensity of the signal. The results from the preliminary data at both facial sites are illustrated Figure 3.20.

The SID was estimated to range from -1.762 mm^{-1} to -2.495 mm^{-1} on the cheek and from -1.499 mm^{-1} to -1.997 mm^{-1} on the neck. Furthermore, it is noted that $n=3/5$ had a higher SID value on the cheek (median = -1.896 mm^{-1}) than on the neck (median = -1.806 mm^{-1}). Any changes between the values estimated from the scattering of the OCT signal might be attributed to the nature and density of the collagen fibres, which have been reported to be different on the neck and cheek sites (Luebberding et al. 2014).

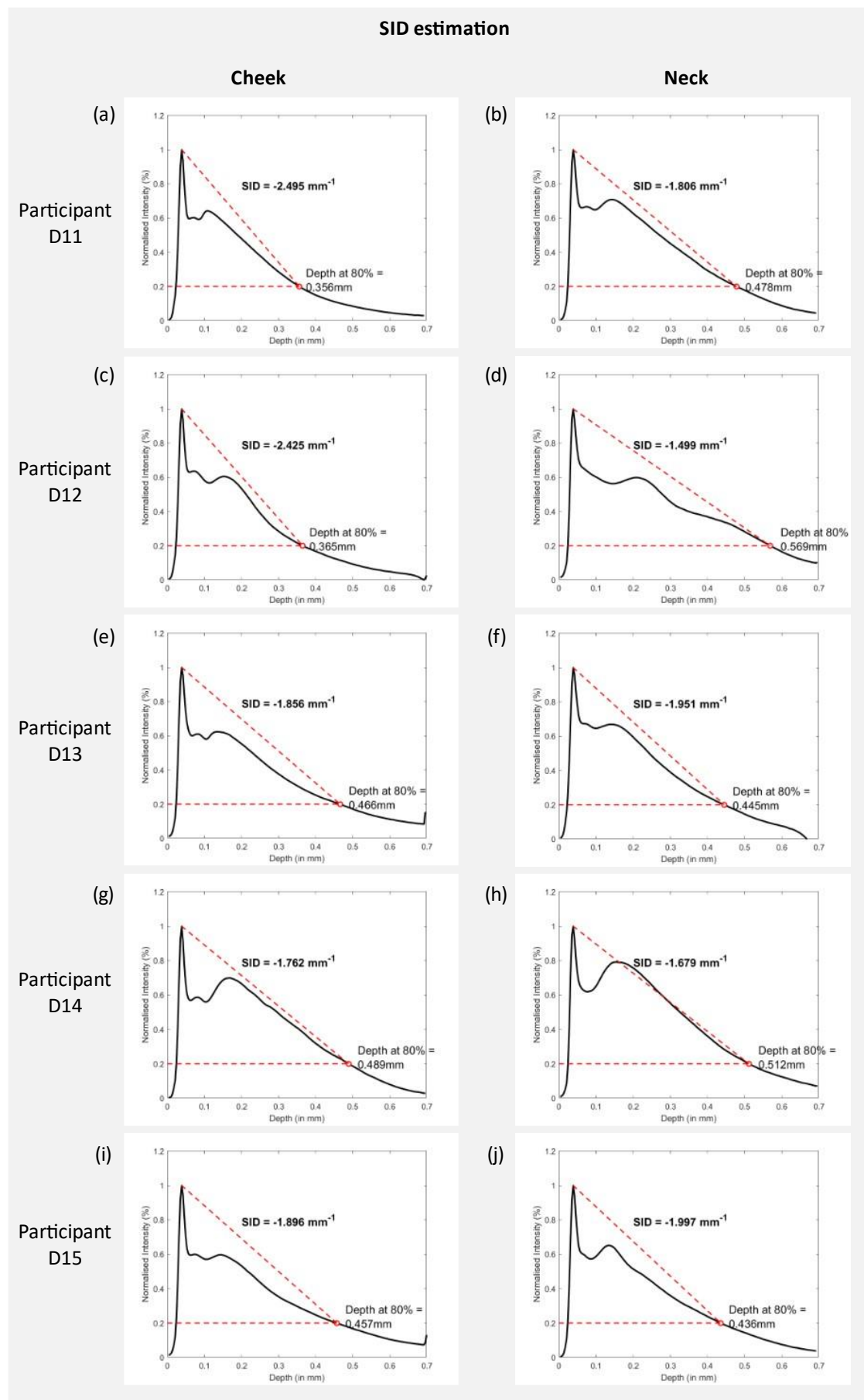


Figure 3.20 A-scans from the 3D-OCT scans highlighting the SID on the cheek for (a) D11, (c) D12, (e) D13, (g) D14, (i) D15 and on the neck for (b) D11, (d) D12, (f) D13, (h) D14, (j) D15.

3.3.5 Surface roughness

Surface roughness values can be estimated from the 2D-OCT as well as 3D-OCT scans. First, the skin surface without artefacts was extracted, as detailed in version 2 of the skin surface detection algorithm. To offset any possible curvature of the skin tissue due to, for example, the measurement system or anatomical location, the detected skin surface needs to be adjusted. Here, the same process as adopted previously in “surface flattening” (Figure 3.16) is not appropriate because it creates a smooth skin surface without any undulations. Instead, first, a moving average of the skin heights is estimated along the X-direction, discarding values at the tails of the curve where the moving mean resulted in errors. After subtracting the newly defined curve from the detected skin surface, an adjusted surface is obtained in 3D with peaks and troughs along the zero value on the Y-axis. Thus, the heights of these irregular peaks and troughs in the adjusted OCT image can be defined. The RMS value (R_q) for each B-mode is then used as a metric of the surface roughness of the 3D scan. Figure 3.21 illustrates the intermediate steps in estimating the surface roughness on both the cheek and neck for the B-modes indicated in Figure 3.9.

The R_q was estimated for each participant on the cheek and neck and has been reported for exemplar B-modes from the 3D-OCT scan (Figure 3.22). Overall, the R_q for the cheek ranged from 10.0 to 14.1 μm with a median value of 12.3 μm . For the neck, the roughness values ranged from 12.6 to 22.7 μm , with a median value of 14.8 μm . These values are similar to those reported by others with the cheek roughness stated as $17.5 \pm 4.4 \mu\text{m}$ and neck roughness stated as $25.3 \pm 5.2 \mu\text{m}$ (Cowley et al. 2012).

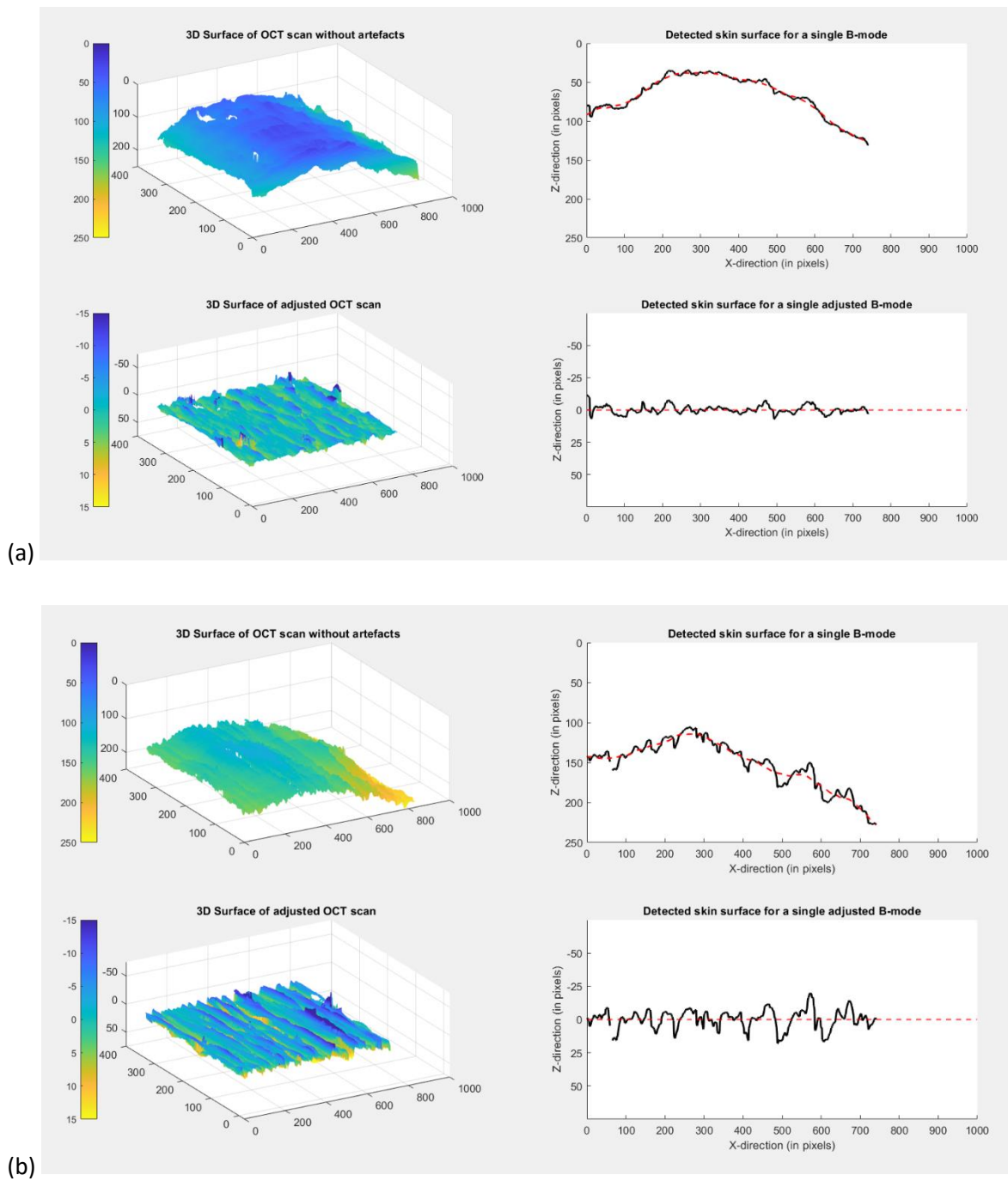
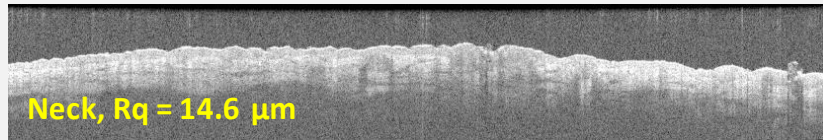
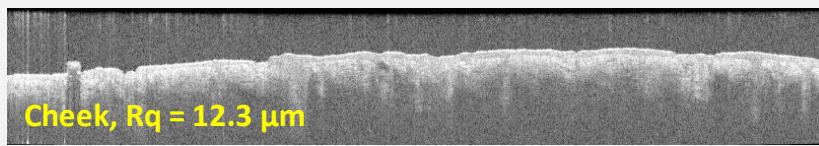


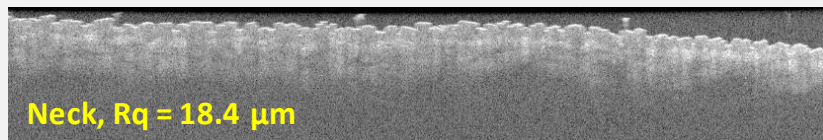
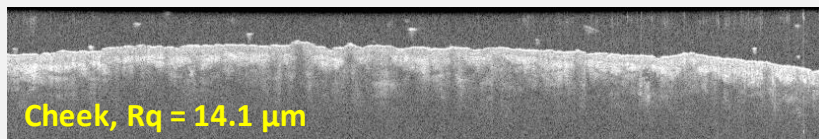
Figure 3.21 Example of participant D13 surface roughness calculation. (a) For the Cheek; $R_q = 11.5 \mu\text{m}$; (b) For the neck; $R_q = 22.7 \mu\text{m}$.

Roughness

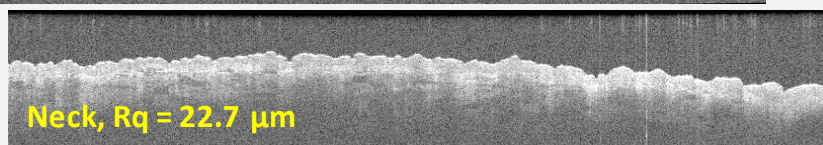
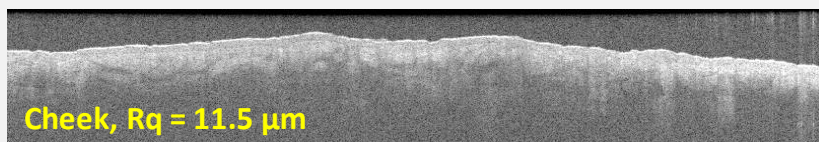
Participant D11



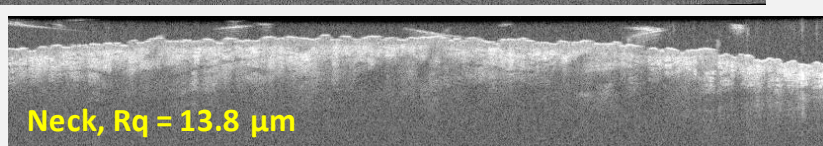
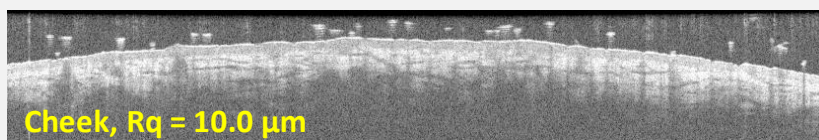
Participant D12



Participant D13



Participant D14



Participant D15

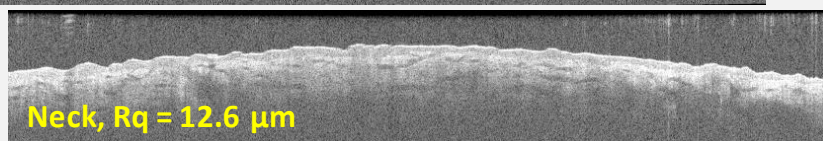
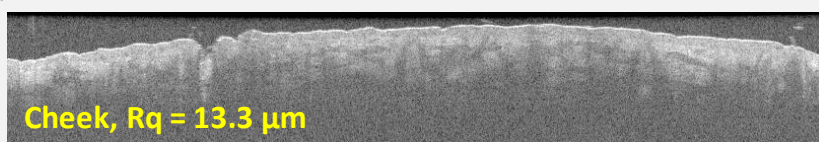


Figure 3.22 Estimated roughness on the cheek and neck for each participant.

3.4 Protocol Development Summary

Preliminary experiments were conducted with the goal of exploring the use and usefulness of OCT in characterising skin parameters in prospective consumer studies. Accessories were developed in-house for this specific OCT system to ensure that it was suitable for imaging facial locations and reduce interference due to the measurement apparatus. A combination of pixel sizes and field of views were evaluated to guarantee a practical acquisition time (

[Table 3.1](#)) in which motion artefacts introduced by the participants breathing and pulse are limited. Ultimately, an image acquisition time of 20 seconds, a pixel size of $6 \times 6 \mu\text{m}$ and field of view of $4 \times 4 \text{ mm}$ was selected to be used in prospective studies. A significant part of the protocol development activities was focused on detecting the true skin surface and distinguishing it from artefacts due to hair follicles and noise. The processing steps cited in the literature generally included protocols for imaging non-hairy skin surfaces. However, the present research is focused on examining the skin response at both the cheek and neck, specifically at sites where there is beard growth. This is a critical element associated with the project aims, namely, to investigate the influence of complex mechanical loading such as electrical shaving on various skin parameters.

Thus, it is essential to include artefact removal processes, which detected hair on the skin surface and distinguished it from the surface itself. This was achieved by the development of the algorithm version 2. In addition, due to inherent variation in skin response, it will be important to perform repeat measurements and estimate the average values for each skin parameter. OCT-Skin parameters have been identified as epidermal thickness, scaled intensity drop (SID), and skin roughness, R_q . These will provide complimentary data to biophysical parameters to characterise the skin. As a summary, the results from these newly defined parameters have been listed in [Table 3.4](#).

Table 3.4 Summary of OCT parameters from the preliminary dataset, listed in ascending order by the participant's age. SID is represented by the magnitude of the result.

Participant	Cheek				Neck			
	Thickness (mm)		SID (mm ⁻¹)	Roughness, Rq (μm)	Thickness (mm)		SID (mm ⁻¹)	Roughness, Rq (μm)
	wrt Peak 2	wrt Peak 3			wrt Peak 2	wrt Peak 3		
D12	0.032	0.112	2.43	14.1	0.169	N/A	1.50	18.4
D14	0.042	0.130	1.76	10.0	0.116	N/A	1.68	13.8
D15	0.035	0.105	1.90	13.3	0.095	N/A	2.00	12.6
D13	0.042	0.095	1.86	11.5	0.105	N/A	1.95	22.7
D11	0.032	0.070	2.50	12.3	0.035	0.102	1.81	14.8

As this dataset was primarily collected to initiate the algorithm development for OCT parameters to characterize skin, the test conditions were not standardised to the level required in a human study. There was no pre-requisite based on gender or even the shaving and grooming habits for the male volunteers, implying that the skin may not reflect a standard baseline state for all participants. Additionally, the precise location on both the cheek and neck for image acquisition was not prescribed. Thus, the analysis of the results obtained has been limited to evaluating the range of values for each parameter, and only initial observations based on anatomical locations.

In summary, the following recommendations were proposed for the prospective consumer study:

1. The physical imaging setup required optimisation. This included a bespoke interface with the skin and mechanical arm to position the device for the neck and cheek. This was critical to avoid tissue distortion in the skin due to contact pressure.
2. The following imaging parameters were selected to provide optimal data: pixel size 6x6 μm, field of view 4x4 mm, acquisition time 20 seconds. These provided a suitable compromise between image acquisition time, skin area imaged, resolution is required, and participant comfort.
3. Repeat measurements will be conducted to improve the precision of the parameters extracted from the scans.
4. Differences were observed between participants and anatomical locations when comparing the Averaged A-scans for epidermal thickness characterization. The algorithm for this parameter

requires additional validation based on data acquired from a controlled study with a larger sample size.

5. The attenuation coefficient of the OCT signal has been approximated by calculating the SID, which has been defined as the coefficient of the slope from Peak 1 where the depth of the signal is 80% of the maximum intensity.
6. The roughness parameter, R_q , depends on the window size supplied to the algorithm. This parameter will be optimized for the images from a controlled study.

Chapter 4 A consumer study to evaluate the skin's biophysical response to mechanical challenges

4.1 Introduction

Several reviews have been published regarding the widespread prevalence of skin sensitivity (SS) and the challenges associated with its identification and treatment (Berardesca et al. 2013; Duarte et al. 2017; Do et al. 2020). Due to its impact on the quality of life, this topic is of interest to healthcare researchers in academia and industry. However, the descriptions of skin sensitivity often involve terms such as burning, stinging, and discomfort. The variability in its perceptions make it difficult to identify the mechanisms underlying the condition. Consequently, there is no consensus regarding an objective quantifiable definition for SS.

Many experimental studies conducted by the cosmetic industry aim to define characteristics of SS but their findings are generally not reported in the public domain. Such studies often focus on the relationship between the response of skin tissues and the chemical triggers of skin sensitivity (Seidenari et al. 1998; Balsam et al. 2009; Sun et al. 2016). However, in the present project, the motivation is driven by the mechanical interactions of skin when exposed to pressure, shear, and friction associated with consumer devices.

Thus, the present research aimed to evaluate the skin response within a cohort of individuals following three distinct insults involving mechanical loading. A study was designed to purposefully sample individuals with varying levels of skin sensitivity to assess any associations between the subjective and objective parameters of SS. A series of biophysical and anatomical/structural measurements were recorded at two selected sites of the face, representing common sites for consumer device interactions. Skin parameters were assessed at baseline and at several time points following the mechanical insults.

The results from only the biophysical measurement tools have been reported in this chapter. Those from the OCT have been reported in [Chapter 5](#). Thus, the objectives of this chapter were as follows:

- Purposefully recruit a cohort of individuals with varying degrees of perceived skin sensitivity assessed using a standardised questionnaire.
- Establish basal skin characteristics on the cheek and neck using biophysical parameters.

- Perform standardized mechanical insults (involving tape stripping, rubbing with a frictional surface, and shaving) to provoke changes in skin health parameters.
- Evaluate the temporal effects of the mechanical insults on the selected biophysical parameters.
- Investigate the relationship in skin responses between the cheek and neck for all participants.
- Compare skin responses between participants categorised with different skin sensitivity.

4.2 Methods

The study was approved by the research ethics panel at Philips (internal document).

4.2.1 Skin sensitivity questionnaire

To identify associations between the perceived and observed parameters of skin sensitivity, participants were purposefully selected based on a questionnaire which is detailed in [Appendix A](#). This short version of the questionnaire was developed in-house at Phillips Consumer Lifestyle (PCL) from a more detailed version previously published (Richters et al. 2017).

To review briefly, the original questionnaire contained 32 questions including details of the presence and extent of typical responses associated with SS following interaction with various stimuli, such as toiletries and weather conditions. This questionnaire was developed based on inputs obtained from 481 responders and was validated in the clinical studies based on both non-invasive and histological data obtained from human volunteers. Benchmarking against the score derived from the original questionnaire, the PCL team aimed to reduce the number of questions related to the various stimuli. Subsequently, models were developed to evaluate the effects of reducing the number of input parameters. The predictive performance of these models was then assessed in terms of the r-squared values (goodness of fit), percentage of classification errors, and their ability to derive the pre-determined class sizes. The classification error calculation estimated how many individuals with true “very SS”, as responded in the original questionnaire, were re-classified as “normal”. Thus, stating the desired class sizes, threshold values were chosen, which should be reconsidered for new studies with different observations. Based on the results of the performance indicators, the following model was selected to estimate the skin sensitivity score (i.e., Q-score):

$$\text{Q-score} = 81.02 + 4.93 * Q1 + 36.89 * Q2 + 27.77 * Q3 - 35.2 * Q4 \quad (\text{Equation 4.1})$$

where the variables were coded as shown in [Table 4.1](#).

Considering the specific focus of the research, an explicit question regarding the skin response to mechanical stimulation (Q5) was added to the questionnaire and subsequently to the selection criteria.

Table 4.1 Coding values for the responses from the SS Questionnaire.

Q. No.	Questions from the screener	Answers	Coding values
Q1	Which skin type best describes you? (Fitzpatrick Skin Type)	1, 2, 3, 4, 5, 6	1, 2, 3, 4, 5, 6
Q2	How frequently does your skin breakout?	Acne Sometimes No	1 0 0
Q3	What is your facial skin like in the morning (before washing)?	Tight Comfortable Oily	1 0 0
Q4	Do you think you have sensitive skin?	Yes A bit No	0 1 2
Q5	Does your skin react during or after shaving or contact with fabrics like clothes or towels?	1, 2, 3, 4, 5 (Never to Always)	-

4.2.2 Participant Selection and Recruitment

A screening email was sent to the cohort of Philips consumer testing panel, who have previously consented to take part in studies affiliated with the product range. This included information regarding the prospective study and the short questionnaire on skin sensitivity. After 72 hours, a total of 262 responses were received (out of 588 individuals invited). Within the following week, the responses were analysed to identify suitable participants. The following inclusion and exclusion criteria were used, as detailed in the Ethics form:

Inclusion criteria –

- Individuals enrolled on the Philips consumer testing panel
- Individuals of any ethnicity
- Males with clean shave
- Individuals presented with the mental capacity and English/Dutch proficiency to provide informed consent

Exclusion criteria –

- Individuals with broken skin
- Individuals presented with current active skin condition on the areas of measurement

Following the 262 responses received, respondents were filtered based on the self-assessed SS category (i.e., Q4), the response to the mechanical stimulus question (i.e., Q5), and the calculated Q-Score. Identifying the first and third quartile values for the distribution of the Q-Score, three groups were created. Thus, 81 potential participants were identified. When age-related inclusion criteria were employed, this number resulted in 12-20 participants per group (Figure 4.1). Aiming to recruit a minimum of 7 volunteers per group, 9 respondents from each group were called back to confirm their participation.

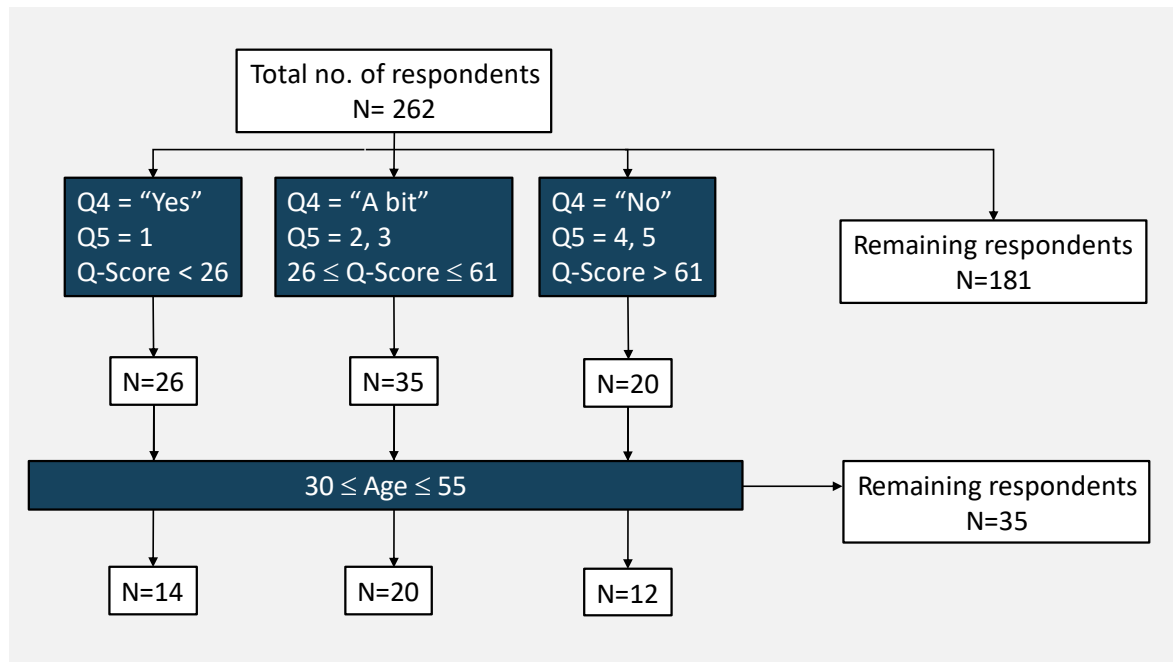


Figure 4.1 Participant selection criteria flowchart.

4.2.3 Skin Sensitivity label assignment

To understand the group skin characteristics of individuals with Low, Mild, and High Skin Sensitivity, the participants needed to be assigned SS labels based on thresholds from their questionnaire responses. Furthermore, to achieve a more thorough assignment of the SS labels, the participants were requested to fill out the short questionnaire on skin sensitivity after the study was completed (i.e., 6 months later). Thus, there were two sets of Q-scores calculated for all participants - those recorded in July 2021 prior to starting the data collection (i.e., Q score July), and those in December 2021 after completing the data collection (i.e., Q score Dec). It has already been established that the Q-score did not account for the participants answer to the question explicitly enquiring the skin response to mechanical stimulation (i.e., Mech SS Score). Thus, a new criterion was developed to assign the SS labels based on the following S-score:

$$S\text{-Score } \% = 1/4 \left(\frac{Q\text{-score July}}{\text{Highest possible } Q\text{-score}} + \frac{Q\text{-score Dec}}{\text{Highest possible } Q\text{-score}} + \frac{\text{Mech SS score July}}{\text{Highest possible score}} + \frac{\text{Mech SS score Dec}}{\text{Highest possible score}} \right) \times 100 \quad (\text{Equation 4.2})$$

By normalising the Q-scores and Mech SS scores to the highest possible values that can be achieved respectively, both variables have been reduced to a scale from 0 to 1. Thus, this approach assigns equal weights to the Q-scores and Mech SS scores while ranking the respondents in an ascending order from Low to High skin sensitivity. Identifying the first and third quartile values for the S-score distribution obtained, the participants were categorised as follows:

- Low SS – individuals with S-score lesser than the first quartile value
- Mild SS – individuals with S-score greater than the first quartile value, but lesser than the third quartile value
- High SS – individuals with S-score greater than the third quartile value

4.2.4 Measurement Protocol

Participants attended the test sessions in an environmentally controlled consumer lab at the Drachten campus of Philips, NL. The temperature in the lab ranged from 21.1°C to 22.3°C and the relative humidity ranged from 51.4% to 56.4%. All participants were instructed to shave 24 hours before each test session.

Using a stencil (70 mm x 50 mm) with a cut-out (15 mm x 15 mm), a square was drawn on both the cheek and neck for each participant to standardize the location of the skin sample across multiple visits (Figure 4.2). For the cheek (Figure 4.2a), a corner of the stencil was aligned with the outer corner of the participants left eye, such that the longer edge of the stencil was placed adjacent to the nose, along the skin towards the chin. The square was outlined on the cheek skin using the cut-out as a boundary. If the cut-out overlapped with the cheek bone, the stencil was shifted down vertically by 15 mm and then the square was drawn. For the neck (Figure 4.2b), the shorter edge of the stencil was placed below the earlobe such that the corner of the stencil coincided with the junction of the earlobe and the neck. Aligning the longer edge in the direction of the collarbone, the cut-out was used to mark the square on the skin. If the cut-out overlapped with the jawbone, the stencil was position vertically below the cheek square, and approximately 15 mm below the jawline.

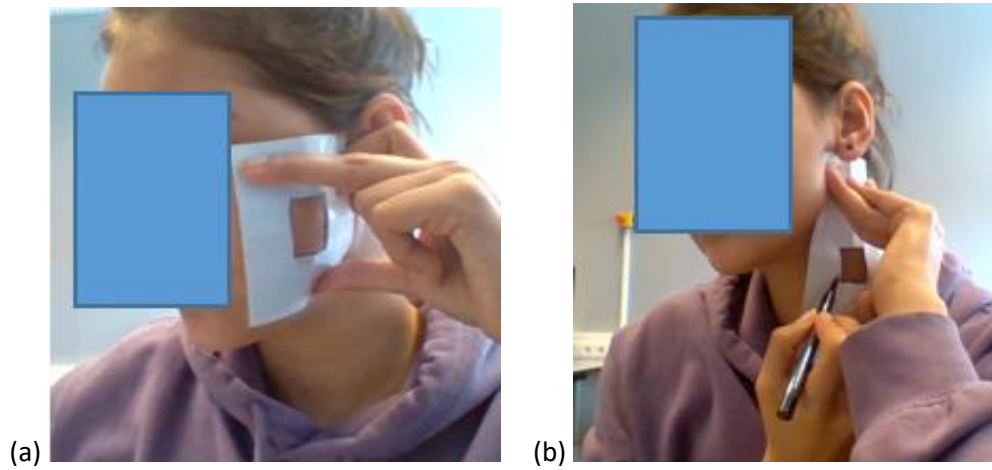


Figure 4.2 Stencil placement to identify skin area for measurements on the (a) cheek and (b) neck.

The baseline skin parameters were then recorded within the highlighted skin area using the OCT (Thorlabs, Inc., USA), Mexameter (MX18, Courage and Khazaka, Germany), Tewameter (TM300, Courage and Khazaka, Germany), and Corneometer (CM825, Courage and Khazaka, Germany) in the sequence and the acquisition time detailed in Table 4.2, based on established methods (Kottner et al. 2014).

Table 4.2 Sequence of biophysical measurements of skin and acquisition times for each site.

Biophysical measurements	Measurement system	Acquisition time	# of measurements	Approx. Total time
1. OCT images	Telesto, Thorlabs	20 seconds	3 times	1 minute
2. Redness values	Mexameter, C+K	5 seconds	5 times	0.5 minutes
3. TEWL, temperature values	Tewameter, C+K	1 minute	2 times	2 minutes
4. SC hydration values	Corneometer, C+K	5 seconds	5 times	0.5 minutes

The first parameter involved placing the probe of the **OCT (Thorlabs Telesto Spectral Domain OCT, USA)** such that the participant could sit with their cheek/neck resting against the camera (Figure 4.3). The position was adjusted as described in Section 3.1. Subsequently, three scans were acquired per site per participant.



Figure 4.3 Example of a participants position when measured with the OCT system.

The **Mexameter (MX18, Courage & Khazaka)** was used to quantify changes in skin redness or erythema, as well as the melanin content of the skin. This measurement is based on the principle of absorption/reflection of three different light wavelengths. The output from the device was obtained following the average of 5 repeated measures recorded through gentle contact with the skin. The resulting parameter is converted into arbitrary units (a.u.) (Clarys et al. 2000; Kleesz et al. 2011).

A **Tewameter (TM300, Courage & Khazaka, Germany)** is a probe which uses the open-chamber method to assess Transepidermal Water Loss (TEWL). This is defined by the amount of water that diffuses passively through the skin as a result of the pressure gradient of water vapour across the skin barrier. TEWL was measured by placing the device in gentle contact with the skin acquired at 1Hz for 1 minute, the final parameter is determined from the average of five TEWL measurements recorded when a period of equilibrium is achieved. TEWL values are expressed in grams of water per square meter of skin per hour (g/h.m^2) (Kleesz et al. 2011; van Erp et al. 2016). Additionally, a temperature sensor is housed within the TEWL chamber with temperatures recorded in °C.

A **Corneometer (CM825, Courage & Khazaka, Germany)** provides an estimation of the hydration of the stratum corneum (SC). The device measures the variations in the dielectric properties of the skin due to changes in surface hydration. The output from the device was estimated following the average of 5 repeated measures recorded through gentle contact with the skin. Its parameter is converted into a.u. (Tupker et al. 1990; Kleesz et al. 2011).

4.2.5 Mechanical stimuli: Tape stripping, friction, and shaving

The study was divided into 3 sequential sessions distinguished by the nature of mechanical insult:

1. Session 1 – Tape stripping (July 2021)
2. Session 2 – Rubbing with a frictional surface (October 2021)
3. Session 3 – Shaving (November – December 2021)

For session 1, tape stripping was conducted using in-house designed metal plates with a small aperture (Rodijk et al. 2016) and tape (Sellotape Original 1109, UK), as indicated in [Figure 4.4](#). Considering safety guidelines due to COVID-19 and subsequent minimum distance requirements, the participants were requested to apply the tape and remove it themselves with the researcher monitoring from a distance away. Overall, tape stripping was conducted 10 times at each location (Gorcea et al. 2013).



Figure 4.4 Tape stripping equipment used in session 1.

For sessions 2 and 3, a commercially available Philips shaver from the S9000 series was used for mechanical stimulation of the skin ([Figure 4.6](#)). The S9000 shaving handle is equipped with load sensors to estimate the amount of force applied onto the shaver head. In this model, the shaver head is not rigidly attached to the shaver handle. Rather, a spring system is employed which allows movement in one axis only. Furthermore, the moving element is mounted with a magnet which enables estimation of the displacement due to the force on the shaver head. This displacement is recorded by a Hall effect sensor, which is built into the shaver handle unit, and is converted to a voltage value. Subsequently, the voltage reading has been calibrated to three colour options, providing light feedback to the user ([Figure 4.7](#)). It is noted that the sensor has an upper limit of force estimation at 7N, which is well-suited for shaving facial hair. The raw force data can be recorded using a proprietary firmware and transferred to a computer using Bluetooth.



Figure 4.5 Annotated image of the Philips S9000 shaver used in the study.

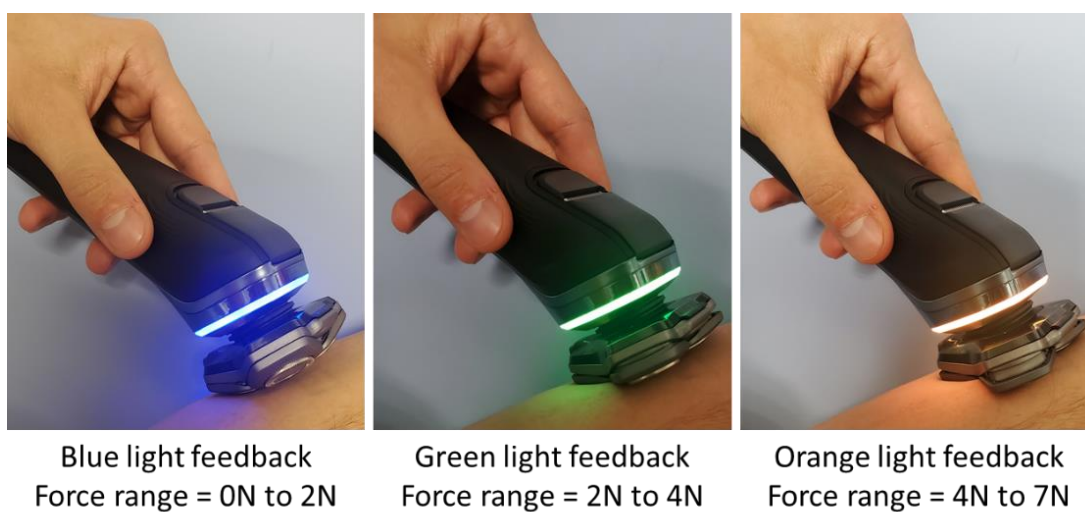


Figure 4.6 Colour feedback options of the S9000 shaving handle.

For session 2, an in-house designed frictional surface was mounted onto the shaving handle (Figure 4.7). A prototype with frictional coefficient equivalent to a surface roughness $1.725 \mu\text{m}$ was selected for this study based on the institutional regulations regarding the ethical concern of providing a suitable irritation to the facial skin of participants. For each participant, the Bluetooth connection of the shaver handle to the laptop was confirmed, and the participant ID was entered

into the associated software before starting the test session. Additionally, it was ensured that the shaving handle had a battery level of at least 30%. Once the baseline measurements were completed using the OCT and biophysical tools, the participants were requested to switch on the shaving handle and rub the frictional surface over the square drawn on their cheek/neck, maintaining contact with the skin surface and mimicking the actions of their normal shaving protocol. Furthermore, the participants were requested to maintain the light feedback from the shaving handle at the orange level (i.e., $> 4\text{N}$) as this study aimed to elicit SS responses from the skin. Simultaneously, force values were saved on the computer at a frequency of 20 milliseconds. After 60 seconds, the participants were requested to stop and switch off the shaving handle. After the mechanical stimulus was applied, the exact time was noted, and post-stimulus measurements were conducted at 0 minutes, 10 minutes, 20 minutes, and 30 minutes intervals. The schematic in [Figure 4.8](#) shows an overview of the timeline for each participant.

For session 3, a commercial shaver head was mounted on to the same shaving handle used in session 2 ([Figure 4.7](#)). The shaver head was specifically selected for this project based on a range of “cap” and “cutter” combinations (detailed in [Figure 4.7](#)). As the distance between the cap and the cutter is decreased, the skin exposure through the cap slots increases, and thus, the chances of the skin getting injured increases. Following institutional regulations regarding the ethical concern of purposely irritating the facial skin of participants, a cap and cutter combination yielding an exposure of 1.16 mm was selected for this study. For each participant, the equipment was set up according to that described for session 2. After the baseline measurements were completed, the participants were requested to switch on the shaving handle and shave over the square drawn on their cheek/neck. After 30 seconds, the participants were requested to stop shaving and switch off the shaving handle. A similar sequence of recording post-stimulus measurement intervals as session 2 was adopted in this session.

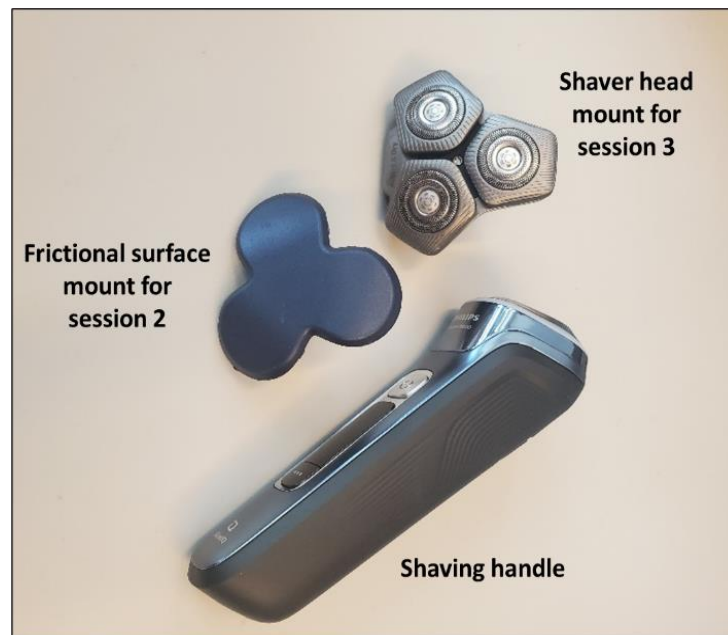


Figure 4.7 Shaving handle and mounts used in sessions 2 and 3.

It is evident that the duration of the mechanical stimulus interaction differed for sessions 2 and 3. This is because the average shaving experiments at PCL span approximately 2 minutes, where the consumer shaves the skin on both sides of their cheek and neck. For the present protocol, the mechanical insult was concentrated to a small area of the skin on only one side of the cheek and neck of each participant. Based on the irritation reported in preliminary tests, 30 seconds of shaving with the prototype device was determined as the upper limit, particularly for the neck. Thus, the shaving session was restricted to 30 seconds at each site. By contrast, there were no reports of irritation using the frictional surface within 30 seconds. Thus, the protocol in session 2 involved interaction with the frictional surface for 60 seconds.

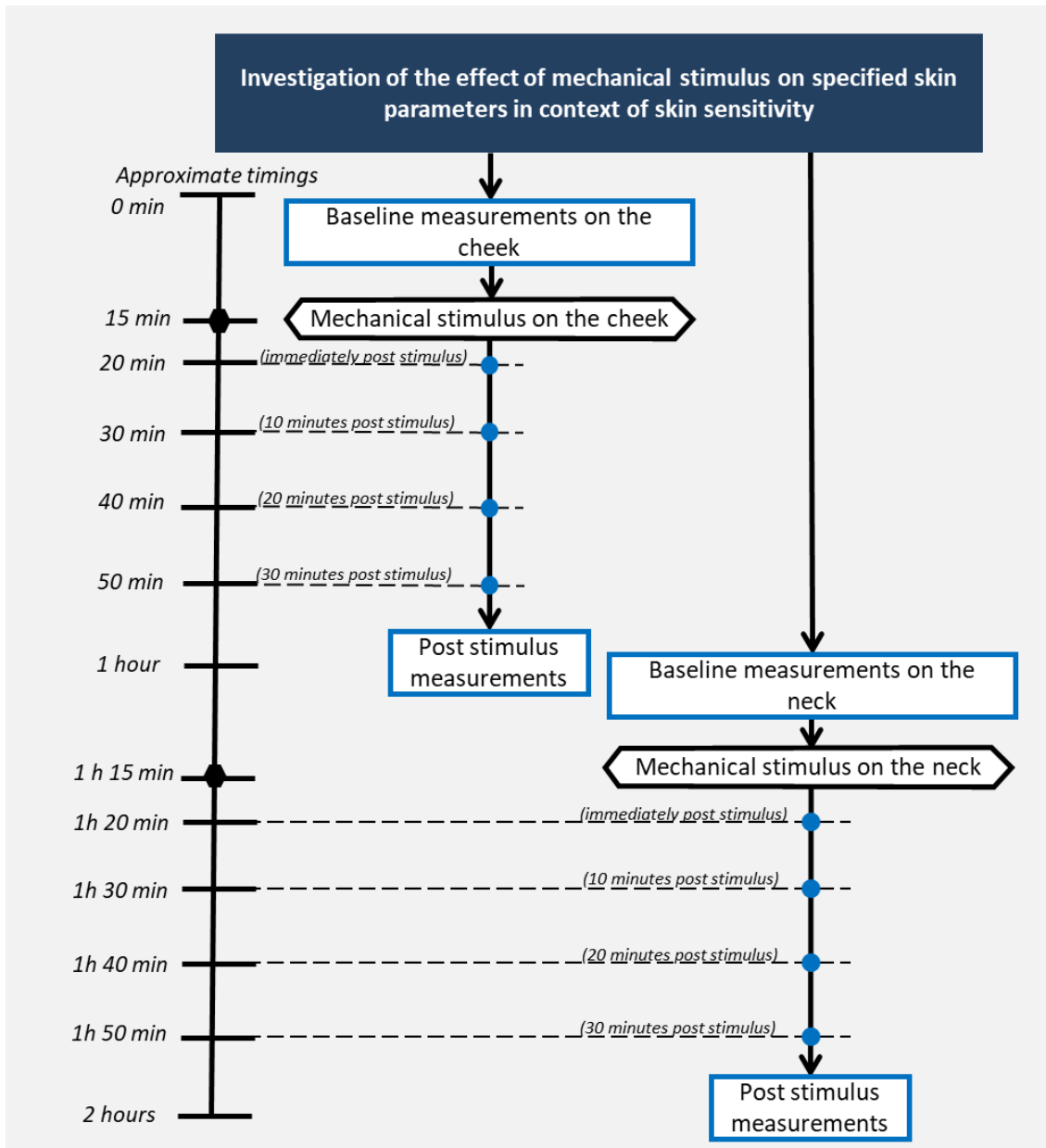


Figure 4.8 Protocol for Mechanical response study at Philips.

4.2.6 Statistical analysis

The distribution of the biophysical values was checked for normality using the Anderson - Darling (AD) normality test and the resultant p-values were determined ([Appendix C](#)). Descriptive statistics such as medians, quartiles, ranges were used. Temporal trends in biophysical parameters at each site, and those between participants from different SS groups, were evaluated for statistical significance using the Mann Whitney U test. Correlations between the biophysical responses on the cheek and neck were estimated using regression analysis and subsequent p-values were determined.

The values from each biophysical measurement for the SS groups were normalised with respect to their baseline value by calculating the ratio, thus estimating the fold changes in the biophysical parameters. This normalisation method allowed the comparison of values from different biophysical parameters in addition to the comparison of the values between SS groups and anatomical site. Furthermore, distinct thresholds were defined based on the following steps:

1. Calculate the fold changes for all participants.
2. Identify the 95th percentile value for each biophysical parameter at each anatomical location.
3. Round up the 95th percentile value such that 4 equal increments could be defined starting from 0.

It is noted that the temperature values were recorded by the temperature sensor in the TEWL probe and were not indicative of the actual skin temperature.

4.3 Results

22 volunteers participated in the study, as detailed in Table 4.3. It is noted that 18 individuals participated in all three sessions, while P6 participated in Session 1 only; P9 participated in Session 1 and only the cheek measurements of Session 2; and P10 and P15 participated in Sessions 1 and 2 only. Furthermore, TEWL and temperature values were not recorded for P11 in Session 2 on the neck due to malfunctioning of the probe. Additionally, the S-score results and SS Label for each participant have been reported.

Table 4.3 Participant details from the study. Where blank, the data was not available.

Participant No.	Age	Shaving tool (Blade/Rota/Combination)	Shaving Frequency (#/week)	S-score	SS Label
P1	37	Combination	< 2	66%	High SS
P2	42	Blade	< 2	69%	High SS
P3	50	Rota	< 2	59%	High SS
P4	47	Blade	> 5	63%	High SS
P5	35	Combination	> 5	46%	Mild SS
P6	54	-	-	75%	High SS
P7	53	Combination	3, 4	69%	High SS
P8	30	Combination	< 2	56%	High SS
P9	55	-	-	17%	Low SS
P10	49	-	-	17%	Low SS
P11	51	Rota	> 5	17%	Low SS
P12	53	Blade	> 5	28%	Low SS
P13	48	Combination	3, 4	52%	Mild SS
P14	50	Combination	3, 4	31%	Mild SS
P15	49	-	-	16%	Low SS
P16	49	Combination	> 5	46%	Mild SS
P17	48	Combination	> 5	41%	Mild SS
P18	48	Blade	3, 4	18%	Low SS
P19	51	Combination	> 5	37%	Mild SS
P20	53	Rota	> 5	23%	Low SS
P21	33	Combination	3, 4	52%	Mild SS
P22	42	Blade	3, 4	16%	Low SS

4.3.1 Baseline skin characteristics

The medians and inter-quartile values of the biophysical parameters at baseline for both the cheek and neck are summarised in Table 4.4. For each biophysical parameter, the median values on the neck are greater than that on the cheek for that session.

Table 4.4 Summary of the baseline values of the biophysical parameters at the three test sessions.

CHEEK		TEWL (g/m ² .h)	Hydration (a.u.)	Redness (a.u.)	Temperature (C)
Session 1	Median	10.8*	43.4	509.7	25.8**
	Quartiles (Q1, Q3)	(9.0, 12.6)	(39.3, 51.04)	(463.5, 538.2)	(25.1, 26.1)
Session 2	Median	10.2	40.5	471.6	23.9**
	Quartiles (Q1, Q3)	(8.8, 13.2)	(33.4, 46.8)	(405.6, 550.8)	(23.4, 24.2)
Session 3	Median	11.7	46.7	387.7	24.4**
	Quartiles (Q1, Q3)	(9.8,14.7)	(37.1, 57.2)	(368.2, 488.6)	(23.4, 24.7)
NECK		TEWL (g/m ² .h)	Hydration (a.u.)	Redness (a.u.)	Temperature (C)
Session 1	Median	13.5*	49.7	537.9	27.3**
	Quartiles (Q1, Q3)	(11.8, 17.6)	(42.1, 58.2)	(482.4, 655.1)	(26.8, 27.9)
Session 2	Median	12.6	41.4	487.6	26.4**
	Quartiles (Q1, Q3)	(10.7, 14.0)	(32.4, 46.7)	(456.4, 518.2)	(26.1, 26.6)
Session 3	Median	14.2	52.2	446.6	25.7**
	Quartiles (Q1, Q3)	(12.3, 15.6)	(42.8, 60.9)	(404.7, 488.8)	(25.2, 25.9)

* $p < 0.05$; ** $p < 0.001$

Figure 4.9 details the baseline values for each biophysical parameter on the cheek and neck for participants at all three sessions. For TEWL on the cheek, shown in Figure 4.9a, the difference in intra-subject TEWL values ranged from 0.1 to 20 g/m².h, with a median difference of 2.6 g/m².h. Furthermore, most of the participants (15/22 or 71%) demonstrated consistent values across the three sessions i.e., a difference between sessions on the cheek of less than 5g/m².h, emphasizing a good degree of reliability between tests. However, there was no evident trend in these values attributed to the test session. The corresponding baseline TEWL values on the neck are presented in Figure 4.9b. The difference in intra-subject TEWL values ranged from 0.5 to 21.4 g/m².h, with a median difference of 3.4 g/m².h. In a similar manner to the cheek, the participants demonstrated consistent TEWL values on the neck across the three sessions with 15/20 of the participants (75%) demonstrating a difference of less than 5 g/m².h. Close examination of the data revealed that in

10/20 of the participants (50%), the maximum TEWL value occurred during Session 1, whereas 9/20 (45%) demonstrated the minimum TEWL values during Session 2. It was noted that P16 has a large variation in TEWL values across the three sessions at both sites, with the maximum occurring during Session 3 for the cheek and Session 1 for the neck.

The individual baseline values for skin hydration on the cheek are presented in [Figure 4.9c](#). The intra-subject hydration values had a difference ranging between 4.3 a.u. to 27.1 a.u., with a median value of 12.6 a.u. Accordingly, some individuals e.g., P22, demonstrated a limited variation between sessions, while others e.g., P8 demonstrated a larger variation. Close examination of the data revealed that for 12/21 of the participants (57%), the maximum hydration values occurred during Session 3 whereas minimum values coincided with Session 2. Similarly, the baseline values for skin hydration on the neck are presented in [Figure 4.9d](#). The differences in the intra-subject hydration values ranged between 4.2 a.u. to 42.6 a.u. with a median value of 13.3 a.u., with P8 again demonstrating the largest variation. Furthermore, in a similar manner to the cheek, 12/20 of participants (60%) demonstrated maximum hydration values at Session 3 and a minimum at Session 2.

The individual baseline values for redness on the cheek are presented in [Figure 4.9e](#). A large intra-subject difference was observed in some participants with redness values ranging from 21.2 a.u. to 296.8 a.u. with a median value of 74.0 a.u. In 9/21 of the participants (43%) the difference in redness values on the cheek was greater than 100 a.u. across the sessions. For 11/21 participants (53%), the maximum redness values occurred during Session 1, whereas for 13/21 participants (62%) the minimum redness values occurred during Session 3. The corresponding baseline redness values on the neck are presented in [Figure 4.1f](#). It is noted that the intra-subject difference redness on the neck was larger than that observed on the cheek with values ranging from 24.0 a.u. to 269.4 a.u. with a median difference of 101.4 a.u. Indeed, 11/20 of the participants (55%) revealed a difference greater than 100 a.u. in redness values across sessions. However, in a similar manner to the cheek, n=14/21 participants (67%) demonstrated the maximum redness values occurred during Session 1, whereas for 13/21 participants (62%) the minimum redness values coincided with Session 3.

The individual baseline values for temperature on the cheek are presented in [Figure 4.9g](#). The intra-subject temperature values demonstrated differences ranging from 0.1°C to 3.6°C, with a median value of 2.1°C. In addition, it was evident that most participants (19/21, i.e., 90%) demonstrated the maximum temperature values at Session 1, whereas 13/21 participants (62%) demonstrated the minimum values at Session 2. The baseline temperatures on the neck are presented in [Figure 4.9h](#), with values markedly higher than that on the cheek. Interestingly, the intra-subject values on

the neck were smaller with the difference ranging from 0.3°C to 2.9°C and a median value of 1.6°C. It was evident that 16/20 participants (80%) demonstrated the maximum temperature values at Session 1, whereas 15/20 participants (71%) demonstrated the minimum values at Session 3.



Figure 4.9 Baseline values for all three sessions for (a) TEWL at cheek, (b) TEWL at neck, (c) Hydration at cheek, (d) Hydration at neck, (e) Redness at cheek, (f) Redness at neck, (g) Temperature at cheek, (h) Temperature at neck.

4.3.2 Temporal responses of the mechanical insults

The temporal changes in biophysical parameters following mechanical stimuli are presented with respect to the two anatomical locations. For each parameter, the baseline values have been denoted by $t=-1$. Subsequent measurement time intervals are denoted by $t=0$, $t=10$, $t=20$, and $t=30$ corresponding to 0 minutes, 10 minutes, 20 minutes, and 30 minutes post insult, respectively. Furthermore, the three sessions have been labelled based on the mechanical stimuli involved with Session 1 denoted by Tape Stripping, Session 2 by Friction, and Session 3 by Shaving.

The Mann Whitney test for statistical significance was used for differences between the values at baseline and subsequent measurement times. Only those differences which are statistically significant ($p < 0.05$) are indicated.

4.3.2.1 Temporal response to insults on the cheek

Figure 4.10 details the temporal changes in the median values for all parameters on the cheek for each of the three sessions. The results for Sessions 1 and 3 revealed increases in parameter values for each time point post tape stripping and shaving, respectively, with differences from baseline which were statistically significant in a large proportion of cases. By contrast, data from Session 2 generally revealed smaller variations in all the biophysical parameters, except for temperature. Indeed, following the friction stimulus there were fewer statistically significant differences.

Closer examination of the individual data for TEWL (Figure 4.10a), revealed that within each session a few participants e.g., P12 consistently demonstrated high outlier TEWL values following all three mechanical insults. For hydration (Figure 4.10b), there was a large variation in the cohort values as demonstrated by the spread in the quartile values. Although there appears to be a temporal increase in hydration values in Sessions 1 and 3, there were only two statistically significant differences compared to basal values, namely, at $t=0$ following tape stripping and at $t=30$ following shaving. Similarly, for the redness values (Figure 4.10c), a large spread was observed in the values at both baseline and post-insults. Furthermore, there appears to be a small temporal increase in the values in both Sessions 1 and 3, although no changes associated with Session 2. By contrast, the temperature values (Figure 4.10d), demonstrated a clear increase in values for all the time points following each of the stimuli, with differences from baseline which were all statistically significant. Furthermore, it is noted that for Session 3 involving shaving, the maximum temperature values occurred at $t=0$, although at subsequent time points the values were higher than baseline.

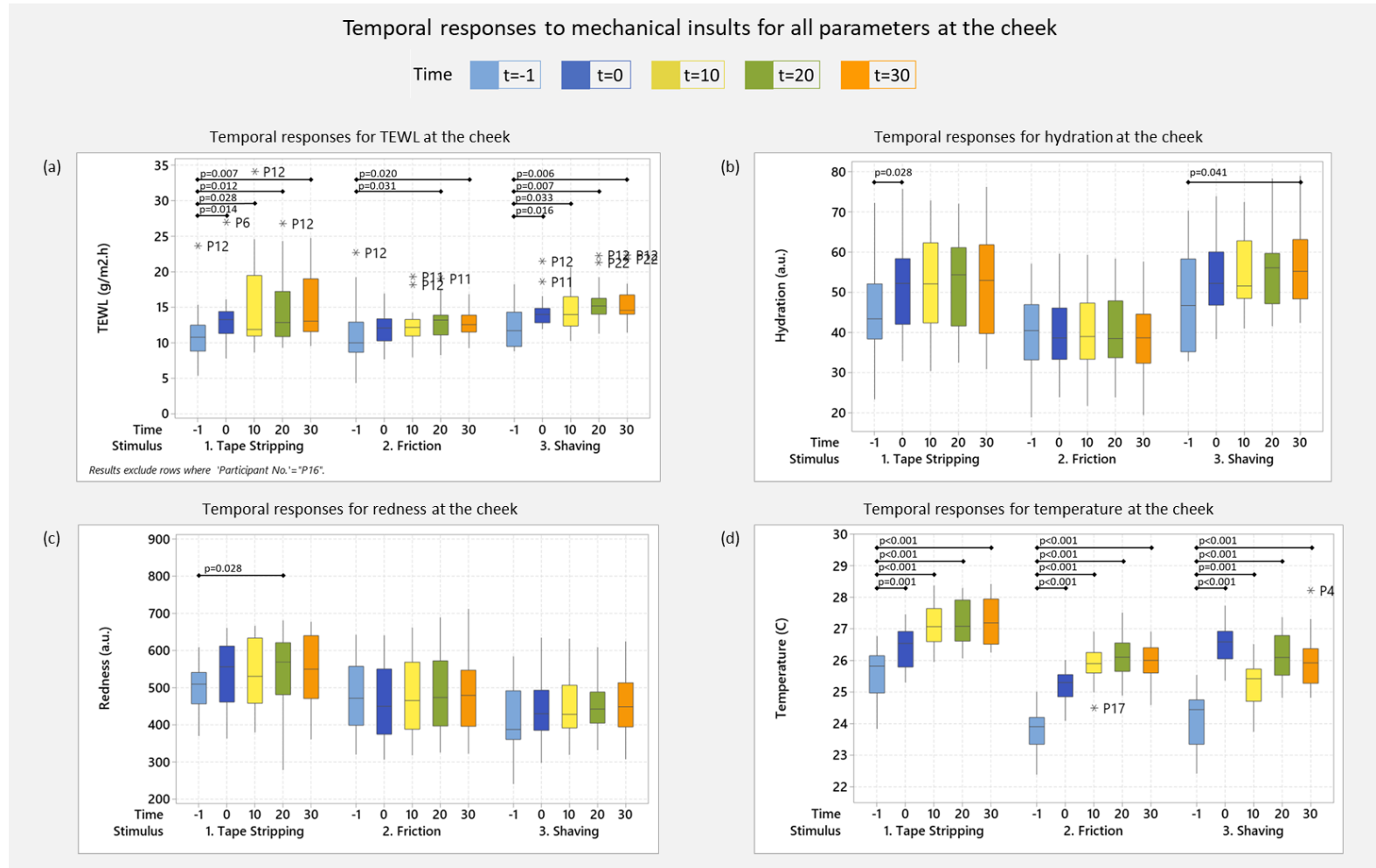


Figure 4.10 Temporal responses to the mechanical stimuli on the cheek for (a) TEWL, (b) Hydration, (c) Redness, (d) Temperature. Outlier values for individual participants are also indicated, as are statistically significant differences from baseline.

Table 4.5 details an alternative analysis of the individual data, namely, the number and percentage of participants that demonstrated fold changes in each biophysical parameter according to defined thresholds for each of the three mechanical stimuli on the cheek. Following the method detailed in Section 4.2.6, the threshold levels were defined as increments of 25% for TEWL, 10% for hydration, 8% for redness, and 3% for temperature.

There was a substantial proportion (33% – 72%) of participants who demonstrated an increase in TEWL values from baseline of at least 25% for each timepoint following all three mechanical insults. However, only in Session 1 were the increases greater than 50% as evidenced for 32%-45% of the cohort.

For skin hydration, clear differences in the skin responses were evident dependent on the nature of the stimuli. Specifically, it was noted that up to 48% of participants revealed a lower hydration value from baseline following the friction stimulus in Session 2, and which continued till 30 minutes post stimulus. By contrast, 50% – 67% of the participants demonstrated an increase of at least 10% in Session 3, and 36% – 59% of the participants demonstrated an increase of at least 20% in Session 1.

For redness, there were small differences in the percentages of participants demonstrating fold increases in values across the three test sessions. However, like that for hydration, 48% to 67% of individuals demonstrated a lower redness value from baseline following the friction stimulus in Session 2.

With respect to temperature changes, most participants demonstrated an increase from baseline of at least 3% for each timepoint following all three mechanical insults. For higher temperature changes of between 9% and 12%, a proportion of participants were implicated following some of the sessions at different timepoints. An example of this variation is evident in Session 3 which revealed 50% of participants demonstrating temperatures values above this threshold at time $t=0$ compared to 0% at $t=10$.

Table 4.5 Analysis of the fold changes in the biophysical parameters post stimulus for each test session on the cheek. Within each session for each biophysical parameter, the values have been shaded from white to blue in ascending order.

Parameter	Threshold (fold change)	Number (and percentage) of participants according to the threshold for the cheek											
		Session 1 (Tape stripping)				Session 2 (Friction)				Session 3 (Shaving)			
		t = 0	t = 10	t = 20	t = 30	t = 0	t = 10	t = 20	t = 30	t = 0	t = 10	t = 20	t = 30
TEWL	<= 0%	6 (27%)	4 (18%)	3 (14%)	4 (18%)	7 (33%)	3 (14%)	4 (19%)	3 (14%)	3 (17%)	2 (11%)	3 (17%)	3 (17%)
	> 0%	16 (73%)	18 (82%)	19 (86%)	18 (82%)	14 (67%)	18 (86%)	17 (81%)	18 (86%)	15 (83%)	16 (89%)	15 (83%)	15 (83%)
	> 25%	11 (50%)	14 (64%)	15 (68%)	14 (64%)	8 (38%)	9 (43%)	10 (48%)	13 (62%)	8 (44%)	6 (33%)	13 (72%)	13 (72%)
	> 50%	9 (41%)	9 (41%)	7 (32%)	10 (45%)	4 (19%)	1 (5%)	3 (14%)	3 (14%)	2 (11%)	0 (0%)	2 (11%)	1 (6%)
	> 75%	4 (18%)	3 (14%)	3 (14%)	4 (18%)	3 (14%)	1 (5%)	1 (5%)	1 (5%)	0 (0%)	0 (0%)	0 (0%)	0 (0%)
	> 100%	1 (5%)	1 (5%)	1 (5%)	1 (5%)	1 (5%)	0 (0%)	0 (0%)	1 (5%)	0 (0%)	0 (0%)	0 (0%)	0 (0%)
	> 100%	1 (5%)	1 (5%)	1 (5%)	1 (5%)	1 (5%)	0 (0%)	0 (0%)	1 (5%)	0 (0%)	0 (0%)	0 (0%)	0 (0%)
Hydration	<= 0%	0 (0%)	1 (5%)	4 (18%)	3 (14%)	10 (48%)	8 (38%)	8 (38%)	10 (48%)	4 (22%)	1 (6%)	1 (6%)	0 (0%)
	> 0%	22 (100%)	21 (95%)	18 (82%)	19 (86%)	11 (52%)	13 (62%)	13 (62%)	11 (52%)	14 (78%)	17 (94%)	17 (94%)	18 (100%)
	> 10%	16 (73%)	15 (68%)	18 (82%)	15 (68%)	3 (14%)	3 (14%)	3 (14%)	5 (24%)	9 (50%)	11 (61%)	11 (61%)	12 (67%)
	> 20%	12 (55%)	8 (36%)	10 (45%)	13 (59%)	1 (5%)	2 (10%)	2 (10%)	2 (10%)	5 (28%)	6 (33%)	5 (28%)	7 (39%)
	> 30%	3 (14%)	6 (27%)	6 (27%)	7 (32%)	0 (0%)	2 (10%)	1 (5%)	1 (5%)	5 (28%)	3 (17%)	4 (22%)	3 (17%)
	> 40%	1 (5%)	1 (5%)	2 (9%)	3 (14%)	0 (0%)	0 (0%)	0 (0%)	1 (5%)	1 (6%)	3 (17%)	2 (11%)	1 (6%)
	> 40%	1 (5%)	1 (5%)	2 (9%)	3 (14%)	0 (0%)	0 (0%)	0 (0%)	1 (5%)	1 (6%)	3 (17%)	2 (11%)	1 (6%)

Redness	<= 0%	4 (18%)	3 (14%)	2 (9%)	2 (9%)	14 (67%)	14 (67%)	10 (48%)	14 (67%)	6 (33%)	5 (28%)	5 (28%)	5 (28%)
	> 0%	18 (82%)	19 (86%)	20 (91%)	20 (91%)	7 (33%)	7 (33%)	11 (52%)	7 (33%)	12 (67%)	13 (72%)	13 (72%)	13 (72%)
	> 8%	12 (55%)	11 (50%)	12 (55%)	10 (45%)	1 (5%)	3 (14%)	3 (14%)	3 (14%)	8 (44%)	8 (44%)	9 (50%)	10 (56%)
	> 16%	2 (9%)	4 (18%)	6 (27%)	4 (18%)	1 (5%)	1 (5%)	1 (5%)	1 (5%)	6 (33%)	4 (22%)	3 (17%)	7 (39%)
	> 24%	1 (5%)	1 (5%)	0 (0%)	1 (5%)	1 (5%)	1 (5%)	1 (5%)	1 (5%)	1 (6%)	3 (17%)	3 (17%)	4 (22%)
	> 32%	0 (0%)	0 (0%)	0 (0%)	0 (0%)	1 (5%)	1 (5%)	1 (5%)	1 (5%)	0 (0%)	3 (17%)	2 (11%)	1 (6%)
	<= 0%	1 (5%)	0 (0%)	0 (0%)	0 (0%)	0 (0%)	0 (0%)	0 (0%)	0 (0%)	0 (0%)	0 (0%)	0 (0%)	0 (0%)
	> 0%	21 (95%)	22 (100%)	22 (100%)	22 (100%)	21 (100%)	21 (100%)	21 (100%)	21 (100%)	18 (100%)	18 (100%)	18 (100%)	18 (100%)
Temperature	> 3%	12 (55%)	21 (95%)	22 (100%)	22 (100%)	21 (100%)	21 (100%)	21 (100%)	21 (100%)	18 (100%)	16 (89%)	18 (100%)	18 (100%)
	> 6%	2 (9%)	11 (50%)	10 (45%)	11 (50%)	8 (38%)	18 (86%)	21 (100%)	19 (90%)	18 (100%)	3 (17%)	15 (83%)	13 (72%)
	> 9%	0 (0%)	2 (9%)	4 (18%)	5 (23%)	1 (5%)	7 (33%)	10 (48%)	10 (48%)	9 (50%)	0 (0%)	7 (39%)	5 (28%)
	> 12%	0 (0%)	0 (0%)	0 (0%)	0 (0%)	1 (5%)	2 (10%)	2 (10%)	2 (10%)	5 (28%)	0 (0%)	1 (6%)	0 (0%)

4.3.2.2 Temporal response to insult on the neck

Figure 4.11 details the temporal changes in the median values for all parameters on the neck for each of the three sessions. For hydration, redness, and temperature, the results from all three sessions revealed increases in values for each time point post stimulus. These increases were statistically different from baseline in a subset of the results. By contrast, data for TEWL revealed smaller variations for all stimuli, with a decrease in values at $t=0$, which was statistically significant only for Session 1 involving tape stripping. Furthermore, it was noted that the magnitude of the signal for all biophysical parameters was consistently lower for Session 2 when compared to Sessions 1 and 3.

Closer examination of the data revealed that for TEWL, as shown in Figure 4.11a, within each session a few participants demonstrated high outlier values. Indeed, P6 demonstrated consistently higher outlier values following tape stripping. For hydration and redness, as shown in Figure 4.11 (b) and (c) respectively, there was a large spread in the values between participants for all time points and sessions. However, this spread was significantly different from the basal values for redness during Sessions 1 and 3. By contrast, for temperature as shown in Figure 4.11d, there is a clear time-dependent change in Sessions 2 and 3. The values demonstrate an increase up to $t=20$, and then reduce slightly. It is noted that in Session 1, the temperature value peaks at $t=20$, although this difference was not statistically significant from baseline.

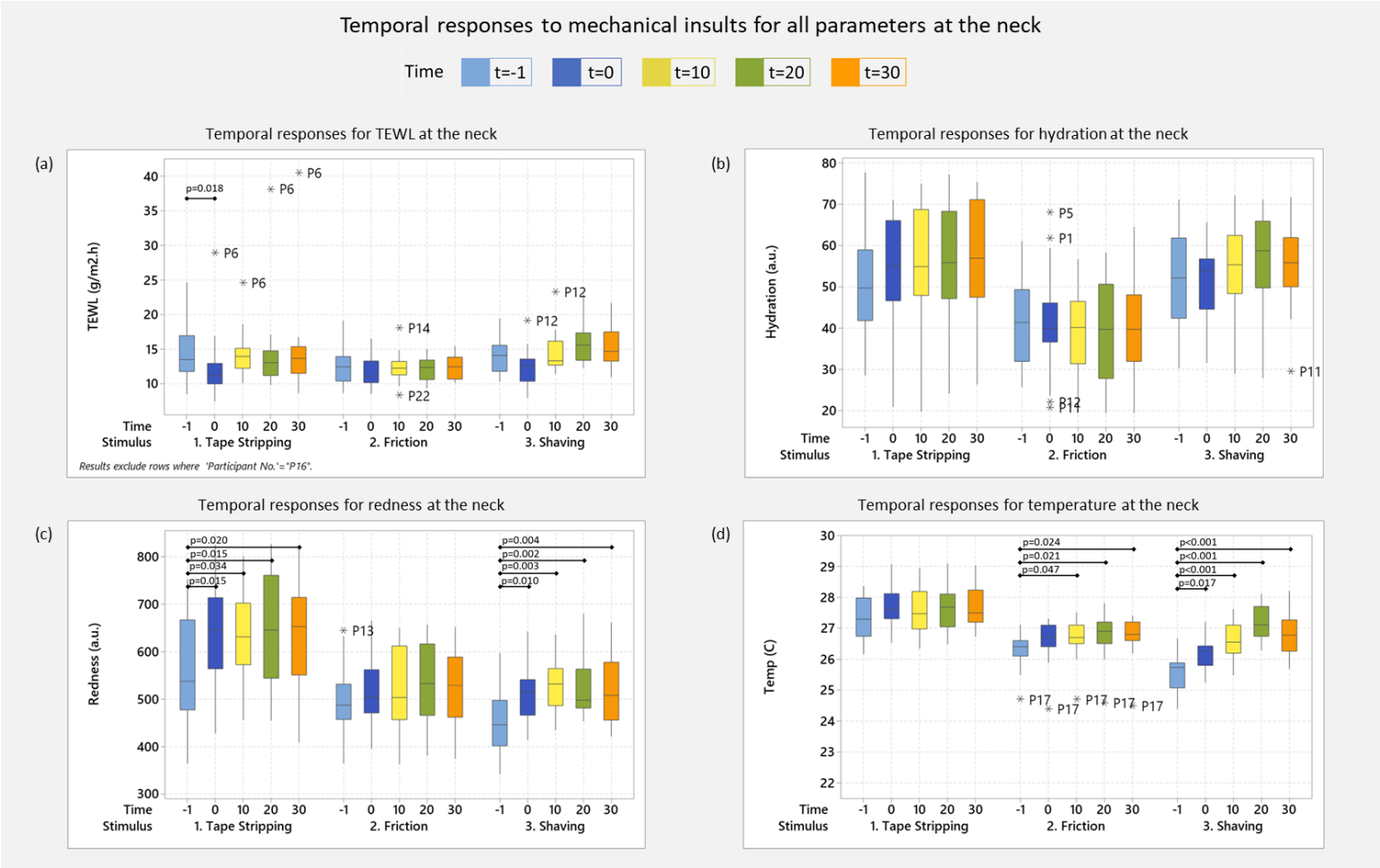


Figure 4.11 Temporal responses to the mechanical stimuli on the neck for (a) TEWL, (b) Hydration, (c) Redness, (d) Temperature. Outlier values for individual participants are also indicated, as are statistically significant differences from baseline.

Table 4.6 details the number and percentage of participants that demonstrated fold changes in the temporal biophysical parameters according to defined thresholds for each of the three mechanical stimuli on the neck. Similar to that on the cheek, the threshold levels were defined as increments of 25% for TEWL, 10% for hydration, 8% for redness, and 3% for temperature.

It is noted that for all parameters following all three stimuli, there was a large percentage of participants demonstrating a negative fold change from baseline. For TEWL, there were small differences in the percentages of participants demonstrating fold increases in values across the three test Session. However, there were some differences based on the nature of stimuli. For example, a range of 5% - 18% of the cohort exceeded this 50% threshold at the four time points in Session 1 (tape stripping), compared to 0% - 39% for Session 3 (shaving).

For hydration, clear differences in the skin responses were evident dependent on the nature of the stimuli. In Session 1, 27% - 50% of the cohort (i.e., 6 to 11 participants) revealed fold increases in values greater than 20%. By contrast, there were considerably fewer fold increases in skin hydration values during Sessions 2 and 3. For redness, there were small differences in the percentages of participants demonstrating fold increases in values across the three test sessions. For temperature, it was noted that all participants exceeding the 12% threshold corresponded to Session 3 only. For all three test sessions, fold increases were evident for a minimum of 16% of the cohort at all time points in excess of 3%. However, when the threshold was raised, there were some differences dependent on the nature of the stimuli. For example, the none of the participants exceeded a fold threshold of 9% for Sessions 1 and 2, whereas up to 4 participants (i.e., 22%) for exceeded this threshold in Session 3.

Table 4.6 Analysis of the fold changes in the biophysical parameters post stimulus for each test session on the neck. Within each session for each biophysical parameter, the values have been shaded from white to blue in ascending order.

Parameter	Threshold (fold change)	Number (and percentage) of participants according to the threshold for the neck											
		Session 1 (Tape stripping)				Session 2 (Friction)				Session 3 (Shaving)			
		t = 0	t = 10	t = 20	t = 30	t = 0	t = 10	t = 20	t = 30	t = 0	t = 10	t = 20	t = 30
TEWL	<= 0%	17 (77%)	10 (45%)	13 (59%)	13 (59%)	13 (68%)	10 (53%)	11 (58%)	10 (53%)	13 (72%)	6 (33%)	5 (28%)	5 (28%)
		5 (23%)	12 (55%)	9 (41%)	9 (41%)	6 (32%)	9 (47%)	8 (42%)	9 (47%)	5 (28%)	12 (67%)	13 (72%)	13 (72%)
	> 0%	3 (14%)	7 (32%)	5 (23%)	7 (32%)	2 (11%)	5 (26%)	4 (21%)	4 (21%)	2 (11%)	8 (44%)	12 (67%)	10 (56%)
		1 (5%)	2 (9%)	1 (5%)	4 (18%)	1 (5%)	3 (16%)	4 (21%)	4 (21%)	0 (0%)	5 (28%)	7 (39%)	7 (39%)
	> 25%	1 (5%)	1 (5%)	1 (5%)	2 (9%)	1 (5%)	3 (16%)	2 (11%)	3 (16%)	0 (0%)	2 (11%)	3 (17%)	5 (28%)
		1 (5%)	1 (5%)	1 (5%)	1 (5%)	1 (5%)	2 (11%)	1 (5%)	2 (11%)	0 (0%)	0 (0%)	2 (11%)	3 (17%)
	> 50%	1 (5%)	1 (5%)	1 (5%)	1 (5%)	1 (5%)	2 (11%)	1 (5%)	2 (11%)	0 (0%)	0 (0%)	2 (11%)	3 (17%)
		1 (5%)	1 (5%)	1 (5%)	1 (5%)	1 (5%)	2 (11%)	1 (5%)	2 (11%)	0 (0%)	0 (0%)	2 (11%)	3 (17%)
Hydration	<= 0%	4 (18%)	4 (18%)	6 (27%)	5 (23%)	10 (50%)	11 (55%)	11 (55%)	8 (40%)	9 (50%)	6 (33%)	5 (28%)	5 (28%)
		18 (82%)	18 (82%)	16 (73%)	17 (77%)	10 (50%)	9 (45%)	9 (45%)	12 (60%)	9 (50%)	12 (67%)	13 (72%)	13 (72%)
	> 0%	12 (55%)	16 (73%)	13 (59%)	15 (68%)	6 (30%)	5 (25%)	7 (35%)	6 (30%)	5 (28%)	8 (44%)	8 (44%)	9 (50%)
		6 (27%)	9 (41%)	11 (50%)	11 (50%)	4 (20%)	2 (10%)	4 (20%)	4 (20%)	2 (11%)	6 (33%)	7 (39%)	7 (39%)
	> 10%	3 (14%)	3 (14%)	6 (27%)	4 (18%)	2 (10%)	1 (5%)	3 (15%)	2 (10%)	1 (6%)	2 (11%)	2 (11%)	2 (11%)
		1 (5%)	1 (5%)	0 (0%)	2 (9%)	1 (5%)	1 (5%)	1 (5%)	0 (0%)	1 (6%)	1 (6%)	1 (6%)	2 (11%)
	> 20%	1 (5%)	1 (5%)	0 (0%)	2 (9%)	1 (5%)	1 (5%)	1 (5%)	0 (0%)	1 (6%)	1 (6%)	1 (6%)	2 (11%)
		1 (5%)	1 (5%)	0 (0%)	2 (9%)	1 (5%)	1 (5%)	1 (5%)	0 (0%)	1 (6%)	1 (6%)	1 (6%)	2 (11%)

Redness	<= 0%	1 (5%)	1 (5%)	0 (0%)	0 (0%)	7 (35%)	5 (25%)	4 (20%)	6 (30%)	2 (11%)	1 (6%)	1 (6%)	2 (11%)
		21 (95%)	21 (95%)	22 (100%)	22 (100%)	13 (65%)	15 (75%)	16 (80%)	14 (70%)	16 (89%)	17 (94%)	17 (94%)	16 (89%)
	> 0%	13 (59%)	12 (55%)	13 (59%)	12 (55%)	7 (35%)	9 (45%)	7 (35%)	5 (25%)	11 (61%)	11 (61%)	12 (67%)	11 (61%)
		4 (18%)	5 (23%)	4 (18%)	3 (14%)	1 (5%)	3 (15%)	3 (15%)	3 (15%)	4 (22%)	5 (28%)	5 (28%)	5 (28%)
	> 8%	2 (9%)	2 (9%)	2 (9%)	2 (9%)	1 (5%)	1 (5%)	1 (5%)	1 (5%)	1 (6%)	2 (11%)	3 (17%)	3 (17%)
		2 (9%)	2 (9%)	2 (9%)	2 (9%)	0 (0%)	0 (0%)	0 (0%)	0 (0%)	1 (6%)	1 (6%)	2 (11%)	1 (6%)
	> 16%	2 (9%)	2 (9%)	2 (9%)	2 (9%)	0 (0%)	0 (0%)	0 (0%)	0 (0%)	1 (6%)	1 (6%)	2 (11%)	1 (6%)
		2 (9%)	2 (9%)	2 (9%)	2 (9%)	0 (0%)	0 (0%)	0 (0%)	0 (0%)	1 (6%)	1 (6%)	2 (11%)	1 (6%)
Temperature	<= 0%	3 (14%)	6 (27%)	6 (27%)	8 (36%)	4 (21%)	7 (37%)	5 (26%)	3 (16%)	2 (11%)	0 (0%)	0 (0%)	0 (0%)
		19 (86%)	16 (73%)	16 (73%)	14 (64%)	15 (79%)	12 (63%)	14 (74%)	16 (84%)	16 (89%)	18 (100%)	18 (100%)	18 (100%)
	> 0%	6 (27%)	5 (23%)	9 (41%)	8 (36%)	3 (16%)	7 (37%)	9 (47%)	5 (26%)	9 (50%)	14 (78%)	18 (100%)	15 (83%)
		2 (9%)	3 (14%)	2 (9%)	1 (5%)	1 (5%)	1 (5%)	2 (11%)	2 (11%)	1 (6%)	9 (50%)	17 (94%)	9 (50%)
	> 3%	0 (0%)	0 (0%)	0 (0%)	0 (0%)	0 (0%)	0 (0%)	0 (0%)	0 (0%)	0 (0%)	2 (11%)	9 (50%)	6 (33%)
		0 (0%)	0 (0%)	0 (0%)	0 (0%)	0 (0%)	0 (0%)	0 (0%)	0 (0%)	0 (0%)	0 (0%)	4 (22%)	2 (11%)
	> 6%	0 (0%)	0 (0%)	0 (0%)	0 (0%)	0 (0%)	0 (0%)	0 (0%)	0 (0%)	0 (0%)	0 (0%)	4 (22%)	2 (11%)
		0 (0%)	0 (0%)	0 (0%)	0 (0%)	0 (0%)	0 (0%)	0 (0%)	0 (0%)	0 (0%)	0 (0%)	4 (22%)	2 (11%)

4.3.3 Comparison of the skin responses between the cheek and neck

4.3.3.1 Cheek and neck relationship for Session 1

The relationships between the TEWL values on the cheek and the neck for Session 1 involving tape stripping are presented in Figure 4.12. It is noted that the plots have axes till 30 g/m².h, except at t = 10, where the axes have been extended till 40 g/m².h. The linear models indicate that TEWL on the neck is greater than that on the cheek for all time points, as determined by the positive intercept of the regression equations. It is noted that the slope of the linear models is at a maximum immediately after the stimulus i.e., t=0, and at a minimum at t=10.

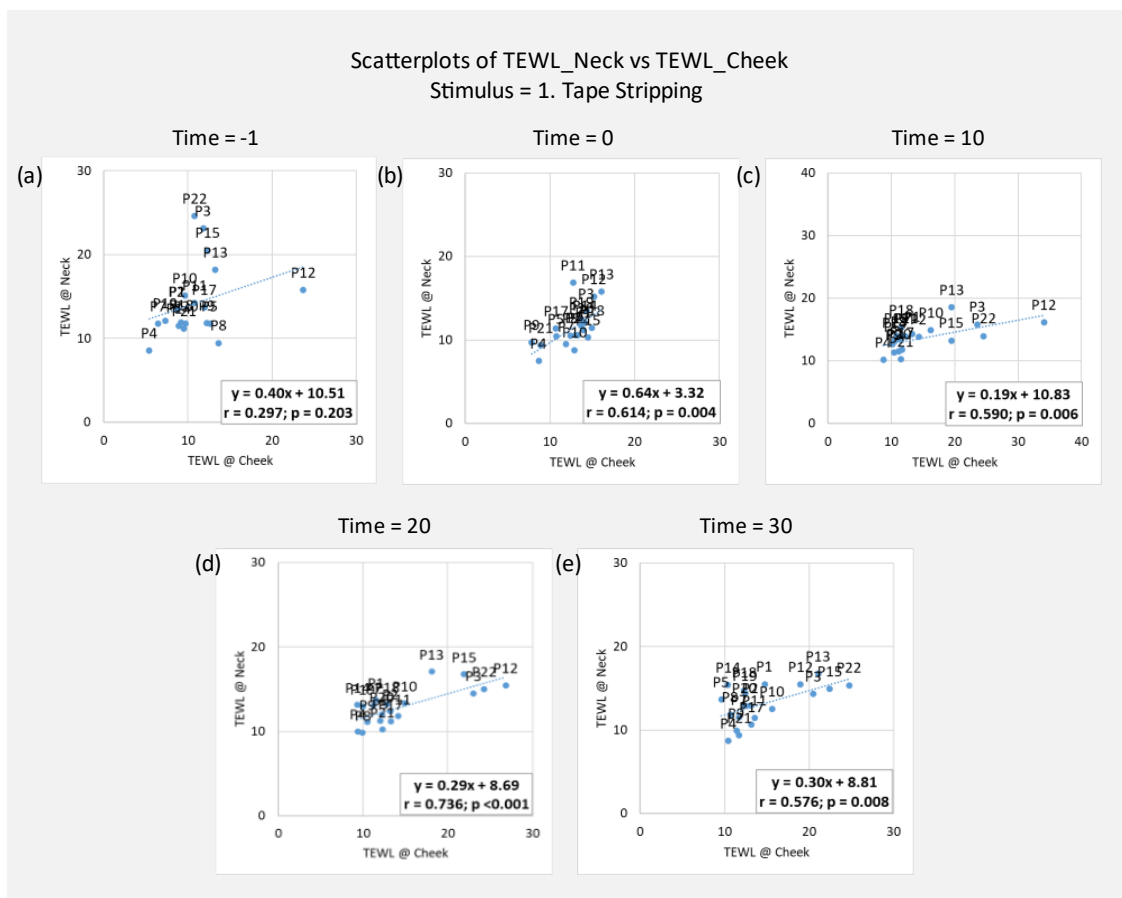


Figure 4.12 Relationship between the TEWL on the cheek and the neck for Session 1 at (a) Time = -1, (b) Time = 0, (c) Time = 10, (d) Time = 20, (e) Time = 30.

The corresponding relationships between the skin hydration values on the cheek and the neck for Session 1 are presented in Figure 4.13. The linear models indicate that hydration on the neck is greater than that on the cheek for all time points, as determined by the positive intercept of the regression equations. It is noted that the hydration data is more consistent than the TEWL data with linear models at all times statistically significant with corresponding slopes ranging from 0.69 to 0.84.

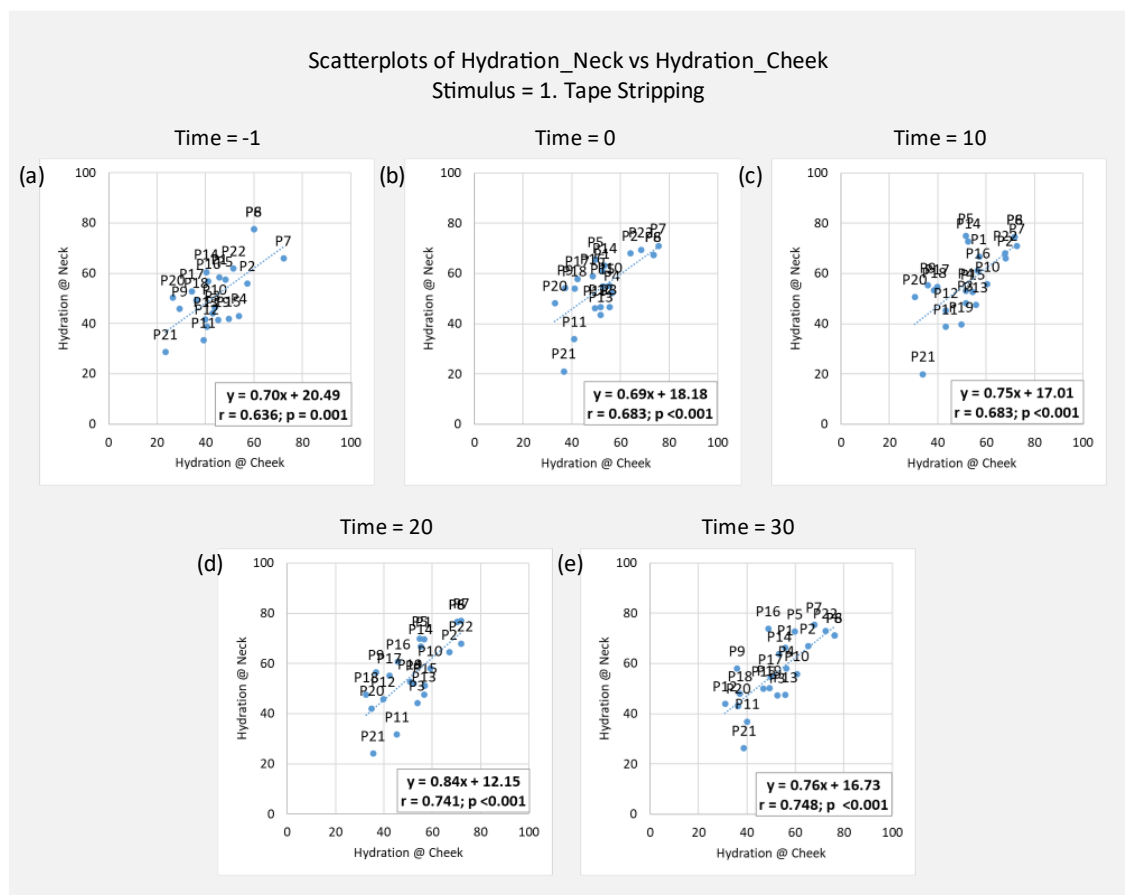


Figure 4.13 Relationship between the skin hydration on the cheek and the neck for Session 1 at

(a) Time = -1, (b) Time = 0, (c) Time = 10, (d) Time = 20, (e) Time = 30.

The relationships between the redness on the cheek and the neck for Session 1 are presented in Figure 4.14. The linear models indicate that redness on the neck is always greater than that on the cheek for all time points, as determined by the positive intercept of the regression. It is noted that the redness data is fairly consistent with linear models at time points post stimuli statistically significant with corresponding slopes ranging from 0.70 to 0.88.

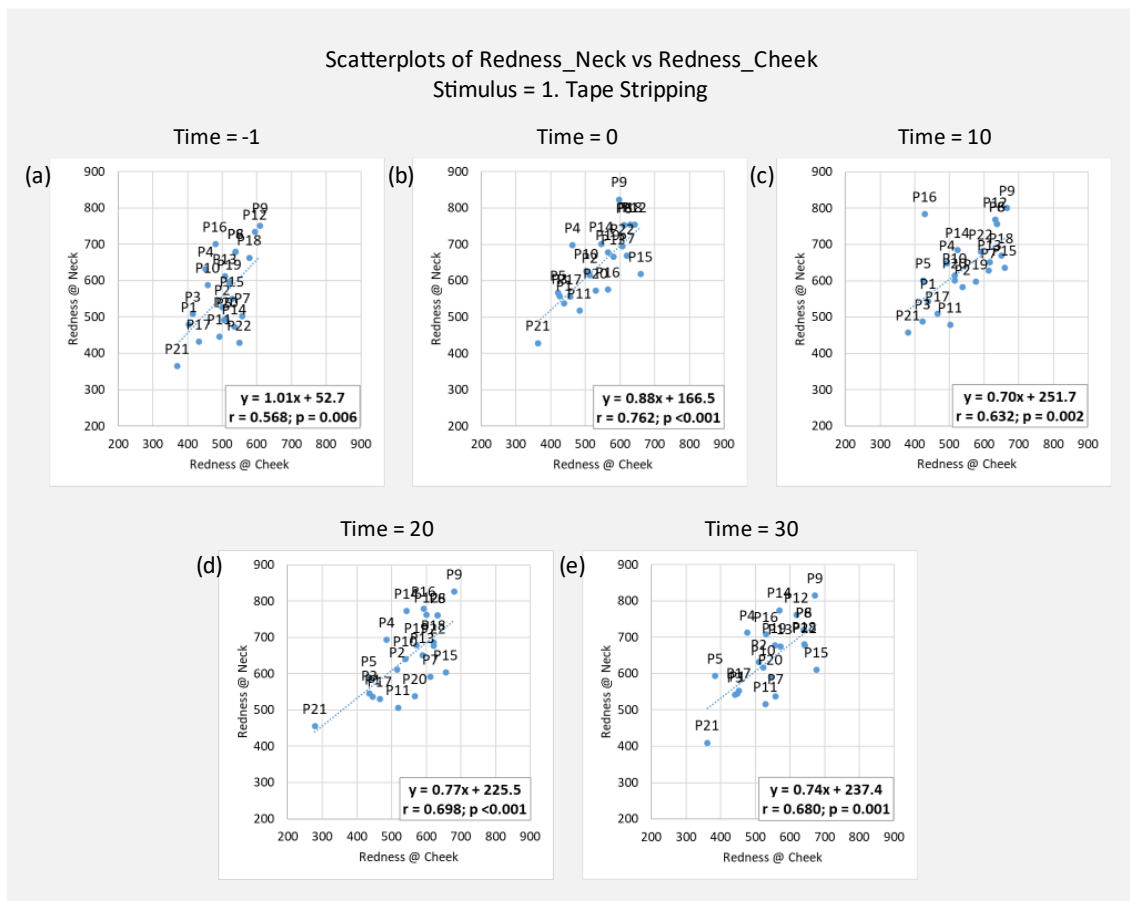


Figure 4.14 Relationship between the redness on the cheek and the neck for Session 1 at (a) Time = -1, (b) Time = 0, (c) Time = 10, (d) Time = 20, (e) Time = 30.

The relationships between the skin temperature on the cheek and the neck for Session 1 are presented in Figure 4.15. The linear models indicate that the temperature on the neck is greater than that on the cheek for all time points, as determined by the positive intercept of the regression equations. It is noted that the temperature data is consistent with linear models at time points yield a statistically significant slope with values increasing across the time points from 0.44 to 0.67.

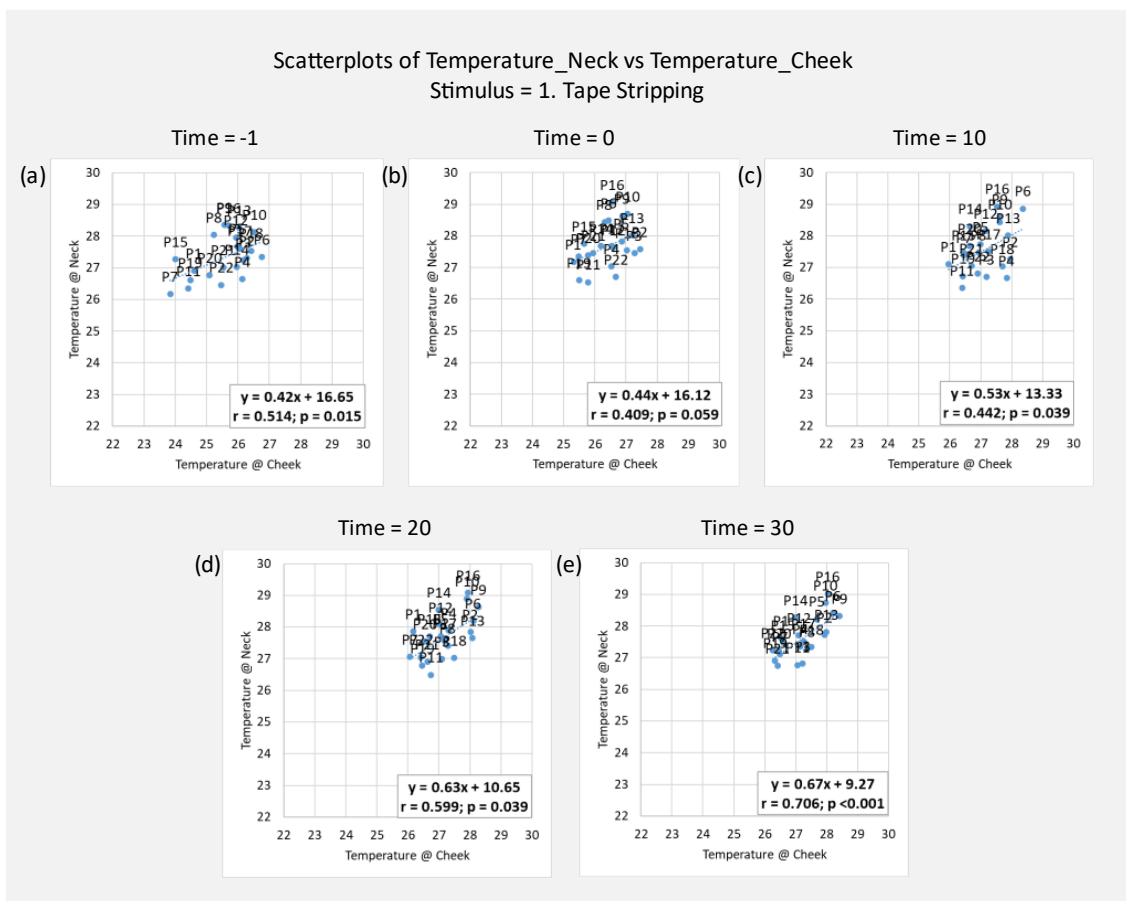


Figure 4.15 Relationship between the temperature on the cheek and the neck for Session 1 at (a) Time = -1, (b) Time = 0, (c) Time = 10, (d) Time = 20, (e) Time = 30.

4.3.3.2 Cheek and neck relationship for Session 2

The relationship between the TEWL values on the cheek and the neck for Session 2 has been demonstrated in [Figure 4.16](#). This model indicates that TEWL on the neck is generally greater than that on the cheek, further confirmed by the positive intercept of the regression equation. However, there is a temporal influence on this relationship which is depicted by the different slopes at each measurement interval. Specifically, at $t = 0$ and $t = 20$, the slope is positive while at $t = 10$ and $t = 30$, the slope is negative.

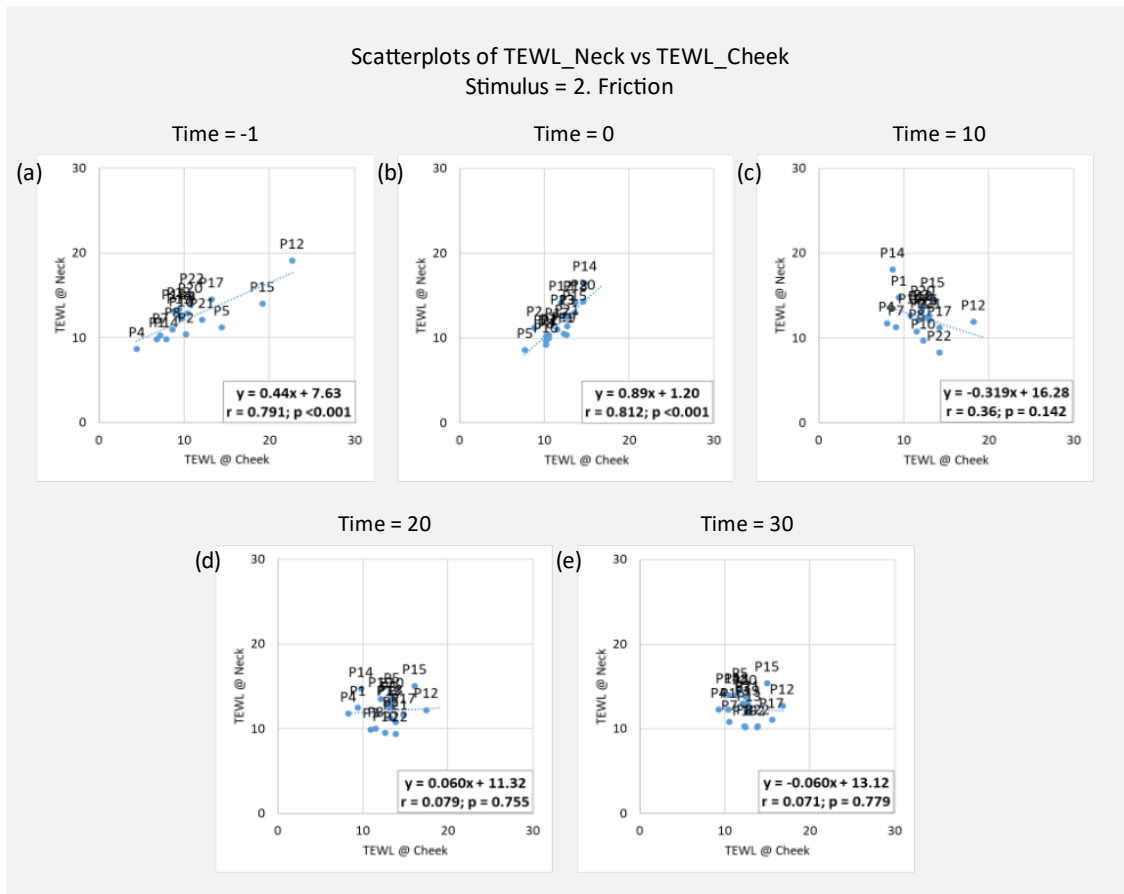


Figure 4.16 Relationship between the TEWL on the cheek and the neck for Session 2 at (a) Time = -1, (b) Time = 0, (c) Time = 10, (d) Time = 20, (e) Time = 30.

The relationship between the cheek and neck during Session 2 for hydration, redness, and temperature have been shown in [Appendix C](#) as they are like those revealed in Session 1. The models indicates that each biophysical parameter has a value on the neck is that is always greater than that on the cheek.

4.3.3.3 Cheek and neck relationship for Session 3

The relationship between the TEWL on the cheek and the neck for Session 3 has been demonstrated in Figure 4.17. Like Session 1, this model indicates that TEWL on the neck is always greater than that on the cheek, further confirmed by the positive intercept of the regression equations. At baseline, it is noted that P11 and P14 influence the trend, which is otherwise highly linear. Furthermore, the modelled relationship post stimulus is fairly consistent with that at baseline, except at t=30 where the slope changes from 0.43 to 0.22.

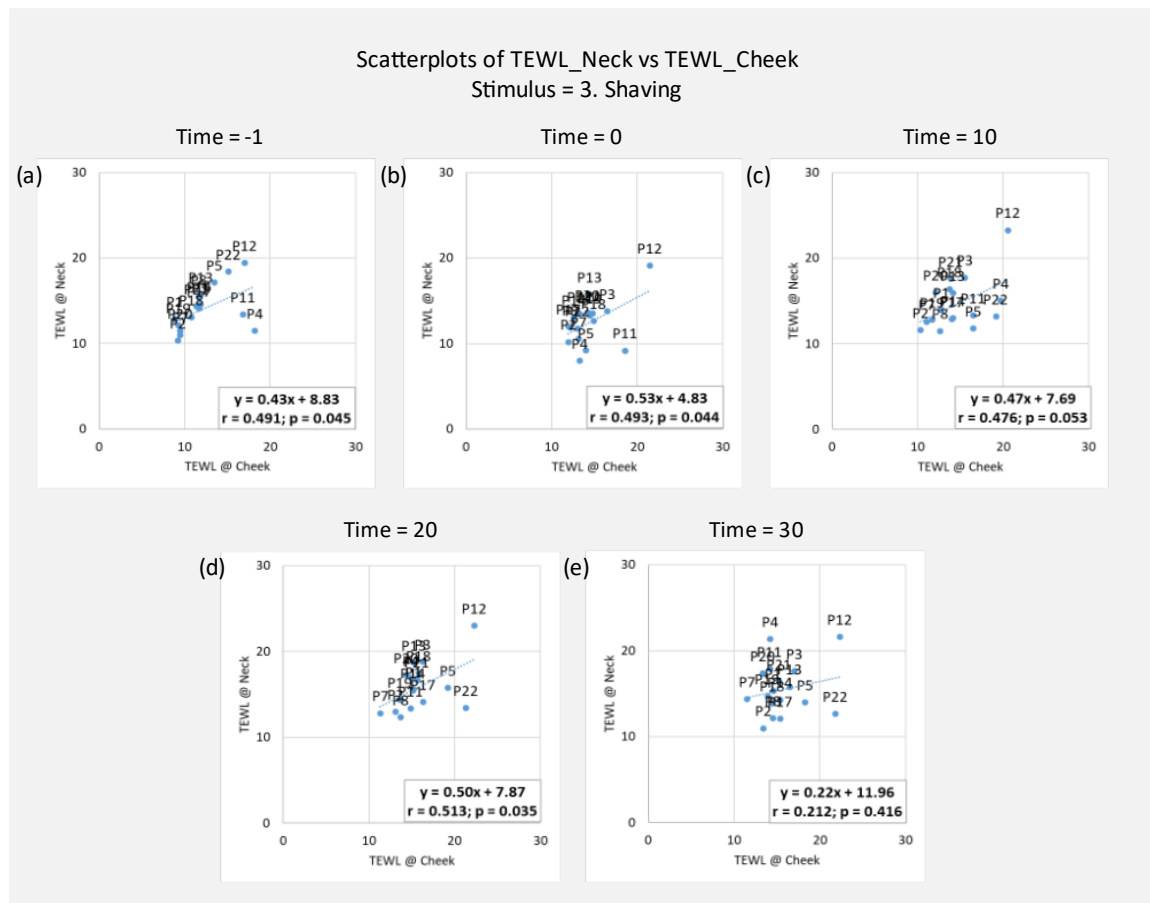


Figure 4.17 Relationship between the TEWL on the cheek and the neck for Session 3 at (a) Time = -1, (b) Time = 0, (c) Time = 10, (d) Time = 20, (e) Time = 30.

The relationship between the cheek and neck during Session 3 for hydration, redness, and temperature have been shown in the Appendix C as they are similar to those revealed in Session 1. The models indicate that each biophysical parameter has a value on the neck is that is always greater than that on the cheek.

4.3.4 Comparison of skin responses between participants categorised with different skin sensitivity

4.3.4.1 TEWL

Figure 4.18 details the temporal changes in the TEWL values for participants categorized by their respective SS labels. On the cheek (Figure 4.18a), the median TEWL values varied between the SS categories for each session. Specifically, the lowest baseline values corresponded to the participants of the High SS group with the median TEWL values ranging from 7.2 g/m²h to 9.5 g/m²h across the sessions. Whereas the Mild and Low SS groups had a median baseline TEWL ranging from 10.4 g/m²h to 15.1 g/m²h in Sessions 1-3. However, this difference was only statistically significant ($p < 0.05$) for Session 2 when comparing the Mild and the High SS groups. Subsequently, following the mechanical stimuli in each session, the Low SS group demonstrated consistently highest TEWL values at all time points post stimulus. However, a large spread was observed between participants within each group. Specifically, following the tape stripping stimulus, the Low SS group demonstrated inter-quartile values ranging from 3.11 g/m²h to 10.91 g/m²h. Subsequently, the differences in TEWL values between the SS groups were revealed to be significant only at $t=10$ and $t=30$ following the friction insult in Session 2. Additionally, it is noted that in Session 2, the High SS group showed statistically significant differences from the Mild SS group at $t = 10$ and $t = 20$, with median values for the High SS group ranging from 12.6 g/m²h to 13.4 g/m²h and those for the Mild SS group ranging from 9.4 g/m²h to 10.9 g/m²h. By contrast, there were smaller non-statistically significant variations between the Low and Mild SS groups.

For TEWL on the neck (Figure 4.18b), the baseline values clearly revealed differences between the SS categories for Sessions 2 and 3. Specifically, the High SS group demonstrated lower baseline TEWL values when compared to the Mild SS group, with medians ranging from 10.3 g/m²h to 11.46 g/m²h for the High SS group and 12.6 g/m²h to 14.56 g/m²h for the Mild SS group. Furthermore, the High SS group also demonstrated significant differences ($p < 0.05$) in baseline TEWL when compared to the Low SS group with median values ranging from 10.3 g/m²h to 13.55 g/m²h. By contrast, smaller variations in TEWL values were evident across the different sessions for each time point post stimuli.

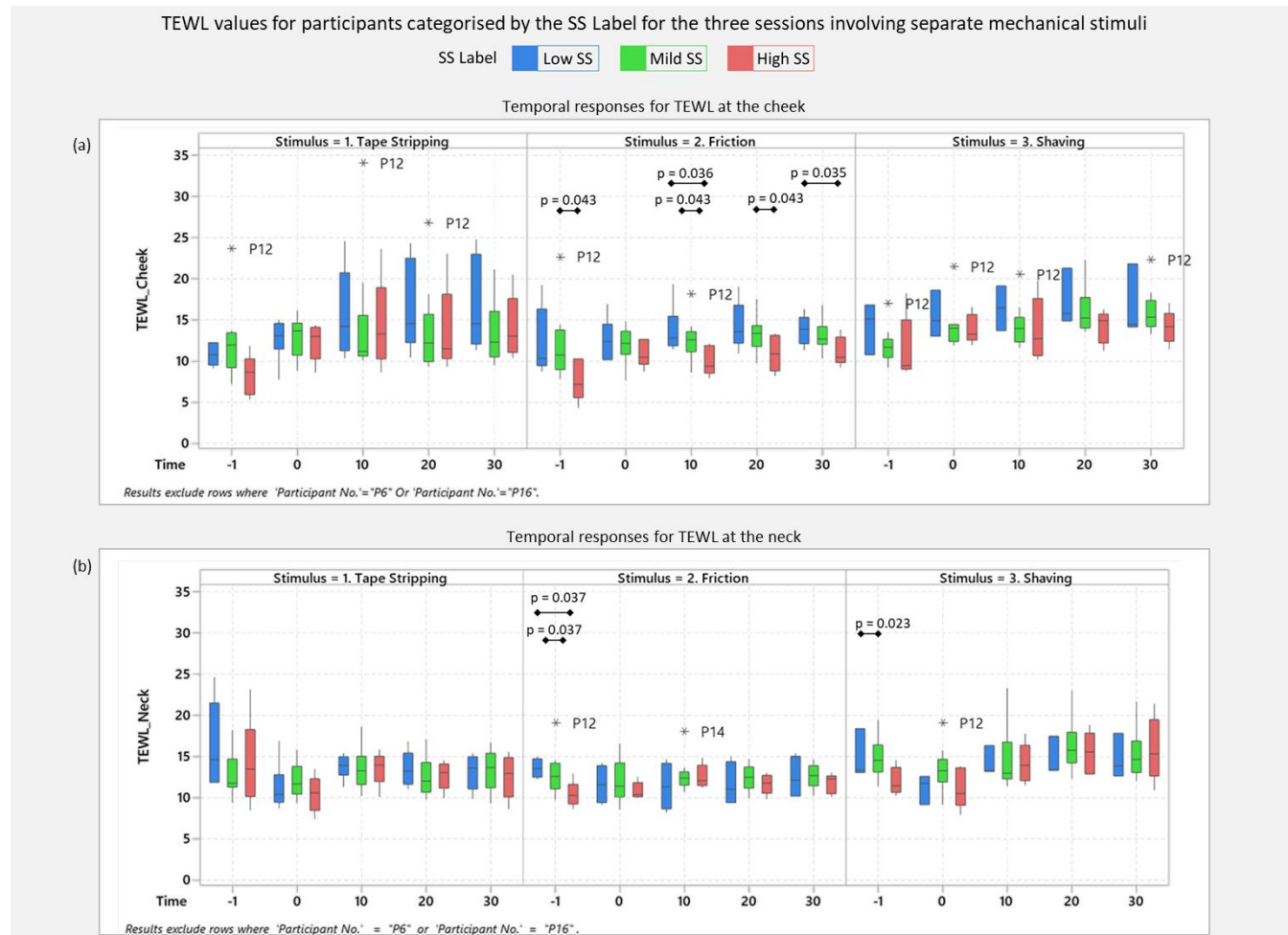


Figure 4.18 TEWL values for each SS category for the three sessions involving separate mechanical insults on the (a) cheek and (b) neck. Outlier values for individual participants are also indicated, as are significant differences ($p < 0.05$) between the SS categories.

4.3.4.2 Hydration

Figure 4.19 details the temporal changes in the hydration values for participants categorized by the SS labels. At baseline for each session, the hydration for the High SS group corresponded to the highest values with the medians ranging from 46.8 a.u. to 59.5 a.u. on the cheek and 45.3 a.u. to 66.4 a.u. on the neck. Whereas the Mild and Low SS groups had a median baseline hydration ranging from 37.9 a.u. to 46.7 a.u. on the cheek and 37.1 a.u. to 52 a.u. on the neck in Sessions 1-3. However, this difference was only statistically significant on the cheek (Figure 4.19a) for Session 1. Following the different stimuli in each session on the cheek, the High SS group continued to reveal the highest median hydration values when compared to the other groups. Indeed, this difference was statistically significant ($p < 0.05$) between the High and Mild SS groups at $t=0$, $t=20$, and $t=30$ for Sessions 1 and 2, with median hydration values ranging from 44.9 a.u. to 61.87 a.u. for the High SS group and 34.45 a.u. to 49.69 a.u. for the Mild SS group. Furthermore, this difference was statistically significant between the High and Low SS groups only at $t=20$ for Session 2. By contrast, there were smaller variations evident between the Low and Mild SS groups, which were not statistically significant.

For hydration on the neck (Figure 4.19b), the groups clearly reveal a large proportion of overlapping values with the High SS group demonstrating highest median hydration values at a majority of time points across all sessions. However, no statistically significant differences were determined for hydration values on the neck between the different SS categories for any of the sessions.

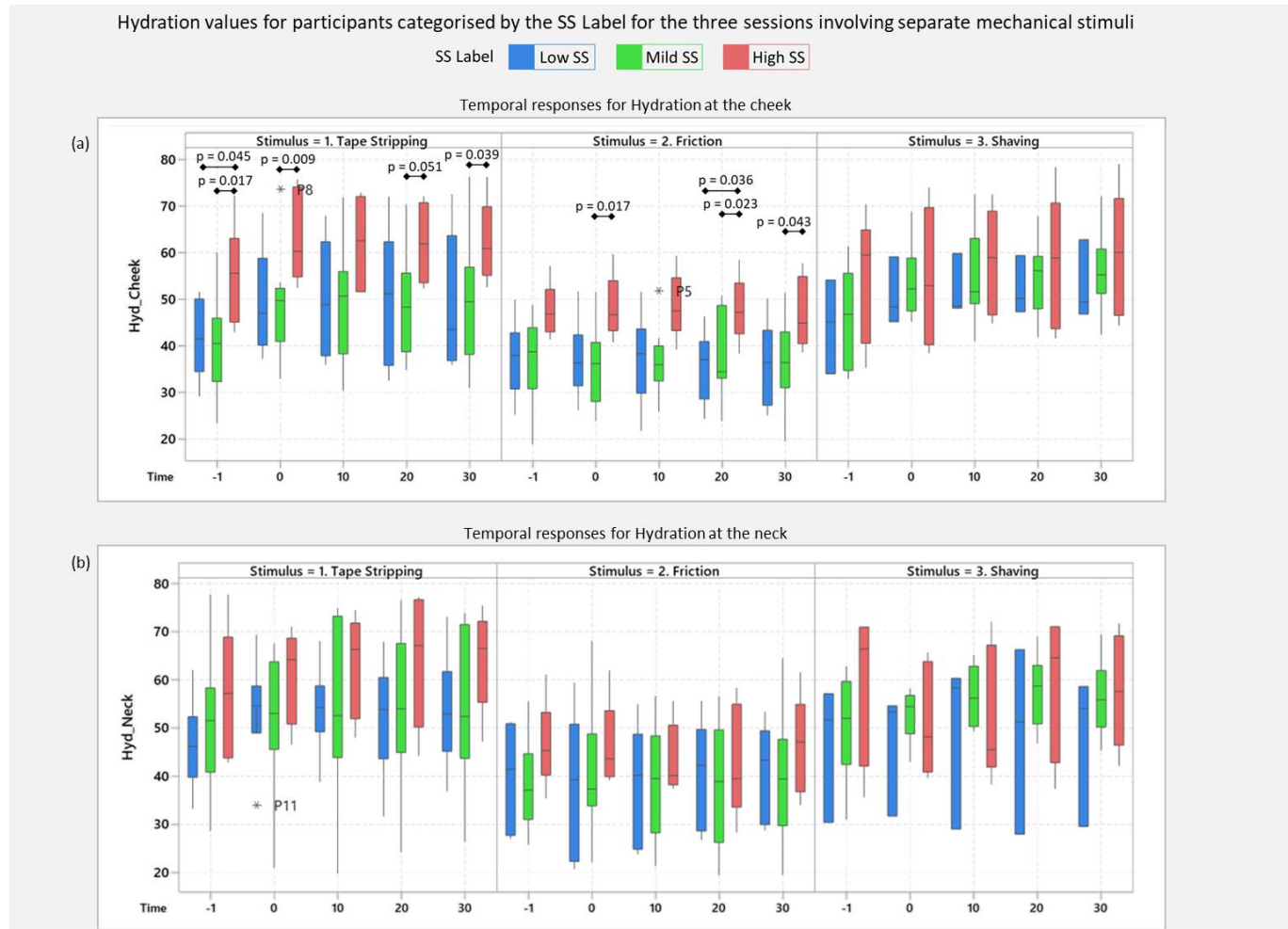


Figure 4.19 Hydration values for each SS category for the three sessions involving separate mechanical insults on the (a) cheek and (b) neck. Outlier values for individual participants are also indicated, as are significant differences ($p < 0.05$) between the SS categories.

4.3.4.3 Redness

Figure 4.20 details the temporal changes in the redness values for participants categorized by the SS labels. Interestingly, it is noted that for most sessions on the cheek and neck, the High SS group revealed the lowest median redness values. Furthermore, it is noted that the Mild SS group revealed peak median redness values at $t=20$ and $t=30$. However, due to the large spread in the values, no statistically significant differences were observed between the different groups. Following tape stripping on the cheek in Session 1 (Figure 4.20a), the Low SS group demonstrated the highest redness values, with the median redness ranging from 606.6 a.u. to 642.3 a.u. This difference was statistically significant only at $t=30$ between the High and Low SS groups, where median redness was observed to be 587.9 a.u. and 647 a.u. respectively.

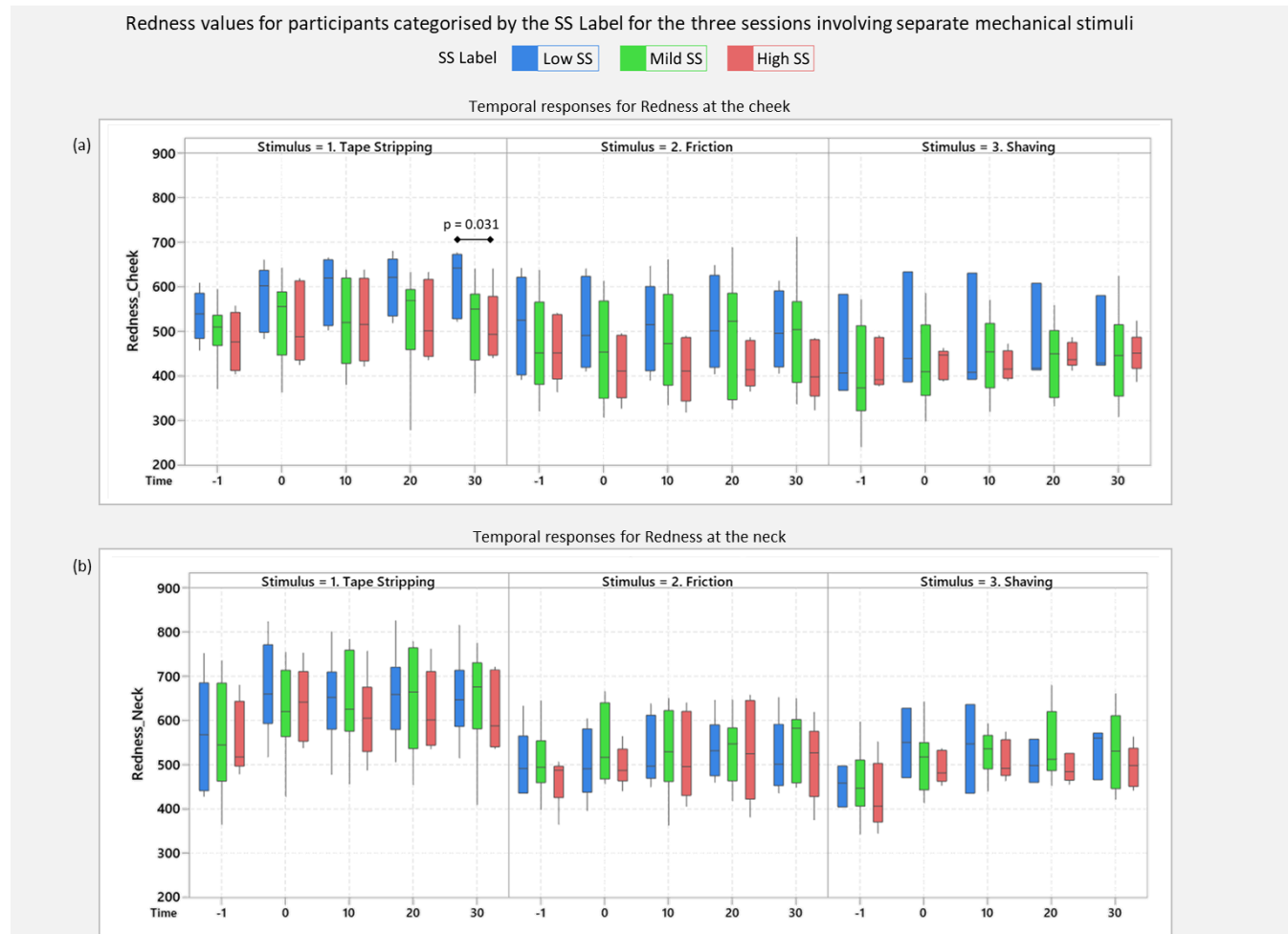


Figure 4.20 Redness values for each SS category for the three sessions involving separate mechanical insults on the (a) cheek and (b) neck. Outlier values for individual participants are also indicated, as are significant differences ($p < 0.05$) between the SS categories.

4.3.4.4 Temperature

Figure 4.21 details the temporal changes in the temperature values for participants categorized by the SS labels. It is noted that for most sessions at baseline, the High SS group demonstrated the highest temperature values with medians ranging from 24.1°C to 26.16°C on the cheek and 25.96°C to 27.07°C on the neck. The exception was observed for Session 1 on the neck (Figure 4.21b), where the High SS group revealed the lowest basal median temperature values. Furthermore, following the mechanical stimulus, the High SS group continued to reveal the higher temperature values for Sessions 2 and 3. However, this difference was statistically significant only between the Mild and the High SS groups. Specifically, on the cheek (Figure 4.21a), at t=30 for Session 3, the median temperatures were observed as 25.66°C for the Mild SS group and 26.37°C for the High SS group. Furthermore, on the neck, at t=0 for Session 2, the median temperature was observed as 26.4°C and 27.1°C for the Mild and High SS groups respectively. It was noted that one participant (P17) from the Mild SS group demonstrated consistently low outlier temperature values in Session 2. For Sessions 1 and 3, no such trends were observed.



Figure 4.21 Temperature values for each SS category for the three sessions involving separate mechanical insults on the (a) cheek and (b) neck. Outlier values for individual participants are also indicated, as are significant differences ($p < 0.05$) between the SS categories.

4.4 Discussion

The aim of this study was to evaluate inter- and intra- subject variability in skin response due to mechanical insults in consumer cohort of male shavers (Section 4.1). Specifically, the basal and transient skin characteristics were examined across individuals with reported differences in perceived skin sensitivities. The study was completed over three test sessions, each involving a distinct mechanical stimulus on the cheek and neck. An array of skin parameters selected following the literature review (Section 2.3) were assessed to evaluate the basal characteristics and corresponding post-insult response (Chaturvedi et al. 2021).

In the present study, participants were purposefully selected based on a self-assessment of skin sensitivity (S-score), providing categories of perceived SS. Six months later, at the end of the study, the participants were re-assessed. Strikingly, out of the 18 participants who completed both assessments, all but one (P7), showed changes in some of their scoring. This corresponded to a increase/decrease in the S-scores such that 6 participants demonstrated a change in the SS category, where 3 participants moved from High SS to Mild SS, 2 participants moved from Mild SS to Low SS, and 1 participant moved from Low SS to Mild SS (Table 4.7). A modification was thus proposed (detailed in Section 4.2.3) where the average of the S-scores from the two assessments was considered for the final SS category grouping. However, it remains to be investigated whether the inherent variability associated with the self-assessed skin sensitivity is due to objectifiable changes in skin parameters.

For the biophysical parameters at baseline and post stimulus, very few statistically significant differences were observed between the different SS groups (Figure 4.18 - Figure 4.21). On closer examination of the data, at baseline, it was observed that the High SS group demonstrated the lowest TEWL values ($p < 0.05$ in Session 2, for the cheek and neck) and the highest hydration values ($p < 0.05$ in Session 1 on the cheek). These findings contrast previous studies where it was found that individuals with SS demonstrated higher TEWL and lower hydration values when compared to those without SS (Muizzuddin et al. 1998; Seidenari et al. 1998; Roussaki-Schulze et al. 2005; Farage et al. 2006; Falcone et al. 2017). However, the clinical significance of this small, yet statistically significant difference is unknown and requires further investigation. Following mechanical stimulation on the cheek, the High SS group exhibited significant increases at specific measurement times ($t = 0, 20, 30$) for both tape stripping and frictional stimulus, but not for shaving. However, as the basal values for this group were also elevated, it is uncertain if the subsequent difference between groups was in response to the stimulus alone.

Table 4.7 Summary of responses from SS questionnaire in July and December. Only 18 participants completed both assessments. Where blank, the response stayed the same. The corresponding S-scores and SS labels are stated.

Participant No.	Q1. Skin Type	Q2. Breakout frequency	Q3. Face Dryness	Q4. SS Response	Q5. Mechanical Stimulus Response	July		December		AVERAGE	
						S-Score	SS category	S-Score	SS category	S-Score	SS category
P1			↑	↓		75%	High SS	57%	Mild SS	66%	High SS
P2				↑		64%	High SS	74%	High SS	69%	High SS
P3		↑			↓	64%	High SS	54%	Mild SS	59%	High SS
P4			↓↓			59%	High SS	67%	High SS	63%	High SS
P5	↓↓		↓	↓	↑	47%	Mild SS	44%	Mild SS	46%	Mild SS
P7						69%	High SS	69%	High SS	69%	High SS
P8	↑		↑	↓	↓↓	74%	High SS	37%	Mild SS	56%	Mild SS
P11		↑				17%	Low SS	17%	Low SS	17%	Low SS
P12	↑	↓		↓	↓	37%	Mild SS	19%	Low SS	28%	Mild SS
P13			↑	↑		47%	Mild SS	57%	Mild SS	52%	Mild SS
P14		↑		↓	↓↓	46%	Mild SS	16%	Low SS	31%	Mild SS
P16	↓↓					47%	Mild SS	45%	Mild SS	46%	Mild SS
P17					↑	36%	Mild SS	46%	Mild SS	41%	Mild SS
P18	↑	↓				17%	Low SS	19%	Low SS	18%	Low SS
P19					↓	47%	Mild SS	27%	Mild SS	37%	Mild SS
P20	↑				↑	17%	Low SS	29%	Mild SS	23%	Mild SS
P21	↓	↑			↑	47%	Mild SS	56%	Mild SS	52%	Mild SS
P22		↓				16%	Low SS	16%	Low SS	16%	Low SS

↑/↓ Increase/ decrease in response by one increment

↑↑/↓↓ Increase/ decrease in response by two increments

Categorisation based on self-assessed perceptions of sensitivity did not provide distinct differences in biophysical parameters of the skin. Indeed, there was a large spread in the subjective responses obtained from the participants but the biophysical values at baseline were narrowly clustered (Figure 4.9). Thus, addressing the objectives of the study to investigate the relationship between the cheek and neck, and evaluate stimuli specific changes in the skin, the biophysical parameters have been discussed for the cohort as a whole in the following sections. Future studies investigating the relationship between the subjective and objective parameters of SS may consider recording the stimuli specific sensitivity using a visual analogue scale. This has been implemented in the subsequent study (Chapter 6).

Basal skin characteristics - Cheek versus Neck

In the present study, the skin on the neck demonstrated consistently higher values for all the biophysical parameters when compared to the corresponding basal values on the cheek (Table 4.4). These results are consistent with the few studies reporting elevated values in TEWL, hydration, and temperature on the neck (Shriner and Maibach 1996; Marrakchi and Maibach 2007; Firooz et al.

2012). Mechanistically, the combination of higher TEWL and hydration is often associated with skin lesions involving a compromised barrier function of the stratum corneum, e.g., due to fresh scars, or disruption to the intracellular matrix (Tagami 2008). The higher hydration values in such cases may be caused by presence of oedema, which is associated with local inflammation and accumulation of fluid in the epidermal skin layer. Indeed, the neck skin may be more prone to mechanical irritation due to the thinner skin morphology when compared to the cheek (Firooz et al. 2016). Furthermore, the elevated temperature values on the neck could be attributed to increased physiological activity resulting in a greater blood perfusion when compared to that on the cheek (Rubinstein and Sessler 1990), also explaining the higher redness values observed on the neck in the present study. By contrast, other studies have reported higher redness values on the cheek than the neck at baseline, hypothesised to be due to the higher density of fatty tissues and blood vessels (Firooz 2012). However, this study does not state the exact measurement site on the cheek or neck, which will influence the underlying morphology of the skin and sub-dermal tissues. In the present study, given the interest in the region with significant beard growth, the protocol involved measuring on the cheek area which was off centred towards the ear. This sampled area has a less dense network of blood vessels as typically encountered at the centre of the cheek (von Arx et al. 2018), which could explain the lower redness values observed in the present study.

Furthermore, at baseline, intra-subject differences were observed for all parameters at the separate test sessions. These could be associated with seasonal variations, with Session 1 corresponding to the summer (July 2021), Session 2 to autumn (October 2021), and Session 3 to winter (December 2021). The results from the present study demonstrated the following between session trends (Table 4.4):

- For TEWL and hydration (on cheek and neck), the median values in autumn < summer < winter
- For redness (on cheek and neck), the median values in autumn < winter < summer
- For temperature –
 - On the cheek, autumn < winter < summer
 - On the neck, winter < autumn < summer

There were consistencies in the seasonal differences for three of the four biophysical parameters at both cheek and neck. This was particularly noted for TEWL and SC hydration where the values in the winter (Session 3) were generally higher than the other two test seasons. However, the temperature values were different on the cheek and neck between sessions. It has previously been reported that winter correlates with elevated TEWL values, and lower values of hydration, redness, and skin temperature when compared to the summer (Black et al. 2000; De Paepe et al. 2009; Galzote et al. 2014; Song et al. 2015). Furthermore, autumn corresponded to an “intermediate

season with no clear trends” (Dolečková et al. 2021). Thus, considering the results only for the summer and winter sessions, the values for TEWL indeed revealed higher values in the winter. Additionally, the combination of decreased redness and skin temperature in the winter is associated with the decrease in sun exposure (Sklar et al. 2013). In contrast to the literature, results of the present study revealed higher basal hydration values in the winter than those in the summer. This may be explained by the experimental protocol which included requesting the participants to clean shave their beard 24 hours before the scheduled tests. It is likely that for the winter session, the participants had flaky skin surface due to the overall dry environment (Verdier-Sévrain and Bonté 2007). The shaving prerequisite on such skin may have influenced the basal values in the experiment leading to an inflammatory response or oedema, which is recorded as elevated hydration values. There is a need for a longitudinal study design to characterise the effects of repeated shaving which has been further explored in the subsequent study ([Chapter 6](#)).

Post stimulus skin characteristics

The protocol included three distinct mechanical insults on the skin surface. These included tape stripping as a positive control (Gorcea et al. 2013; Rodijk et al. 2016). A frictional stimulus and electric shaving period were included as distinct mechanical stimuli eliciting changes in skin properties, representing real-world loads that the skin is commonly exposed to. The frictional stimulus involved a combination of pressure and shear which can alter the microclimate at the skin surface (Zhang and Roberts 1993). This process was observed in the temperature values where localized heat was generated due to the stimulus interaction. The shaving stimuli includes cutting and pulling of hair, in addition to the pressure and shear forces at the skin surface (Maurer et al. 2016). This process is known to activate the mast cells, in the tissue surrounding the hair follicles. These cells, which are responsible for the sensory and immune function of the skin, reacting to different stimuli within minutes after their activation and contribute to the redness, swelling, and pain (Metz et al. 2008). To our knowledge, this is the first study utilising an array of biophysical and imaging parameters to evaluate frictional and electrical shaving stimulus ([Section 2.3](#)).

During the present study, the tape stripping protocol involved the application of 10 consecutive tapes on each site. However, only a mild to moderate change in skin parameters was observed following the stimulus for the majority of participants. This was significantly less than the two-fold change in TEWL on the cheek reported following the application of only five or six tapes (Gorcea et al. 2013). This difference could be attributed to several factors. For example, with COVID-19 restrictions there was a prescribed minimum distance between individuals of 1.5 m. The researcher was thus prohibited from performing the mechanical stimulus. Instead, each participant applied

the strips to their own skin, using the applicator device (Figure 4.4), with the inevitable tendency to minimise pain. This created a risk of inappropriate technique, where the duration of application and the speed of removing the tape has been reported as crucial in damaging the skin barrier (Breternitz et al. 2007). For the friction and shaving stimuli, the diminished skin response could be attributed to either the low magnitude of force or the short duration of interaction. However, the duration of stimulus interaction was limited based on institutional guidelines for consumer studies.

Another reason for the diminished response may be the prior mechanical conditioning of the facial skin which, in many cases, would have been exposed to a regular shaving stimulus for a prolonged period. It is known that the skin and soft tissues can adapt to prolonged exposure to mechanical loads as demonstrated by soft tissues at the stump of amputees as they bear load through prosthetic limbs (Wang and Sanders 2003). However, the influence of a comparatively smaller and infrequent load remains to be examined with respect to the skin adaptations. In the present study, it is likely that the technique used by the participants did not conform to the standard required to strip the SC and that the friction and shaving interaction with the load was not harsh enough to elicit a significant response.

Investigating the temporal trends in the skin responses, most biophysical parameters across the cohort revealed mild to moderate increases in values immediately following the mechanical insults (Figure 4.10 and Figure 4.11). Additionally, most group medians for the skin responses did not return to baseline values even 30 minutes post insult. For the tape stripping stimulus, this is consistent with findings from other studies involving different protocols (Mihaela Gorcea et al. 2013; Richters et al. 2016). However, a high degree of inter-subject variability was evident, which limited statistically significant differences from baseline values. By contrast, the TEWL values on the neck demonstrated a decreasing trend in values immediately after the stimulus. This trend in TEWL was also observed for the other two mechanical stimuli on the neck. This unexpected result required further investigation, which will be addressed in Chapter 5 when the effects of the mechanical stimuli on the structural aspects of the skin were examined using OCT.

Investigating the trends in the skin responses to the different mechanical stimuli on the cheek (Table 4.5), the fold changes from baseline across the cohort were greatest following tape stripping for the two parameters, TEWL and hydration. Indeed, it is well established that the mechanical stripping of cell layers from the SC increase TEWL values. It also influenced the hydration values, which are measured by the electrical capacitance of the tissue and records increased values due to removal of the dead skin cells. Furthermore, the increase in hydration values following tape stripping could be linked to local inflammation due to the stimulus or hyperaemia. By contrast, friction produced the largest response for temperature. This heating was apparent in the absence

of changes to TEWL and hydration. The decoupled effect may be a result of the low magnitude of frictional stimulus included in the experimental protocol. With reference to the parameter reflecting redness, the greatest response was observed following the shaving stimulus. This supports the previous hypothesis involving the mechanism of electrical shaving, discussed earlier, which activates mast cells and contributes to redness, swelling, and pain response (Metz et al., 2008).

On the neck (Table 4.6), the fold changes in biophysical parameters from baseline revealed that of the three mechanical insults, shaving generally produced the largest response across the cohort with respect to TEWL, redness, and temperature. This corresponds to the widely reported areas of shaving irritation (Cowley et al. 2012). The difference in the findings on the cheek and neck could be attributed to the different structure and morphology of the skin sites, with the neck having horizontally orientated hair follicles and a thinner skin structure. There was a corresponding higher basal TEWL value than the cheek on the neck site. Following the insults, there were elevated values for TEWL, redness, and temperature post shaving. By contrast, it was observed that the tape stripping stimulus produced the largest response on the neck for hydration. Here, it can be argued that the damage mechanisms introduced by the different stimuli are distinct in their influence on the skin response. Tape stripping leads to removal of dead cell layers, revealing an immediate increase in the skin hydration, whereas shaving involves a combination of mechanical forces that do not reveal the same magnitude of increase in hydration values. It is proposed to examine the influence of these stimuli over a longer time period, recording recovery characteristics at 24 hours to determine the physiological processes associated with each stimulus.

Conclusions

The present study included participants with distinct differences in self-reported SS. There was a large spread in the subjective responses obtained from the participants but the biophysical values at baseline were narrowly clustered. The protocol developed has generated a novel dataset characterising biophysical parameters of the hirsute skin on the cheek and neck. However, the insult model limited the magnitude of the skin response post stimulus. Nevertheless, differences in the damage mechanisms of each mechanical insult have been discussed, as well as hypothesis for differing results between the cheek and neck skin. Furthermore, suggestions have been made to optimise the protocol to investigate the influence of mechanical stimuli on these sites.

Chapter 5 Characterisation of OCT parameters following mechanical challenges in the consumer cohort

5.1 Introduction

Optical Coherence Tomography (OCT) has been identified as a promising tool for characterizing structural and physiological skin parameters ([Table 2.1](#)). Furthermore, a need for an array of multi-modal parameters for the assessment of enhanced skin sensitivity has also been identified ([Section 2.3.9](#)). Thus, a protocol was designed to characterize skin combining biophysical measurements and OCT and evaluate the influence of mechanical stimuli ([Section 4.2](#)).

Following the development of algorithms to estimate specified skin parameters from OCT images ([Section 3.3](#)), this chapter aimed to evaluate their feasibility in distinguishing different anatomical sites and participants with varying degrees of skin sensitivity. Thus, the objectives of this chapter were as follows:

1. Establish baseline characteristics on the cheek and neck of participants using OCT-skin parameters.
2. Evaluate the temporal effects of the mechanical stimuli on the OCT-skin parameters.
3. Establish the relationship between the OCT-skin parameters on the cheek and neck for all participants.
4. Investigate the relationship between the OCT-skin parameters and the biophysical parameters.
5. Investigate the relationship between the OCT-skin parameters with respect to the SS categories.

5.2 Methods

The protocol implemented in this chapter has been detailed in [Section 4.2.4](#). Exemplar OCT scans are illustrated in [Figure 5.1](#).

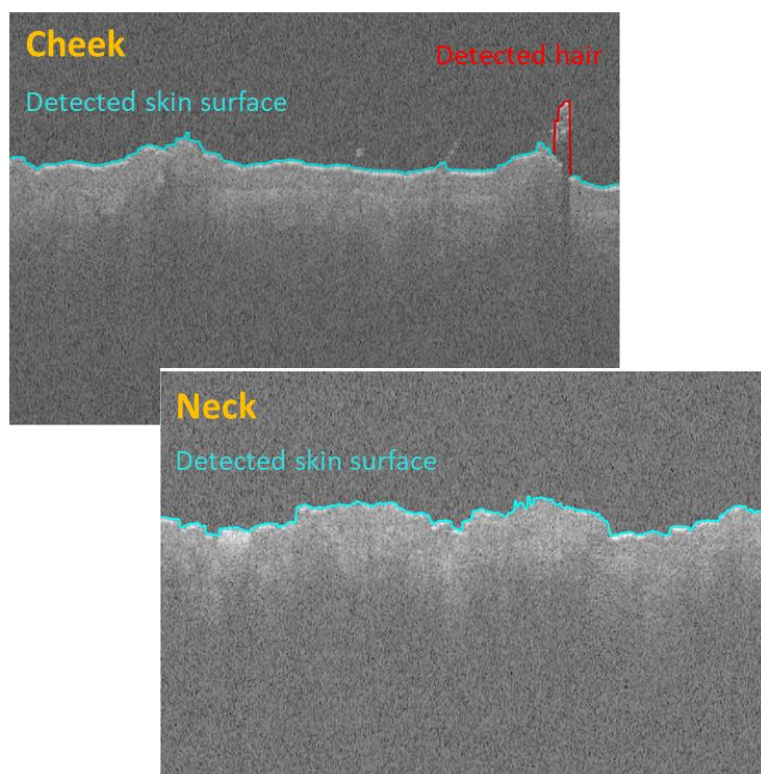


Figure 5.1 OCT scans from the cheek and neck for one participant at baseline. The skin surface detected from the MATLAB algorithm has been highlighted in blue. Additionally, detected artefacts have been highlighted in red.

The methodology and algorithms for derivation of the OCT-skin parameters have been detailed in [Chapter 3](#). Exemplar A-lines have been illustrated in [Figure 5.2](#).

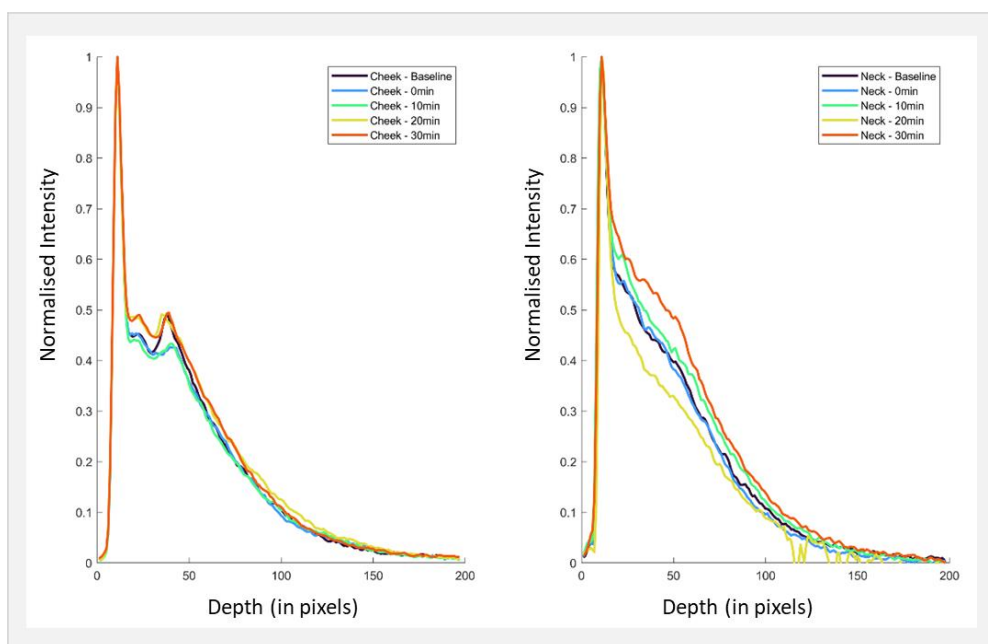


Figure 5.2 Temporal A-scans for the cheek and neck for one participant.

5.2.1 Area under the Curve (AuC) estimation

As described in [Chapter 3](#), the OCT scans were analysed for estimating the epidermal thickness. However, results from the present study revealed errors in detecting a second peak. Upon closer examination, it was determined that these errors occurred in approximately 50% scans of the cheek and 70% scans of the neck, as illustrated in [Figure 5.3](#) for two individuals.

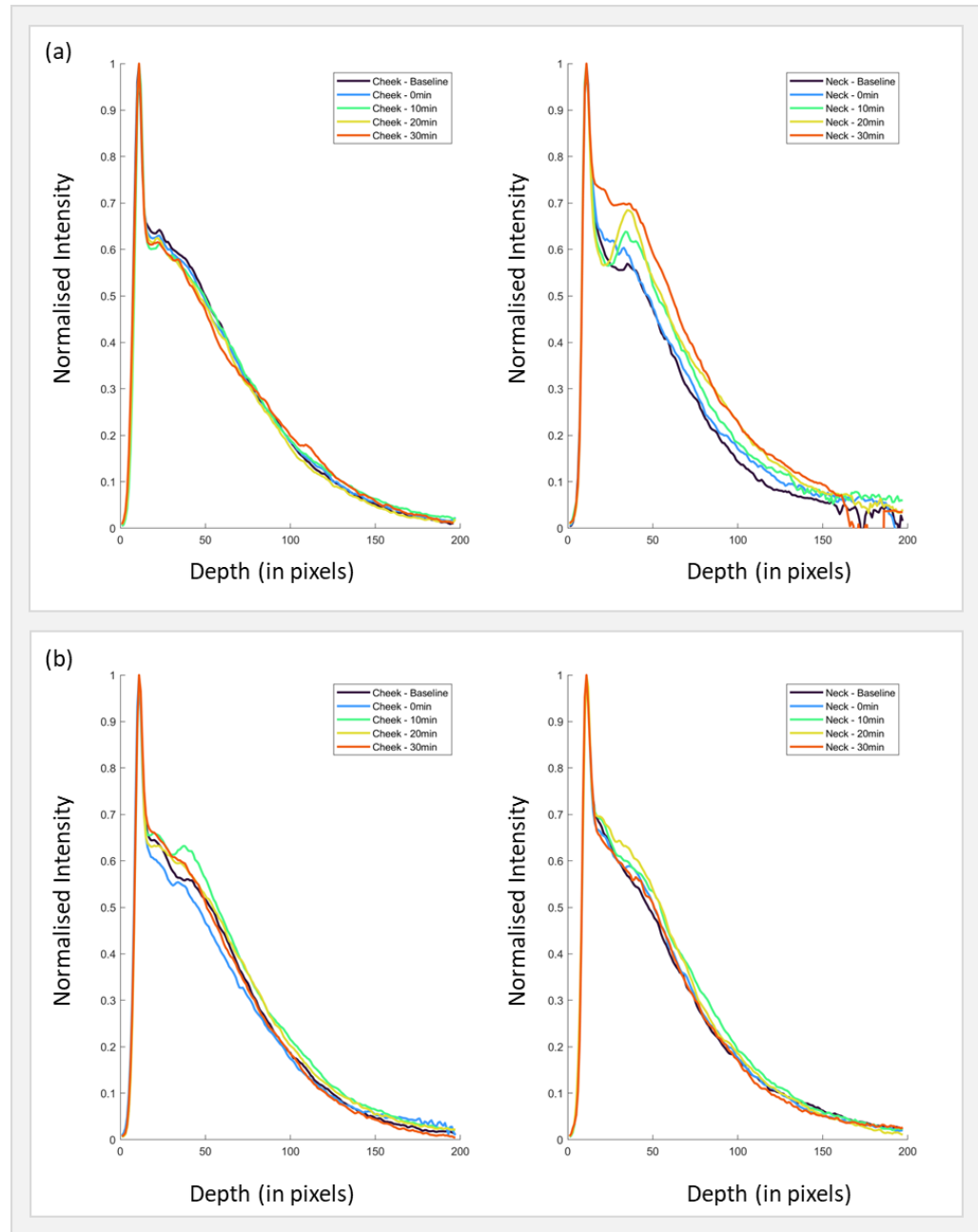


Figure 5.3 Exemplar A-lines for two individuals. (a) Individual 1 reveals missing second peaks for the A-lines mostly on the cheek. (b) Individual 2 reveal missing second peaks for several A-lines on the cheek and neck.

Thus, a new parameter, namely Area under the Curve (AuC), was developed to characterise the A-lines. AuC is estimated as the area under the A-line curve from the Peak 1 up to a defined depth, as illustrated in [Figure 5.4](#). As epidermal thickness is widely approximated as 0.1mm (Graham et al. 2019), a value of 0.2mm depth was selected ensuring a buffer in the estimation for the variability between participants. Thus, the AuC serves as a proxy for the epidermal thickness, quantifying the superficial skin tissue and has been included in the results presented in this chapter.

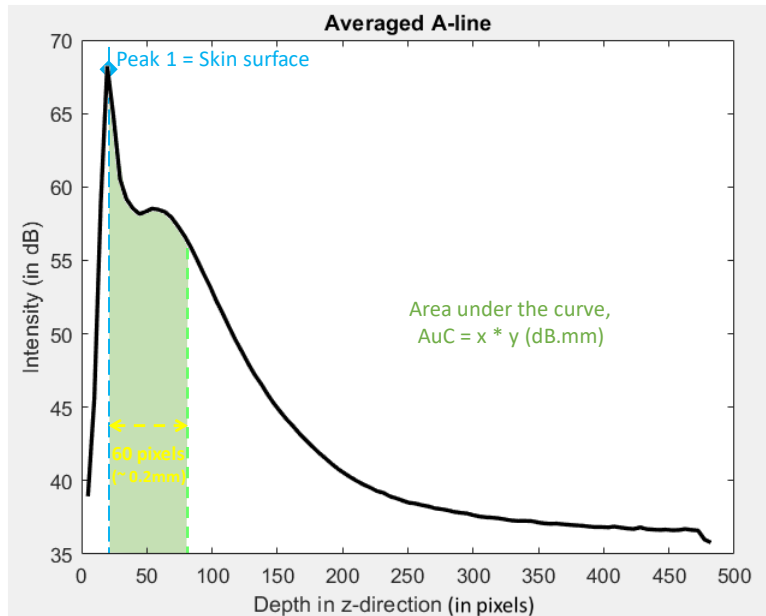


Figure 5.4 Illustration of Area under the curve calculation from an Averaged A-line

5.2.2 Statistical Analysis

Normality of the distribution of the values was checked using the Anderson - Darling (AD) normality test ([Appendix D](#)). Accordingly, descriptive statistics such as medians, quartiles, ranges were used. Differences between sessions and temporal trends in the OCT-skin parameters at each site were evaluated for statistical significance using the Mann Whitney U test. Correlations between the OCT-skin parameters on the cheek and neck have been estimated using regression analysis. However, due to the diminished response observed from the mechanical stimuli, the results have been presented for baseline only. Correlations between the OCT-skin parameters and the biophysical parameters were estimated using the Pairwise Spearman test.

For the visual investigation of the influence of extrinsic factors on the OCT-skin parameters, the participants were ranked for each parameter in each session, based on descending order of the values. The values were then colour coded from dark to light blue in each column. Lastly, the rows were arranged in groups based on the SS category.

5.3 Results

The demographic details of the participants from this study have been presented in [Table 4.3](#). It is noted that 18 individuals participated in all three sessions, where P6 participated only in Session 1, P9 participated in Session 1 and only the cheek measurements of Session 2, and P10 and P15 participated only in Sessions 1 and 2. However, the OCT-skin parameters have not been estimated for P6 due to poor quality of the OCT scans. Similarly, there is no data for P12 only from Session 1.

5.3.1 Baseline characteristics

The medians and interquartile values of the OCT-skin parameters at baseline for the cheek and neck are summarised in [Table 5.1](#). Comparing the median values for each parameter between the sessions, distinct trends were observed. Specifically, for SID, the values in Session 1 were smaller than those in Session 2, which were smaller than those in Session 3. These differences were statistically significant between each session on the cheek, whereas only between Sessions 1 and 2, and Sessions 1 and 3 on the neck. Conversely, the AuC demonstrated median values in Session 1 greater than those in Session 2, which were greater than those in Session 3. On both sites, Session 3 revealed statistically significant differences from Sessions 1 and 2. For the Rq, the data in Session 3 revealed the largest values ($p > 0.05$) on both sites.

When comparing the values between the cheek and neck, it was observed that the median SID and Rq on the neck were greater than those on the cheek for each session ($p < 0.001$). Furthermore, it is noted that the median AuC on the cheek was greater than that on neck for each session ($p < 0.001$).

Table 5.1 Summary of the baseline values of the OCT-skin parameters for the three test sessions.

Statistically significant differences between the sites and sessions have been noted using the Mann-Whitney test @.

CHEEK		SID (mm ⁻¹)	AuC (dB.mm)	Rq (μm)
Session 1	Median	2.58 *^	11.65 ^	15.73
	Quartiles (Q1, Q3)	(2.46, 2.69)	(11.21, 11.97)	(12.27, 18.77)
Session 2	Median	2.93 *#	11.52 #	14.60
	Quartiles (Q1, Q3)	(2.72, 3.09)	(11.19, 11.77)	(11.63, 18.68)
Session 3	Median	3.31 ^#	10.63 ^#	16.93
	Quartiles (Q1, Q3)	(3.05, 3.37)	(10.2, 10.9)	(12.05, 22.45)
NECK		SID (mm ⁻¹)	AuC (dB.mm)	Rq (μm)
Session 1	Median	2.38 *^	11.07 ^	22.15
	Quartiles (Q1, Q3)	(2.23, 2.57)	(10.87, 11.32)	(19.6, 27.62)
Session 2	Median	02.65 *	10.85 #	22.85
	Quartiles (Q1, Q3)	(2.51, 2.76)	(10.49, 11.18)	(17.4, 26.57)
Session 3	Median	2.85 ^	10.25 ^#	24.10
	Quartiles (Q1, Q3)	(2.72, 2.92)	(10.11, 10.82)	(20.24, 28.46)

@ $p < 0.001$ between cheek and neck for all parameters in each session; * $p < 0.05$ between Session 1 and Session 2; ^ $p < 0.05$ between Session 1 and Session 3; # $p < 0.05$ between Session 2 and Session 3

Furthermore, the individual values of each OCT-skin parameter have been plotted in [Figure 5.5](#). For the SID on the cheek, shown in [Figure 5.5a](#), the difference in the intra-subject SID values ranged from 0.00 mm⁻¹ to 1.15 mm⁻¹ as demonstrated by P12 and P3, respectively. Furthermore, 86% of participants (n=18/21) demonstrated the lowest SID values in Session 1 ($p < 0.05$ between all sessions), while 66% of participants (n=14/21) demonstrated the highest SID values in Session 3 ($p < 0.05$ between all sessions). Similarly, the corresponding baseline SID values on the neck are presented in [Figure 5.5b](#). The SID on the neck demonstrated a smaller variability within the participants such that the intra-subject SID values ranged from 0.17 mm⁻¹ to 0.88 mm⁻¹ across the sessions, with a median of 0.48 mm⁻¹. Additionally, similar to that on the cheek, 70% of participants (n=14/20) revealed the lowest SID values in Session 1 ($p < 0.05$ between all sessions) and 65% of

participants (n=13/20) revealed the highest SID values in Session 3 ($p<0.05$ between Sessions 1 and 3 only).

For the AuC on the cheek, presented in [Figure 5.5c](#), the intra-subject differences in the values on the cheek ranged from 0.20 dB.mm to 2.00 dB.mm, where P3 continued to demonstrate the largest spread. Furthermore, 52% of participants (n=11/21) revealed the highest AuC values in Session 1 ($p<0.05$ between Sessions 1 and 3 only), while 76% of participants (n=16/21) revealed the lowest values in Session 3 ($p<0.05$ between all sessions). The corresponding AuC values on the neck are presented in [Figure 5.5d](#). The variability for AuC within participants on the neck is observed to be smaller than that on the cheek, with the intra-subject differences in AuC ranging from 0.32 dB.mm to 1.80 dB.mm, as demonstrated by P18 and P2 respectively. However, similar to that on the cheek, 55% of participants (n=11/20) revealed the highest AuC values on the neck in Session 1 ($p<0.05$ between Sessions 1 and 3 only), while 70% (n=14/20) revealed the lowest AuC values in Session 3 ($p<0.05$ between all sessions).

For the roughness on the cheek, shown in [Figure 5.5e](#), the differences in the intra-subject Rq values ranged from 0.21 μm to 13.56 μm as demonstrated by P10 and P11 respectively. Furthermore, 43% of the participants (n=9/21) revealed the highest Rq values occurring in Session 3 ($p>0.05$), while 52% of participants (n=11/21) revealed the lowest Rq values in Session 2 ($p>0.05$). Similarly, the roughness values on the neck are presented in [Figure 5.1f](#). The variability between participants is greater on the neck, with the difference in intra-subject Rq values from 1.69 μm to 31.50 μm , where P11 revealed the largest difference again. Similar to that on the cheek, 45% of participants (n=9/20) revealed the highest Rq values in Session 3 ($p>0.05$), while 50 % of participants (n=10/20) revealed the lowest Rq values in Session 2 ($p>0.05$).

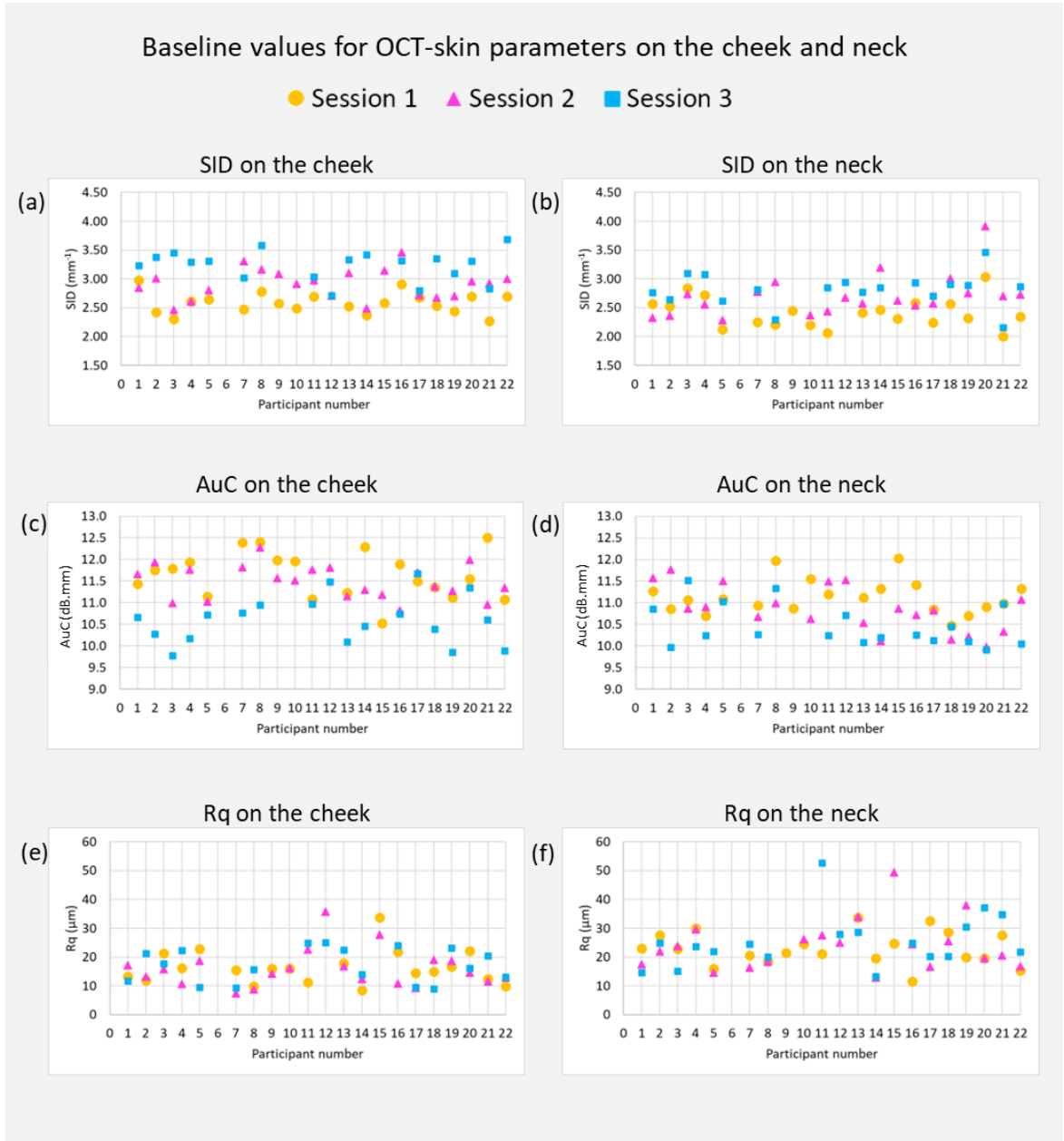


Figure 5.5 Baseline values for SID, AuC, and Rq for the three sessions for (a) SID on the cheek, (b) SID on the neck, (c) AuC on the cheek, (d) AuC on the neck, (e) Rq on the cheek, (f) Rq on the neck.

5.3.2 Temporal responses to mechanical stimuli

Figure 5.6 illustrates the temporal changes in the median values of the OCT-skin parameters on the cheek for the three sessions involving different mechanical stimuli. Overall, small variations were observed in response to the stimulus for each OCT-skin parameter. Closer examination of the individual trends for SID, presented in Figure 5.6a, revealed that within each session a few participants e.g., P9 and P16 repeatedly demonstrated high outlier values. Furthermore, the response in SID revealed a small increasing trend in post stimulus values for Sessions 1 and 2. For the tape stripping session, the increase in the median SID from baseline ($p>0.05$) ranged from 0.08 mm^{-1} to 0.13 mm^{-1} . Similarly, for the frictional stimulus, a small increase in the median SID was observed post stimulus such that the values continued to increase up till $t=30$, where the difference from baseline revealed statistically significant changes ($p=0.05$) with an increase from 2.93 mm^{-1} to 3.04 mm^{-1} . By contrast, for the shaving stimulus session, the median SID values demonstrated a decrease ($p>0.05$) post stimulus such that the change in the medians ranged from 0.03 mm^{-1} to 0.13 mm^{-1} .

For the AuC on the cheek, shown in Figure 5.6b, fewer outliers are noted as compared to the results for SID. The tape stripping and frictional stimuli revealed small changes ($p>0.05$) from baseline in the post stimulus values with the differences ranging from 0.01 dB.mm to 0.10 dB.mm and 0.01 dB.mm to 0.20 dB.mm in magnitude, respectively. Additionally, P9 and P18 are noted as low responding outliers in Session 1 at $t=30$. By contrast, the shaving stimulus demonstrated a consistently increasing trend in values, with the median AuC revealing a statistically significant increase from baseline at $t=20$ ($p=0.045$) and $t=30$ ($p=0.041$).

For the Rq on the cheek, presented in Figure 5.6c, all three sessions revealed a decrease in Rq post stimulus. Furthermore, there were a few participants e.g., P12 and P15, repeatedly demonstrating higher outlier values. For the tape stripping stimulus, there was a decrease in Rq values such that the median Rq decreased from $15.72 \text{ }\mu\text{m}$ to $11.60 \text{ }\mu\text{m}$ at $t=0$ ($p=0.044$) and $12.35 \text{ }\mu\text{m}$ at $t=30$ ($p=0.022$). Similarly, following the shaving stimulus, the values decreased from $16.93 \text{ }\mu\text{m}$ to $10.71 \text{ }\mu\text{m}$ at $t=10$ ($p=0.024$), $12.14 \text{ }\mu\text{m}$ at $t=20$ ($p=0.041$), and $11.70 \text{ }\mu\text{m}$ at $t=30$ ($p=0.048$). By contrast, the frictional stimuli revealed smaller changes in the Rq values such that the difference in Rq from baseline ranged from $0.63 \text{ }\mu\text{m}$ to $2.62 \text{ }\mu\text{m}$ ($p>0.05$).

Temporal responses to mechanical insults for all parameters on the cheek

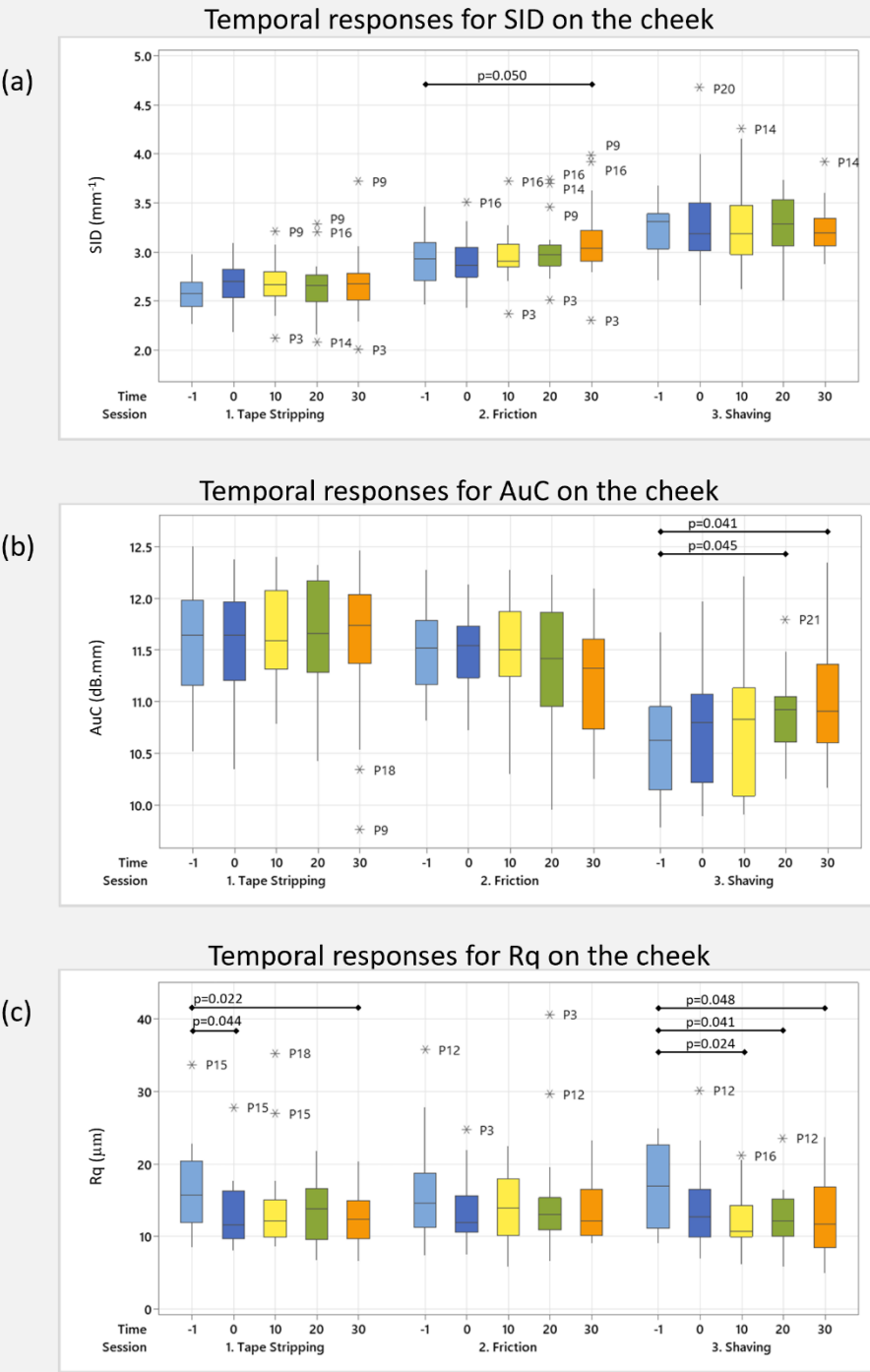


Figure 5.6 Temporal response to mechanical insults on the cheek for (a) SID, (b) AuC, (c) Rq. Outlier values for individual participants are also indicated, as are statistically significant differences from baseline using the Mann Whitney test.

Figure 5.7 illustrates the temporal changes in the median values of the OCT-skin parameters on the neck for the three sessions involving different mechanical stimuli. Like that on the cheek, small variations were observed overall in response to the stimulus for each OCT-skin parameter. Upon closer examination of the individual trends for SID, shown in Figure 5.7a, an increasing trend in the median SID values was observed post stimulus. However, these differences did not reveal statistically significant differences from baseline in any of the sessions. P8, P10, P20, and P21 were noted as outliers, however, only P20 demonstrated recurring outlier values.

For the AuC on the neck, presented in Figure 5.7b, all three sessions revealed an increase in the post stimulus values. However, due to the large spread in the data, these changes were not statistically significant from baseline. Specifically, the difference in the median values from baseline ranged from 0.14 dB.mm to 0.36 dB.mm for the tape stripping stimulus, from 0.05 dB.mm to 0.23 dB.mm for the frictional stimulus, and 0.14 dB.mm to 0.39 dB.mm for the shaving stimulus.

For the Rq on the neck, presented in Figure 5.7c, similar to that on the cheek, all three sessions revealed a decrease in the values post stimulus. Within each session a few participants e.g., P11 and P15 consistently demonstrated high outlier values. For the session involving tape stripping, small changes were observed post stimulus, with the difference in median Rq values from baseline ranging from 1.72 μm to 3.86 μm ($p>0.05$). For the session involving the frictional stimulus, the values at $t=0$ were significant lower ($p=0.047$) than that at baseline, with the median Rq equal to 18.75 μm . Smaller changes were observed at subsequent intervals ($p>0.05$), with the Rq remaining lower than that at baseline. However, P12 was noted as an extreme outlier at $t=20$ with Rq equal to 74.47 μm . For the shaving stimulus, the difference in the post stimulus Rq values from baseline ranged from 1.97 μm to 3.16 μm . However, this difference was statistically significant only at $t=20$ ($p=0.006$), where the median Rq was estimated as 21.14 μm .

Temporal responses to mechanical insults for all parameters on the neck

Time t=-1 t=0 t=10 t=20 t=30

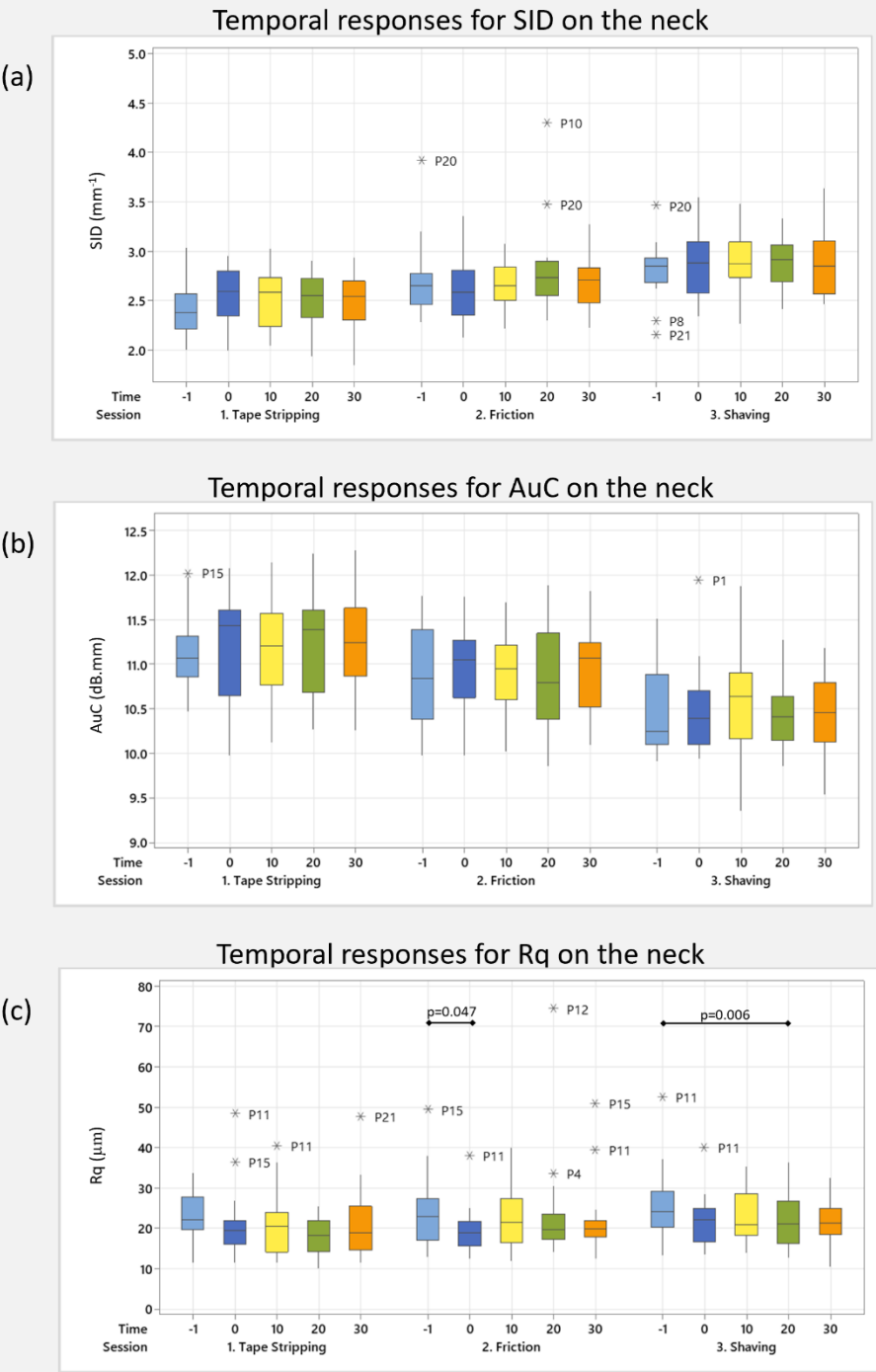


Figure 5.7 Temporal response to mechanical insults on the neck for (a) SID, (b) AuC, (c) Rq. Outlier values for individual participants are also indicated, as are statistically significant differences from baseline using the Mann Whitney test.

5.3.3 Correlation between the OCT-skin parameters on the cheek and neck

The relationship between the OCT-skin parameters on the cheek and neck have been presented in [Figure 5.8](#). This analysis is limited to the values recorded at baseline only due to the small influence of the mechanical stimuli observed in each session ([Figure 5.6](#) and [Figure 5.7](#)). For each parameter, the relationship between the values on the cheek and neck are observed to be dependent on the session. Specifically for SID, shown in [Figure 5.8 \(a\) – \(c\)](#), the linear models indicate that the SID on the neck is greater than that on the cheek as revealed by the positive coefficient of the slope for sessions 1 and 3, with the values estimated as 0.15 and 0.16, respectively. By contrast, in Session 2, the coefficient of the slope is revealed to be negative with a value of -0.16, indicating higher SID values on the cheek than on the neck. However, due to the large spread between the participants, these trends do not achieve statistical significance ($p>0.05$).

Similarly, for the AuC, shown in [Figure 5.8 \(d\) – \(f\)](#), the linear models reveal differences in the direction of the slopes across the sessions, such that the coefficients are determined as -0.04, 0.34, and -0.02 for Sessions 1, 2, and 3, respectively. However, the large spread between the participants limits the statistical significance of these trends ($p>0.05$).

Like that for SID and AuC, the linear models generated for the Rq between the cheek and neck, presented in [Figure 5.8 \(g\) – \(i\)](#), the direction of the slopes are different depending on the session. However, Sessions 2 and 3 indicate the Rq on the neck is greater than that on the cheek, with the coefficient of the slope estimated as 0.66 ($p=0.024$) and 0.87 ($p=0.019$), respectively.

Scatterplots of OCT-skin parameters on the cheek versus neck

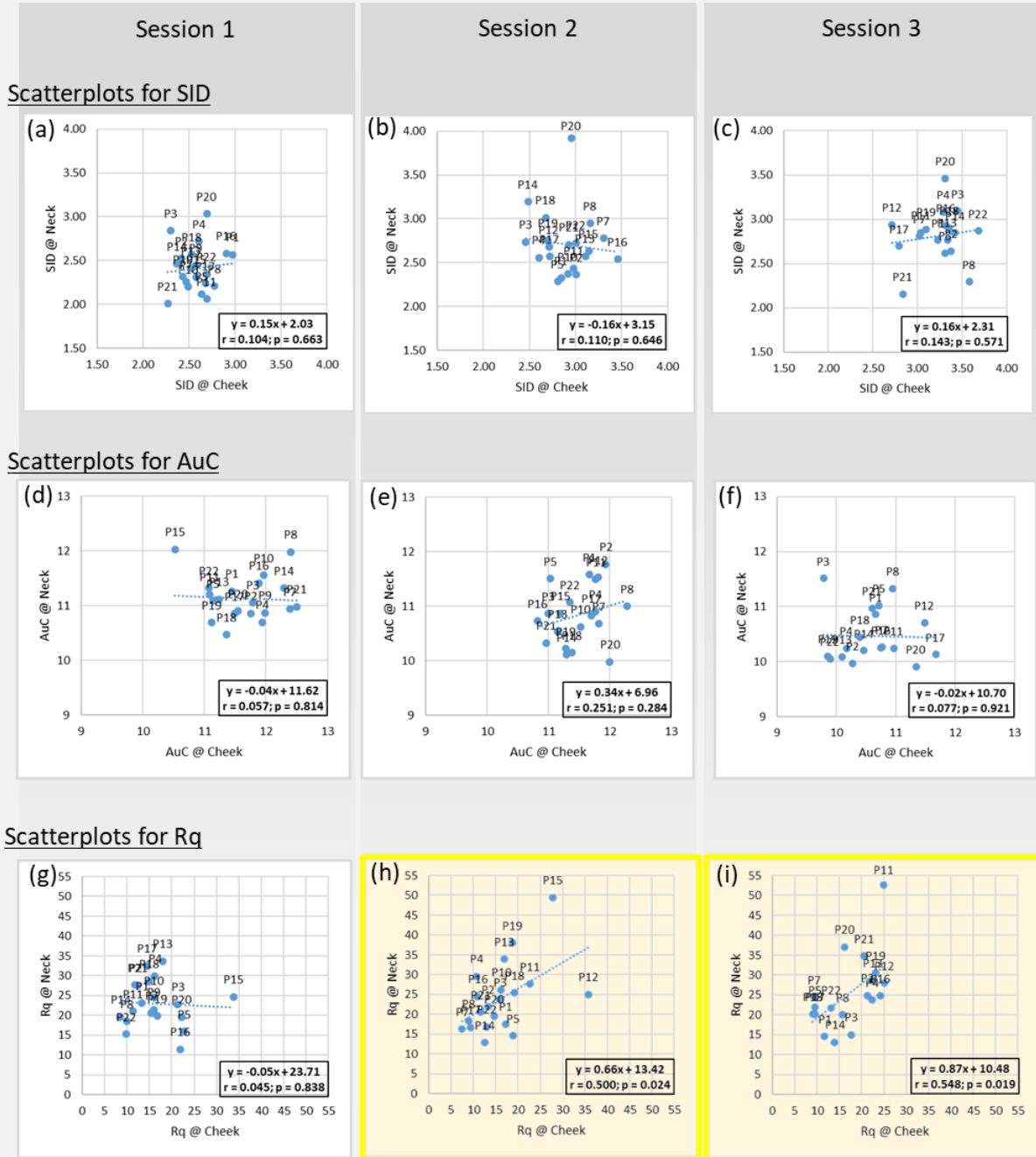


Figure 5.8 Relationship between the cheek and neck at baseline for SID in (a) Session 1, (b) Session 2, (c) Session 3; for AuC in (d) Session 1, (e) Session 2, (f) Session 3; for Rq in (g) Session 1, (h) Session 2, (i) Session 3. Where $p < 0.05$, the plots have been highlighted in yellow.

5.3.4 Relationship between OCT-skin parameters and biophysical parameters

The relationship between each OCT-skin parameter and biophysical parameter was investigated for correlation and statistical significance. This analysis was conducted at baseline only as limited influence of the mechanical stimuli was noted in the previous sections. Figure 5.9 represents an exemplar plot of this analysis with the scatterplots, Spearman correlation coefficients, and p-values for each pair of parameters from Session 2 on the neck. It is observed that of the 21 scatterplots, only 4 pairs revealed statistically significant correlations, namely SID and AuC ($p=0.002$), SID and temperature ($p=0.014$), AuC and temperature ($p=0.010$), and roughness and hydration ($p=0.003$). Furthermore, the magnitude of the r-value in each case ranged from 0.555 to 0.659, revealing a moderate association between the parameters. However, similar trends were not observed for Sessions 1 and 3 (Appendix D), with the exception for roughness and hydration where the Spearman correlation coefficients and p-values were revealed as $r = -0.507$ and $p = 0.023$, and $r = -0.434$ and $p = 0.072$, respectively, as illustrated in Figure 5.10. Conversely, the correlation for the roughness and hydration on the cheek (Appendix D) did not achieve statistical significance ($p>0.05$).

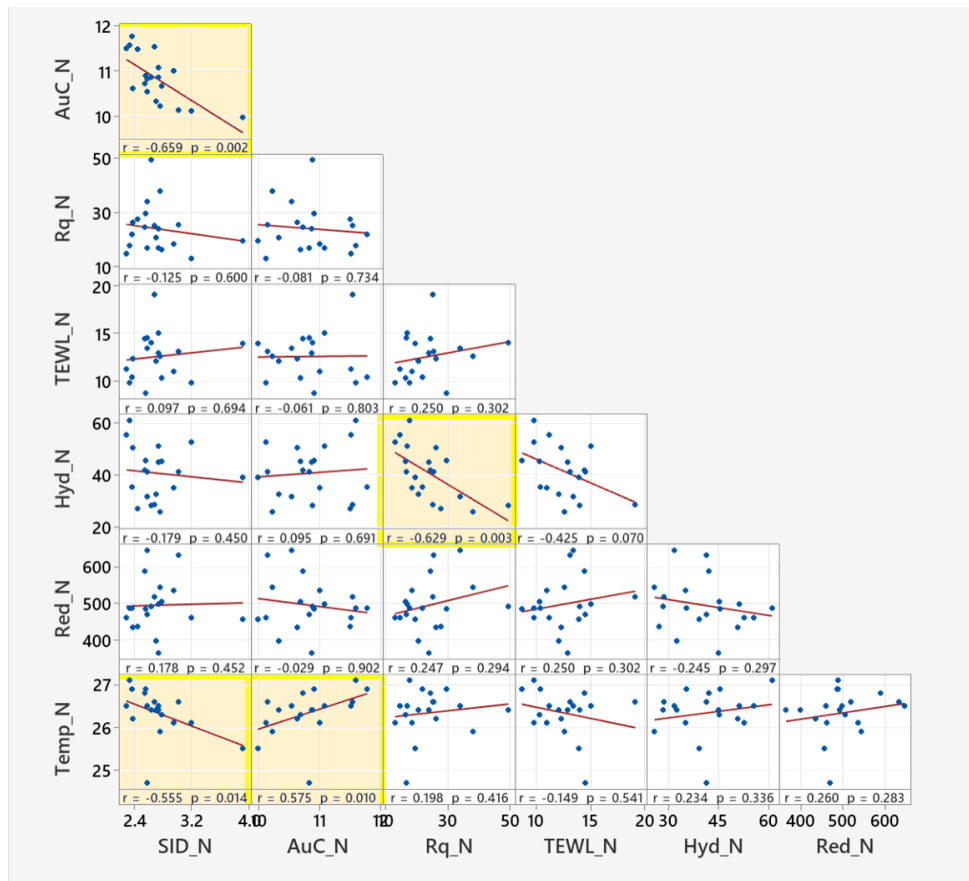


Figure 5.9 Spearman correlation scatterplots between OCT-skin parameters and biophysical parameters on the neck at baseline for Session 2. Where $p < 0.05$, the plots have been highlighted in yellow.

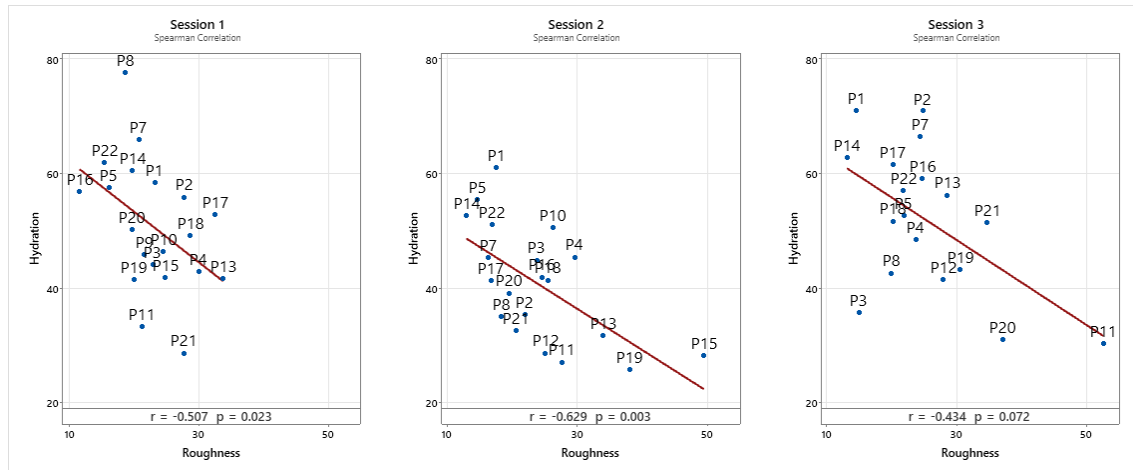


Figure 5.10 Spearman correlation between the roughness and hydration on the neck for Sessions 1, 2, and 3 at baseline.

5.3.5 Relationship between OCT-skin parameters and SS categories

The trends across participants skin parameters were investigated with respect to others in the group by ranking the participant for each parameter. This exploratory analysis aimed to identify clusters for participants where the OCT-skin parameters and the biophysical parameters yielded values of differing units and orders of magnitude. [Table 5.2](#) illustrates the ranks obtained from Session 1 at baseline for the 17 participants where the results were recorded for all sessions. Those from Sessions 2 and 3 are included in [Appendix D](#).

On both sites, a large variability was observed when examining the ranks across the SS groups. For example, on the cheek, the High SS group included individuals such as P1 where the values for 5 of the 7 of the parameters yielded ranks greater than 11. Conversely, P4, also from the High SS group, revealed ranks ranging from 4 to 17 across all 7 skin parameters.

Table 5.2 Ranks for participants from Session 1 at baseline for all the skin parameters, sorted by the SS category.

	Participant	SS Category	Shaving method	Shaving Frequency	Rank SID	Rank AuC	Rank Rq	Rank TEWL	Rank Hyd.	Rank Red.	Rank Temp.
Cheek	P11	Low SS	Rota	>5	14	16	14	7	13	11	16
	P18	Low SS	Blade	3, 4	8	12	9	11	14	1	1
	P22	Low SS	Blade	3, 4	13	17	16	8	5	3	11
	P5	Mild SS	Combination	>5	10	14	1	4	6	9	7
	P8	Mild SS	Combination	<2	15	2	15	2	2	4	12
	P13	Mild SS	Combination	3, 4	7	13	5	3	12	8	6
	P14	Mild SS	Combination	3, 4	3	4	17	12	11	5	8
	P16	Mild SS	Combination	>5	16	6	3	1	10	12	9
	P17	Mild SS	Combination	>5	11	10	10	5	15	14	5
	P19	Mild SS	Combination	>5	5	15	6	15	8	6	15
	P20	Mild SS	Rota	>5	12	9	2	9	16	7	13
	P21	Mild SS	Combination	3, 4	1	1	12	10	17	17	10
	P1	High SS	Combination	<2	17	11	11	13	7	16	14
	P2	High SS	Blade	<2	4	8	13	14	3	10	2
	P3	High SS	Rota	<2	2	7	4	6	9	15	3
	P4	High SS	Blade	>5	9	5	7	17	4	13	4
	P7	High SS	Combination	3, 4	6	3	8	16	1	2	17
Neck	P11	Low SS	Rota	>5	2	6	9	5	16	14	16
	P18	Low SS	Blade	3, 4	13	17	4	10	11	3	6
	P22	Low SS	Blade	3, 4	8	3	16	2	3	16	15
	P5	Mild SS	Combination	>5	3	8	15	12	6	11	4
	P8	Mild SS	Combination	<2	4	1	14	16	1	2	3
	P13	Mild SS	Combination	3, 4	9	7	1	4	14	5	2
	P14	Mild SS	Combination	3, 4	10	4	12	14	4	13	9
	P16	Mild SS	Combination	>5	14	2	17	1	7	1	1
	P17	Mild SS	Combination	>5	5	14	2	6	9	15	5
	P19	Mild SS	Combination	>5	7	16	11	9	15	6	14
	P20	Mild SS	Rota	>5	17	12	13	11	10	10	12
	P21	Mild SS	Combination	3, 4	1	10	6	15	17	17	10
	P1	High SS	Combination	<2	12	5	7	8	5	12	11
	P2	High SS	Blade	<2	11	13	5	7	8	7	7
	P3	High SS	Rota	<2	16	9	8	3	12	8	8
	P4	High SS	Blade	>5	15	15	3	17	13	4	13
	P7	High SS	Combination	3, 4	6	11	10	13	2	9	17

5.4 Discussion

This chapter aimed to characterise the skin on two facial locations using parameters extracted from OCT images. Subsequently, the SID, AuC, and Rq have been reported from a cohort of consumer detailed in [Section 4.3](#). To the authors' knowledge, there are no studies that have estimated these parameters on bearded cheek and neck skin. Consequently, the results from the present chapter create an opportunity to investigate the feasibility of the OCT-skin parameters to distinguish the inter- and intra-subject variability in the skin tissue at these specific sites.

Based on the definitions of SID and AuC ([Section 3.3.4](#) and [5.2.1](#)), it is expected that these two parameters would reveal inversely proportional results. Indeed, this was observed in the present study, where within each participant, the SID and AuC demonstrated opposite trends between the different sessions ([Figure 5.5](#)). However, examining the correlation between the parameters, varying trends between the different sites and sessions were revealed with only results from the cheek in session 3 and neck in session 2 achieving statistically significant values ([Figure 5.6](#) and [Figure 5.7](#)). These variations can be explained by the difference in features characterised by the two parameters. While SID estimates the coefficient of the relative optical density, the AuC estimates the optical density of the skin tissue with respect to a standardized depth. Combination of these parameters provides a composite analysis of the superficial skin, corresponding to microvessels and fibrous structures. For example, of the 17 participants that were ranked with respect to each parameter ([Table 5.2](#)), P21 revealed the lowest SID and highest AuC in the group. Conversely, P3 ranked second for SID but ranked seventh for AuC. These results indicate that while the relative decrease in optical density for the two participants was similar, they demonstrated differences in the composition of the skin tissue. [Figure 5.11](#) illustrates exemplar B-mode images for P3 and P21 where differences in the frequency domain can be observed. While P3 reveals a higher contrast in the grey pixels, P21 presents a smoother transition in the pixel values revealing an overall brighter image. Clinically, blood vessels, hair follicles, and sebaceous glands create dark cavities in the OCT scan, while collagen and elastin fibres appear as bright clusters (Welzel et al. 2004; Mogensen et al. 2008; Schmitz et al. 2013). Thus, in the present example, it can be hypothesized that while both participants have a similar degree of attenuating features, P21 could have higher fibrous content in the papillary dermis.

Overall results from the present study revealed a lower median SID and higher median AuC for the cheek when compared to the neck ([Table 5.1](#); $p < 0.001$). While there are no directly comparable studies, some researchers have examined the echogenicity of various skin tissues using ultrasound imaging, revealing a significantly higher density of the dermal tissue on the neck than on the cheek, stating that these differences require additional investigation (Firooz 2016). Furthermore, as a large

degree of variability was observed in the trends between participants, the results from the present study did not reveal statistically significant correlations between the two sites for the SID or AuC. Thus, these parameters may be influenced by specific morphological and physiological properties of the skin, which change in isolation to one another. For instance, it can be hypothesized that the cheek is more conditioned to mechanical stimuli than the neck, as it receives more exposure to a variety of environmental factors (Black et al. 2000). However, further research is needed to address identify such trends.

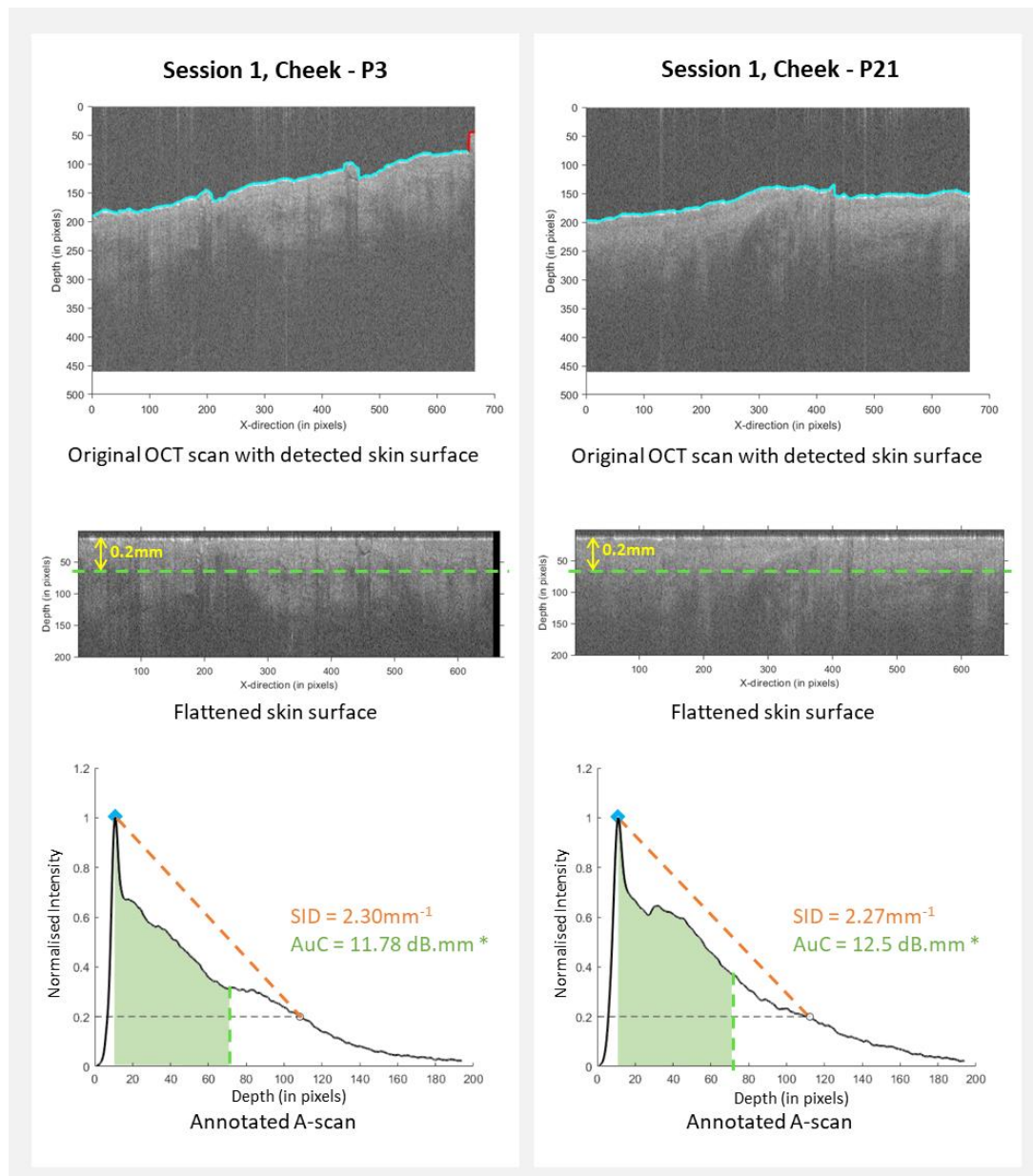


Figure 5.11 Exemplar OCT scans and A-scans for P3 and P21 at baseline in session 1 on the cheek.

* AuC is calculated from the non-normalized A-scans as this parameter is standardised with respect to the depth *in vivo*. However, the estimation method has been plotted on the normalised A-scan for visual comparison with the SID estimation.

For skin surface roughness, the methodology employed in this study was based on the root-mean-square estimation of the skin surface (Section 3.3.5). While several researchers have reported skin roughness values (Table 5.3), the anatomical sites investigated do not represent skin with beard growth. It has been reported that there is a large degree of variability between anatomical sites. Furthermore, for those from seemingly similar sites, the precise location under investigation is often unclear. Thus, the results presented in this chapter provide novel information, with median roughness at baseline ranging from 14.6 μm to 16.93 μm on the cheek and 22.15 μm to 24.10 μm on the neck ($p < 0.001$ between cheek and neck). The correlation between these two sites also revealed statistically significant values in Sessions 2 and 3 at baseline (Figure 5.8; $p < 0.024$), with the neck demonstrating consistently larger roughness than the cheek. Functionally, as the neck supports the mobility of the head, increased cutaneous elasticity of the tissue is expected (Trojahn et al. 2015). Consequently, the neck skin presents a higher number of folds and wrinkles. One researcher has compared the biomechanical properties of the cheek and neck in a female cohort, revealing that the wrinkles on the neck were fivefold deeper than those on the cheek (Kim et al. 2013). Others have also presented rougher neck skin discussing the impact of these findings on male grooming behaviour (Maurer et al. 2016). However, the association of higher basal skin roughness remains to be established with respect to enhanced skin sensitivity.

Table 5.3 Roughness values obtained from OCT images for various anatomical sites reported in literature. Results have been included for healthy skin at baseline.

Reference	Roughness (μm)	Anatomical location	Age range	Sample size
Present study (Session 1)	15.73	Cheek	30 – 55 years old	22 (male only)
	22.15	Neck		
(Vingan et al. 2023)	16	Cheek	20 – 89 years old	70
(Askaruly et al. 2019)	0.98 \pm 0.22	Forearm	27 years old (mean)	5
	2.08 \pm 0.40	Cheek		
	2.34 \pm 0.34	Eye rim		
	1.58 \pm 0.67	Forearm	55 years old (mean)	5
	4.23 \pm 1.94	Cheek		
	5.22 \pm 1.53	Eye rim		
(Welzel, Bruhns, and Wolff 2003)	12.7 \pm 2.1	Forearm	24 – 27 years old	15 (female only)
(Maiti et al. 2020)	3	Forearm	18 – 35 years old	12
	2	Cheek		
	4	Neck (backside)		

	3	Eye bag		
--	---	---------	--	--

The correlations between the OCT-skin parameters and biophysical parameters were investigated in the present study revealing few statistically significant trends. Across all three sessions, roughness and hydration on the neck revealed inversely proportional relationships ([Figure 5.10](#); $p=0.072$), demonstrating a rougher skin surface for dryer skin. Similar trends have been reported by researchers (Eberlein-König et al. 2000; Dąbrowska et al. 2016), where a decrease in roughness values was observed as a result of exposure to water. Furthermore, statistically significant correlations were observed between temperature and either SID, AuC or redness. These trends can be explained by the influence of cutaneous blood flow (CBF) in estimation of the parameter (Tzen et al. 2010). Increased blood flow corresponds with the increase in vessel morphology (Rubinstein and Sessler 1990), which in turn will change the optical density of the skin tissue and the skin surface colour. Interestingly, however, the SID, AuC, and redness did not reveal correlations in values. These trends in results are unclear and need to be further investigated. Functional adaptations of OCT have been implemented in dermatological research (Kennedy et al. 2011; Wang et al. 2015; Wang and Larin 2016; Zaveri 2016; Jiang et al. 2020). As such, Dynamic-OCT provides an opportunity to investigate the microcirculation in the skin tissue, in addition to the structural parameters. Thus, the subsequent study has been designed using a Dynamic-OCT system ([Chapter 6](#)). Advantages of these features are pending validation.

Results for estimating the epidermal thickness revealed errors in approximately 60% of the images. Typically, thickness values from OCT scans are calculated based on the distance between the first two peaks in the A-line plots, where the first peak is regarded as the skin surface and the second peak as the Dermal-Epidermal Junction (DEJ, [Figure 3.6](#)). However, analysis of the OCT scans revealed gradually decreasing intensity values in the A-lines as the optical signal penetrated deeper into the skin such that only one clear peak was observed in most cases, corresponding to the skin surface. Similar features were observed by other researchers, which has been attributed to the digital smoothing of the wavy DEJ as the A-lines are averaged (Welzel et al. 2003). Subsequently, epidermal thickness was not estimated in the present study. A new parameter was defined, AuC, characterising the density of the superficial skin layers. This parameter can be further optimised for different applications.

Conclusions

The feasibility of newly defined OCT-skin parameters to distinguish the inter- and intra-subject variability were investigated in this chapter. Results were discussed for basal skin OCT parameters

only. SID and Rq revealed greater values on the neck, whereas the cheek had a larger AuC. However, only Rq demonstrated statistically significant correlations between the cheek and neck. Furthermore, Rq on the neck also correlated with hydration, presenting larger values for less hydrated skin. TEWL did not reveal statistically significant correlations with any of the OCT-skin parameters. Categorization of the participants based on self-assessed skin sensitivities did not reveal clusters with respect to the biophysical or OCT-skin parameters. The protocol can be modified to create a larger signal post-stimulus through a modified mechanical insult and new dynamic properties can be assessed in skin through Dynamic-OCT technique.

Chapter 6 **Assessment of skin integrity at different anatomical locations in response to shaving**

6.1 Introduction

The motivation of the PhD programme is driven by the inter-subject differences in tolerance thresholds to mechanical stimulation introduced by skin contacting consumer devices such as electrical shavers ([Section 1.2](#)). Thus, an experimental protocol was designed to include tape stripping and shaving as mechanical stimuli to characterise skin parameters between individuals with varying degrees of perceived skin sensitivities. The previous study ([Chapter 4](#) and [Chapter 5](#)) revealed limited differences in the selected skin parameters within a cohort of consumers, associated with insult and measurement restriction imposed during the COVID-19 pandemic. Indeed, the mechanical stimulation of the skin did not elicit a significant response, possibly due to the protocol design. Additionally, the selected anatomical sites limited the comparison with studies from the literature. Thus, a modified protocol was developed to address the limitations and has been presented in this chapter.

In addition to the small changes in biophysical parameters, there was little change in the morphology of the skin characterised with OCT. The review of the scientific literature identified cutaneous blood flow (CBF), amongst others, as a relevant parameter in the assessment of enhanced skin sensitivity ([Section 2.3](#)). Consequently, there was an opportunity to include CBF-associated parameters in the present study as part of a modified OCT evaluation. A new OCT system, Vivosight (Michelson Diagnostics Ltd., UK), with dynamic imaging capabilities was rented, and the associated VivoTools software enabled the quantification of several CBF features. Thus, an enhanced array of parameters to characterise the skin were explored alongside a modified insult model.

Along with the optical and biophysical methods of skin characterisation, the present study also created an opportunity to collaborate with another researcher with expertise in analysis of surface biomarkers associated with early detection of skin damage (Jayabal et al. 2022). Based on the literature review ([Section 2.3](#)), pro-inflammatory cytokines revealed a significant increase in their expression following mechanical loading. Subsequently, the present study included non-invasive sampling of sebum for exploratory analysis of biomarkers associated with shaving. The methodology associated with these inflammatory markers is detailed in [Section 6.2.5](#).

Aims and Objectives

The present study aimed to characterise the skin responses to mechanical stimulus in the form of electric shaving using biophysical, optical, and biochemical techniques. The specific objectives of this study were as follows:

- Develop a new the array of parameters to characterise the skin.
- Establish baseline skin characteristics with respect to the biophysical, optical, and biochemical parameters on the forearms, cheek, and neck.
- Introduce mechanical loading in the form of electric shaving.
- Investigate the temporal skin response to shaving and tape stripping on the forearms. Further examine any changes in the response due to repetitive loading
- Evaluating the feasibility of tape stripping as a surrogate for shaving on the forearm.
- Investigate the spatial and temporal skin response to shaving on the cheek and neck. Further examine any changes in the response due to repetitive loading.

The results from this study have been divided into two chapters, with the present chapter focusing on the objective parameters of the skin (e.g., TEWL, roughness, and redness), and the following chapter ([Chapter 7](#)) detailing the subjective parameters associated with enhanced skin sensitivity (e.g., S-scores, visual analogue scores, and shaving habits).

6.2 Methods

The study was approved by the local Faculty Ethics committee of the University of Southampton (FoHS-Ethics-71825). The test protocol ([Appendix B](#)) was performed in the Biomechanics Testing Laboratory in the Clinical Academic Facility at Southampton General Hospital, Southampton, UK. The room temperature was maintained at $24^{\circ}\text{C} \pm 2^{\circ}\text{C}$. The study was a repeated measures cohort design, where healthy volunteers were recruited to be exposed to repeated mechanical insults.

6.2.1 Participant recruitment and preparation

Participant recruitment was conducted by means of poster advertisements and word of mouth, excluding those who had an underlying skin disease (such as atopic dermatitis). Each potential participant was given an information sheet and requested to confirm their decision if they wished to participate. The participant inclusion criteria were as follows:

- Healthy volunteers
- Minimum age of 18 years
- Individuals of any ethnicity

- Males willing to be clean shave
- Individuals presented with the mental capacity and English proficiency to provide informed consent
- Individuals with availability for at least 2 hours on two consecutive days.

The sample size was set at a minimum of 10 participants, for this exploratory study. Upon recruitment, participants were requested to clean shave 72 hours before the first test session. At the first test session, each individual was able to ask the researcher questions and was then asked to sign the consent form and complete the Skin Sensitivity Questionnaire ([Appendix A](#)). Using a stencil (70 mm x 50 mm) with a cut-out (15 mm x 15 mm), non-permanent squares were drawn on both forearms, cheek, and neck for each participant to standardize the location of measurement across multiple visits ([Figure 4.2](#)). On the forearms, a point was marked along the volar forearm 10 cm away from the wrist joint line, towards the elbow. Placing the middle of the shorter edge of the stencil above the point, the square was drawn using the cut-out ([Figure 6.1](#)). For the cheek and neck, the region of interest was modified from that used in the previous study to mark areas of the skin away from bony prominences. As such, first, a scale ruler was aligned from the top of the ear to the corner of the participant's mouth. Then, a point was marked at 5 cm from the top of the ear. Next, the stencil was placed on the cheek such that a corner of the cut-out aligned with the point marked previously. The square was outlined on the cheek skin using the cut-out as a boundary. For the neck, the scale ruler was used to mark a point vertically below the square draw on the cheek, such that the point was located 1 cm above the end of the hairline. Using the stencil, the square was drawn on the neck by aligning a corner of the cut-out with the identified point ([Figure 6.1](#)). This method enabled personalisation of the region of interest, which is considered important given the different shapes of heads.

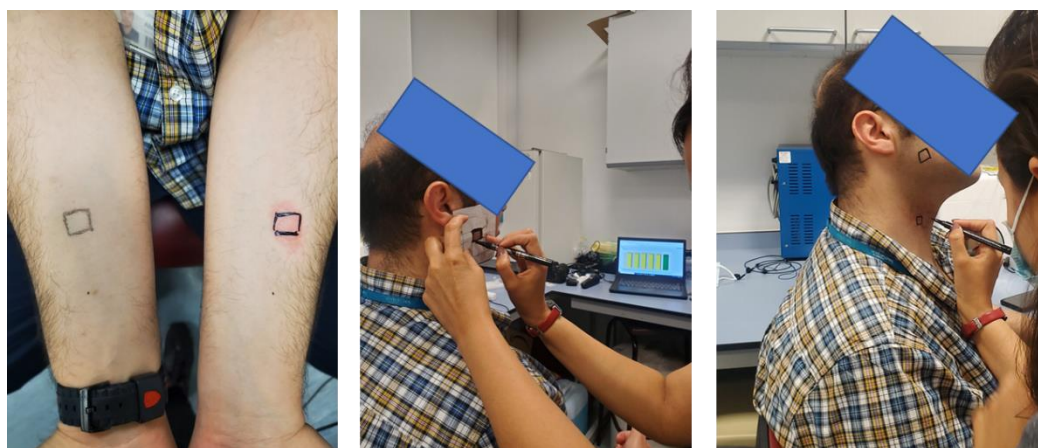


Figure 6.1 Region of interest highlighted on the forearms, cheek, and neck by drawing a square.

6.2.2 Protocol

The measurement protocol was designed to estimate skin parameters on the forearm, cheek, and neck at baseline, then following repeated mechanical insults. The methodology was modified following analysis of results from the previous study (Chapter 4 and Chapter 5) to elicit a greater response in the skin. A sequential protocol was designed whereby measurements could be taken pre- and post-stimulus at each location (Figure 6.2). This enabled efficient data collection at each site, with its feasibility confirmed by pilot testing.

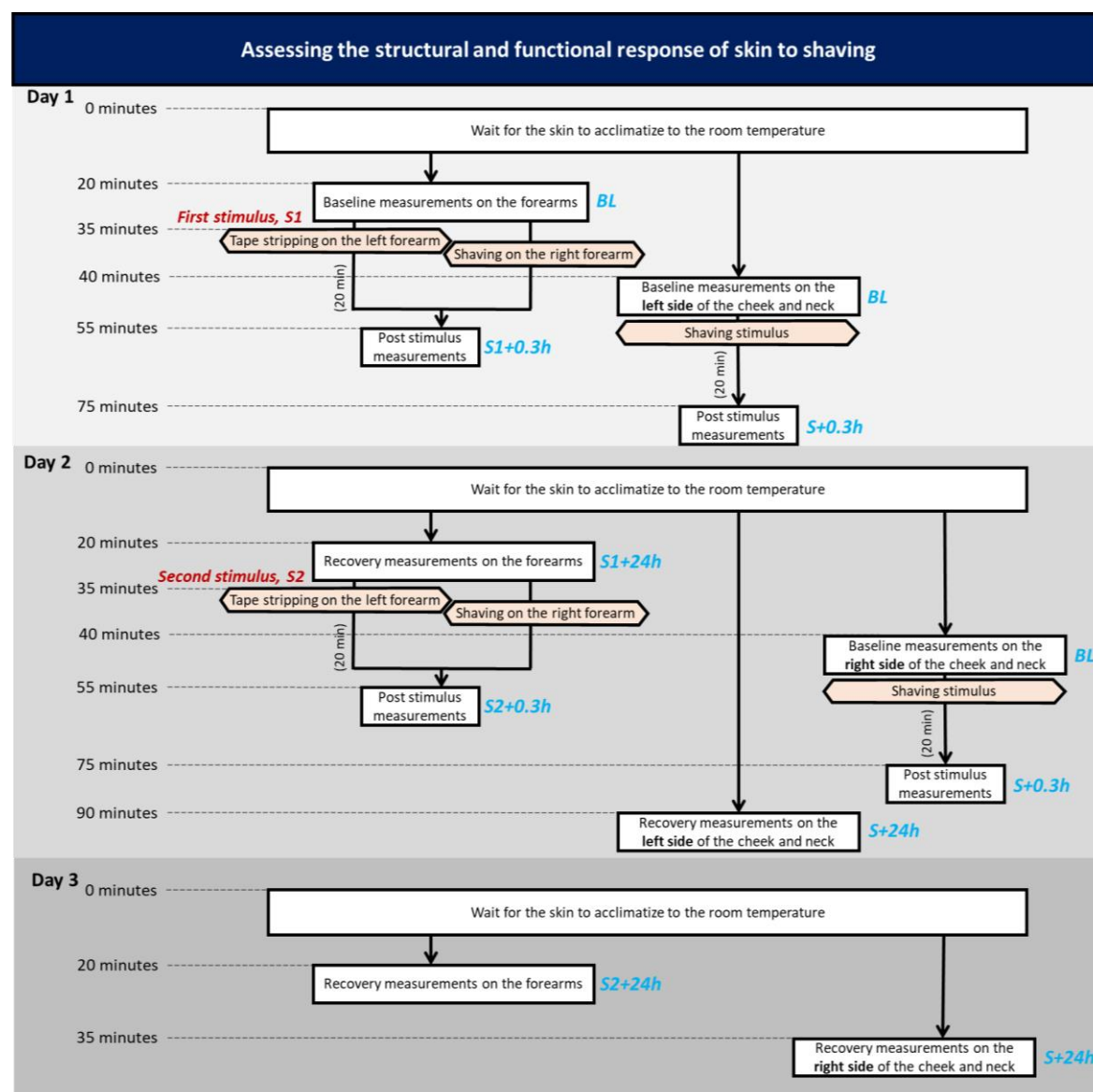


Figure 6.2 Protocol for assessing the structural and functional response of the skin to shaving.

The skin parameters were recorded within the highlighted skin area using an OCT system (Vivosight, Michelson Diagnostics Ltd., UK), a Tewameter (TM300, Courage and Khazaka, Germany), a Corneometer (CM825, Courage and Khazaka, Germany), and Sebutapes in the sequence detailed in

Table 6.1. The sequence of measurement was based on established methodology which aims to minimise the risk of bias and carry over effects (Kottner et al. 2014). Macroscopic photographs of the highlighted skin areas were also captured using a Dermalite Foto II Pro lens (USA) mounted on a Canon EOS R5 DSLR camera. Modifying the protocol from the previous study, the redness was estimated using these digital images, as detailed in [Section 6.2.4](#). Furthermore, sebum samples were collected from the skin surface using Sebutapes ([Figure 6.3](#)). These were placed on the skin for 2 minutes using blunt forceps. The tapes were then removed and placed in 2mL tubes, prior to being stored in a -80°C freezer for future analysis.

Table 6.1 Sequence of measurements of skin and acquisition times for each site

Measurement	Measurement system	Acquisition time	Number of measurements	Approx. Total time
1. DSLR pictures	Dermalite lens	30 seconds	1	0.5 minutes
2. OCT scans	Vivosight	30 seconds	2	1 minute
3. TEWL values	Tewameter	1 minute	2	2 minutes
4. SC hydration values	Corneometer	5 seconds	5	0.5 minutes
5. Sebum sample	Sebutpes	2 minutes	1	2 minutes

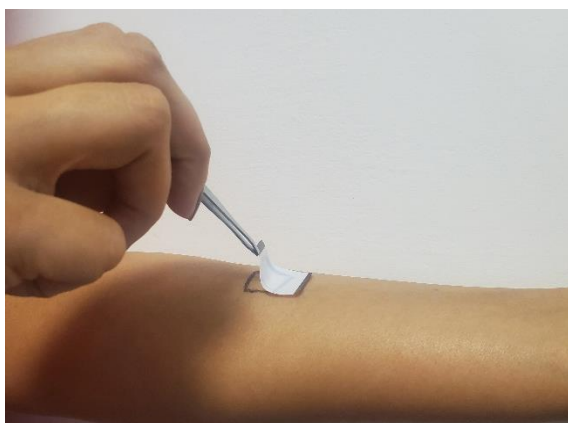


Figure 6.3 Placement of the Sebutape on the arm.

A shaving stimulus was performed on the right forearm and tape stripping was performed on the contra-lateral forearm (left) as a positive control, using 20 consecutive tapes. Shaving was also performed on the cheek and neck to investigate different facial sites ([Figure 6.4](#)). Similar to the protocol discussed in [Section 4.2.4](#), the participants were requested to increase the shaving contact pressure such that the light ring on the shaver handle was in the orange zone, indicating force values between 4N and 7N at the skin/device interface ([Figure 4.6](#)). The main modification to the protocol involved an increase in time exposure to shaving from 30 seconds to 60 seconds. Increasing the time rather than the magnitude of load was assumed to represent the real-world shaving conditions

more closely. In addition, the magnitude and frequency of shaving strokes was characterised using a built-in load cell and has been detailed in [Chapter 7](#).

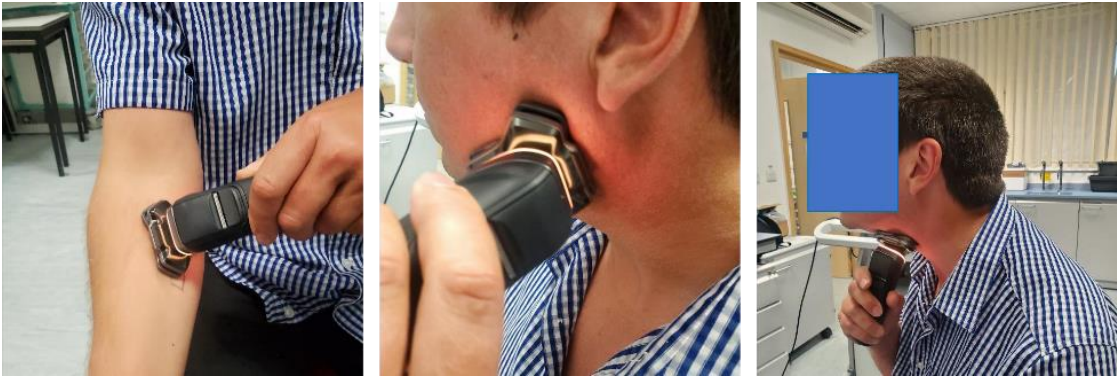


Figure 6.4 Example of the shaving stimulus on the forearm, cheek, and neck.

Following the mechanical stimulus, skin response was characterised after an interval of 20 minutes, i.e., 0.3 hours. Additionally, the protocol was designed to investigate the influence of repetitive loading on the skin and subsequent recovery. Thus, the participants were requested to attend two sessions over three days where Session 1 involved the first round of mechanical stimulus and corresponds to skin characteristics at baseline (Day 1), 20 minutes post stimulus (Day 1), and 24 hours post stimulus (Day 2). Subsequently, Session 2 involved the second round of mechanical stimulus at the same site, followed by characterising the skin response at 20 minutes post stimulus (Day 2), and 24 hours post stimulus (Day3). Thus, the figures and tables illustrated in the Results section include the labels illustrated in [Figure 6.5](#).

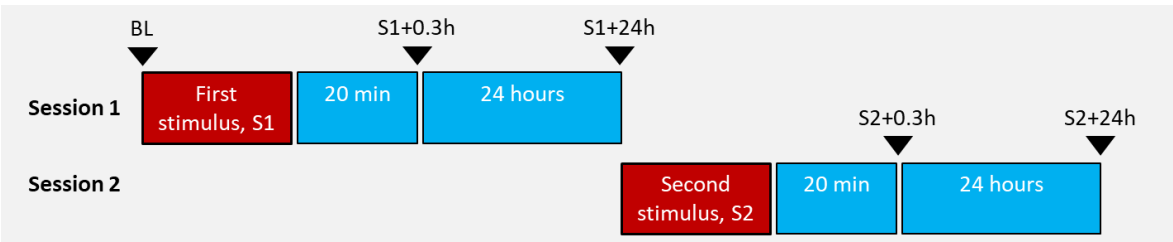


Figure 6.5 Labels for the timepoints of the data collection on the forearms: BL → Baseline;
S1+0.3hr → 20 minutes post first stimulus; S1+24hr → 24 hours post first stimulus;
S2+0.3hr → 20 minutes post second stimulus; S2+24hr → 24 hours post second stimulus.

However, during pilot tests, it was determined that the repetitive shaving stimulus on the cheek and neck was not ethical as the first stimulus elicited dermatitis symptoms within 24 hours ([Figure](#)

6.6). Thus, the protocol was modified to evaluate the influence of repetitive loading on the cheek and neck on the contralateral side. This was executed by initially requesting the participants to prepare for the study by clean shaving their beard 72 hours before the scheduled tests.



Figure 6.6 Exemplar dermatitis response on the neck in the preliminary test.

During Session 1, the shaving stimulus (60 seconds, orange zone) on the cheek and neck was performed on the left side of their face. Immediately after completing the measurements on Day 1, the participants were requested to clean shave the remaining area of their beard per their regular shaving habits (documented by the researcher). This step introduced a proxy for the first stimulus on the right side of the face while leaving the left side available for skin recovery characterisation at 24 hours post stimulus. Thus, for the cheek and neck, the tests were scheduled such that Session 1 involved characterisation of the skin with 72-hours-beard (labelled as “Long Beard”) at baseline (Day 1) and 20 minutes post-shaving (Day 1). The following day, the 24 hours post stimulus values were recorded on the left side of their face (Day 2), concluding Session 1. Additionally, Session 2 was used to characterise the skin on the right side of the face with the 24-hours-beard (labelled as “Short Beard”) at baseline (Day 2), 20 minutes post stimulus (Day 2). The corresponding 24 hours post stimulus was then conducted on Day 3, as illustrated in Figure 6.7.

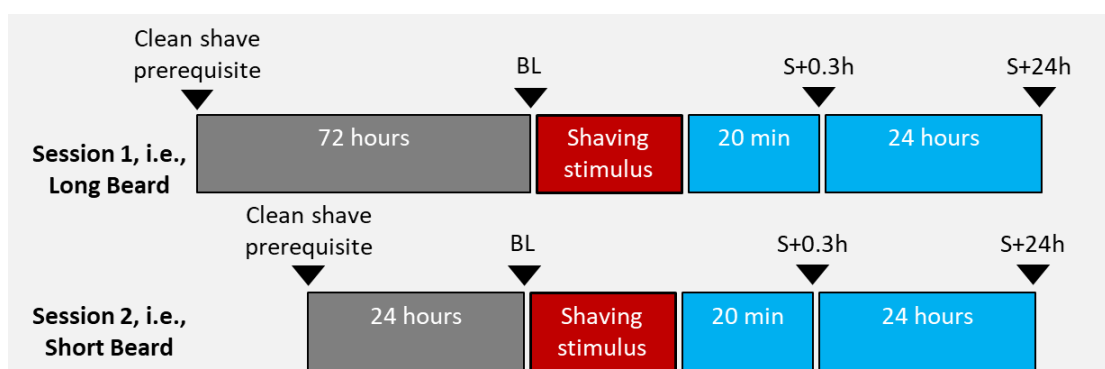


Figure 6.7 Labels for the timepoints of the data collection on the cheek and neck: BL → Baseline; S+0.3hr → 20 minutes post stimulus; S+24hr → 24 hours post stimulus. It is noted that Session 1 is referred to as “Long Beard” and Session 2 as “Short Beard”.

6.2.3 Imaging parameters selection and optimization

The Vivosight and VivoTools OCT system provides several parameters that allow real-time quantification of the skin (Figure 6.8). However, as algorithms were previously developed to characterise skin properties derived from the Thorolabs OCT system (Chapter 3), there is an opportunity to compare and optimise the array of parameters that will be used in this study. An overview of the optical parameters has been provided in Table 6.2.

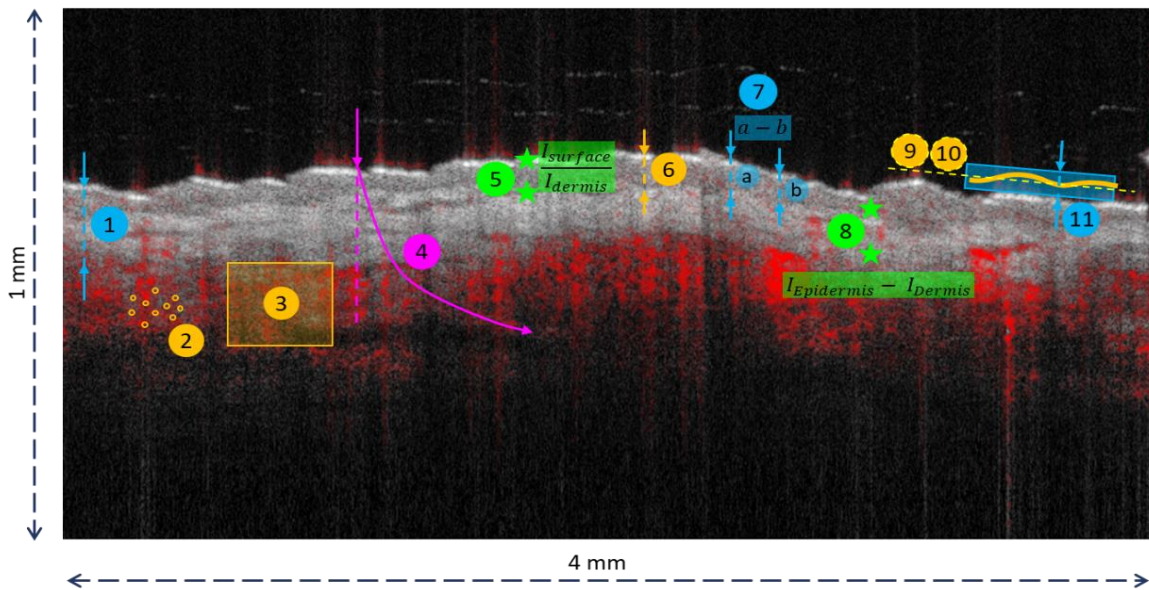


Figure 6.8 Annotated Dynamic OCT image with parameters from the Vivosight OCT system as follows: 1. Plexus depth (μm), 2. Vessel diameter (μm), 3. Vessel density (%), 4. Optical attenuation coefficient (mm^{-1}), 5. Surface reflectivity ratio, 6. Epidermal thickness (μm), 7. Epidermal thickness variation (μm), 8. Epidermal contrast (%), 9. Mean variation of surface height, R_a , 10. RMS variation of surface height, R_q , 11. Peak-to-trough difference of the surface height, R_z .

Table 6.2 Overview of imaging parameters that can be extracted in the present study, including previously developed OCT-skin parameters and Vivosight parameters.

Imaging Parameters	Unit	Measurement system	Measurement definition	Advantages	Limitations
Scaled Intensity Drop, SID	mm ⁻¹	Vivosight and MATLAB	Coefficient of the slope from the highest peak of the A-line to the point where the intensity reduces by 80%	Algorithm has been fine-tuned to estimate skin parameters for the cheek and neck	Not validated by other researchers
Area Under the Curve, AuC	a.u.	Vivosight and MATLAB	Area under the A-line curve corresponding to a depth of 60 pixels from the highest peak		
Roughness, Rq	μm	Vivosight and MATLAB	Root mean square of the deviation of the peaks and troughs from the surface height		
Plexus depth	μm	Vivosight	Depth of the superficial plexus, measured by the depth at which the red pixels in the OCT image exceed a specified threshold	Real-time output, no post-processing required. Closely linked with visible redness of the skin surface.	Automatically calculated; parameter cannot be fine-tuned
Vessel diameter	μm	Vivosight	Modal vessel diameter at the identified plexus depth	Real-time output, no post-processing required.	Automatically calculated; parameter cannot be fine-tuned
Vessel density	%	Vivosight and Vivotools	The average brightness of the Dynamic OCT image across all pixels in the en-face image, at the selected depth	Can detect differences in the superficial vasculature	Result is not reliable for depths > 0.5 mm
Optical attenuation coefficient, OAC	mm ⁻¹	Vivosight and Vivotools	Rate at which the OCT signal brightness falls with depth below the skin surface	Expected to correlate with collagen content as it is believed to be the main optical scattering agent in the skin	Influenced by transient increase in blood flow
Surface reflectivity ratio, SRR	-	Vivosight and Vivotools	Ratio of the OCT signal intensity from the skin surface to that from the dermal-epidermal junction.	Expected to correlate with collagen content as it measures the optical scattering intensity from cells in the dermis	Influenced by treatments directly affecting the optical properties of the skin surface, such as creams, make-up, or tape stripping.
Epidermal thickness	μm	Vivosight and Vivotools	Extracted by analysing the average OCT intensity profile	A fundamental parameter across imaging modalities	These parameters have not been optimised for different anatomical locations and fails to yield results in certain in vivo scans.
Epidermal thickness variation	μm	Vivosight and Vivotools	Difference between the thinnest and thickest sections of the epidermis	Can differentiate between young and old people as older skin tends to have a flatter dermal-epidermal junction and therefore a low thickness variability	
Epidermal contrast	%	Vivosight and Vivotools	The average OCT intensity difference from the epidermis compared to the dermis	May give information regarding skin conditions that affect the epidermis cellular content and structure, such as skin fibrosis.	
Roughness	μm	Vivosight and Vivotools	<ul style="list-style-type: none"> • Ra is the mean variation of the surface height • Rq is the root-mean-square variation of the surface height • Rz is the peak-to-trough difference of the surface height at the lowest and highest points 	Validated for use with repeatability estimated as ± 1.8 μm for Ra, ± 2.2 μm for Rq, and ±12 μm for Rz.	Automatically calculated; parameter cannot be fine-tuned

It is noted that certain parameters may be providing similar outputs. Thus, comparative analysis was conducted between selected parameters to optimize the characterisation of the skin, as detailed in the following sections.

6.2.3.1 Scaled Intensity Drop and Optical Attenuation Coefficient

Scaled Intensity Drop (SID) is estimated as the coefficient of the slope from the point of maximum intensity to the point where the signal reduces by 80% (Figure 3.8). Similarly, Optical Attenuation Coefficient (OAC) is defined by Vivosight as the slope of the OCT intensity signal versus the depth profile in the upper dermis (Vivotools User Guide, Issue 4), illustrated in Figure 6.9. The VivoTools software scales the intensity values depending on the maximum measurable value, such that the y-axis in the A-scans ranges from 0 to 1 corresponding to approximately 0 to 100 dB. The OAC is extracted from the curve which is mathematically fitted to the Intensity profile as follows,

$$OCT\ Intensity = A \cdot e^{-2\mu z} + Noise \quad (\text{Equation 6.1})$$

where A is a constant defined by the input beam intensity and the sensitivity of the detection system; z is depth below the surface; and μ is the attenuation coefficient. The factor of 2 is used because the OCT probe light traverses a total path length 2z (into the skin and back out again to the probe).

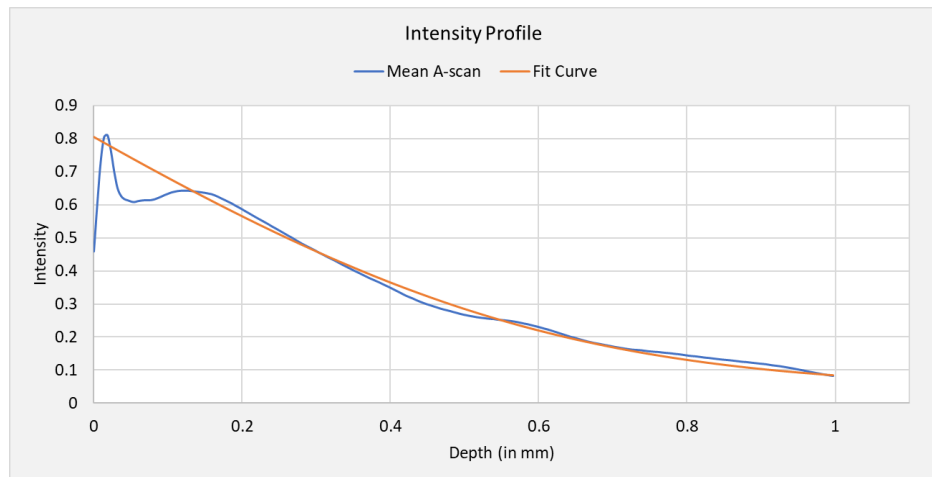


Figure 6.9 Exemplar A-line for an OCT scan of the cheek at baseline. The plot was created using the average Intensity values from the OCT images stack using the VivoTools software.

As SID and OAC are estimates of the attenuation of the OCT signal, these parameters were investigated for correlations. For the entire dataset from the present study, the data was non-normally distributed. The Spearman Correlation test of the SID versus the OAC revealed a strong correlation with the $r = 0.807$ and $p < 0.001$ (Figure 6.10). Interestingly, some clusters are observed

based on the anatomical locations, notably with the cheek having higher values than the arm and neck. Consequently, the SID values will be used for further analysis allowing comparison of the results from the present study with those from [Chapter 5](#).

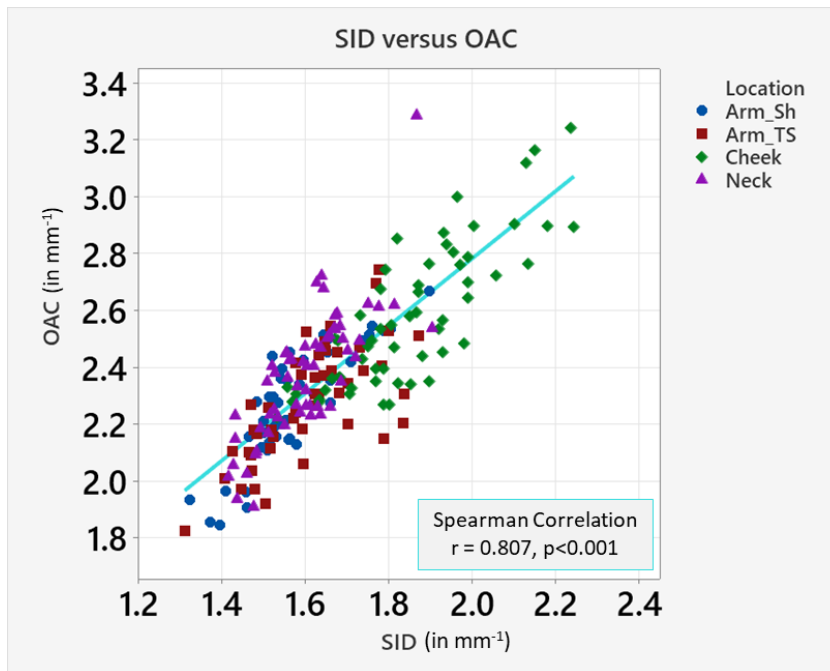


Figure 6.10 Scatterplot of SID vs OAC for all OCT scans in the present study.

6.2.3.2 Plexus Depth, Vessel Diameter, and Vessel Density

The **Vivosight** software yields a value corresponding to the Plexus Depth and Vessel Diameter for each OCT scan. Vessel Density is estimated by the accompanying **VivoTools** software which measures the active vasculature in the skin as a function of depth, yielding values from 0.0 (no vessels) to 1.0 (100% of the tissue is vessels) in increments of 0.05 mm for depth. An exemplar en-face image of a dynamic OCT scan is illustrated in [Figure 6.11a](#). For the corresponding OCT scan, the depth versus Vessel Density plot has been illustrated in [Figure 6.11c](#). The dynamic OCT algorithm accuracy reduces when the OCT signal is weak. In practice, the result is not reliable for depths > 0.50 mm. Furthermore, the manufacturer recommends assessing the Vascular Density at depths of 0.15 mm, 0.30 mm, or 0.50 mm which corresponds roughly to measurements in the papillary dermis, top of the superficial plexus, and just below the top of the superficial plexus, respectively ([Section 2.1](#)).

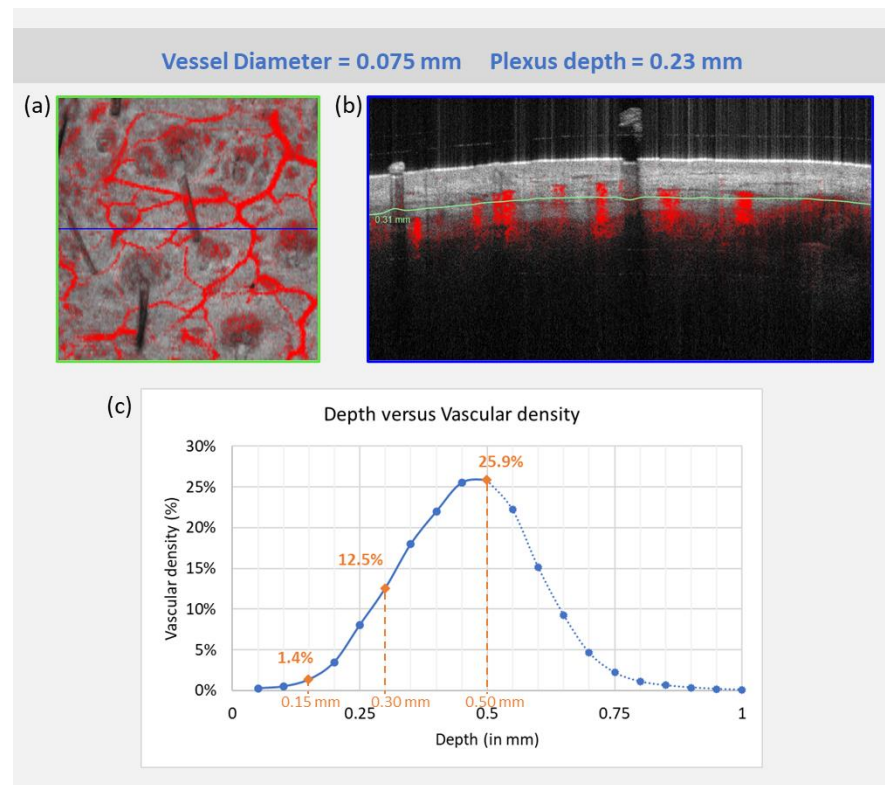


Figure 6.11 Dynamic OCT scan of the cheek at baseline. (a) En-face image of the stack at a depth of 0.3 mm, (b) exemplar 2D-OCT scan from the stack, (c) plot of depth versus vascular density for the OCT scan.

For the characterisation of the skin with respect to the Plexus Depth and Vessel Diameter (Figure 6.12), it is noted that the correlation between the parameters is not strong ($r = -0.477$, $p < 0.001$). Furthermore, there appears to be a site-specific shift in the values for both parameters. Consequently, both the Plexus Depth and Vessel Diameter will be included in further analysis.

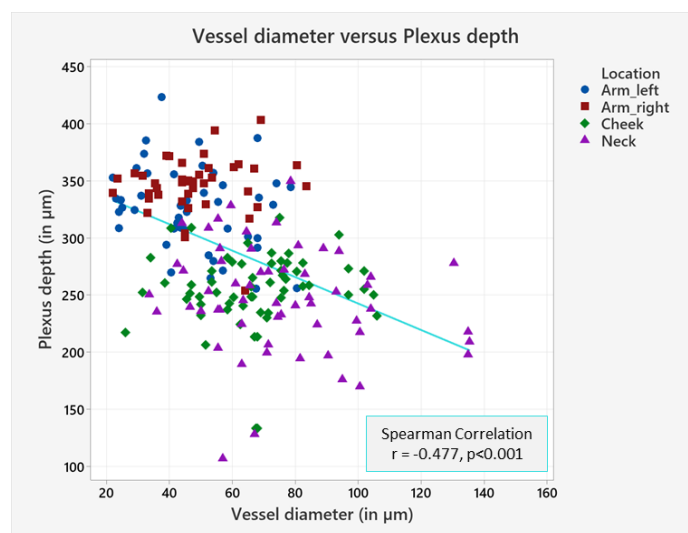


Figure 6.12 Scatterplot of Plexus Depth versus Vessel Diameter from all the OCT scans from the present study.

For the Vascular Density, an exemplar plot of results from the cheek for the Short Beard is illustrated in Figure 6.13. The values from 0.15mm depth demonstrated an increase from baseline at S+0.3h, with the difference almost reaching statistical significance ($p=0.053$). However, the recovery at S+24h did not reveal large differences from the baseline or S+0.3h. The results from 0.30mm depth demonstrated statistically significant differences between BL and S+0.3h ($p=0.006$), and between S+0.3h and S+24 ($p=0.018$). Recovery characteristics were observed as the S+24h values returned to BL. For the Vascular Density at 0.5mm depth, there were no significant differences between time points. As the Vascular Density at a depth of 0.30 mm provided the highest degree of distinction between different measurement times for the anatomical location being examined, this parameter was included in further analysis.

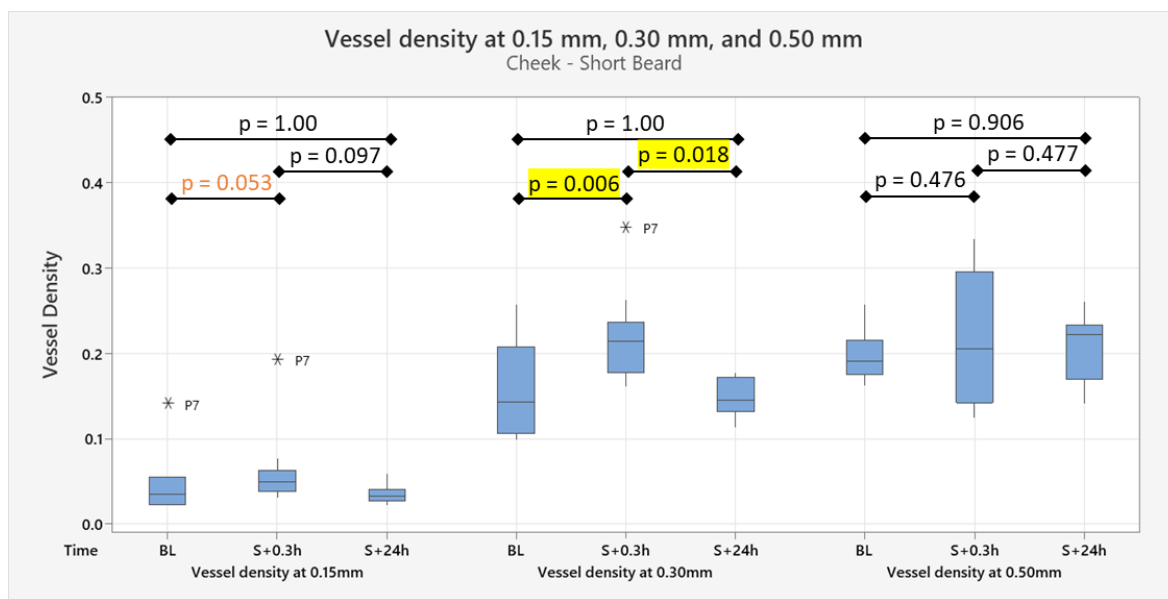


Figure 6.13 Exemplar Vascular Densities plots for OCT scans of the cheek corresponding to the Short Beard from the present study. Statistically significant differences between measurement times are calculated using Wilcoxon Signed Rank test.

6.2.3.3 Epidermal Parameters

The Epidermal Parameters include Epidermal Thickness, Epidermal Thickness Variation, and Epidermal Contrast. The estimation of these parameters is based on the peak detection in the A-line profiles as demonstrated in Figure 3.6. Similarly, the VivoTools software extracts the average epidermal thickness by analysing the OCT intensity profile. If it cannot find the epidermis due to a diminished second peak in the A-scan, then VivoTools will report 'N' for 'Epidermis detected' and the rest of the Epidermal Parameters are set to zero.

In the present study, the software failed to produce an output for the Epidermal Parameters in 29% scans from the cheek and 69% scans from the neck. An exemplar intensity profile of such a scan is shown in Figure 6.14. The thickness estimation was also attempted using the MATLAB algorithm previously developed (Section 3.3.3) on the raw Vivosight OCT scans. As demonstrated in Figure 6.14c, the algorithm was able to detect a second peak in the A-scan, and subsequently estimate a thickness value. However, upon examination of the scans for the entire cohort, it was revealed that the MATLAB algorithm was unable to estimate the thickness in 15% of the scans on the cheek and 41% of the scans on the neck. Therefore, the Epidermal Parameters have not been included in the analysis of the results from the present study.

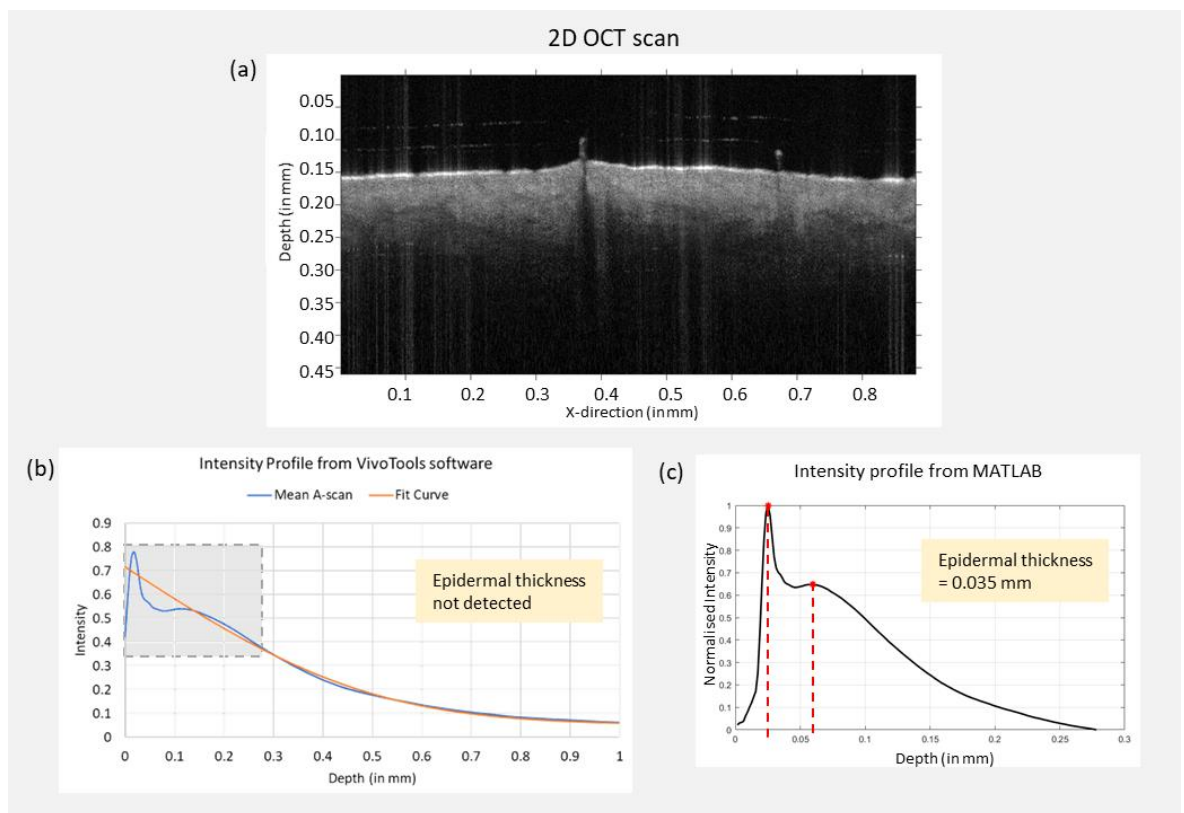


Figure 6.14 Exemplar Intensity profile for OCT scan of the cheek. (a) 2D-OCT scan; (b) A-scan from the VivoTools software where Epidermal thickness is not detected; (c) A-scan from the MATLAB algorithm with estimation of the Epidermal thickness.

6.2.3.4 Roughness from MATLAB and Roughness from Vivotools

The VivoTools software yields average roughness, RMS roughness, and peaks-to-trough roughness values of the skin surface for each OCT scan (Table 6.2). For direct comparison between the VivoTools outputs and those from the MATLAB algorithm, the RMS roughness will be further investigated. Furthermore, VivoTools also provides a rendering of the detected surface, enabling visualization of the post-processed surface. Thus, a detailed comparative analysis of the roughness estimation for one OCT scan is conducted and illustrated in Figure 6.15.

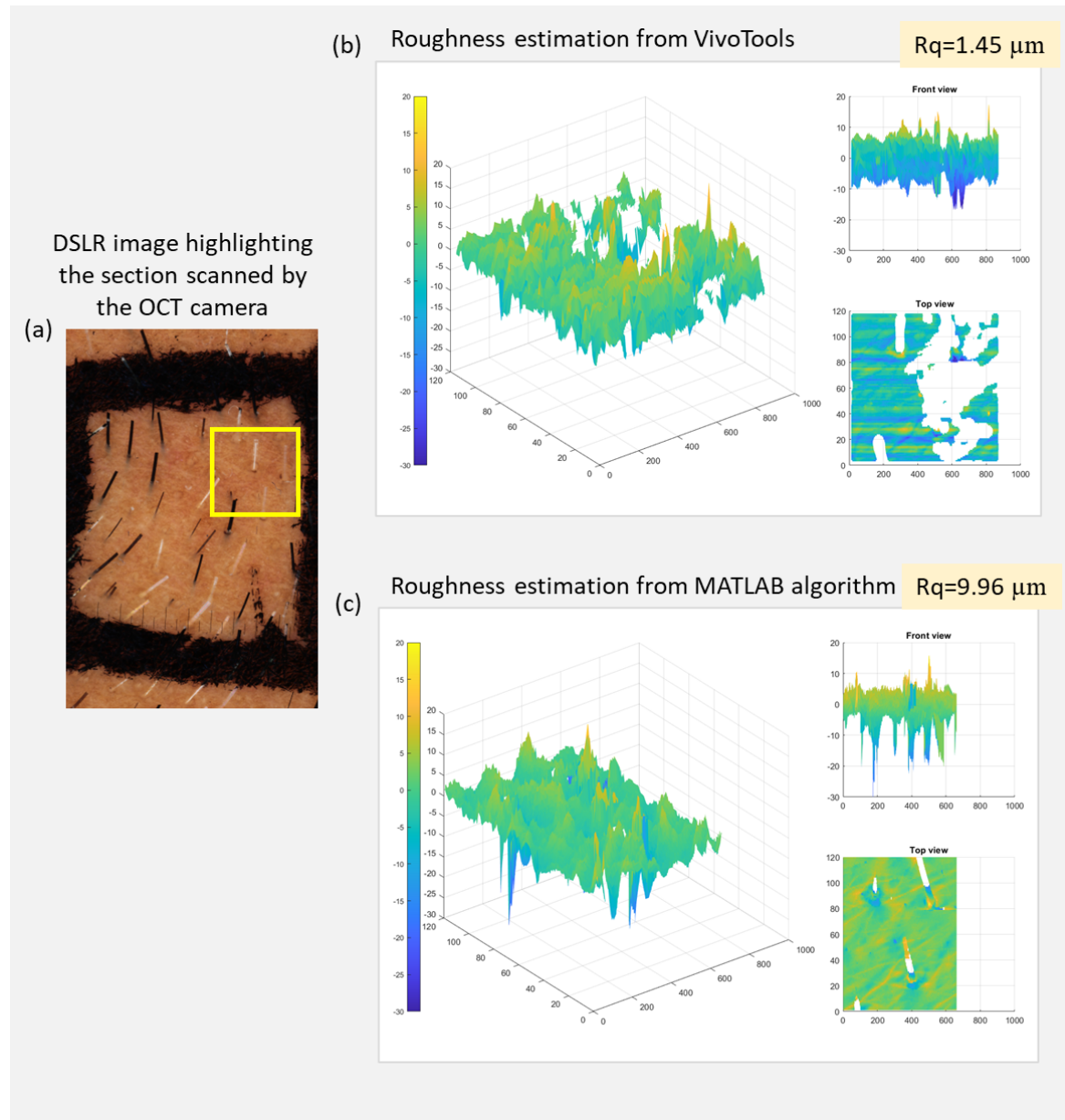


Figure 6.15 Comparison of RMS Roughness estimation from the VivoTools software and the MATLAB algorithm. a) Exemplar DSLR image of the cheek; (b) Post-processed surface rendering from VivoTools; (c) Surface rendering from MATLAB algorithm.

The surface plots in Figure 6.15 (b) and (c) have been generated from an OCT scan of the cheek where the skin sample is shown in Figure 6.15 (a). It is noted that the VivoTools software may have a filtering step which distinguishes noise (such as hair) and removes the associated pixels before calculating the roughness parameters. Indeed, it is observed that the Vivosight surface in Figure 6.15 (b) has many pixels removed. Similarly, the MATLAB algorithm detailed in Section 3.3.2 has been optimized to distinguish hair from skin and calculate the roughness of the remaining pixels. However, upon closer examination of Figure 6.15 (c), it is noted that the hair was more closely detected by this method, preventing the removal of relevant skin-pixels from the image. This difference in skin detection is evident in the roughness values generated by the two methods, where, for the example shown in Figure 6.15, the VivoTools software provided a value of $1.45\text{ }\mu\text{m}$ and the MATLAB algorithm provided a value of $9.96\text{ }\mu\text{m}$.

This trend in the two roughness values was noted for the results from the entire cohort (Figure 6.16), where the dispersion in the data increases with higher roughness values. Additionally, a strong correlation was revealed between the values with the $r=0.795$ ($p<0.001$). However, the slope and the intersect point indicted a systematic difference. Furthermore, site-specific clusters are observed with the roughness of the neck demonstrating the largest values from both estimation methods. This detail is considered important, especially in the context of shaving. The difference in the results from the two methods requires further investigation. However, for the purpose of the present study, one parameter can be selected to evaluate the temporal trends in roughness due to mechanical stimuli. Given the closer skin detection using the MATLAB algorithm, the MATLAB estimated roughness values will be analysed further in the present study.

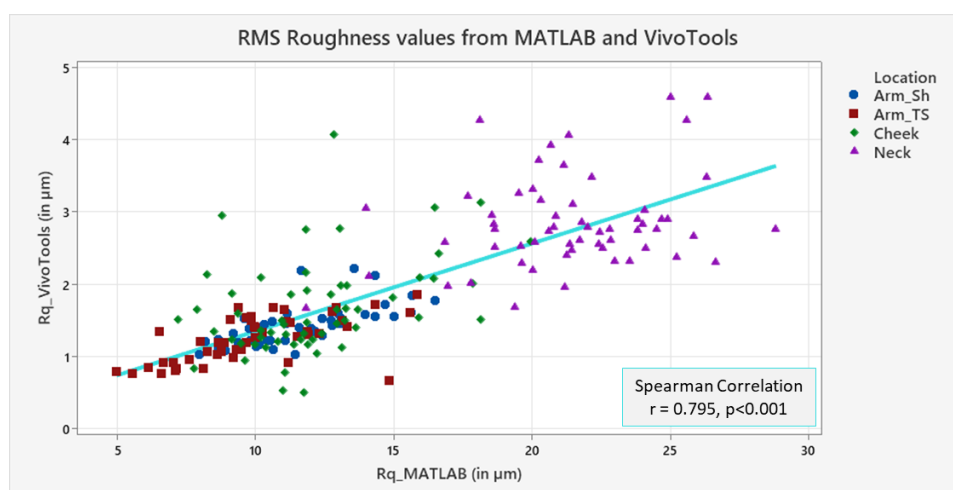


Figure 6.16 Scatterplot of Roughness values from MATLAB and VivoTools from all the OCT scans from the present study.

6.2.4 Redness estimation

Redness of the skin surface can be estimated from the DSLR images in the CIELAB colour space (Weatherall and Coombs 1992; Ly et al. 2020). Briefly, a CIELAB colour value expresses the lightness (black to white), red/green intensity, and yellow/blue intensity, as L^* , a^* , and b^* values, respectively (Figure 6.17). The L^* , a^* , and b^* values can be transcribed to dermatological parameters, where the L^* value correlates with the level of pigmentation of the skin; the a^* value correlates with erythema; and the b^* value correlates with pigmentation. Thus, in the present study, the a^* values have been generated to quantify the redness of the skin surface.

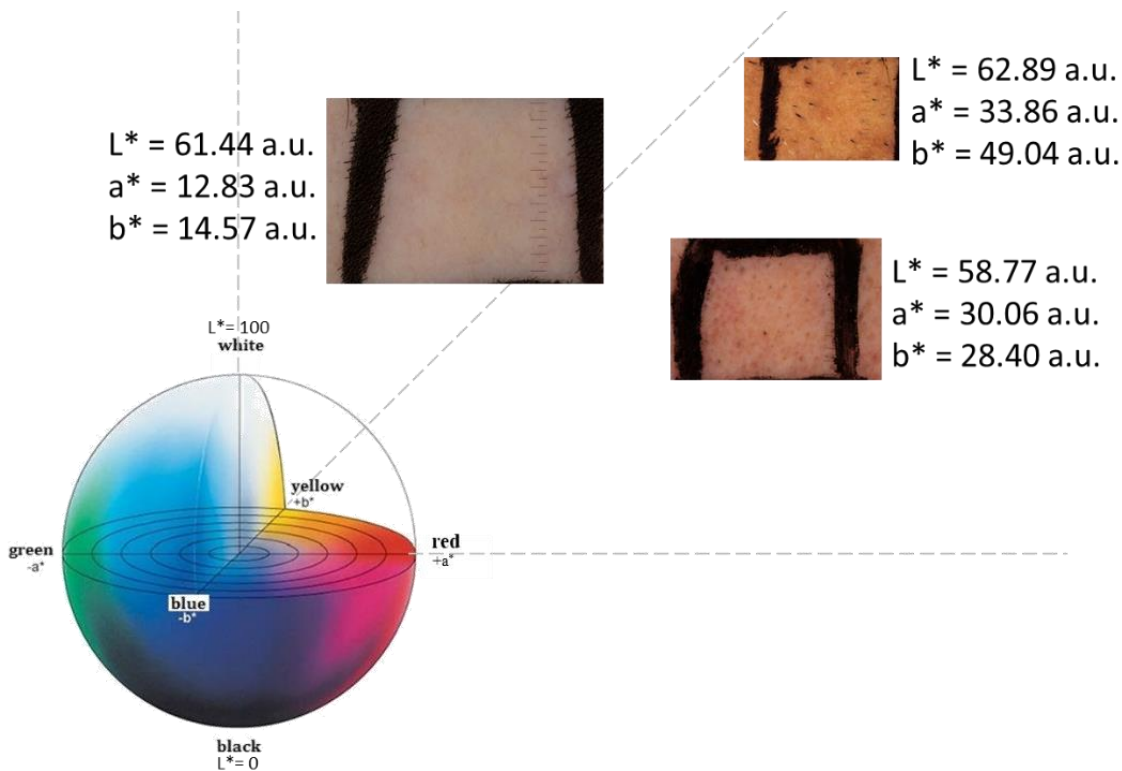


Figure 6.17 CIELAB colour sphere (Tang, Cai, and Xu 2015) with exemplar images from the present study.

Prior to estimation of the skin redness, the DSLR images were filtered to define a standardized region of interest ignoring the black square drawn on the skin with a mask designed to remove the hair in the images (Figure 6.18). Using the RGB2LAB function in MATLAB, the mean a^* values were then estimated for each image.

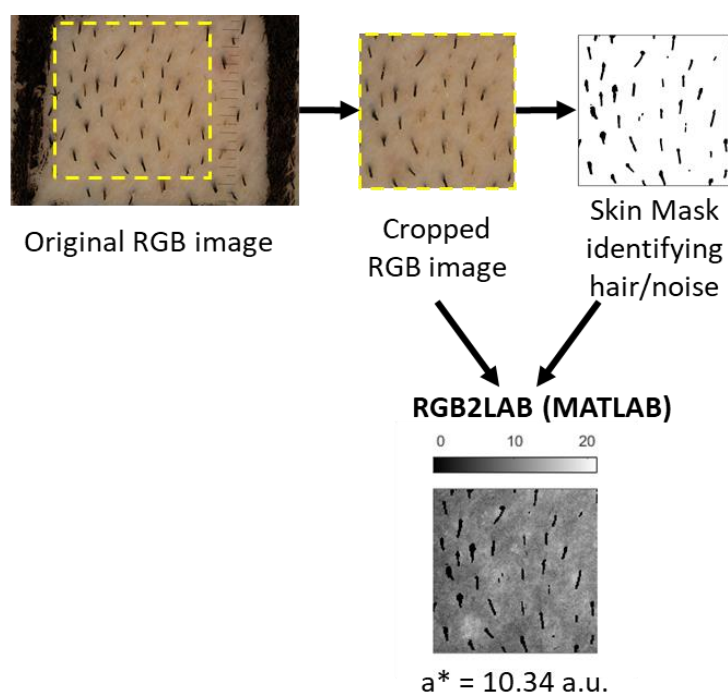


Figure 6.18 Schematic for redness estimation highlighting the region of interest in the original RGB image, skin mask generation, and the resulting a^* image.

6.2.5 Biochemical analysis

The extraction of skin inflammatory biomarkers was performed in collaboration with another researcher, who recently developed an optimised approach to protein recovery (Jayabal et al. 2022). The number of sebum samples had to be reduced to accommodate the capacity of the ELISA analysis. Consequently, the samples from the cheek and neck were prioritized over those from the forearms due to the overarching aims of the present study. Furthermore, the samples from the Short Beard session were prioritised over those from the Long Beard session, hoping to achieving a stronger signal due to the repetitive loading. Thus, Sebutapes obtained only from the cheek and neck in the Short Beard session were selected for the exploratory analysis.

Extraction and analysis followed a standard operating procedure. To review briefly, frozen Sebutape samples were thawed to room temperature, and a 0.85 ml solution of phosphate-buffered saline (PBS) (Sigma-Aldrich Co, St. Louis, Missouri, USA) and 0.1% dodecylmaltoside (DDM) (Thermo Fisher Scientific, UK) was added to each container. After 1 hour of vigorous shaking and immersion in the solution, the containers were sonicated for 5 minutes, the Sebutapes discarded, and 0.5 ml of the extraction buffer was transferred into vials for centrifugation. Subsequently, the vials were centrifuged for 10 min at 15000 g, whilst being maintained at a constant temperature of 4°C. The supernatants were discarded and the pellets vortexed for 10 s. The samples were then

processed using U-Plex immuno-assay kits (Meso Scale Diagnostics, USA) to quantify the concentration of specified cytokines. The panel of cytokines investigated include high-abundant cytokines such as IL-1 α and IL-1RA and low abundant cytokines, namely, IL-8 as they have been identified to be highly relevant in the context of skin damage owing to their upregulation following mechanical stimuli in tissue models (Terui et al. 1998; Perkins et al. 2001). Furthermore, low abundant cytokines such as IL-6, INF- γ , and TNF- α are also included as they have been highlighted for their role in the inflammatory cascade following insults and in the formation of skin barrier (Ulfgren et al. 2000).

Analysis of the sebum samples was conducted over two sessions involving calibrators and plates from different batches. Consequently, the samples from P5 and P7 were analysed in a different batch compared to the other remaining samples. As a result, the chemical evaluation for P5 and P7 was limited to IL-1 α , IL-1RA, and IFN- γ .

6.2.6 Statistical analysis

Most parameters have $p < 0.05$ for the Anderson Darling normality test ([Appendix E](#)), indicating that the data is non-normally distributed. Thus, non-parametric statistics were chosen. To investigate the difference between anatomical locations at baseline, the values for both the arms, and the Long Beard session for the cheek and neck were considered. The groups medians of the parameters were tested for statistical significance using the Wilcoxon signed rank test. To investigate the influence of time at each location, the group medians of the parameters were tested for statistical significance using the Friedman test. Each anatomical site was subsequently analysed in more detail with differences from baseline, tested for significance using the Wilcoxon signed rank test. Furthermore, final recovery characteristics were also tested for statistical significance using the Wilcoxon signed rank test after the first and second stimulus, respectively.

6.3 Results

Ten volunteers were recruited for this study, as detailed in Table 6.3. Only one participant, P9, was unable to attend Day 3 and thus, there is no data for S2+24h from the forearms and S+24h from the Short Beard on the cheek and neck. Furthermore, S2+24h values were not recorded for P1 and P2 from the forearms as the protocol was later modified to include this measurement in the cohort. Also, only 15 tapes were used for the second forearm stimulus (S2) as the positive control for P6 because the participant complained of discomfort.

Table 6.3 Participant details from the study with the calculated S-score and SS Label.

Participant No.	Age	Shaving tool	Shaving frequency (#/week)	S-Score	SS Label
P1	35	Combination	<2	29%	Mild SS
P2	28	Non-electric	<2	52%	Mild SS
P3	25	Non-electric	<2	26%	Mild SS
P4	37	Electric	3, 4	40%	Mild SS
P5	24	Combination	3, 4	27%	Mild SS
P6	38	Non-electric	<2	52%	Mild SS
P7	36	Non-electric	<2	54%	Mild SS
P8	37	Electric	<2	62%	High SS
P9	41	Non-electric	<2	59%	High SS
P10	41	Non-electric	3, 4	43%	Mild SS

6.3.1 Comparison of baseline characteristics for each anatomical site

The baseline values for the skin parameters at each anatomical location are illustrated in Figure 6.19. Overall, for all parameters, the results from each arm had largely overlapped values such that no statistically significant differences ($p>0.05$) were observed. Comparing the results from the arms with those from the facial sites, 7 of the 10 parameters, namely TEWL (Figure 6.19a), redness (Figure 6.19c), AuC (Figure 6.19e), plexus depth (Figure 6.19g), vessel diameter (Figure 6.19h), vessel density (Figure 6.19i), and SRR (Figure 6.19j), revealed statistically significant differences ($p<0.05$) from the cheek and neck. Furthermore, the arms revealed the highest median values for hydration (Figure 6.19b, $p<0.05$ compared to the cheek), AuC, and plexus depth. Additionally, there

were differences in the inter-subject variability in several parameters for the different locations, such that the vessel density revealed three-fold larger ranges in the results on the facial sites, while redness and vessel diameter revealed 50% larger ranges. The plexus depth was observed to be shallower on the facial sites with the results revealing 30% higher median values for the arms.

The cheek demonstrated the highest median values for 6 of the 10 parameters, namely TEWL, Redness, SID ([Figure 6.19d](#)), Vessel diameter, Vessel density, and SRR ($p < 0.05$ compared to the arms). In addition, large inter-subject variability was observed on the cheek for AuC and SRR, such that the range of values was 2 times and 1.5 times greater than the other sites, respectively. The neck revealed the highest values for the Rq ([Figure 6.19f](#), $p < 0.05$ compared to arms and cheek), which was approximately 1.5 times greater than the medians from the other sites. Furthermore, TEWL revealed a high degree of inter-subject variability such that the range of values was almost 2-fold greater than the other sites. In addition to the Rq, results from the cheek and neck demonstrated statistically significant differences for the SID and SRR. In both cases, the cheek revealed larger variability between participants.

Values of the medians, ranges, and outliers have been detailed in the following sections.

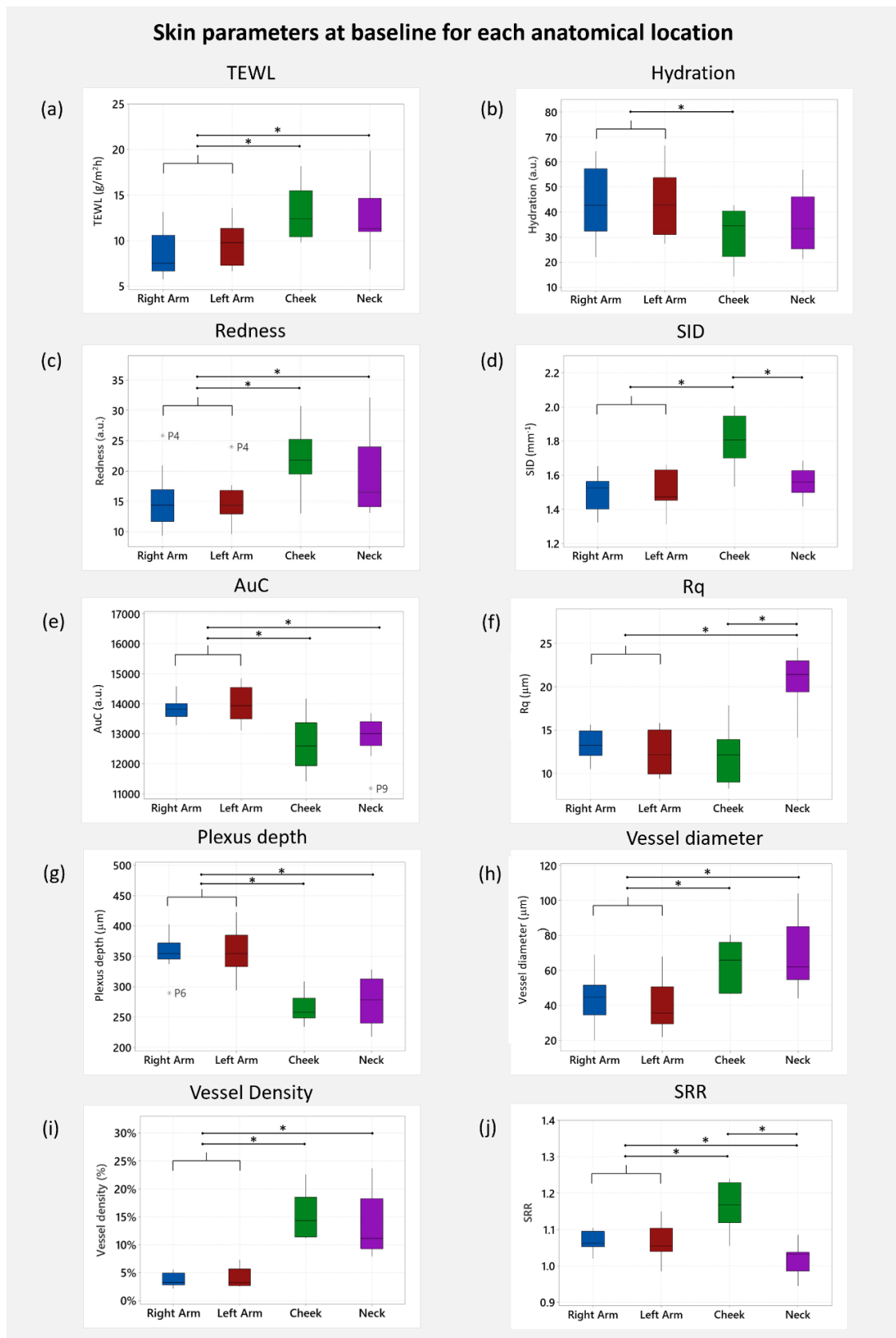


Figure 6.19 Baseline characteristics for all anatomical locations for (a) TEWL, (b) Hydration, (c) Redness, (d) SID, (e) AuC, (f) Rq, (g) Plexus depth, (h) Vessel diameter, (i) Vessel Density, (j) SRR. Outlier values are indicated, as are statistically significant differences between groups using the Wilcoxon test (* $p < 0.05$).

6.3.2 Temporal response for each anatomical site

For the temporal effect of the mechanical stimuli on each site, the p-values from the Friedman test are summarised in Table 6.4. Furthermore, the results from the Long and Short Beards on the cheek and neck have been investigated independently to explore the influence of beard length for each skin parameter.

Table 6.4 P-values from the Friedman Test investigating the influence of time on each location for the selected parameters. $p < 0.05$ has been highlighted in yellow. Arm_Sh and Arm_TS refer to the shaving and tape stripping stimulus on the each arm, respectively.

Parameter	Arm_Sh (n=7)	Arm_TS (n=7)	Cheek_ Long Beard (n=10)	Cheek_ Short Beard (n=9)	Neck_ Long Beard (n=10)	Neck_ Short Beard (n=9)
TEWL*	0.080	<0.001	0.013 (n=9)	0.030 (n=8)	0.002 (n=9)	0.002 (n=8)
Hydration	0.100	0.020	0.001	0.003	0.001	0.001
Redness	0.060	0.002	<0.001	<0.001	<0.001	0.001
SID	0.010	0.004	0.025	0.097	0.002	0.016
AuC	0.060	0.008	0.082	0.062	0.002	0.032
Rq	0.200	0.010	0.741	0.368	0.670	0.368
Plexus Depth	0.454	0.013	0.407	0.013	0.001	0.002
Vessel Diameter	0.014	<0.001	0.009	0.001	0.207	0.025
Vessel Density	0.096	0.007	0.082	0.004	<0.001	<0.001
SRR	0.189	0.002	0.407	0.256	0.076	0.002

*Sample size for TEWL measurements were different than that noted in the column headers due to malfunctioning of the probe for one participant.

Tape stripping revealed statistically significant temporal effects on the arm for all 10 skin parameters ($p < 0.05$). Conversely, the only significant changes on the shaving arm were for SID and Vessel Diameter parameters ($p < 0.05$). Smaller changes were observed in TEWL, redness, and AuC, which were all close to statistical significance ($p \leq 0.082$).

For the cheek and neck, the shaving stimuli revealed statistically significant temporal effects for TEWL, hydration, and redness, whereas the Rq demonstrated smaller changes. The Plexus Depth and Vessel Density showed statistically significant changes in most cases, excluding the Cheek_Long Beard, where the temporal trend for Vessel Density was approaching statistical significance ($p=0.082$). Additionally, SID and Vessel Diameter also revealed statistically significant temporal trends for most cases, excluding the SID for the Cheek_Short Beard ($p=0.097$) and Vessel Density for the Neck_Long Beard ($p=0.207$). The AuC revealed distinct temporal trends based on the anatomical location such that the results for the neck were statistically significant. However, those for the cheek were approaching significant values ($p\leq 0.082$). Similarly, the SRR also demonstrated distinct trends based on the anatomical locations, where the results for the Neck_Short Beard revealed statistically significant temporal trends ($p=0.002$), whereas those for the cheek revealed smaller changes such that the differences were not statistically significant ($p=0.407$ for Long Beard and $p=0.256$ for Short Beard).

6.3.2.1 Shaving on the arm

The temporal effect of shaving on the arm is illustrated for each parameter in [Figure 6.20](#). For TEWL ([Figure 6.20a](#)), at baseline (BL) the results were clustered around normative values, ranging from 5.78 g/m²h to 13.15 g/m²h, with a median of 7.54 g/m²h. The first shaving stimulus and subsequent recovery did not reveal remarkable changes in the TEWL values. An exception to this trend was P9, who was an outlier with a value of 29.26 g/m²h at S1+24h. A significant increase ($p=0.035$) in TEWL values was observed after the second shaving stimulus (S2+0.3h), where the relative change between the participants varied as the values ranged from 7.01 g/m²h to 25.29 g/m²h, while the median demonstrated an increase of 2.12 g/m²h. Additionally, P7 was observed as a outlier with TEWL equal to 32.92 g/m²h. Subsequently, the cohort revealed partial recovery after 24 hours (S2+24h) as the values ranged from 6.92 g/m²h to 14.03 g/m²h but the median remained significantly elevated from baseline (median=10.28 g/m²h, $p=0.033$).

For hydration ([Figure 6.20b](#)), a considerable variation in values was evident between participants at baseline, where the results ranged from 22.0 a.u. to 64.3 a.u. with a median of 42.7 a.u. However, following the first shaving stimulus, a statistically significant increase ($p=0.014$) in values was observed (median: 51.2 a.u., range: 37.0 a.u. to 65.6 a.u.). At 24 hours post stimulus, the group characteristics remained similarly elevated from basal values ($p=0.041$). Following the second shaving stimulus, the results continued to demonstrate an increase (median: 53.6 a.u., range: 43.1 a.u. to 68.9 a.u.), which was statistically significant ($p=0.006$) compared to baseline. By contrast, at

24 hours post second stimulus, there was some recovery in hydration values where the differences to baseline were no statistically significant ($p>0.05$).

For redness (Figure 6.20c), the basal values ranged from 9.3 a.u. to 21.0 a.u., with a median of 14.4 a.u. Furthermore, P4 was noted as an outlier with the redness value of 25.8 a.u, demonstrating highest basal redness values in the cohort. Overall, there were only a few remarkable changes in the results following the shaving stimuli. After the first insult, there was a statistically significant ($p=0.025$) increasing trend in the results such that the values ranged from 9.9 a.u. to 25.8 a.u., while the median demonstrated an increase of 1 a.u. Subsequent measurements revealed smaller changes in results ($p>0.05$).

For SID (Figure 6.20d), the results at baseline ranged from 1.32 mm^{-1} to 1.65 mm^{-1} with a median value of 1.53 mm^{-1} . Following the first shaving stimulus there was a statistically significant increase ($p=0.025$) in SID with the values ranging from 1.40 mm^{-1} to 1.81 mm^{-1} . After an interval of 24 hours, the group demonstrated a return to baseline, with values clustered between 1.46 mm^{-1} and 1.60 mm^{-1} and P9 as an outlier ($\text{SID}=1.75 \text{ mm}^{-1}$). After the second shaving stimulus, there was a significant increase in SID ($p=0.006$), with the median value equal to 1.65 mm^{-1} (range: 1.46 mm^{-1} to 1.90 mm^{-1}). Subsequently, the group demonstrated recovery characteristics with a statistically significant difference from $\text{S2}+0.3\text{h}$ ($p=0.022$) where the values ranged between 1.49 mm^{-1} to 1.55 mm^{-1} and P8 was observed as an outlier ($\text{SID}= 1.74 \text{ mm}^{-1}$).

For AuC (Figure 6.20e), the baseline values ranged from 13,288 a.u. to 14,586 a.u. with a median of 13,824 a.u. Overall, there were few remarkable changes in the results following the insults. Notably, there was a decrease in AuC after each shaving stimuli, and a return towards baseline at $\text{S1}+24\text{h}$. However, 24 hours after the second shaving stimulus, the group demonstrated a significant increase ($p=0.022$) from baseline, where the difference in median AuC was estimated as 185 a.u.

For Rq (Figure 6.20f), the basal values ranged from $10.5 \mu\text{m}$ to $15.7 \mu\text{m}$ with a median on $13.3 \mu\text{m}$. Following the first shaving stimulus, there was statistically significant decrease ($p=0.006$) in values with the median roughness equal to $11.5 \mu\text{m}$ (range: $7.9 \mu\text{m}$ to $13.0 \mu\text{m}$). 24 hours after the first stimulus, the group median continued to decrease to $10.4 \mu\text{m}$, which remained statistically lower than baseline ($p=0.006$). However, the trends between participants were different as the values ranged from $8.7 \mu\text{m}$ to $16.5 \mu\text{m}$. Following the second shaving stimulus, the Rq remained low with the median value equal to $10.9 \mu\text{m}$ ($p=0.006$). After 24 hours, a small increase was observed in the group characteristics such that the median Rq was equal to $11.1 \mu\text{m}$, which was not statistically significant when compared to BL.

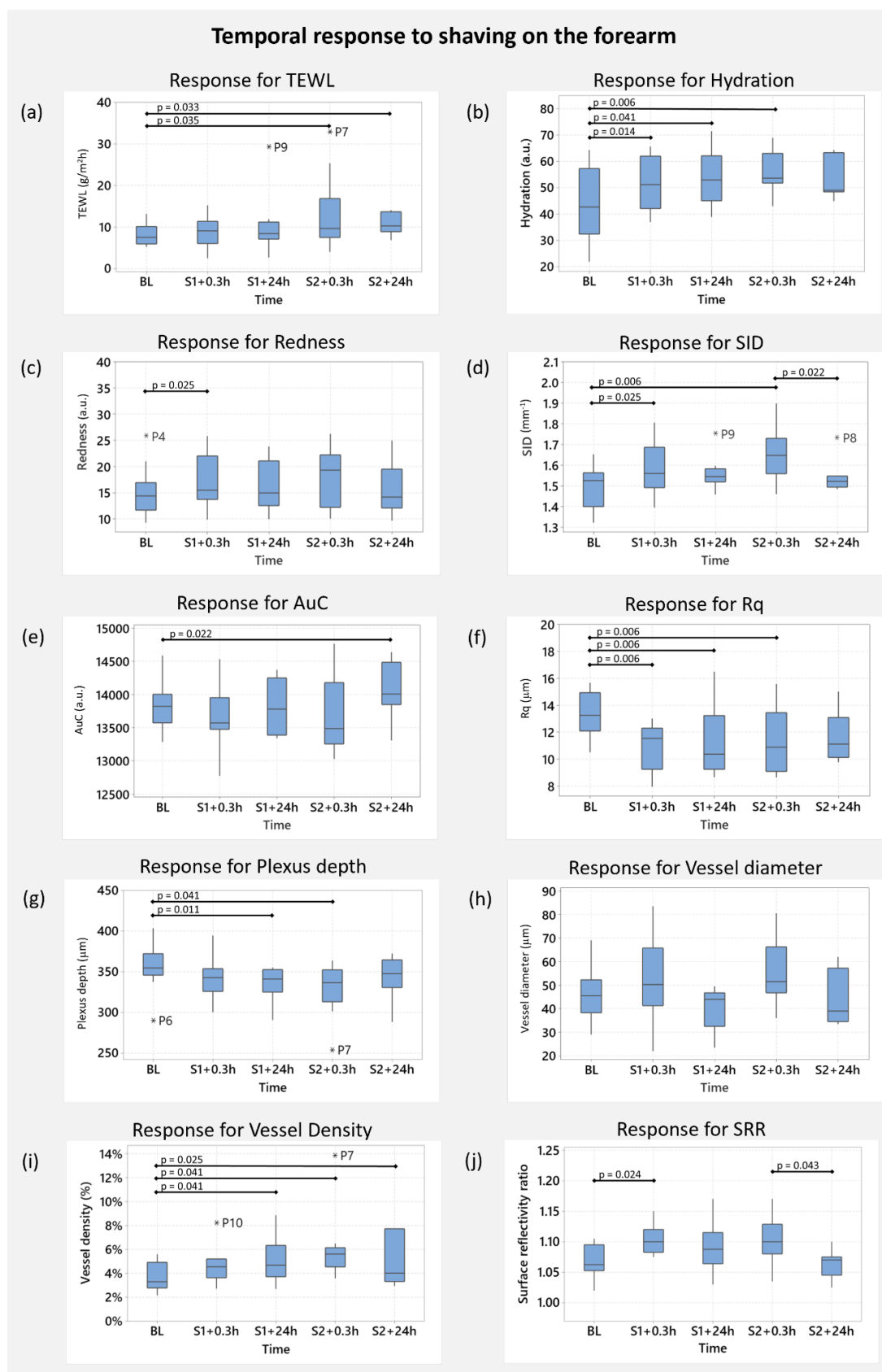


Figure 6.20 Temporal response following shaving on the arm for (a) TEWL, (b) Hydration, (c) Redness, (d) SID, (e) AuC, (f) Rq, (g) Plexus depth, (h) Vessel diameter, (i) Vessel Density, (j) SRR.

Outlier values are indicated, as are statistically significant differences from baseline and statistically significant recovery from stimulus using the Wilcoxon test.

For plexus depth (Figure 6.20g), the results at baseline ranged from 338 μm to 403 μm with a median value of 355 μm . Furthermore, P6 was observed as an outlier with the plexus depth as 290 μm , indicating the shallowest depth in which basal vascular flow recorded for this cohort. After initial shaving, there was a small decrease in the plexus depth (median: 34.3 μm , range: 300 μm to 394 μm). The plexus depth continued to decrease up to 24 hours post stimulus reaching values that were then statistically lower than those at baseline ($p=0.011$), corresponding to a median change of 13 μm (range: 291 μm to 355 μm). After the second shaving stimulus, the plexus depth remained low such that the values were still significantly different ($p=0.041$) from baseline. Here, P7 was noted as an outlier with a plexus depth of 245 μm . Partial recovery was observed at 24 hours after the second stimulus such that the distribution of values was no longer statistically different from baseline ($p > 0.05$).

For vessel diameter (Figure 6.20h), the baseline values ranged from 20 μm to 69 μm with a median of 45 μm . Overall, there were few remarkable changes in the results in response to the shaving insults. There was an increase ($p>0.05$) in the vessel diameter after each round of shaving where the difference in medians from baseline estimated as 5 μm at S1+0.3h and 6 μm at S2+0.3h. Furthermore, both recovery periods revealed a decrease ($p>0.05$) in vessel diameter towards baseline.

For vessel density (Figure 6.20i), the values at baseline ranged from 2.2% to 5.6% with a median of 3.3%. Over the course of the study there was an incremental increase in vessel density values, where 24 hours after the initial stimulus (S1+24) and for both time points after the second stimulus, values statistically higher than baseline. During both 24-hour recovery periods, there was a high degree of inter-subject variability, evidenced by the wide range between values (range: 2.7% to 8.9% at S1+24h and 3.0% to 7.7% at S2+24h). In addition, outliers were noted, for example P7 had a vessel density equal to 13.9% at S2+0.3h.

For SRR (Figure 6.20j), the basal values ranged from 1.02 to 1.11 with a median of 1.06. After the first shaving stimulus, a statistically significant increase ($p=0.02$) was observed in the cohort with median value of 1.1. After 24 hours, differences in relative trends were observed for individual participants, as the results ranged from 1.03 to 1.17 with a median of 1.09. For example, P4 revealed a decrease in SRR values from 1.1 at S1+0.3h to 1.03 at S1+24h, while P10 revealed an increase in SRR from 1.08 to 1.11, respectively. Following the second shaving stimulus, a small increase ($p>0.05$) in group median value was observed, although there was a high degree of variation between participants with values ranging from 1.04 to 1.17. The final time point revealed some recovery of values back to baseline, where there was a significant reduction in SRR between S2+0.3h and S2+24h ($p=0.043$).

6.3.2.2 Tape stripping on the arm

The temporal effect of tape stripping on the arm is illustrated for each parameter in [Figure 6.21](#). All parameters demonstrated a statistically significant increase in values from baseline following each tape stripping insult. Exception to this trend is observed for AuC, Rq, and Plexus depth, where values demonstrated a statistically significant decrease following simulation. Results for each parameter have been reviewed in detail in the following paragraphs.

For TEWL ([Figure 6.21a](#)), the basal values ranged from 6.63 g/m²h to 13.60 g/m²h with a median of 9.78 g/m²h. After the first round of tape stripping, there was a statistically significant increase ($p=0.022$) in the values and in the variation between participants such that the median TEWL was equal to 12.94 g/m²h (range: 9.48 g/m²h to 29.32 g/m²h). After 24 hours, there was a small increase of 2.83 g/m²h in the median, which continued to reveal statistically significant elevation ($p=0.009$) from baseline. Furthermore, a large variation was observed between participants (range: 8.66 g/m²h to 46.67 g/m²h). After the second round of tape stripping, there was a 6-fold increase in median TEWL from BL ($p=0.009$, median: 60.34 g/m²h). P5 was noted as an outlier, demonstrating a smaller increase (TEWL=16.57 g/m²h). Partial recovery was observed at S2+24h for most participants as the group demonstrated a decrease ($p=0.0035$) in values with the median equal to 39.28 g/m²h, which was 4-fold greater than BL ($p=0.009$).

For hydration ([Figure 6.21b](#)), the results at baseline ranged from 27.4 a.u. to 66.6 a.u. with a median of 42.8 a.u. An increase in values ($p=0.008$) was observed after the initial tape stripping with median hydration equal to 57.7 a.u. After 24 hours, the participants revealed differences in relative trends, as the results ranged from 35.4 a.u. to 80.8 a.u. indicating a drying effect for some participants. However, the median revealed statistically significant differences from BL ($p=0.014$). After the second round of tape stripping, there was a 2-fold increase in values from BL ($p=0.006$), with median hydration equal to 92.2 a.u. Additionally, large variation was observed between individuals as results ranged from 29.7 a.u. to 100.6 a.u. Subsequently, recovery characteristics were observed for the group as hydration values decreased towards baseline ($p>0.05$).

For redness ([Figure 6.21c](#)), the basal values ranged from 9.59 a.u. to 17.68 a.u. with a median of 14.36 a.u. Like that on the other forearm, P4 was noted as an outlier with redness equal to 24.01 a.u. The results revealed a 40% increase ($p=0.006$) in the median following the first tape stripping stimulus. Subsequently, the group demonstrated initial recovery characteristics after 24 hours as the redness values decreased significantly ($p=0.008$) towards baseline. Following the second tape stripping stimulus, the group demonstrated a 50% increase ($p=0.006$ from BL). In contrast to the previous 24 hours interval, the group did not reveal recovery characteristics at S2+24h as the results

remained elevated from baseline ($p=0.035$). However, P5 was noted as a low responding outlier with redness equal to 10.06 a.u.

For SID (Figure 6.21d), the basal values ranged from 1.31 mm^{-1} to 1.66 mm^{-1} with a median of 1.47 mm^{-1} . The first round of tape stripping revealed a significant increase ($p=0.006$) in SID such that the median was equal to 1.65 mm^{-1} (range: 1.48 mm^{-1} to 1.84 mm^{-1}). After 24 hours, the group demonstrated initial recovery characteristics as the results returned towards baseline ($p=0.014$ from S1+0.3h). Following the second round of tape stripping, there was a significant increase ($p=0.006$) in SID again (range: 1.50 mm^{-1} to 1.87 mm^{-1}). Subsequently, the results returned towards baseline ($p>0.05$ from BL).

For AuC (Figure 6.21e), the results at baseline ranged from 13,114 a.u. to 14,849 a.u. with a median of 13,940 a.u. After the first round of tape stripping, there was a significant decrease ($p=0.006$) in AuC from baseline (median=13,255 a.u.). Following an interval of 24 hours, initial recovery characteristics were observed as the AuC demonstrated an increase ($p=0.008$) which was statistically significant from the first stimulus. However, the spread between the values was smaller than that observed at baseline as the results ranged from 13,226 a.u. to 14,452 a.u. After the second round of tape stripping, the group revealed a decrease ($p>0.05$) in the AuC (difference in median = 335 a.u.). Interestingly, after an interval of 24 hours, recovery characteristics were not observed as the AuC continued to demonstrate a decrease such that group revealed statistically significant differences from baseline ($p=0.035$).

For the surface roughness (Figure 6.21f), the basal values ranged from $9.4 \text{ }\mu\text{m}$ to $15.8 \text{ }\mu\text{m}$ with a median of $12.2 \text{ }\mu\text{m}$. After the first stimulus, there was a significant decrease ($p=0.006$) in values such that the median Rq was $9.48 \text{ }\mu\text{m}$ (range: $7.1 \text{ }\mu\text{m}$ to $12.9 \text{ }\mu\text{m}$). Recovery was not observed after 24 hours as the Rq remained significantly lower than BL ($p=0.006$). After the second round of tape stripping, the values decreased again ($p=0.006$), revealing a median Rq of $7.7 \text{ }\mu\text{m}$. Subsequently, recovery was not observed after 24 hours as a small increase in Rq was revealed which remained significantly lower than basal values ($p=0.022$). However, two outliers were observed as P5 and P7 revealed Rq values of $11.88 \text{ }\mu\text{m}$ and $4.98 \text{ }\mu\text{m}$ at S2+24h.

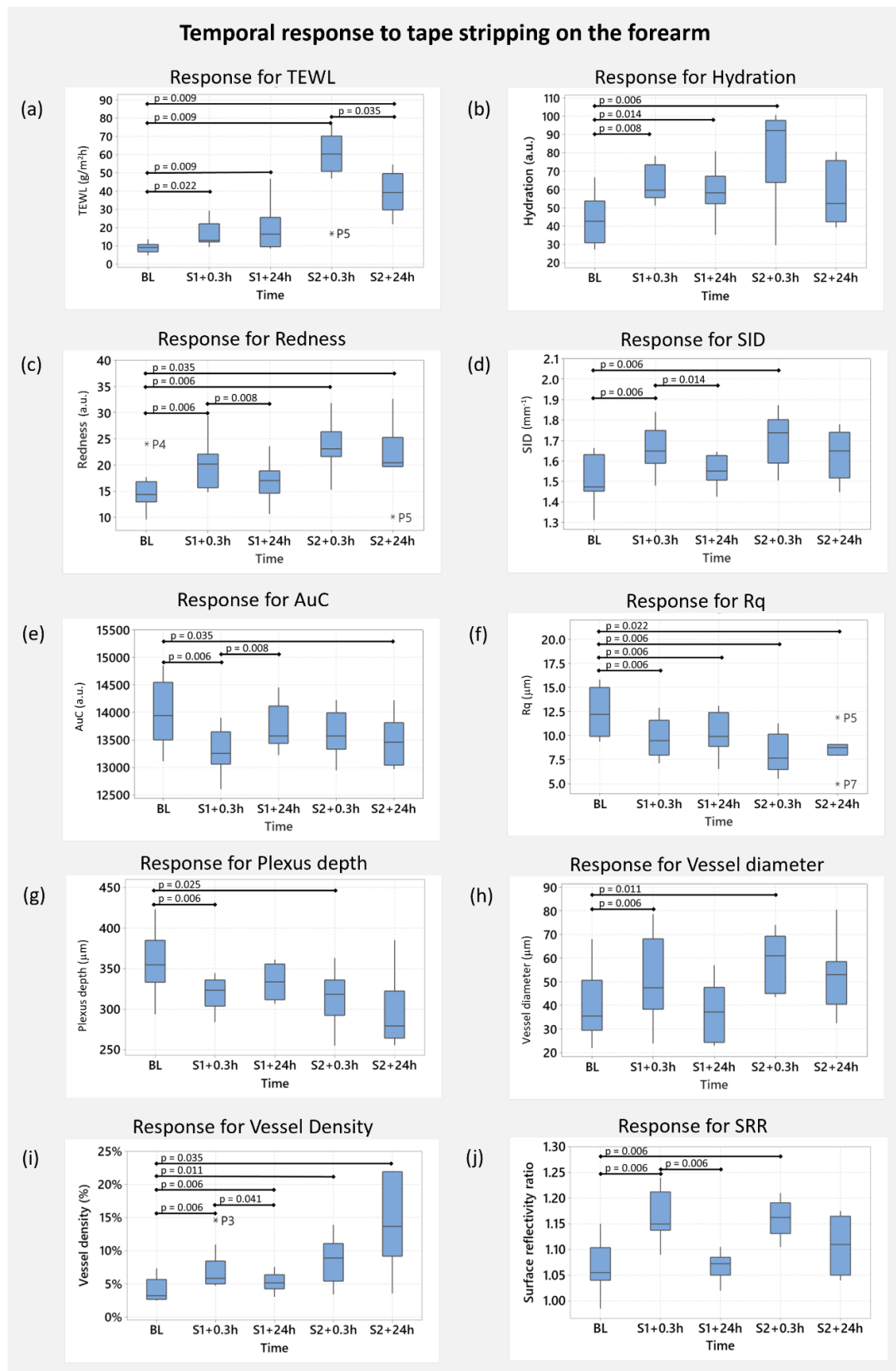


Figure 6.21 Temporal response following tape stripping on the arm for (a) TEWL, (b) Hydration, (c) Redness, (d) SID, (e) AuC, (f) Rq, (g) Plexus depth, (h) Vessel diameter, (i) Vessel Density, (j) SRR. Outlier values are indicated, as are statistically significant differences from baseline and statistically significant recovery from stimulus using the Wilcoxon test.

For the plexus depth (Figure 6.21g), the values at baseline ranged from 294 μm to 423 μm with a median of 355 μm . Following tape stripping, an overall decreasing trend in plexus depth was observed. After the initial tape stripping stimulus, there was a statistically significant decrease ($p=0.006$) in values from baseline (median: 343 μm , range: 285 μm to 345 μm). No significant changes were observed in the subsequent recovery period. After the second tape stripping stimulus, the cohort revealed a significant decrease ($p=0.025$) from baseline (median: 319 μm , range: 256 μm to 363 μm). After 24 hours, the median plexus depth continued to decrease, but did not reveal any significant changes due to a large variation within the cohort which ranged from 256 μm to 385 μm .

For the vessel diameter (Figure 6.21h), the values at baseline ranged from 22 μm to 68 μm with a median of 36 μm . Significant changes in results were observed after each tape stripping stimulus where the median values increased by 12 μm at S1+24h ($p=0.006$) and 25 μm at S2+24h ($p=0.011$). Both recovery periods revealed a decrease ($p>0.05$) in values towards baseline, however large variability was observed between participants at S2+24h (range: 33 μm to 81 μm).

For the vessel density (Figure 6.21i), the values at baseline ranged from 2.5% to 7.3% with a median of 3.2%. Similar to the shaving stimuli on the contralateral arm, there was an incremental increase in vessel density such that each time point revealed significantly higher values from baseline. Furthermore, partial recovery was observed at S1+24h as the results revealed a significant decrease from stimulus ($p=0.041$). Conversely, the results at S2+24h demonstrated an increase ($p=0.035$ from BL) and a high degree of inter-subject variability (range: 3.5% to 21.9%)

For the SRR (Figure 6.21j), the results at baseline ranged from 0.99 to 1.15 with a median of 1.06. Both tape stripping sessions revealed significant increases in values such that the median was estimated as 1.15 at S1+0.3h ($p=0.006$) and 1.16 at S2+0.3h ($p=0.006$). Furthermore, initial recovery was observed at S1+24h as the SRR decreased significantly ($p=0.006$ from stimulus) where the median was similar to baseline (difference in median = 0.01). Conversely, the second recovery period revealed a large spread in individuals was observed with results ranging from 1.04 to 1.18.

6.3.2.3 Shaving on the Cheek

The temporal effect of shaving on the cheek for the Long and Short Beard is illustrated for each parameter in Figure 6.22. For TEWL (Figure 6.22a), the results at baseline for the Long and Short Beards revealed similar medians of 12.38 $\text{g/m}^2\text{h}$ and 14.61 $\text{g/m}^2\text{h}$, respectively. The shaving stimulus demonstrated an increase in TEWL values for both sessions where the difference in medians from baseline was estimated as 3.3 $\text{g/m}^2\text{h}$ ($p=0.013$) for the Long Beard and 8.93 $\text{g/m}^2\text{h}$

($p=0.018$) for the Short Beard. Furthermore, the variability between participants also increased as the values ranged from 10.39 g/m²h to 29.56 g/m²h and 10.36 g/m²h to 34.51 g/m²h, respectively. Both sessions demonstrated recovery characteristics as the TEWL decreased significantly towards baseline with the median for the Long Beard session estimated as 13.67 g/m²h and that for the Short beard as 12.09 g/m²h ($p=0.013$ and $p=0.021$ from stimulus, respectively).

For hydration (Figure 6.22b), the results at baseline for the Long and Short Beards revealed differences in medians with values equal to 34.49 a.u. and 44 a.u., respectively. However, both sessions revealed a large variation within the cohort such that the hydration values ranged from 14.22 a.u. to 42.84 a.u. and 19.04 a.u. to 52.88 a.u., respectively. For the Long Beard session, the results demonstrated a statistically significant increase ($p=0.006$) from baseline with the median clustered around 45.85 a.u. No recovery was observed as the group continued to demonstrate elevated values ($p=0.006$) with the median difference from baseline estimated as 13.7 a.u. For the Short Beard session, a similar increase ($p=0.006$) was observed post shaving, with the median hydration equal to 53.37. Conversely, however, the recovery period revealed an overall drying effect as the values decreased ($p=0.013$ from stimulus) for most participants (median: 42.34 a.u., range: 19.5 a.u. to 58.8 a.u.).

For redness (Figure 6.22c), the basal values for the Long and Short Beards revealed similar medians of 21.77 a.u. and 20.98 a.u., respectively. However, the variability between participants was different as the Short Beard session revealed P6 as a low responding outlier (redness=10.29 a.u.). Both sessions revealed similar trends in the skin response with statistically significant increases in values post shaving where difference in medians from baseline were estimated as 7.6 a.u. ($p=0.006$) and 6.2 a.u. ($p=0.008$), respectively. Furthermore, both sessions revealed a decrease in values after 24 hours. However, this difference was significant for the Long Beard session only ($p=0.009$) when compared to baseline.

For SID (Figure 6.22d), the results at baseline for both sessions revealed medians of 1.81 mm⁻¹. Furthermore, there were statistically significant increases in values post shaving as the difference in medians from baseline were estimated as 0.15 mm⁻¹ ($p=0.032$) and 0.08 ($p=0.008$), respectively. Subsequent decrease in SID was observed after 24 hours. For the Long Beard session, this difference was statistically significant from baseline ($p=0.008$) as the results ranged from 1.57 mm⁻¹ to 2.06 mm⁻¹ with median equal to 1.77 mm⁻¹. Conversely, the Short Beard sessions revealed results ranging from 1.64 mm⁻¹ to 1.99 mm⁻¹ and median equal to 1.85 mm⁻¹ ($p>0.05$).

For AuC (Figure 6.22e), the results at baseline for Long and Short Beards revealed similar medians of 12,602 a.u. and 12,755 a.u., respectively. For both sessions, there was a decrease in AuC following the shaving stimulus. However, this difference statistically significant ($p=0.008$) for the

Short Beard session only where the difference in median from baseline was 614 a.u. After 24 hours, both sessions revealed an increase in AuC. This difference was significant post stimulus ($p=0.025$) for the Long Beard session only as the difference in median was 748 a.u. Additionally, P8 was noted as a low responding outlier in the Short Beard session ($AuC=10,393$ a.u.).

For Rq (Figure 6.22f), the results at baseline for both sessions revealed medians of $12\text{ }\mu\text{m}$. There were no significant changes in results post shaving for either of the sessions as the difference in medians ranged from $1.3\text{ }\mu\text{m}$ to $1.6\text{ }\mu\text{m}$ throughout the experiment. However, the Short Beard session revealed a higher variation in results between participants at S+24h as the values ranged from $7.18\text{ }\mu\text{m}$ to $18.16\text{ }\mu\text{m}$. Furthermore, P5 was noted as a high responding outlier in the Long Beard session at S+0.3h ($Rq=20\text{ }\mu\text{m}$).

For the plexus depth (Figure 6.22g), the results at baseline for Long and Short Beards revealed similar medians of $258\text{ }\mu\text{m}$ and $255\text{ }\mu\text{m}$, respectively. 20 minutes post shaving, there was a decrease in the plexus depth for both sessions, with the medians equal to $251\text{ }\mu\text{m}$ and $240\text{ }\mu\text{m}$, respectively. This difference was statistically significant only for the Short Beard session ($p=0.014$). However, P7 was noted as an outlier with a plexus depth of only $133\text{ }\mu\text{m}$ for the Long Beard session, while the Short Beard session did not reveal any outliers as results ranged from $133\text{ }\mu\text{m}$ to $278\text{ }\mu\text{m}$. After 24 hours, the group values were clustered around the medians which were equal to $255\text{ }\mu\text{m}$ and $262\text{ }\mu\text{m}$, respectively. Furthermore, these differences were statistically significant for the Short Beard session when compared to the stimulus ($p=0.018$), indicating recovery in characteristics.

For the vessel diameter (Figure 6.22h), the results at baseline for the Long and Short Beards revealed medians of $66\text{ }\mu\text{m}$ and $55\text{ }\mu\text{m}$ respectively. For both sessions, similar trends in results were observed as the vessel diameter increased significantly post stimulus where the difference in medians from baseline was $7\text{ }\mu\text{m}$ ($p=0.006$) and $15\text{ }\mu\text{m}$ ($p=0.009$) respectively. However, the variability between participants was different for the sessions, with the values for the Long Beard sessions ranging from $64\text{ }\mu\text{m}$ to $97\text{ }\mu\text{m}$ and those for the Short Beard from $50\text{ }\mu\text{m}$ to $106\text{ }\mu\text{m}$. Subsequent recovery revealed a decrease in vessel diameters, however only the Short Beard group demonstrated statistically significant recovery from stimulus ($p=0.009$) with median vessel diameter estimated as $63\text{ }\mu\text{m}$.

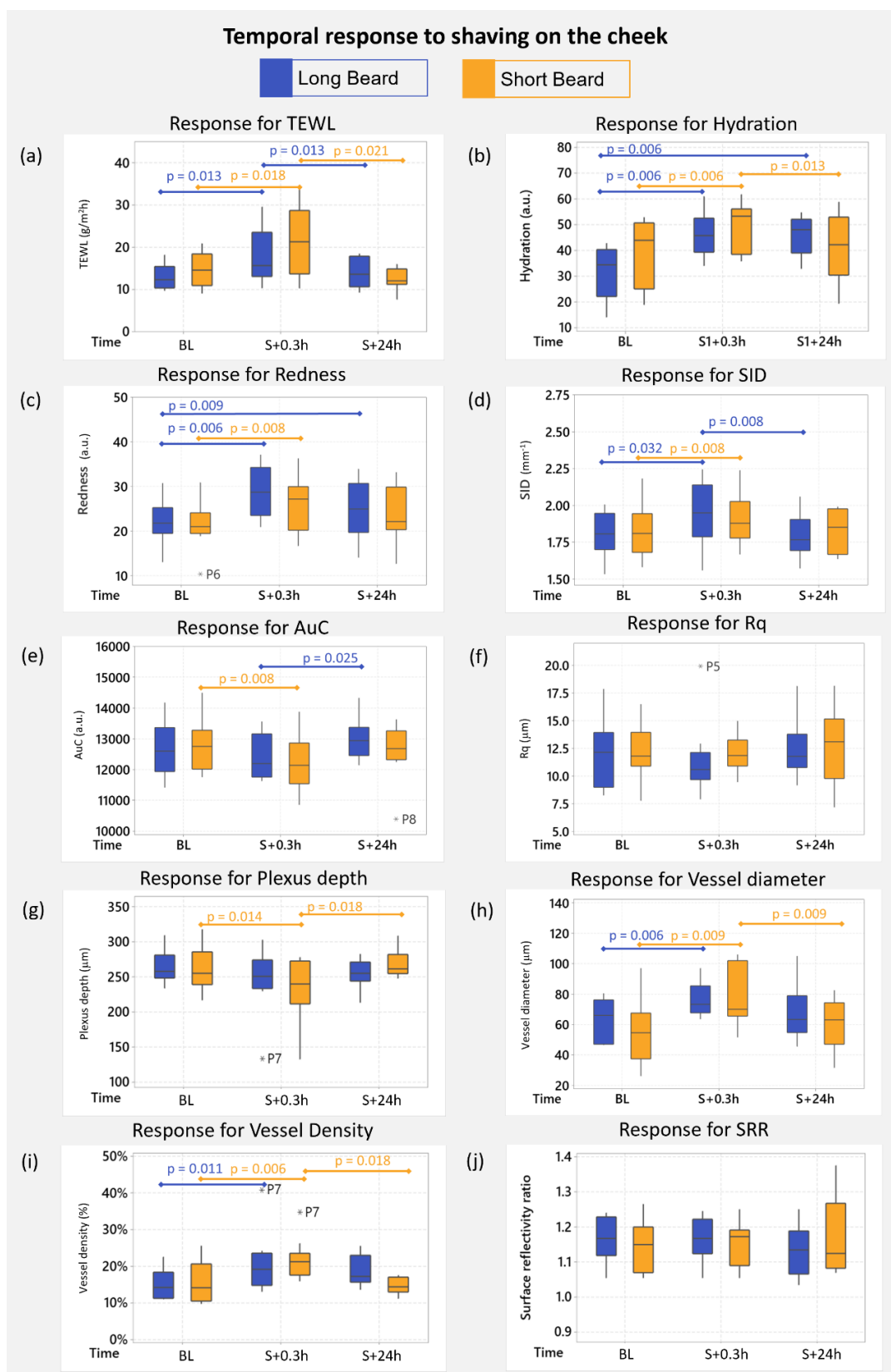


Figure 6.22 Temporal response following shaving on the cheek for (a) TEWL, (b) Hydration, (c) Redness, (d) SID, (e) AuC, (f) Rq, (g) Plexus depth, (h) Vessel diameter, (i) Vessel Density, (j) SRR.. Outlier values are indicated, as are statistically significant differences from baseline and statistically significant recovery from stimulus using the Wilcoxon test.

For the vessel density (Figure 6.22i), the results at baseline for the Long and Short Beards revealed similar medians of 14.3% and 14.2%, respectively. Results from both sessions demonstrated significant increases in vessel densities with medians equal to 19.3% ($p=0.011$) and 21.3% ($p=0.006$), respectively. In both sessions, P7 was observed as an outlier at S+0.3h with vessel density equal to 41% and 34.8%, respectively. After 24 hours, results from both sessions demonstrated decreasing values clustered around the medians which were equal to 17.3% and 14.5%, respectively. However, these differences were statistically significant for the Short Beard session ($p=0.018$), indicating some recovery characteristics.

For the SRR (Figure 6.22j), the values at baseline for the Long and Short Beards revealed similar medians of 1.17 and 1.15, respectively. There were no significant changes in SRR for either session in response to shaving where the median values ranged from 0 to 0.04 throughout the experiments. However, the variability between participants revealed values ranging from 1.04 to 1.25 for the Long Beard session and 1.07 to 1.38 for the Short Beard session.

6.3.2.4 Shaving on the Neck

For TEWL (Figure 6.23a), the results at baseline for the Long and Short Beards revealed similar medians of 11.32 g/m²h and 11.86 g/m²h, respectively. Both sessions revealed an increase in TEWL in response to shaving as there was an approximately 4-fold ($p=0.009$) and 3.5-fold ($p=0.009$) increase from baseline, respectively. Furthermore, there was large variability between participants in both sessions as the results ranged from 12.74 g/m²h to 91.88 g/m²h and 17.33 g/m²h to 73.44 g/m²h, respectively. Subsequently, recovery characteristics were observed as both sessions demonstrated significant decrease in results with median TEWL estimated as 15.64 g/m²h and 15.72 g/m²h ($p=0.013$ and $p=0.014$ from stimulus, respectively). Additionally, P10 is noted as an outlier at S+24h for the Long Beard with a TEWL value of 36.89 g/m²h.

For hydration (Figure 6.23b), the results at baseline for the Long and Short Beards revealed medians estimated as 33.3 a.u. and 45.8 a.u., respectively. Both sessions revealed a large variation within the cohort at baseline such that the hydration values ranged from 21.3 a.u. to 56.9 a.u. and 28.0 a.u. to 64.2 a.u., respectively. Following mechanical stimulation, the results revealed significant increases in values from baseline such that the medians were estimated as 48.0 a.u. ($p=0.006$) and 60.7 a.u. ($p=0.009$), respectively. However, the results were skewed for the Long Beard sessions as values ranged from 39.78 a.u. to 83.84 a.u. Additionally, the Short Beard session revealed values ranging from 28.4 a.u. to 82.9 a.u. After the recovery period, results from both sessions

demonstrated recovery characteristics as the hydration values decreased significantly towards baseline with median equal to 41.2 a.u. ($p=0.014$) and 33.5 a.u. ($p=0.009$), respectively.

For redness (Figure 6.23c), the results at baseline for the Long and Short Beards revealed median values equal to 16.56 a.u. and 18.18 a.u., respectively. The variability between participants was different for the sessions as P4 was observed as an outlier for the Short Beard session only. Following the shaving stimulus, both sessions revealed a significant increase ($p=0.006$ for both) in redness such that there was an approximately 2-fold increase in the medians. However, there were differences in the spread between participants as the results for the Long Beard session ranged from 23.32 a.u. to 51.61 a.u., and those for the Short Beard ranged from 19.07 a.u. to 42.93 a.u. After 24 hours, both groups demonstrated a statistically significant decrease in redness with medians equal to 21.46 a.u. and 26.14 ($p=0.009$ and $p=0.013$ from stimulus, respectively). However, these differences were significantly elevated when compared to baseline ($p=0.009$ and $p=0.018$, respectively), indicating that recovery was not achieved.

For SID (Figure 6.23d), the results at baseline for the Long and Short Beards revealed median values equal to 1.56 mm^{-1} and 1.58 mm^{-1} , respectively. For both sessions, there was a significant increase ($p=0.008$ for both) in SID post shaving as the difference in medians from baseline was 0.16 mm^{-1} and 0.12 mm^{-1} , respectively. Furthermore, recovery characteristics were observed in both sessions as the SID values demonstrated statistically significant decreases after 24 hours ($p=0.006$ and $p=0.013$, respectively). However, the Short Beard group consistently revealed larger variations in the results when compared to the Long Beard group. For example, at 20 minutes post stimulus, the results for the Long Beard session ranged from 1.61 mm^{-1} to 1.78 mm^{-1} , whereas those for the Short Beard session ranged from 1.51 mm^{-1} to 1.91 mm^{-1} . Additionally, P5 was noted as a low responding outlier for the Long Beard group at 24h post stimulus, with SID equal to 1.43 mm^{-1} .

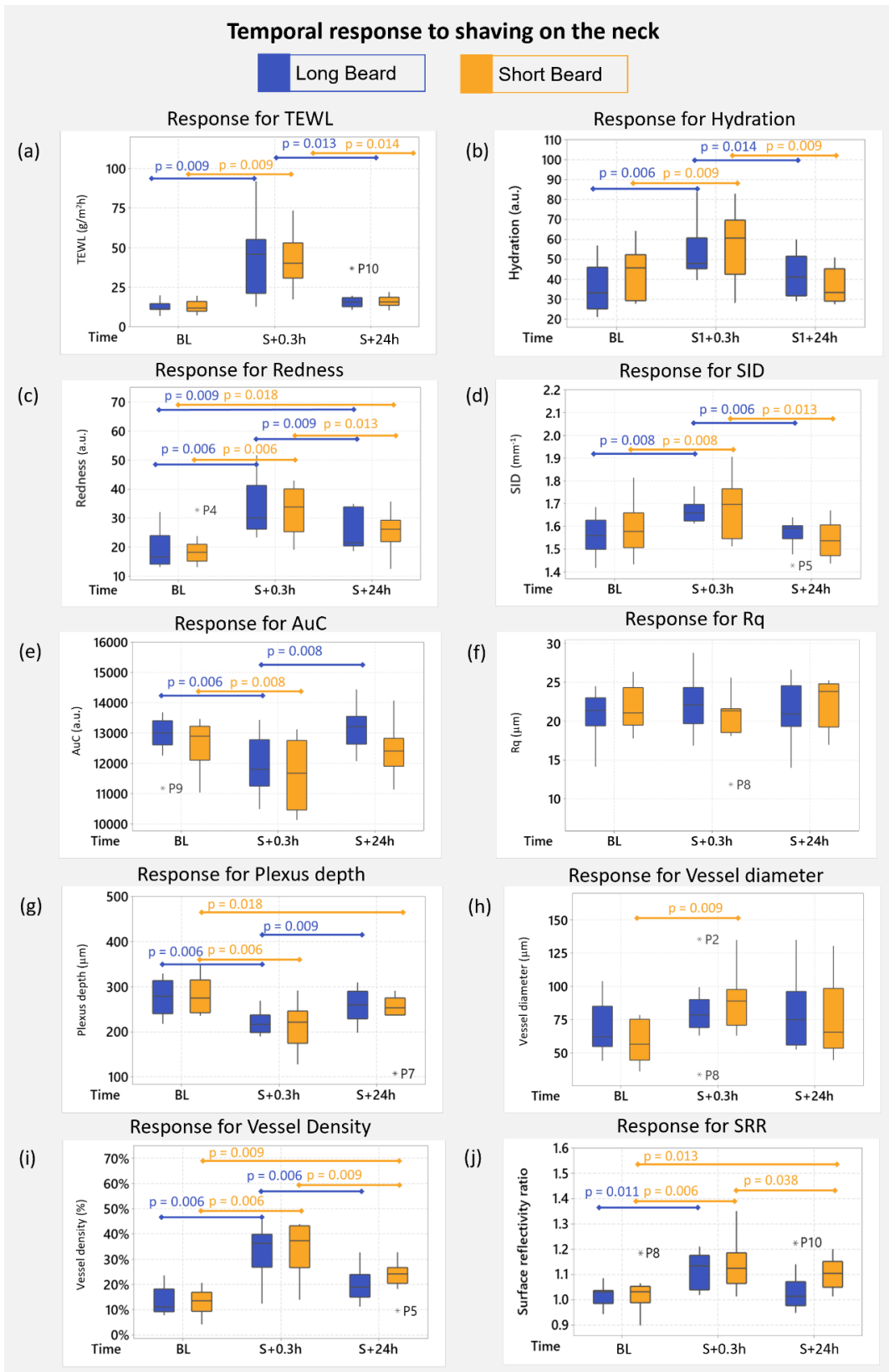


Figure 6.23 Temporal response following shaving on the neck for (a) TEWL, (b) Hydration, (c) Redness, (d) SID, (e) AuC, (f) Rq, (g) Plexus depth, (h) Vessel diameter, (i) Vessel Density, (j) SRR. Outlier values are indicated, as are statistically significant differences from baseline and statistically significant recovery from stimulus using the Wilcoxon test.

For AuC (Figure 6.23e), the results at baseline for the Long and Short Beards revealed medians of 13,004 a.u. and 12,899 a.u., respectively. However, the variability between the participants differed as the results for the Long Beard session ranged from 12,256 a.u. to 13,684 a.u. while P9 was a low responding outlier with AuC equal to 11,182 a.u. The Short beard session revealed a larger range in results with values spread from 11,036 a.u. to 13,467 a.u. Following the shaving stimulus, both sessions revealed a significant decrease in AuC such that the difference from baseline was estimated as 1,204 a.u. ($p=0.006$) and 1,227 a.u. ($p=0.008$), respectively. After 24 hours, both sessions demonstrated an increase in values towards baseline where only the Long Beard session revealed a significant increase (median=13,215 a.u., $p=0.008$).

For Rq (Figure 6.23f), the results at baseline for the Long and Short Beards revealed medians of 21 μm . However, the spread between participants was different as the results for the Long Beard session ranged from 14 μm to 25 μm , and those for the Short Beard session ranged from 18 μm to 26 μm . No significant changes in Rq were observed in response to shaving for either of the sessions. Notably, P8 was revealed as a low responding outlier at S+0.3h for the Short Beard (Rq=16.95 μm), where the group median was 21.34 μm . Subsequent recovery periods demonstrated distinct differences in trends as the Long Beard session revealed a decrease in Rq (median: 21.46 μm , range: 14.0 μm to 26.6 μm , $p>0.05$) while the Short Beard session revealed an increase (median: 35.72 μm , range: 17.0 μm to 25.3 μm , $p>0.05$).

For the plexus depth (Figure 6.23g), the results at baseline for the Long and Short Beards revealed medians equal to 279 μm and 275 μm , respectively. After shaving there was a statistically significant decrease in the plexus depth for both sessions, such that the medians were 217 μm ($p=0.006$) and 222 μm ($p=0.006$) when compared to baseline. However, the Short Beard session revealed a larger variability between participants such that the range in values was two-fold greater than that for the Long Beard. Following an interval of 24 hours, both sessions revealed some recovery characteristics which was statistically significant only for the Long Beard session (median: 260 μm , $p=0.009$ from stimulus). The Short Beard session demonstrated statistically significant differences from baseline ($p=0.018$) with P7 as a low responding outlier (plexus depth=107 μm).

For the vessel diameter (Figure 6.23h), the results at baseline for the Long and Short Beards revealed medians of 62 μm and 56 μm , respectively. Following the shaving stimulus, there was an increase in the vessel diameter for both sessions, with the Short Beard results revealing statistically significant elevation ($p=0.009$) from baseline with difference in medians estimated as 32 μm . However, the Long Beard group revealed a median difference of 17 μm from baseline with P2 (vessel diameter=136 μm) and P8 (vessel diameter=36 μm) demonstrating high and low outlier values, respectively. After 24 hours, an overall decrease in vessel diameter was observed for both

sessions. However, large variability was observed as results ranged from 53 μm to 135 μm for the Long Beard and 45 μm to 131 μm for the Short Beard.

For the vessel density ([Figure 6.23i](#)), the basal values for the Long and Short Beards revealed median values of 11.1% and 13.6%, respectively. Following the shaving stimulus, both sessions revealed statistically significant increases ($p=0.006$ for both) such that the medians were approximately 3-fold greater. Subsequent recovery was observed for the Long Beard group as the results revealed a statistically significant decrease ($p=0.006$) in vessel density from stimulus where the median was estimated as 19.0%. Similarly, the Short Beard group also revealed a statistically significant decrease ($p=0.009$) in values from stimulus, although these results were still significantly elevated ($p=0.009$) from baseline. Furthermore, P5 was observed as a low responding outlier with the vessel density decreasing to 9.6%.

For the SRR ([Figure 6.23j](#)), the values at baseline for the Long and Short Beards revealed medians of 1.03 for both. However, the two sessions demonstrated differences in variability between participants as the values ranged from 0.95 to 1.09 and 0.90 to 1.05, respectively. Furthermore, P8 was noted as a high responding outlier in the Short Beard session with SRR equal to 1.19. Following the shaving stimulus, both sessions demonstrated significant increases ($p=0.011$ and $p=0.006$, respectively) in group characteristics such that the medians revealed 100% increase from baseline. Additionally, the Short Beard session demonstrated a larger spread between participants with the values ranging from 1.02 to 1.35. Following an interval of 24 hours, both sessions demonstrated a decrease in SRR with medians estimated as 1.02 ($p=0.038$) and 1.11 ($p>0.05$), respectively. However, recovery characteristics were not observed for the Short Beard as the results remained significantly elevated from baseline ($p=0.013$). Conversely, the difference in medians for the Long Beard were smaller ($p>0.05$) with P10 observed as an outlier (SRR=1.23).

6.3.3 Biochemical markers

As noted in [Section 6.2.5](#), results for P5 and P7 are limited to IL-1 α , IL-1RA, and IFN- γ . In addition, P9 was not available for the S+24h measurement for the Short Beard session. Also, there was an error in the extraction of cytokines for P6 at S+0.3h on the cheek, P6 at S+24h on the neck, and P10 at BL on the neck, and consequently no results were found. Furthermore, the IL-6 values for P1 on the cheek and the TNF- α values on the neck for P2 at S+24h and P4 at BL were below for detection limits, yielding erroneous results.

For all the biomarkers in the panel, the temporal response to shaving on the cheek has been illustrated in Figure 6.24. For IL-1 α (Figure 6.24a), the basal values ranged from 33 pg/mL to 469 pg/mL, with a median of 145 pg/mL. However, P7 was observed as a high responding outlier with a basal value of 782 pg/mL. After the shaving stimulus, there was a statistically significant increase ($p=0.009$) in the IL-1 α concentration, such that the median was more than two-fold greater. Furthermore, a large spread was observed between participants as the values ranged from 157 pg/mL to 1,418 pg/mL. After 24 hours, the group demonstrated a return towards baseline as the results revealed a statistically significant decrease ($p=0.014$) in the parameter, with the median estimated as 149 pg/mL.

For IL-1RA (Figure 6.24b), the results at baseline ranged from 485 pg/mL to 3,210 pg/mL, with a median of 1,732 pg/mL. Like the results for IL-1 α , P7 was noted as an outlier with the basal IL-1RA concentration of 6,945 pg/mL. After shaving there was a statistically significant upregulation ($p=0.009$) in the IL-1RA concentration with a two-fold increase in the median. This trend was also observed for P7, again an outlier for this group with the IL-1RA concentration estimated as 15,802 pg/mL. After 24 hours, recovery characteristics were observed as there was a statistically significant decrease ($p=0.042$) in the parameter, such that the group median was revealed as 2,631 pg/mL with values ranging from 362 pg/mL to 3,424 pg/mL.

For IL-6 (Figure 6.24c), the baseline values ranged from 0.16 pg/mL to 0.64 pg/mL, with a median of 0.24 pg/mL. Following the shaving stimulus, there was an increase ($p>0.05$) in the cytokine concentration (median: 0.48 pg/mL, range: 0.25 pg/mL to 0.83 pg/mL). After 24 hours, the group demonstrated a decrease in the IL-6 concentration such that the median was 0.27 pg/mL and results ranged from 0.15 pg/mL to 0.43 pg/mL. For all the measurement times, P8 was noted as a consistent outlier. However, a similar temporal trend for P8 was observed with the basal value of 0.64 pg/mL, post stimulus value of 3.54 pg/mL, and recovery value of 0.88 pg/mL.

For IL-8 (Figure 6.24d), the basal values ranged from 0.36 pg/mL to 2.15 pg/mL with a median of 1.57 pg/mL. After the shaving stimulus, there was an increase ($p>0.05$) in the concentration and spread between participants such that the results ranged from 0.62 pg/mL to 16.21 pg/mL with a median of 3.08 pg/mL. After 24 hours, most of the group demonstrated a decrease in the IL-8 concentration, which was 2.5-fold greater ($p=0.052$) than baseline. However, P10 demonstrated an increase in the cytokine with the IL-8 concentration estimated as 22.45 pg/mL.

For IFN- γ (Figure 6.24e), the results at baseline ranged from 3.20 pg/mL to 11.52 pg/mL with a median of 5.85 pg/mL. Here, P2 was noted as an outlier with the IFN- γ concentration estimated as 87 pg/mL. Following the shaving stimulus, the group demonstrated a statistically significant increase ($p=0.009$) in the IFN- γ concentration such that the group median was 2.5 times greater.

Again, P2 was noted as an outlier, with the cytokine concentration of 257 pg/mL. After 24 hours, the group demonstrated recovery as there was a statistically significant decrease ($p=0.014$) in results with values returning to baseline (median: 5.99 pg/mL, range: 2.55 pg/mL to 11.31 pg/mL).

For TNF- α (Figure 6.24f), the results at baseline ranged from 0.45 pg/mL to 1.55 pg/mL with a median of 0.84 pg/mL. Additionally, P2 was noted as an outlier with the result estimated as 13.5 pg/mL. No significant changes were observed in the TNF- α concentration in response to shaving. At S+0.3h, there was an increase ($p>0.05$) in the group characteristics such that the values ranged from 0.69 pg/mL to 3.68 pg/mL with a median of 1.31 pg/mL. After an interval of 24 hours, the group demonstrated a decrease in the parameter such that the results ranged from 0.34 pg/mL to 1.65 pg/mL with a median of 0.69 pg/mL.

Temporal response for biomarkers to shaving on the cheek for the Short Beard

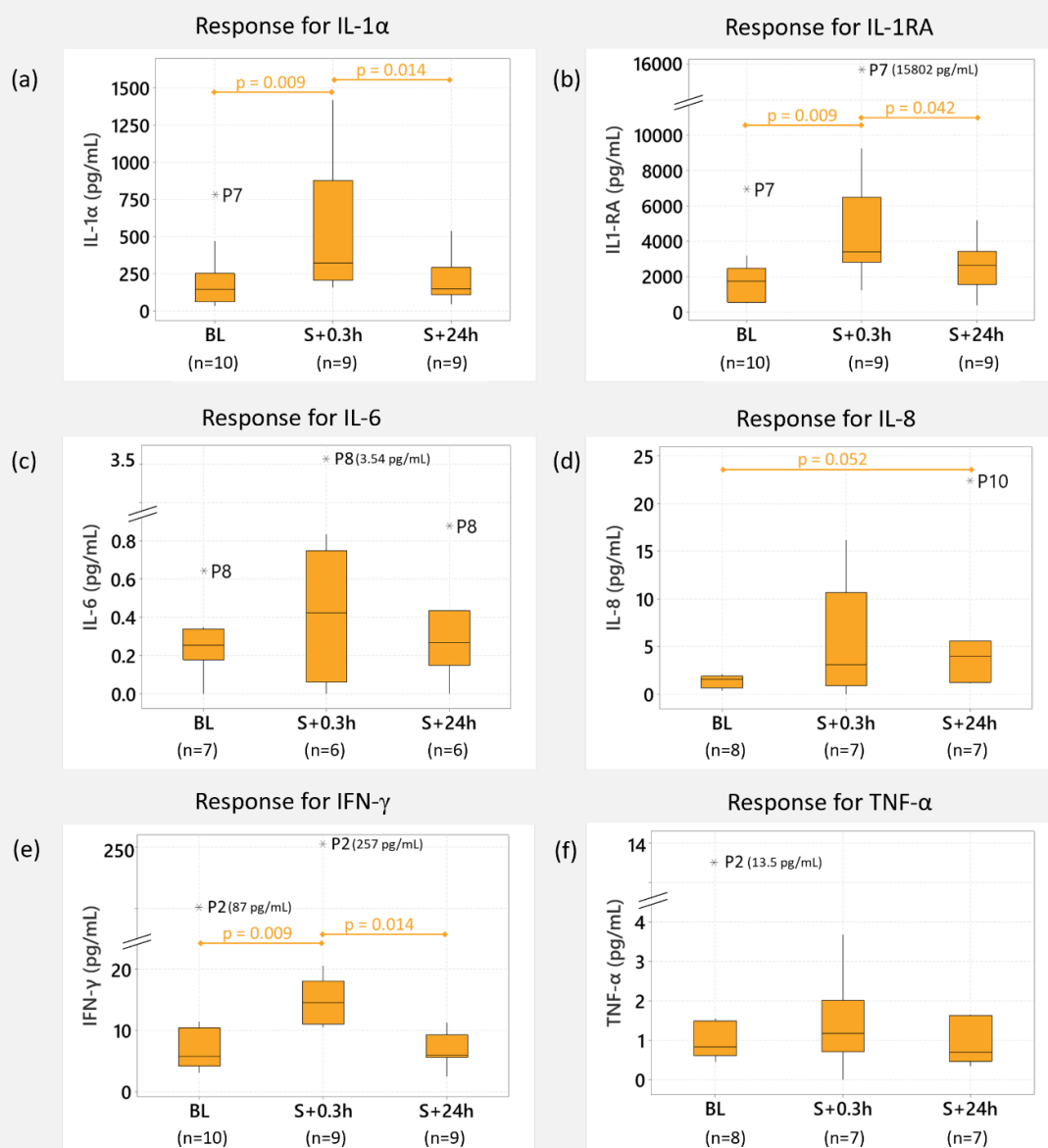


Figure 6.24 Temporal response following shaving on the cheek for the Short Beard for (a) IL-1 α , (b) IL-1RA, (c) IL-6, (d) IL-8, (e) IFN- γ , (f) TNF- α . Sample sizes and outlier values are indicated, as are statistically significant differences from baseline and statistically significant recovery from stimulus using the Wilcoxon test.

The temporal response to shaving on the neck has been illustrated in [Figure 6.25](#). For IL-1 α ([Figure 6.25a](#)), the basal values ranged from 127 pg/mL to 993.71 pg/mL with a median of 257 pg/mL. After the shaving stimulus, there was a statistically significant increase ($p=0.009$) in the IL-1 α concentration, such that the median was 3-fold greater. Furthermore, a large spread was observed between participants as the values ranged from 282 pg/mL to 2,635 pg/mL. After 24, the group demonstrated a decrease towards baseline as the results revealed a statistically significant decrease ($p=0.014$) in the parameter, with a median estimated as 225 pg/mL. Consistently, P7 was noted as an outlier with a basal value of 5,492 pg/mL, a post stimulus value of 6,545.37 pg/mL, and a recovery value of 2,835.62 pg/mL.

For IL-1RA ([Figure 6.25b](#)), the results at baseline ranged from 255 pg/mL to 2,090 pg/mL, with a median of 1,329 pg/mL. Following the shaving stimulus, there was a statistically significant increase ($p=0.009$) in with the median revealing a 2.5-fold greater value. After 24 hours, recovery characteristics were observed as there was a statistically significant decrease ($p=0.014$), such that the group median was revealed as 1,172 pg/mL. Similar to the results for IL-1 α , P7 was consistently noted as an outlier with the basal IL-1RA concentration of 14,985 pg/mL, post stimulus value of 19,219 pg/mL, and a recovery value of 16,928 pg/mL.

For IL-6 ([Figure 6.25c](#)), the baseline values ranged from 0.13 pg/mL to 0.34 pg/mL with a median of 0.27 pg/mL. After shaving there was a two-fold statistically significant increase ($p=0.014$) in the cytokine concentration such that the values ranged from 0.35 pg/mL to 1.17 pg/mL. After 24 hours, the group demonstrated a statistically significant decrease ($p=0.052$) in the IL-6 concentration such that the values returned to baseline (median: 0.26 pg/mL range: 0.18 pg/mL to 0.41 pg/mL). Furthermore, P8 was noted as an outlier with a value of 0.96 pg/mL.

For IL-8 ([Figure 6.25d](#)), the basal values ranged from 1.10 pg/mL to 6.90 pg/mL with a median of 1.33 pg/mL. Furthermore, P6 was observed as an outlier with the IL-8 value estimated as 18.49 pg/mL. Following the shaving stimulus, there was a seven-fold statistically significant increase ($p=0.030$) in the concentration such that the results ranged from 1.23 pg/mL to 29.94 pg/mL. After 24 hours, most of the group demonstrated a decrease in the IL-8 concentration, which did not achieve statistical significance. However, P8 demonstrated an increase in the cytokine with the IL-8 concentration estimated as 187 pg/mL.

For IFN- γ ([Figure 6.25e](#)), the results at baseline ranged from 2.86 pg/mL to 15.39 pg/mL with a median of 7.62 pg/mL. Following the shaving stimulus, the group demonstrated a statistically significant increase ($p=0.009$) in the IFN- γ concentration such that the group median was two-fold greater. Here, P7 was noted as an outlier, with the cytokine value of 61.11 pg/mL. After 24 hours, the group demonstrated recovery as a statistically significant decrease ($p=0.024$) in characteristics

was observed (median= 6.20 pg/mL). Again, P7 was noted as an outlier with the IFN- γ concentration of 41.58 pg/mL.

For TNF- α (Figure 6.25f), the results at baseline ranged from 0.12 pg/mL to 0.53 pg/mL with a median of 0.20 pg/mL. Additionally, P6 was noted as an outlier with the TNF- α concentration estimated as 6.57 pg/mL. Following the shaving stimulus, there was an increase ($p>0.05$) in the cytokine concentration such that the values ranged from 0.95 pg/mL to 2.20 pg/mL and a median of 1.55 pg/mL. However, P8 demonstrated a larger increase as the result was estimated as 60 pg/mL. After an interval of 24 hours, most of the group demonstrated a statistically significant decrease ($p=0.036$) in the parameter such that the median was estimated as 0.40 pg/mL. However, there was a large spread between the participants as the results ranged from 0.23 pg/mL to 8.43 pg/mL. Again, P8 revealed an outlier value of 32 pg/mL, demonstrating a decrease in the parameter after 24 hours.

Temporal response for biomarkers to shaving on the neck for the Short Beard

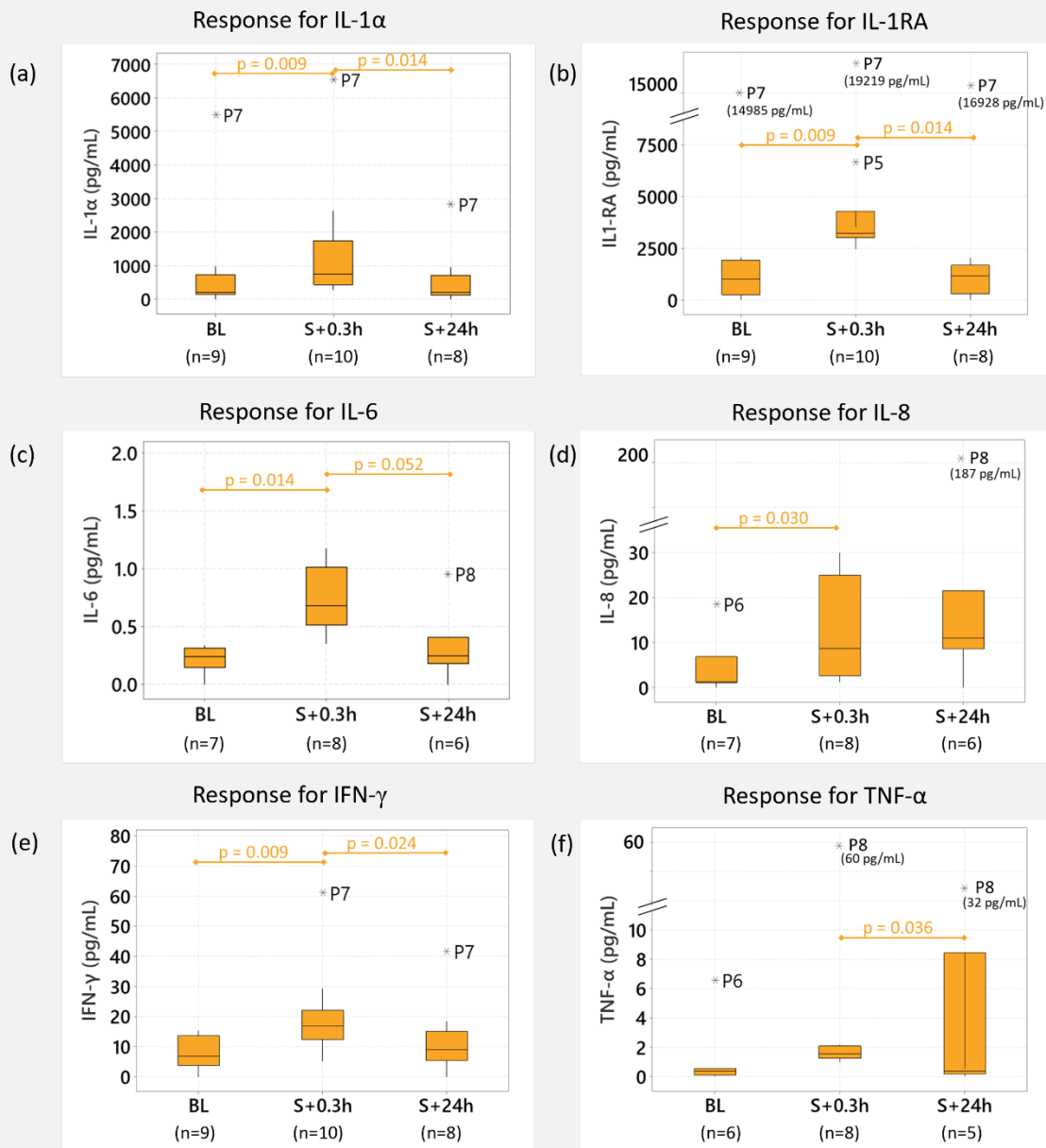


Figure 6.25 Temporal response following shaving on the neck for the Short Beard for (a) IL-1 α , (b) IL-1RA, (c) IL-6, (d) IL-8, (e) IFN- γ , (f) TNF- α . Sample sizes and outlier values are indicated, as are statistically significant differences from baseline and statistically significant recovery from stimulus using the Wilcoxon test.

6.4 Discussion

The present study explored the spatial and temporal changes in skin tissue response with respect to shaving. Addressing limitations of the previous consumer study ([Section 4.4](#)), the stimulus was successfully modified to elicit a change in the structure and function of local skin tissues by increasing the duration of the shaving stimulus from 30 s to 60 s. Furthermore, a new OCT system with dynamic-imaging capabilities was employed for characterisation of blood perfusion. This was integrated into an enhanced array of measurements, which were successfully implemented for the objective assessment of skin. This chapter provides novel data to evaluate the morphological and physiological skin response to shaving, giving a unique perspective on skin response to mechanical stimulation. For example, it was found that the neck skin was significantly rougher than the cheek skin. Additionally, post shaving, biomarkers such as IL-1 α , IL-1RA, and IL-8 revealed >2 fold increase in concentration at both sites. However, as the study was conducted with 10 participants only, the findings should be considered preliminary pending further evaluation on larger cohorts.

Clinical usability of the parameters was evaluated for the newly developed OCT-skin parameters ([Section 3.3](#)) and compared against those obtained from the commercially available Vivosight system ([Section 6.2.3](#)), revealing equivalence for SID and OAC. In contrast, the roughness estimation from the two methods revealed large differences in the magnitude of the corresponding results ([Figure 6.15](#)). The underlying reason for these differences may be associated with the estimation of the true skin surface, in particular the tracking of hair which is particularly challenging over facial sites of the cheek and neck. Furthermore, similar to the limitation in Chapter 5 ([Section 5.2.1](#)), both methods failed to detect the epidermal thickness in a large number of scans from the cheek and neck. This has been associated with the undulating nature of dermal-epidermal junction, as discussed in [Section 5.4](#). Alternatively, the AuC was estimated from the OCT scans in the present study, which demonstrated significant spatial and temporal trends in results. However, as the intensity values exported from Vivosight OCT scans were scaled to arbitrary units, the subsequent AuC parameter has been presented in a.u. This contrasts with the results from Chapter 5, where the AuC was estimated in dB*mm. Thus, direct comparison between the values is limited for this parameter.

In addition to the new OCT system, the protocol was modified to estimate redness of the skin surface using macroscopic photographs. Interestingly, the redness response did not reveal recovery characteristics in most cases following the mechanical stimulation. This finding is considered important in the present research as the perception of enhanced skin sensitivity is largely driven by the subjective assessment of skin appearance where skin is regarded as sensitive when it is more red in colour (Seidenari et al. 1998; Farage and Maibach 2010). Furthermore, the protocol included

chemical analysis of sebum as studies exploring characteristics of sensitive skin have reported differences in post-insult biochemistry of SS individuals (Richters et al. 2016; Raj et al. 2017; Yatagai et al. 2018). Remarkably, the results revealed significant increases for the inflammatory biomarkers post shavings, with some also demonstrating upregulation after 24 hours. This is the first time an optimised non-invasive biomarker approach has been used in the context of skin shaving, providing unique insight into the inflammatory cascade of the local tissue.

Dynamic-imaging for skin characterisation

Dynamic-imaging was specifically included in this study as cutaneous blood flow (CBF) parameters allowed examination of the multifactorial nature of enhanced skin sensitivity (Lammintausta et al. 1988; Diogo and Papoila 2010). In particular, it is not currently known how the local microvascular structures in the dermis in response to mechanical stimuli and the dynamic OCT offers the potential for a novel evaluation of changes in local blood flow. In the present study, the CBF parameters demonstrated distinct spatial differences such that the magnitude of values for the Vessel Diameter and Vessel Density were smaller on the forearms than on the cheek/neck at baseline (Figure 6.19) and in response to the mechanical stimuli (Figure 6.20 - Figure 6.23). Conversely, the Plexus Depth on the forearms was higher when compared to the cheek/neck, indicating that the vasculature on the facial sites is more superficial and denser than on the forearm. These results also indicate that the forearm is not be a suitable proxy for the cheek/neck when investigating skin parameters. This finding may be of interest for future research, specifically in the development of site-specific products.

Conversely, the CBF parameters demonstrated largely overlapping values between the cheek and neck skin, demonstrating some equivalence of these facial sites at baseline. However, differences were observed in the skin response to shaving. Specifically, the Plexus Depth and Vessel Density (Figure 6.23 g, i) did not demonstrate complete recovery on the neck in the Short Beard session as the results were significantly different from those at baseline. By contrast, the results from the cheek demonstrated overlapping values between baseline and recovery. No directly comparative studies were found in literature to corroborate this finding. One study (Marrakchi and Maibach 2007) examined the basal blood flow in skin tissue on several facial sites using Laser Doppler Flowmetry and, similar to the presented results, did not reveal any statistically significant differences between the cheek and neck. Another study (Wang et al. 2015) investigated the changes in CBF on the finger following tape stripping using Optical Microangiography (OMAG), revealing significantly increased blood flow at 1-minute post stimulus which recovered after 15 minutes. The results found in this study suggest that there is a distinct hyperaemic response in the

local tissues following mechanical stimulus, where superficial microvascular vessels become perfused as part of a physiological reaction to the load. This could be associated with local damage to the epidermal and dermal tissues, where blood can transport platelets and leukocytes to facilitate coordinated and cooperative activities in normal healing that limit acute inflammation and trigger tissue repair. Consequently, it is likely that despite similarities in basal characteristics, there may be differences in the skin tissue response to stimuli. Indeed, such vascular response have been investigated in the context of the overall skin function, revealing dynamic oscillation of blood flow in response to external stress (Bertuglia et al. 2000; Rossi and Carpi 2004). However, additional research investigating the vasculature of facial skin is needed to understand the differences in the skin response to mechanical stimuli such as shaving. As such, dynamic-imaging and its functional adaptations are promising techniques in the exploration of enhanced skin sensitivity. Preliminary analysis of the presented CBF parameters and associations with intrinsic and extrinsic factors related to SS have been included in [Chapter 7](#).

Shaving on the cheek and neck

The shaving stimulus included in the present study elicited statistically significant changes from baseline for most of the measured skin parameters on the cheek and neck ([Figure 6.22](#) and [Figure 6.23](#)). However, the ratio in values with respect to baseline demonstrated larger differences on the neck than on the cheek ([Table 6.5](#)). Specifically, with respect to TEWL, the post stimulus values on the neck were twice as large as those on the cheek. Indeed, it is widely reported that mechanical stimulation in the form of tape stripping results in an increase in TEWL, explained by the compromise of the functional integrity of the stratum corneum (Bashir et al. 2001; Gao et al. 2013; Gorcea et al. 2019). However, as the functional difference between the skin on cheek and neck remains unclear, the anatomical variations in the TEWL response in the present study implicates the interaction of the stimulus with the skin surface. It is possible that the density and direction of beard hair varied between the two sites leading to differences in the subsequent skin tissue response. Reportedly, the neck skin is more rough than the cheek and the hair has a lower emerging angle which leads to a higher chance of ingrown hairs (Maurer et al. 2016). These factors may contribute to the stimulus introduced in the present study where participants were requested to shave in a small area for 60 seconds. These parameters have been explored and discussed further in [Chapter 7](#). There may also be differences in the pre-conditioning of these skin sites, with cheek skin exposed to environmental challenges (UV, wind, rain) more frequently than the neck site. This may alter the tolerance to external stimuli.

With respect to hydration, the cheek and neck skin revealed similar increase in values post stimulus, corroborated by studies investigating the temporal influence of tape stripping (Loffler et al. 2004; Richters et al. 2016). Interestingly, larger differences from baseline were observed in the Long Beard session. As the accuracy of results for hydration estimation using the Corneometer depends on the contact area between the probe and skin surface (Berardesca et al. 1997), it can be assumed that these basal values may not reflect the true skin hydration status on the facial sites because all participants had a 72-hour long beard which prevented sufficient skin contact. Consequently, the post shaving values may reveal larger differences from baseline due to the improved contact.

Furthermore, redness revealed larger differences on the neck from baseline even after the recovery period. Indeed, other studies have also reported an increase in redness values post shaving (Kolbe et al. 2006; Cowley et al. 2012), however recovery characteristics were not explored. In the present study, redness was estimated by filtering the DSLR images and provided quantification of the visible erythema (Section 6.2.4). Thus, it is expected that larger vessel diameters and densities would be associated with more redness on the skin surface. However, correlations between the various objective parameters remain to be investigated and have been presented in Chapter 7.

Table 6.5 Median ratio in values from baseline. Highlighted cells represent a ratio greater than 1.3 (this threshold was arbitrarily selected).

		Long Beard				Short Beard			
		Post stimulus		Recovery		Post stimulus		Recovery	
		Cheek	Neck	Cheek	Neck	Cheek	Neck	Cheek	Neck
Biophysical	TEWL	1.3	2.8	1.1	1.2	1.3	3.1	0.9	1.1
	Hydration	1.4	1.5	1.3	1.3	1.2	1.3	1.1	0.9
	Redness	1.2	1.9	1.1	1.2	1.2	1.7	1.0	1.3
Structural	SID	1.1	1.1	1.0	1.0	1.0	1.1	1.0	1.0
	AuC	1.0	0.9	1.0	1.0	1.0	0.9	1.0	1.0
	Rq	1.0	1.0	1.0	1.0	1.0	1.0	1.0	1.0
	Plexus Depth	1.0	0.8	1.0	0.9	0.9	0.8	1.0	0.9
	Vessel Diameter	1.2	1.2	1.2	1.1	1.4	1.5	1.3	1.4
	Vessel Density	1.2	2.6	1.2	1.8	1.3	2.4	1.2	1.8
	SRR	1.0	1.1	1.0	1.0	1.0	1.1	1.0	1.1
Biochemical	IL-1alpha	-	-	-	-	2.8	2.2	0.9	0.7
	IL-1RA	-	-	-	-	2.5	3.2	1.2	0.8
	IL-6	-	-	-	-	1.8	3.0	1.1	1.2
	IL-8	-	-	-	-	3.7	3.9	3.9	8.9
	IFN gamma	-	-	-	-	2.9	1.8	1.0	1.5
	TNF-alpha	-	-	-	-	1.5	5.0	0.6	1.4

Smaller changes in the temporal response were observed for the non-dynamic structural parameters, i.e., SID, AuC, Rq, and SRR. Except for AuC, it was noted that these parameters provided distinction between the cheek and neck skin at baseline ([Figure 6.19](#)), with the results for the neck revealing higher Rq values. Comparisons with literature for skin roughness have been presented in Chapter 5 ([Table 5.3](#)). In contrast, the cheek revealed higher SID and SRR values. As the scattering of the OCT signal is influenced by the presence of micro vessels and structural elements such as collagen fibres (Welzel et al. 2003), the results indicate that the neck had a more dense dermis, similar to the observations in Chapter 5 with respect to SID and AuC. However, as the SRR estimates the relative intensity of the top surface of the skin to that of the dermis, a denser dermis is expected to yield lower SRR values (assuming similar intensities for the skin surface). As such, it is unclear which component is driving the spatial differences, requiring further investigation. The SRR is estimated by the VivoTools software and per the manufacturer, it has not been independently validated since its release in November 2021. Optical attenuation of the skin tissue has been studied by a few researchers (Olsen et al. 2018), however, trends between the cheek and neck skin remain to be investigated.

For the array of biochemical parameters, all proteins revealed an upregulation in concentrations post shaving on both facial sites (ratio from baseline ranging from 1.5 to 5.0; [Table 6.5](#)). Indeed, such inflammatory response has been reported following various mechanical insults (De Wert et al. 2015, 2019; Soetens et al. 2019). However, there were large differences in the recovery characteristics observed on the cheek and neck. For example, results for IL-8 revealed an increasing trend in the recovery period with the cheek skin demonstrating a median ratio of 3.9 from baseline, while the neck demonstrated median ratio of 8.9. The authors believe this is a novel finding as the magnitude of the results exceeds those observed in literature where different skin sites have been examined (Feldmeyer et al. 2010; Soetens et al. 2019; Abiakam et al. 2023). This may be explained by the structural properties of perifollicular skin, which is rich in vasculature, innervation, and cells of the innate and adaptive immune system (Maurer et al. 2016). This makes the perifollicular skin a highly responsive and inflammatory system. The presented results indicate that a shaving stimulus activated this system, resulting in shaving-induced skin irritation. Indeed, subjective responses from participants also indicated the perceived discomfort following the stimulus. This has been discussed in more detail in [Chapter 7](#).

With respect to the different sessions, it was hypothesized that the Long Beard session may yield a larger skin response than the Short Beard session due to the mechanics of cutting longer hair at the skin/device interface. This could have increased the likelihood of shearing forces on the hair follicles, creating local damage in the dermis. Indeed, the hair follicle is a sensory organ, and the perifollicular skin is highly responsive to external signals including mechanical and thermal

stimulation. Alternatively, it was hypothesized, that the Short Beard session may yield a larger skin response due to a brief period between the repeated shaving stimuli. As results from the present study revealed a larger post stimulus value in the Short Beard session for most parameters with many not achieving recovery, it can be suggested that for the present cohort, a repetitive shaving stimulus elicited a larger response in the skin than a single shaving stimulus involving a longer beard. Further investigation characterising the shaving load have been presented in [Chapter 7](#).

Tape stripping versus shaving on the forearms

In the present research project, it has been challenging to find comparative studies in literature because of the anatomical region of interest (i.e., bearded skin on the cheek and neck) as well as the nature of the mechanical stimulus (i.e., electric shaving). Consequently, regarding the nature of the stimulus, analysis has been expanded to include studies involving controlled mechanical stimulation of skin in the form of tape stripping. Prior research (Rodijk et al. 2016) indicated that tape stripping using 8-12 tapes was a suitable model for shaving up to 30 seconds when investigating the skin response with Confocal Raman Microscopy. Thus, the protocol developed in Chapter 4 aimed to explore associations between tape stripping and shaving with respect to an array of skin parameters. However, the study did not reveal significant temporal trends due to the magnitude of the stimuli ([Section 4.3.2](#)), preventing further analysis. Accordingly, in this chapter, the skin response to tape stripping versus shaving was conducted on the forearms, with one arm allocated to tape stripping and the contralateral side to shaving. The influence of both stimuli has been summarized in [Table 6.4](#), revealing differences in temporal trends in 8/10 parameters. For example, hydration revealed smaller changes following the shaving stimulus, while tape stripping demonstrated a statistically significant temporal influence ($p=0.020$). Similar results are observed for SRR, where shaving revealed small changes ($p=0.189$) while tape stripping revealed significant changes ($p=0.002$). This can be explained by the damage mechanism of the two stimuli. As discussed in [Section 4.4](#), tape stripping primarily impairs the barrier function of the skin by removing layers of the stratum corneum (Bashir et al. 2001; Lademann et al. 2009) resulting in exposure of the underlying water-saturated epidermis (Tagami et al. 1980). In contrast, shaving involves the cutting and pulling of hair, in addition to the pressure and shear forces at the skin surface (Maurer et al. 2016), not necessarily damaging the skin barrier. This can be observed in [Figure 6.20](#), where shaving on the forearm did not elicit an increase in TEWL. Indeed, years of development effort towards consumer comfort may be minimizing the non-functional aspect of the skin/device interaction. These arguments questioned the hypothesis establishing equivalence between tape stripping and shaving. Consequently, in the present study it was concluded that tape stripping was not a good

surrogate for shaving on the forearm. While tape stripping has many advantages in dermatology, specifically for obtaining minimally invasive skin samples (Hughes et al. 2021; Barber and Boiko 2022), its utility in modelling complex mechanical loads such as shaving seems to be limited.

Conclusions

In the present study, a wide array of skin parameters including biophysical, imaging, and biochemical parameters, were investigated for characterising facial skin. The roughness values were larger on the neck, while the SID and SRR were larger on the cheek. The shaving insult resulted in a decrease in the barrier function accompanied by hyperaemia and inflammation, with the magnitude of the result corresponding to the site and beard length. Subsequent differences were observed in the recovery characteristics as most parameters returned to basal values. Furthermore, the forearm skin was found to be an unsuitable proxy for the cheek/neck, and tape stripping was revealed as an unsuitable surrogate for shaving on the forearm.

Chapter 7 Perceived and observed changes in skin response following shaving

7.1 Introduction

Sensitive skin is considered to be a highly subjective phenomenon (Draelos 1997; Re et al. 2001; Richters et al. 2017). Indeed, perception of changes in skin status is relative to the conditions that an individual is accustomed to. For example, a consumer familiar with redness on the skin surface after shaving may believe it is a typical response of the tissue. Conversely, another user may deem it to be associated with discomfort and sensitivity. Often, such perceptions are governed by factors like the individual's habits (e.g., the type of shaving device and frequency of shaving per week) and are regarded as intrinsic factors contributing to the skin response ([Section 2.2.3](#)). Additionally, there is also an influence from extrinsic factors such as the magnitude, frequency, and duration of the stimulus ([Section 2.2.4](#)), which may impact the local changes in skin structure and function following activities such as shaving.

Consequently, the present chapter aimed to study the associations between intrinsic and extrinsic factors related to a shaving load with the observed changes in skin response to the stimulus in the context of enhanced skin sensitivity. Thus, the specific objectives were as follows:

- Characterise the shaving stimulus.
- Investigate trends within the intrinsic and extrinsic factors associated with shaving loads.
- Evaluate relations within the objectively measured skin responses and a selected array of skin parameters.
- Compare trends between the observed changes in skin tissue and perceived comfort.

7.2 Methods

The protocol used in this study has been detailed in [Section 6.2.2](#). Even though data was also recorded for the forearm, analysis has been limited to the results obtained from the cheek and neck to focus on the effects of shaving on relevant skin sites. These include results from the long and short beard sessions.

7.2.1 Perceived sensitivity and intrinsic factors

The factors evaluated in this chapter include the calculated S-scores and Q-scores. Additionally, responses from the intake questionnaire for “Q5. Does your skin react during or after shaving or contact with fabrics like clothes or towels?” have been included, referred to as the “Mech SS” hereafter. Furthermore, participants’ habitual shaving device and shaving frequency have been detailed. Lastly, post-stimulus visual analogue scores (VAS) were recorded and are presented as VAS_0.3h and VAS_24h.

Furthermore, using an adapted analytical approach presented in [Section 6.2.4](#), DSLR images of the beard were analysed over a fixed region of interest to estimate the count of detected hairs ([Figure 7.1](#)). Subsequently, the baseline images from the cheek and neck were digitally processed to determine the number of hairs as N_{hair} .

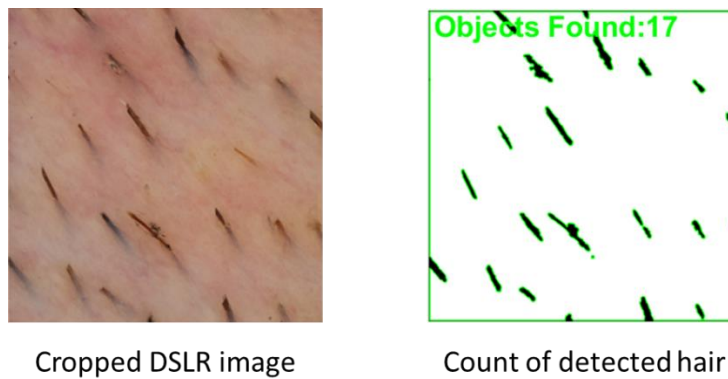


Figure 7.1 Exemplar image of the neck with estimation of the count of detected hair.

7.2.2 Estimation of Extrinsic factors

The present study focuses on mechanical stimulation of two facial locations (cheek and neck) using an electric shaver. The stimulus for each participant was characterized, providing information regarding the extrinsic factors associated with the load. A commercially available Philips shaver that was equipped with load sensors was used ([Section 4.2.5](#)). The force applied during shaving was recorded at 50Hz using a proprietary software and transferred to a computer. [Figure 7.2](#) provides examples of the Force vs Time data that was recorded for the shaving stimuli on different anatomical locations for one participant. It is noted that the load sensor had an upper limit of 7N, above which signal truncation occurs.

For characterisation of the mechanical stimulus, the following metrics were used:

1. F_{rms} – the square root of the arithmetic mean of the squares of the force values (in Newtons).
2. $f_{strokes}$ – the stroke frequency as quantified by the total number of peaks recorded divided by the duration of the shave (in strokes/second).
3. N_{max} – The ratio of peaks with values equal to 7N divided by the total number of peaks (in percentage).

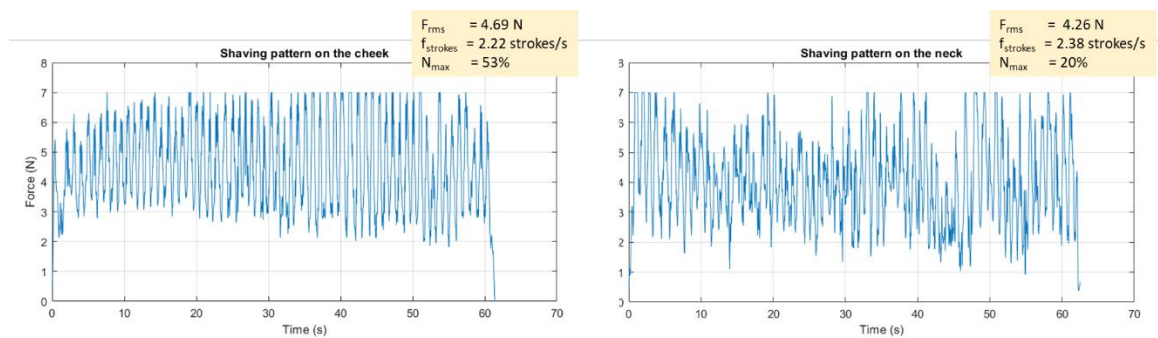


Figure 7.2 Exemplar Force vs Time plots from the shaving stimulus on the cheek and neck for one participant.

7.2.3 Statistical Analysis

Data from the new shaving parameters, participant reported outcomes and beards characteristics were collated and summarised using descriptive statistics. Prior to further analysis, the data was assessed for normality using the Anderson Darling test ([Appendix F](#)). Exploratory analysis was conducted involving case studies to provide exemplar data sets from distinct individuals within the cohort tested. Correlations between the intrinsic and extrinsic factors were investigated using the Spearman Correlation test. The strength and nature of the trends were depicted through colour-coded rankings of participants within each parameter. Furthermore, the rankings for each participant were assessed in the light of perceived sensitivity and shaving behaviours, to evaluate trends between objective parameters and participants.

7.3 Results

In addition to the demographic details presented in Table 6.3, the information has been repeated in Figure 7.3 including the calculated Q-scores and reported Mech SS score. It is observed that of the 10 participants, only two (i.e., P8 and P9) were classified as High SS, while the remaining were Mild SS. There were no Low SS individuals in this cohort. Furthermore, the results obtained from load characterisation has been detailed in Table 7.1. It is observed that the majority of the cohort (n=7/10) reported shaving less than 2 times per week, and most participants commonly used non-electric devices (n=6/10).

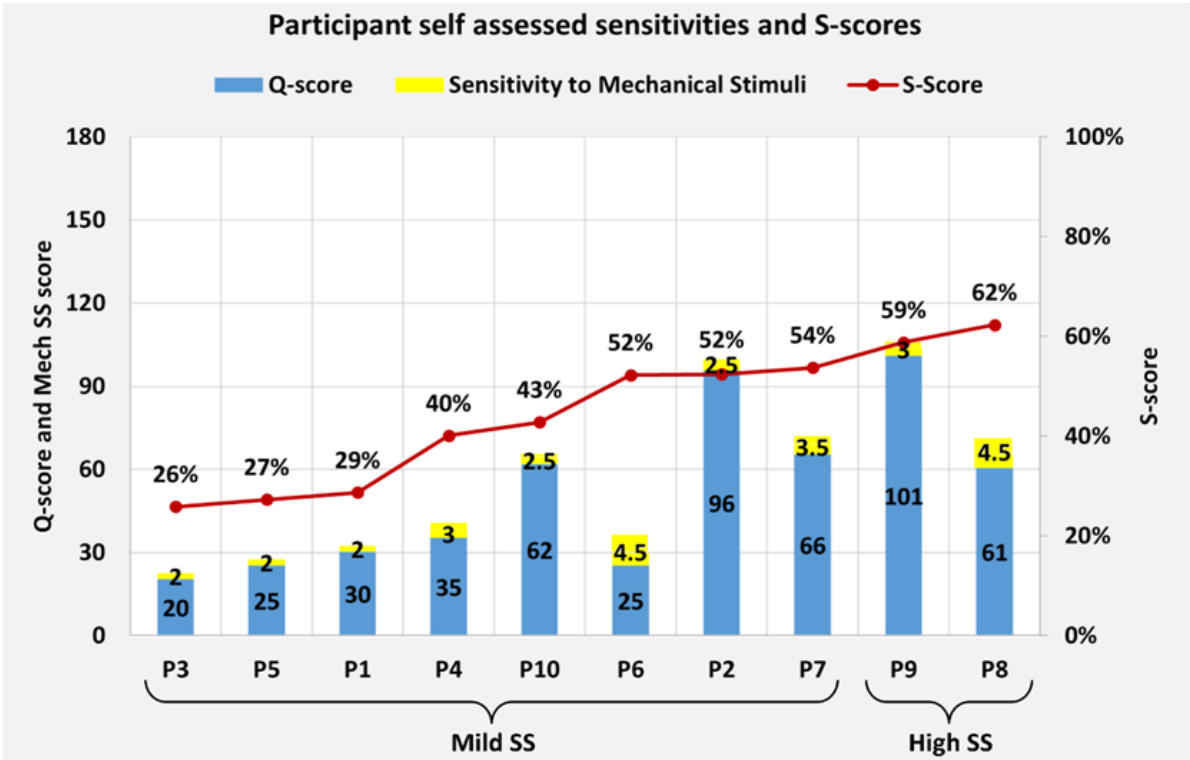


Figure 7.3 S-scores for all participants, sorted in ascending order. Associated Q-scores and Mech SS have also been plotted.

Table 7.1 Participant details including calculated S-scores, self reported Mech SS, and estimated load characteristics.

Location	Participant	S-scores	Mech SS	Shaving freq/week	Shaving device	Long Beard Session				Short Beard Session			
						F _{rms} (N)	f _{strokes} (strokes/s)	N _{max} (%)	N _{hair} (count)	F _{rms} (N)	f _{strokes} (strokes/s)	N _{max} (%)	N _{hair} (count)
Cheek	P1	29%	2.0	< 2	Combination	5.11	1.58	40%	32	4.50	1.88	39%	40
	P2	52%	2.5	< 2	Non-electric	4.84	1.23	45%	20	5.05	1.92	28%	21
	P3	26%	2.0	< 2	Non-electric	-	-	-	12	4.95	1.95	39%	12
	P4	40%	3.0	3, 4	Electric	4.69	2.22	53%	43	4.37	3.08	34%	38
	P5	27%	2.0	3, 4	Combination	4.53	1.78	0%	12	4.33	2.48	29%	19
	P6	52%	4.5	< 2	Non-electric	5.66	3.85	63%	33	5.63	2.73	76%	38
	P7	54%	3.5	< 2	Non-electric	5.35	2.70	50%	26	5.43	1.82	48%	28
	P8	62%	4.5	< 2	Electric	5.42	3.77	86%	38	4.76	2.95	67%	23
	P9	59%	3.0	< 2	Non-electric	6.58	1.10	98%	19	6.43	1.23	99%	31
	P10	43%	2.5	3, 4	Non-electric	5.86	1.23	96%	23	5.58	2.48	50%	9
Neck	P1	29%	2.0	< 2	Combination	4.29	2.17	30%	23	4.79	2.20	23%	23
	P2	52%	2.5	< 2	Non-electric	4.37	2.40	4%	11	4.28	1.28	5%	16
	P3	26%	2.0	< 2	Non-electric	4.21	1.80	1%	24	4.12	2.18	14%	21
	P4	40%	3.0	3, 4	Electric	4.26	2.38	20%	64	3.23	2.82	0%	41
	P5	27%	2.0	3, 4	Combination	3.85	2.05	0%	22	4.36	2.38	38%	10
	P6	52%	4.5	< 2	Non-electric	4.73	2.48	43%	21	4.84	1.88	44%	20
	P7	54%	3.5	< 2	Non-electric	5.76	2.45	67%	29	5.57	1.75	57%	22
	P8	62%	4.5	< 2	Electric	4.81	3.78	59%	13	4.50	3.30	56%	12
	P9	59%	3.0	< 2	Non-electric	5.96	2.62	99%	21	6.11	1.50	90%	16
	P10	43%	2.5	3, 4	Non-electric	5.45	2.22	71%	16	5.36	1.70	71%	15

7.3.1 Case study

An overview of the various skin characteristics recorded in the present study has been illustrated for participant P7, corresponding to the Long Beard shaving session in Figure 7.4 and the Short Beard shaving session in Figure 7.5. P7 reported the use of a non-electric shaving method less than two times per week. Based on the responses to the SS Questionnaire, he was categorised in the Mild SS group. However, he ranked third in the cohort with respect to the S-score which was estimated as 54%. It is noted that the self-assessed SS response for this participant was neutral but he marked a relatively higher score for sensitivity to mechanical stimuli specifically.

Characterisation of the shaving stimulus demonstrated differences in the load at the two anatomical sites, where the F_{rms} and N_{max} was higher on the neck than the cheek. For example, in the long beard session, the results were estimated at 5.35 N and 50% on the cheek and 5.76 N and 67% on the neck, respectively. Conversely, the $f_{strokes}$ were observed to be greater on the cheek than the neck. This implies that the shaving technique employed by P7 on the cheek was at a higher frequency of stroke rate with a lower load when compared to the neck. However, the $f_{strokes}$ in the Long Beard session were greater than the Short Beard session at both sites, indicating that this participant shaved more rapidly in the Long Beard session.

Overall, for P7 there was an increase in the post stimulus values (at S+0.3h) for most measured parameters with the Vessel Density demonstrating consistently high results (e.g., 125% and 172% increase from baseline in the Long Beard session for the cheek and neck, respectively). Conversely, the plexus depth demonstrated a decrease following shaving with difference in results from baseline ranging from 20% to 47%. Indeed, the DSLR images revealed distinct areas of redness on the skin surface post shaving. Following the recovery period, most parameters demonstrated a return towards baseline. In contrast, it was noted that the Rq on the cheek and vessel diameter on the neck revealed a further increase in values in the Long Beard session at S+24h (Figure 7.4), with differences from baseline equal to 58% and 143%, respectively. Additionally, in the Short Beard session (Figure 7.5), there was a higher degree of variability in the temporal trends for the parameters, such that at S+0.3h on the cheek, only the IL-1RA results revealed a fold change >1. Whereas on the neck, the difference in values from baseline demonstrated fold changes >1 for TEWL, redness, vessel density, and IFN- γ . Following recovery, the vessel density and IFN- γ remained elevated on the neck. Interestingly, recovery characteristics on the cheek demonstrated a decrease >50% from basal values for the vessel density and IL-1 α .

Investigating the visual analogue scores (VAS) post stimulus on the cheek and neck in both sessions, the participant reported a higher VAS on the neck indicating greater discomfort than the cheek (for

both sessions, VAS_cheek = 2 and VAS_neck = 8). Interestingly, the VAS on the cheek revealed different trends between the two sessions after the recovery period, with a decrease in the sensitivity observed in the Long Beard session ($\Delta\text{VAS} = -1$), while an increase was observed in the Short Beard session ($\Delta\text{VAS} = +1$). VAS on the neck at S+24h in both sessions remained elevated with values equal to 3 and 5 in the Long and Short Beard sessions, respectively.

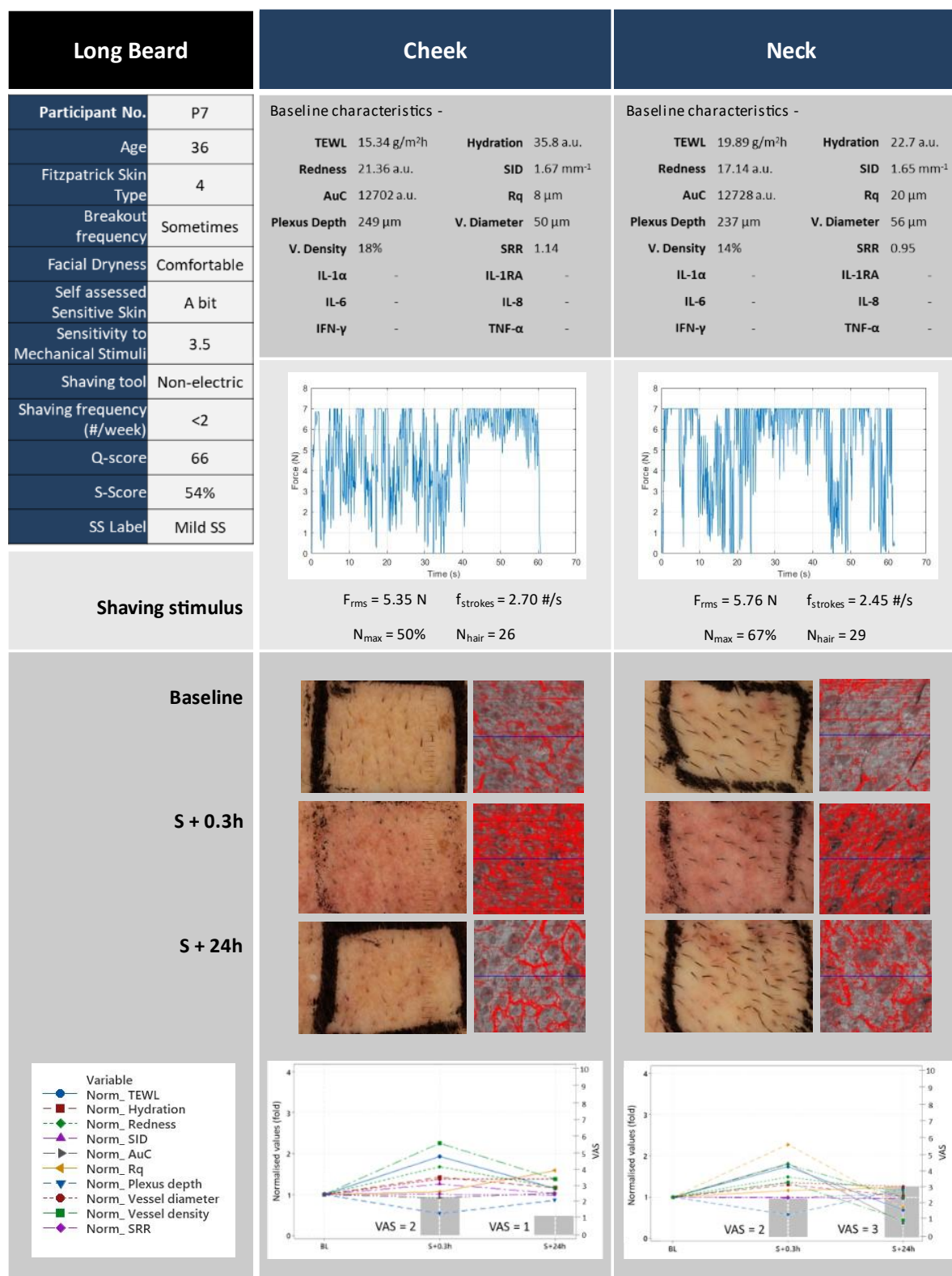


Figure 7.4 Case study for P7 from the Long Beard session (does not include biochemical parameters).

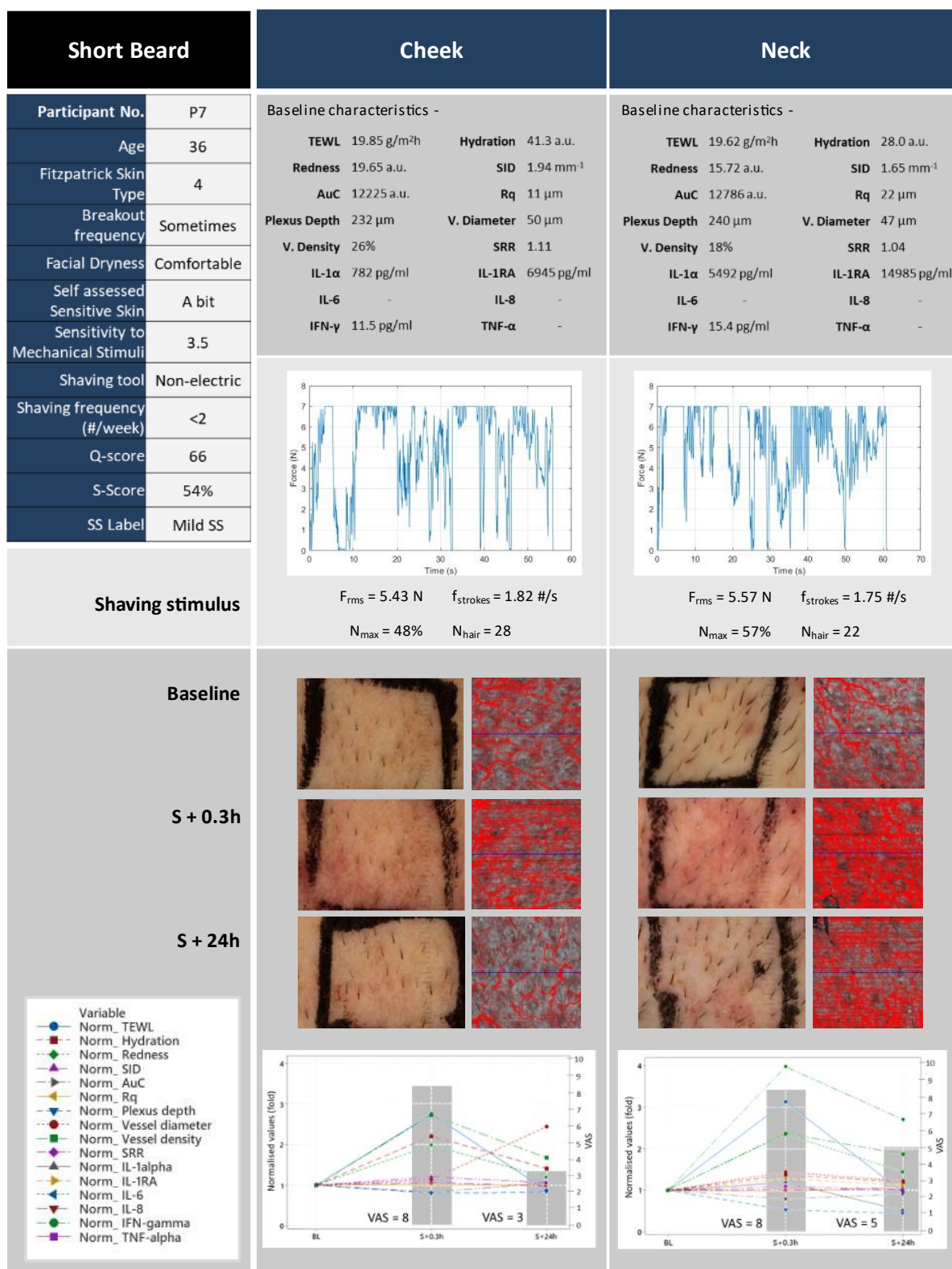


Figure 7.5 Case study for P7 from the Short Beard session.

7.3.2 Intrinsic and Extrinsic factors associated with shaving

Extrinsic factors on the cheek and neck

The shaving load was characterised for each participant, investigating associations between the cheek and neck as illustrated in Figure 7.6 (a) - (c). Additionally, the hair count is also presented (Figure 7.6d).

Overall, the cohort revealed overlapping values in shaving force profiles between the two sessions (Figure 7.6a). This is assumed to be related to the protocol where participants were requested to shave such that the device feedback light was in the orange colour zone (estimated force range 4N – 7N; Section 4.2.4). However, inter- and intra-subject differences were observed. For example, P9 demonstrated similar results in both sessions on the cheek ($F_{rms_Long\ Beard} = 6.58\text{ N}$, $F_{rms_Short\ Beard} = 6.43\text{ N}$) and neck ($F_{rms_Long\ Beard} = 5.96\text{ N}$, $F_{rms_Short\ Beard} = 6.11\text{ N}$). In contrast, P1 did not reveal a consistent trend (for the cheek, $F_{rms_Long\ Beard} = 5.11\text{ N}$, $F_{rms_Short\ Beard} = 4.50\text{ N}$; on the neck, $F_{rms_Long\ Beard} = 4.29\text{ N}$, $F_{rms_Short\ Beard} = 4.79\text{ N}$).

In contrast to the results observed for the Force, the cohort revealed differences in the f_{stroke} trends (Figure 7.6b) with respect to the session. Interestingly, it is noted that P9, while demonstrating high force values, revealed lower stroke frequency. For N_{max} (Figure 7.6c), the results revealed similarities in the profiles when compared for the results for F_{rms} which follows logically as the greater the number of peaks at the maximum force, the greater the overall force value. Lastly, for the count of hair (Figure 7.6d), most participants were clustered around 20 - 40 on the cheek and 10 - 25 on the neck, revealing site-specific differences. However, P4 had a high density of hairs at both sites.

Upon examining the Long and Short beard groups for statistically significant trends, the results revealed $p > 0.05$. However, overall trends between the cheek and neck demonstrated statistically significant trends for several parameters. Specifically, F_{rms} and N_{max} revealed a strong correlation between the cheek and neck ($r = 0.730$, $p < 0.001$ and $r = 0.664$, $p = 0.003$, respectively). Additionally, the correlation for f_{stroke} was approaching significance while results for N_{hair} demonstrated $p > 0.05$.

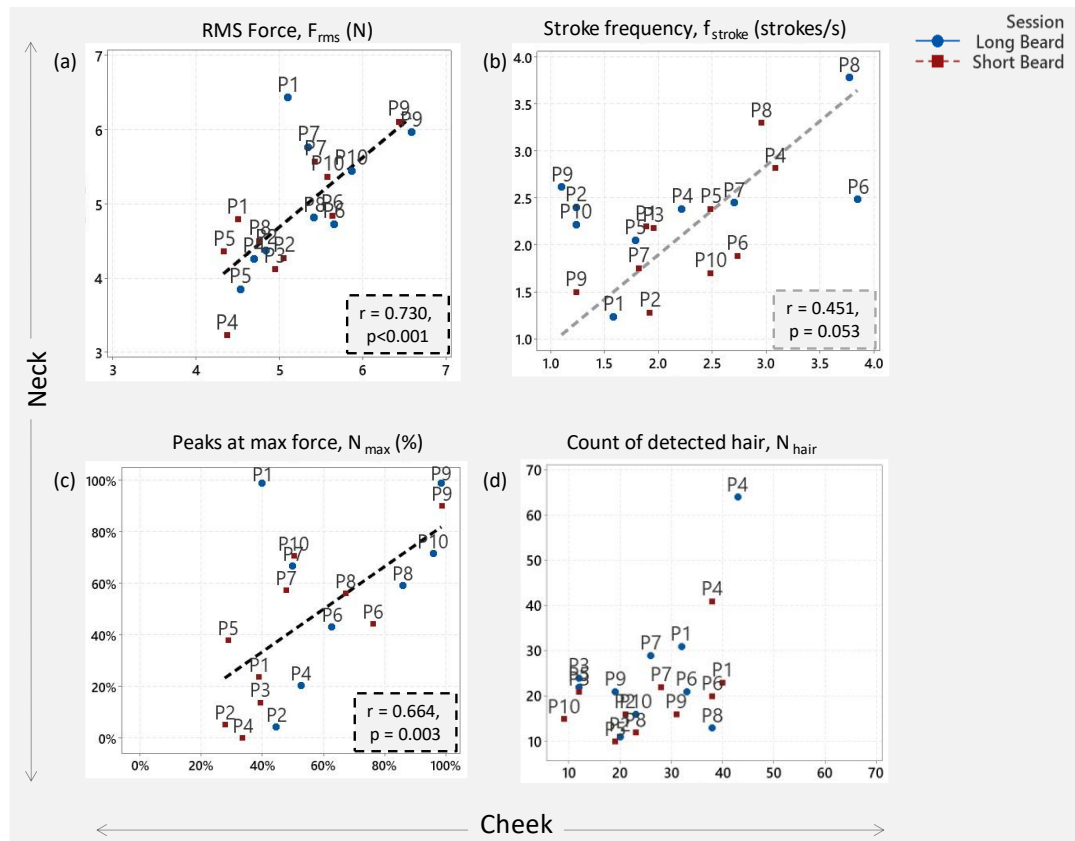


Figure 7.6 Scatterplots of values on the cheek and neck for the Long and Short Beard sessions for (a) F_{rms} , (b) f_{stroke} , (c) N_{max} , (d) N_{hair} .

Correlation between the Intrinsic and Extrinsic factors

Table 7.2 details the results from the Spearman Correlation test for each pair of the identified Intrinsic and Extrinsic factors. It follows logically that the S-scores are significantly correlated with the Q-score ($r=0.723$, $p<0.001$) and the Mech SS ($r=0.826$, $p<0.001$) as the former is defined using the latter two (Section 4.2.3). Furthermore, F_{rms} was also expected to be well-correlated with N_{max} ($r=0.859$, $p<0.001$) based on the definitions of the parameters (Section 7.2.2).

Interestingly, Mech SS revealed statistically significant correlations ($p<0.05$) with $n=7/8$ other parameters. Specifically, this parameter was not correlated only with N_{hair} , which in turn was not correlated with any other parameter. Amongst the Extrinsic factors, F_{rms} and N_{max} demonstrated significant correlations with the S-scores, Q-scores, Mech SS, and $f_{strokes}$. Furthermore, VAS_0.3 revealed statistically significant correlations with most intrinsic factors ($n=4/5$), but none of the extrinsic factors. Given the interest of the present research in consumer comfort, this parameter is considered important and selected for further analysis. Consequently, the Mech SS, F_{rms} , and

VAS_0.3 were selected for further investigations exploring associations with the objective skin responses to shaving (Section 7.3.4).

Table 7.2 Spearman correlation values, p-values, and sample size for all Intrinsic and Extrinsic factors. Pairs with $p < 0.05$ have been highlighted in bold with shades of light to dark blue for ascending positive r values.

	Intrinsic Factors					Extrinsic Factors		
	S-scores	Q-score	Mech SS	VAS_0.3h	VAS_24h	N_hair	F_rms	f_strokes
Intrinsic Factors	Q-score $r = 0.723$ $p < 0.001$ (n = 40)							
	Mech SS $r = 0.826$ $p < 0.001$ (n = 40)	Q-score $r = 0.332$ $p = 0.036$ (n = 40)						
	VAS_0.3h $r = 0.371$ $p = 0.019$ (n = 40)	Q-score $r = 0.365$ $p = 0.020$ (n = 40)	Mech SS $r = 0.439$ $p = 0.005$ (n = 40)					
	VAS_24h $r = 0.327$ $p = 0.052$ (n = 36)	$r = 0.172$ $p = 0.315$ (n = 36)	Mech SS $r = 0.471$ $p = 0.004$ (n = 36)	VAS_0.3h $r = 0.531$ $p = 0.001$ (n = 36)				
	N_hair $r = 0.045$ $p = 0.781$ (n = 40)	$r = -0.048$ $p = 0.767$ (n = 40)	$r = 0.266$ $p = 0.097$ (n = 40)	$r = 0.149$ $p = 0.359$ (n = 40)	$r = 0.233$ $p = 0.171$ (n = 36)			
Extrinsic Factors	F_rms $r = 0.584$ $p < 0.001$ (n = 39)	Q-score $r = 0.543$ $p < 0.001$ (n = 39)	Mech SS $r = 0.398$ $p = 0.012$ (n = 39)	$r = 0.174$ $p = 0.288$ (n = 39)	$r = -0.301$ $p = 0.079$ (n = 35)	$r = -0.02$ $p = 0.903$ (n = 39)		
	f_strokes $r = 0.187$ $p = 0.255$ (n = 39)	$r = -0.253$ $p = 0.120$ (n = 39)	Q-score $r = 0.461$ $p = 0.003$ (n = 39)	$r = 0.115$ $p = 0.488$ (n = 39)	$r = 0.252$ $p = 0.144$ (n = 35)	$r = 0.156$ $p = 0.344$ (n = 39)	$r = -0.18$ $p = 0.274$ (n = 39)	
	N_max $r = 0.691$ $p < 0.001$ (n = 39)	Q-score $r = 0.49$ $p = 0.002$ (n = 39)	Mech SS $r = 0.555$ $p < 0.001$ (n = 39)	$r = 0.195$ $p = 0.235$ (n = 39)	$r = -0.167$ $p = 0.338$ (n = 35)	$r = 0.035$ $p = 0.830$ (n = 39)	F_rms $r = 0.859$ $p < 0.001$ (n = 39)	$r = 0.017$ $p = 0.917$ (n = 39)

7.3.3 Selecting an optimised array of skin parameters

Table 7.3 details the results from the Spearman Correlation test for each pair of the 16 skin tissue parameters. Remarkably, TEWL revealed statistically significant correlations ($p < 0.05$) with 10 of the 15 other parameters, wherein moderately positive relationships were observed (r value ranging from 0.310 to 0.739). The exception to this trend was observed for AuC and plexus depth which demonstrated negative relationships ($r = -0.532$ and $r = -0.566$, respectively). Indeed, the AuC and plexus depth consistently revealed negative correlations with other parameters, which was confirmed by the decreasing temporal trend post stimulation (Figure 6.22 and Figure 6.23).

The vessel density revealed statistically significant correlations ($p < 0.05$) with majority of the parameter array ($n = 11/15$). Upon closer examination, these included the parameters associated with the cutaneous blood flow, namely, redness, plexus depth, and vessel diameter. Furthermore,

the vessel density also demonstrated significant correlations (r-value ranging from 0.341 to 0.520, $p < 0.01$) with most of the inflammatory biomarkers, excluding TNF- α .

For the sub-array of biochemical parameters, all except IL-8 revealed statistically significant correlations with the other cytokines. Indeed, the low abundant IL-8 did not achieve statistical significance in correlations for most pairs from the wider array. However, it is noted that when compared to Rq, the results demonstrated a moderate relationship ($r = 0.352$, $p = 0.021$). Interestingly, both parameters have previously revealed spatial differences when investigating trends on the cheek and neck ([Section 6.3](#)).

Fewer statistically significant correlations were observed for some parameters such as hydration. Indeed, the results for hydration stand out due to the lack of correlations with any of the biochemical parameters and most of the structural parameters and have been discussed further in [Section 7.4](#). A summary of the observations have been listed in [Table 7.4](#), supplemented with information from the spatial and temporal trends from [Section 6.3](#).

Table 7.3 Spearman correlation values, p-values, and sample size for the biophysical, structural, and biochemical parameters. Pairs with $p < 0.05$ have been highlighted in bold with shades of light to dark blue for ascending positive r values and shades of light to dark red for descending negative r values.

		Biophysical Parameters					Structural Parameters					Biochemical Parameters				
		TEWL	Hydration	Redness	SID	AuC	Rq	Plexus depth	Vessel diameter	Vessel density	SRR	IL-1alpha	IL-1RA	IL-6	IL-8	IFN-gamma
Biophysical parameters	Hydration	$r = 0.058$, $p = 0.557$ ($n = 106$)														
	Redness	$r = 0.31$, $p = 0.001$ ($n = 104$)	$r = 0.572$, $p < 0.001$ ($n = 116$)													
	SID	$r = 0.15$, $p = 0.124$ ($n = 106$)	$r = 0.082$, $p = 0.376$ ($n = 118$)	$r = 0.137$, $p = 0.143$ ($n = 116$)												
Structural Parameters	AuC	$r = -0.532$, $p < 0.001$ ($n = 106$)	$r = 0.111$, $p = 0.231$ ($n = 118$)	$r = -0.079$, $p = 0.402$ ($n = 116$)	$r = -0.39$, $p < 0.001$ ($n = 118$)											
	Rq	$r = 0.108$, $p = 0.27$ ($n = 106$)	$r = -0.008$, $p = 0.933$ ($n = 118$)	$r = 0.054$, $p = 0.568$ ($n = 116$)	$r = -0.764$, $p < 0.001$ ($n = 118$)	$r = 0.035$, $p = 0.707$ ($n = 118$)										
	Plexus depth	$r = -0.566$, $p < 0.001$ ($n = 106$)	$r = -0.156$, $p = 0.092$ ($n = 118$)	$r = -0.326$, $p < 0.001$ ($n = 116$)	$r = -0.292$, $p = 0.001$ ($n = 118$)	$r = 0.599$, $p < 0.001$ ($n = 118$)	$r = -0.012$, $p = 0.9$ ($n = 118$)									
	Vessel diameter	$r = 0.085$, $p = 0.388$ ($n = 106$)	$r = 0.442$, $p < 0.001$ ($n = 118$)	$r = 0.513$, $p < 0.001$ ($n = 116$)	$r = -0.174$, $p = 0.059$ ($n = 118$)	$r = 0.201$, $p = 0.029$ ($n = 118$)	$r = 0.099$, $p = 0.284$ ($n = 118$)	$r = -0.103$, $p = 0.269$ ($n = 118$)								
	Vessel density	$r = 0.659$, $p < 0.001$ ($n = 106$)	$r = 0.302$, $p = 0.001$ ($n = 118$)	$r = 0.567$, $p < 0.001$ ($n = 116$)	$r = 0.115$, $p = 0.217$ ($n = 118$)	$r = -0.347$, $p < 0.001$ ($n = 118$)	$r = 0.118$, $p = 0.201$ ($n = 118$)	$r = -0.705$, $p < 0.001$ ($n = 118$)	$r = 0.405$, $p < 0.001$ ($n = 118$)							
Biochemical Parameters	SRR	$r = 0.374$, $p < 0.001$ ($n = 106$)	$r = -0.19$, $p = 0.04$ ($n = 118$)	$r = 0.045$, $p = 0.63$ ($n = 116$)	$r = 0.606$, $p < 0.001$ ($n = 118$)	$r = -0.61$, $p < 0.001$ ($n = 118$)	$r = -0.503$, $p < 0.001$ ($n = 118$)	$r = -0.23$, $p = 0.012$ ($n = 118$)	$r = -0.28$, $p = 0.002$ ($n = 118$)	$r = 0.127$, $p = 0.171$ ($n = 118$)						
	IL-1alpha	$r = 0.388$, $p = 0.006$ ($n = 49$)	$r = 0.178$, $p = 0.192$ ($n = 55$)	$r = 0.043$, $p = 0.758$ ($n = 55$)	$r = -0.066$, $p = 0.631$ ($n = 55$)	$r = -0.29$, $p = 0.031$ ($n = 55$)	$r = 0.274$, $p = 0.043$ ($n = 55$)	$r = -0.337$, $p = 0.012$ ($n = 55$)	$r = 0.163$, $p = 0.234$ ($n = 55$)	$r = 0.341$, $p = 0.011$ ($n = 55$)	$r = -0.113$, $p = 0.409$ ($n = 55$)					
	IL-1RA	$r = 0.554$, $p < 0.001$ ($n = 49$)	$r = 0.085$, $p = 0.539$ ($n = 55$)	$r = 0.191$, $p = 0.162$ ($n = 55$)	$r = 0.421$, $p = 0.001$ ($n = 55$)	$r = -0.309$, $p = 0.022$ ($n = 55$)	$r = -0.16$, $p = 0.244$ ($n = 55$)	$r = -0.379$, $p = 0.004$ ($n = 55$)	$r = 0.044$, $p = 0.751$ ($n = 55$)	$r = 0.378$, $p = 0.004$ ($n = 55$)	$r = 0.229$, $p = 0.093$ ($n = 55$)	$r = 0.681$, $p < 0.001$ ($n = 55$)				
	IL-6	$r = 0.739$, $p < 0.001$ ($n = 34$)	$r = 0.014$, $p = 0.93$ ($n = 40$)	$r = 0.233$, $p = 0.149$ ($n = 40$)	$r = 0.402$, $p = 0.01$ ($n = 40$)	$r = -0.587$, $p < 0.001$ ($n = 40$)	$r = -0.195$, $p = 0.227$ ($n = 40$)	$r = -0.496$, $p = 0.001$ ($n = 40$)	$r = -0.047$, $p = 0.771$ ($n = 40$)	$r = 0.449$, $p = 0.004$ ($n = 40$)	$r = 0.588$, $p < 0.001$ ($n = 40$)	$r = 0.565$, $p < 0.001$ ($n = 40$)	$r = 0.646$, $p < 0.001$ ($n = 40$)			
	IL-8	$r = 0.267$, $p = 0.11$ ($n = 37$)	$r = -0.085$, $p = 0.588$ ($n = 43$)	$r = 0.44$, $p = 0.003$ ($n = 43$)	$r = -0.177$, $p = 0.256$ ($n = 43$)	$r = -0.063$, $p = 0.69$ ($n = 43$)	$r = 0.352$, $p = 0.021$ ($n = 43$)	$r = -0.185$, $p = 0.234$ ($n = 43$)	$r = 0.201$, $p = 0.196$ ($n = 43$)	$r = 0.52$, $p < 0.001$ ($n = 43$)	$r = -0.075$, $p = 0.632$ ($n = 43$)	$r = 0.175$, $p = 0.262$ ($n = 43$)	$r = 0.136$, $p = 0.384$ ($n = 43$)	$r = 0.25$, $p = 0.12$ ($n = 40$)		
	IFN-gamma	$r = 0.514$, $p < 0.001$ ($n = 49$)	$r = 0.128$, $p = 0.353$ ($n = 55$)	$r = 0.153$, $p = 0.264$ ($n = 55$)	$r = 0.016$, $p = 0.908$ ($n = 55$)	$r = -0.253$, $p = 0.063$ ($n = 55$)	$r = 0.141$, $p = 0.303$ ($n = 55$)	$r = -0.335$, $p = 0.012$ ($n = 55$)	$r = 0.194$, $p = 0.156$ ($n = 55$)	$r = 0.39$, $p = 0.003$ ($n = 55$)	$r = 0.07$, $p = 0.61$ ($n = 55$)	$r = 0.672$, $p < 0.001$ ($n = 55$)	$r = 0.496$, $p < 0.001$ ($n = 55$)	$r = 0.474$, $p = 0.002$ ($n = 40$)	$r = 0.228$, $p = 0.141$ ($n = 43$)	
	TNF-alpha	$r = 0.593$, $p < 0.001$ ($n = 36$)	$r = 0.098$, $p = 0.543$ ($n = 41$)	$r = 0.145$, $p = 0.366$ ($n = 41$)	$r = 0.252$, $p = 0.112$ ($n = 41$)	$r = -0.207$, $p = 0.194$ ($n = 41$)	$r = -0.172$, $p = 0.281$ ($n = 41$)	$r = -0.14$, $p = 0.381$ ($n = 41$)	$r = -0.088$, $p = 0.585$ ($n = 41$)	$r = 0.226$, $p = 0.155$ ($n = 41$)	$r = 0.444$, $p = 0.004$ ($n = 41$)	$r = 0.374$, $p = 0.016$ ($n = 41$)	$r = 0.543$, $p < 0.001$ ($n = 41$)	$r = 0.699$, $p < 0.001$ ($n = 38$)	$r = 0.027$, $p = 0.869$ ($n = 41$)	$r = 0.615$, $p < 0.001$ ($n = 41$)

Table 7.4 Decision matrix to reduce the number of variables, minimising the array of skin tissue responses. Spatial and temporal differences have been summarized considering the observations from Chapter 6.

	Parameter	Spatial differences	Temporal differences	Correlations	Rationale
Biophysical parameters	TEWL	-	xx	xx	All biophysical parameters had similar results in distinguishing spatial and temporal trends. TEWL showed a higher number of correlated pairs. Furthermore, TEWL is considered to represent the functional barrier of the skin.
	Hydration	-	xx	x	
	Redness	-	xx	x	
Structural parameters	SID	xx	xx	x	Few structural parameters demonstrated spatial differences, where SID was also sensitive to temporal trends, while SRR showed significant correlations with many parameters. Additionally, for the dynamic structural parameters, the vessel density showed significant correlations with a larger number of parameters and differences in temporal trends following shaving.
	AuC	-	x	xx	
	Rq	xx	-	x	
	Plexus depth	-	xx	xx	
	Vessel diameter	-	x	x	
	Vessel density	-	xx	xx	
	SRR	xx	x	xx	
Biochemical parameters	IL-1 α	xx	xx	xx	Most biochemical parameters showed a significant correlation with a large number of parameters. Additionally, IL-1 α and IL-8 also demonstrated significant differences in basal values from the cheek and neck. Thus, each were selected to represent the high and low abundance biomarkers in the array.
	IL-1RA	-	xx	xx	
	IL-6	-	x	xx	
	IL-8	xx	x	x	
	IFN- γ	-	x	x	
	TNF- α	-	-	x	

- No significant differences observed
- x Moderate significant differences observed
- xx Large significant differences observed

7.3.4 Associations between Intrinsic and Extrinsic factors, and the skin tissue responses

Associations between the parameters selected in Sections 7.3.2 and 7.3.3 were investigated for the Long and Short Beard sessions combined, including the basal, post-stimulus, and recovery responses. Results have been presented in Table 7.5. It is observed that TEWL, SID, and SRR demonstrated statistically significant correlations with the intrinsic and extrinsic factors. Specifically, TEWL and SRR revealed $p < 0.05$ with a weak to moderate correlation with Mech SS, VAS_0.3h, and F_{rms} (r-value ranging from 0.197 to 0.352). However, SRR and VAS_0.3h demonstrated a negative correlation ($r = -0.251$, $p = 0.012$), indicating a decrease in the skin reflectivity with an increase in discomfort. SID revealed statistically significant positive correlations with Mech SS ($r = 0.258$, $p = 0.005$) and F_{rms} ($r = 0.503$, $p < 0.001$), indicating a higher scattering of the optical signal with an increase in the self-assessed sensitivity and the applied force.

Table 7.5 Spearman correlation values, p-values, and sample size between Intrinsic and Extrinsic factors, and the skin tissue responses. Pairs with $p < 0.05$ have been highlighted in bold with shades of light to dark blue for ascending positive r values and shades of light to dark red for descending negative r values.

	Mech SS	VAS_0.3h	F_{rms}
TEWL	$r = 0.352$, $p < 0.001$, (n = 106)	$r = 0.217$, $p = 0.041$, (n = 89)	$r = 0.197$, $p = 0.047$, (n = 103)
SID	$r = 0.258$, $p = 0.005$, (n = 118)	$r = -0.116$, $p = 0.252$, (n = 99)	$r = 0.503$, $p < 0.001$, (n = 115)
Vessel density	$r = 0.041$, $p = 0.660$, (n = 118)	$r = 0.132$, $p = 0.192$, (n = 99)	$r = 0.122$, $p = 0.192$, (n = 115)
SRR	$r = 0.213$, $p = 0.020$, (n = 118)	$r = -0.251$, $p = 0.012$, (n = 99)	$r = 0.294$, $p = 0.001$, (n = 115)
IL-1alpha	$r = 0.109$, $p = 0.429$, (n = 55)	$r = -0.194$, $p = 0.249$, (n = 37)	$r = -0.079$, $p = 0.567$, (n = 55)
IL-8	$r = 0.188$, $p = 0.228$, (n = 43)	$r = 0.002$, $p = 0.991$, (n = 29)	$r = -0.151$, $p = 0.335$, (n = 43)

For closer examination of the trends across the cohort, participants responses were ranked and colour-coded. Table 7.6 illustrates the results for the Short Beard session for the selected array of parameters identified in Table 7.2 and Table 7.3 (similar to the analysis presented in Section 5.3.5).

Participants' shaving frequency and device have also been listed, and the rows have been sorted to display an increasing trend in Mech SS. These parameters represent the intrinsic factors associated with shaving, and thus, stay consistent for each participant spatially and temporally. Similarly, the VAS_0.3 and F_{rms} are linked with the shaving stimulus and thus, the values only differ spatially. In addition, as P9 did not attend the recovery session, there is skin response no data for this participant for S+24h.

The ranks for VAS_0.3 demonstrated differences based on the skin site being investigated. For example, P9 revealed the highest rank on the cheek and the 8th rank on the neck. However, P8 revealed the same rank on both sites (rank = 2). Similarly, the F_{rms} ranks also demonstrated spatial differences. For example, the results revealed that P1 had the 8th rank on the cheek while the 5th rank on the neck. In contrast, P3 demonstrated the 6th rank on the cheek and the 9th rank on the neck. However, only P9 revealed the same rank on both sites, with the highest force values in the cohort (rank = 1).

Furthermore, site specific trends were also observed with respect to the skin tissue responses. For example, at S+0.3h, P8 revealed similar relative force values with the F_{rms} ranks equal to 7 on the cheek and 6 on the neck. However, this participant revealed TEWL rank equal to 1 on the cheek, while on the neck, it was 8. After recovery, the relative values demonstrated differing trends as the rank on the cheek was 3, while it was 6 on the neck. Similar differences in trends were observed when examining the other parameters. These findings highlight the relative intra-subject variability following shaving.

Investigating clusters across all parameters, large inter-subject variability was observed. For example, on the cheek at S+0.3h, P9 demonstrated the 1st rank for SID and IL-1 α , and the 3rd rank for SRR and IL-8. However, with respect to TEWL and vessel density, P9 revealed relatively lower tissue responses as the ranks were equal to 6th and 7th, respectively. On the neck at S+0.3h, P9 revealed ranks ranging from 1st to 4th for all parameters except SRR where the results were the lowest in the group (rank = 10).

Table 7.6 Participant ranks for each parameter in the Short Beard session. Where data is missing, the cells have been filled black.

Location	Time	Participant	Intrinsic factors			Extrinsic factors		Skin tissue responses					
			Shaving freq/week	Shaving device	Mech SS	Rank VAS_0.3	Rank F _{rms}	Rank norm. TEWL	Rank norm. SID	Rank norm. V. Den.	Rank norm. SRR	Rank norm. IL-1α	Rank norm. IL-8
Cheek	S+0.3h	P1	< 2	Combination	2.0	9	8	7	3	9	8	2	5
		P3	< 2	Non-electric	2.0	6	5	8	8	6	4	7	1
		P5	3, 4	Combination	2.0	4	10	4	4	3	1	6	
		P10	3, 4	Non-electric	2.5	5	3	9	2	10	2	8	7
		P2	< 2	Non-electric	2.5	2	5		5	8	6	3	6
		P4	3, 4	Electric	3.0	10	9	3	6	1	5	5	2
		P9	< 2	Non-electric	3.0	1	1		1	7	3	1	3
		P7	< 2	Non-electric	3.5	6	4	2	10	4	9	9	
		P6	< 2	Non-electric	4.5	6	2	5	9	1	10		
		P8	< 2	Electric	4.5	2	7	1	7	5	7	4	4
	S+24h	P1	< 2	Combination	2.0	9	8	8		5	6	7	3
		P3	< 2	Non-electric	2.0	6	5	2	1	6	4	8	2
		P5	3, 4	Combination	2.0	4	10	1	2	1	5	4	
		P10	3, 4	Non-electric	2.5	5	3	6	5	7	3	5	1
		P2	< 2	Non-electric	2.5	2	5		8	2	9	1	6
		P4	3, 4	Electric	3.0	10	9	5	3	3	7	3	5
		P9	< 2	Non-electric	3.0	1	1						
		P7	< 2	Non-electric	3.5	6	4	7	7	9	8	9	
Neck	S+0.3h	P3	< 2	Non-electric	2.0	4	9	2	7	9	6	6	6
		P5	3, 4	Combination	2.0	7	7	9	10	8	9	4	
		P10	3, 4	Non-electric	2.5	9	3		9	10	5		
		P2	< 2	Non-electric	2.5	1	8		4	1	4	1	2
		P4	3, 4	Electric	3.0	9	10	4	6	2	8	5	7
		P9	< 2	Non-electric	3.0	8	1	3	1	4	10	2	1
		P7	< 2	Non-electric	3.5	2	2	5	8	6	7	9	
		P6	< 2	Non-electric	4.5	5	4	7	3	2	2	3	5
		P8	< 2	Electric	4.5	2	6	8	5	7	3	7	4
	S+24h	P1	< 2	Combination	2.0	5	5	5	7	6	1	7	5
		P3	< 2	Non-electric	2.0	4	9	1	2	7	5	5	3
		P5	3, 4	Combination	2.0	7	7	4	5	8	4	3	
		P10	3, 4	Non-electric	2.5	9	3	3	9	9	3		
		P2	< 2	Non-electric	2.5	1	8		1	1	2	2	2
		P4	3, 4	Electric	3.0	9	10	2	6	3	6	1	4
		P9	< 2	Non-electric	3.0	8	1						
		P7	< 2	Non-electric	3.5	2	2	8	4	2	8	6	
		P6	< 2	Non-electric	4.5	5	4	7	3	3	7		
		P8	< 2	Electric	4.5	2	6	6	8	5	9	6	1

7.4 Discussion

The shaving stimulus was characterised in this chapter, yielding participant-specific parameters for the assessment of variability in skin response following loading. The authors believe this is one of the first studies to characterise the shaving stimulus on the cheek and neck. As such, extrinsic factors associated with the stimulus were defined and estimated. Furthermore, intrinsic factors were also defined based on participants' perceived sensitivity and comfort. Comprehensive evaluation of the skin response to shaving was presented as case studies [Section 7.3.1](#), highlighting the novelty of the present protocol in characterising a wide array of skin parameters (as discussed in [Section 6.4](#)) and linking the participant comfort with the skin responses. Indeed, it was observed that there was a higher degree of visible redness ([Figure 7.4](#) and [Figure 7.5](#)) accompanied by an increase in the VAS, indicative of enhanced sensitivity post shaving.

Results revealed statistically significant correlations between several intrinsic and extrinsic factors. For example, it was observed that the higher the mechanical sensitivity, the higher the force applied by the participant (Mech SS and F_{rms} , $r = 0.398$, $p = 0.012$) and the higher the reported discomfort post shaving (Mech SS and VAS_0.3, $r = 0.439$, $p = 0.005$). Subsequently, it can be hypothesized that individuals who apply more force during shaving regard themselves as more sensitive to mechanical stimuli. However, the protocol implemented in this study required participants to shave in a small region on their face for 60 seconds, maintaining a high load such that the device feedback light was in the "orange zone" ([Figure 4.6](#)). Thus, the results obtained from characterising the shaving patterns are not considered the true consumer behaviour. Nevertheless, such parameters may be exemplary of stimuli involving pressure, friction, and combinations thereof, and provide opportunities for future analysis involving mechanical stimulation of skin.

Furthermore, TEWL, SID, and SRR demonstrated statistically significant correlations with Mech SS, VAS_0.3h, and F_{rms} ([Table 7.5](#)). As such, it can be suggested that with an increase in the perception of SS and the force of stimulus application, there is a decrease in the SC integrity, decrease in optical density of the tissue, and a change in the skin reflectivity. As the SRR demonstrated a positive correlation with Mech SS and a negative correlation with VAS_0.3h, the relationship between SRR and skin surface colour/composition requires further investigation to understand the mechanisms underlying perception of SS. The authors believe this is one of the first studies correlating skin tissue response to mechanical stimulation with intrinsic and extrinsic factors in shaving.

The relationship between shaving and skin sensitivity has been conceptualised in [Figure 7.7](#), highlighting the inter-dependent network of physiological actions that are subsequently triggered ([Table 7.3](#)) and the variety of overarching factors that influence the responses ([Table 7.2](#)). The interaction of an electric shaver with the skin surface can be explained with a combination of

intermittent loading and manipulation of hair. Indeed, the former can lead to abrasion of the outer skin layers (Bhaktaviziam et al. 1963) and subsequent removal of corneocytes (Turner et al. 2006). As these cells are crucial for the barrier function of the skin, several pathological pathways are subsequently triggered by such stimuli. For example, increase in TEWL and hydration is observed (Bashir et al. 2001; Loffler et al. 2004; Gorcea et al. 2013; Richters et al. 2016; Jayabal et al. 2021), as well as an upregulation in pro-inflammatory cytokines (Nickoloff and Naidu 1994; De Wert et al. 2015; Soetens et al. 2019). Interestingly, statistically significant correlations were found between these parameters in [Section 7.3.3](#) (e.g., TEWL and IL-1 α , $r = 0.388$ and $p = 0.006$), indicating that the shaving stimulus implemented in the present study impaired the local skin barrier.

Furthermore, the loading component of the stimulus leads to the occlusion and reperfusion of blood vessels in the underlying tissue. Physiologically, this has been linked with microvascular remodelling (Wang et al., 2015). Indeed, significant changes were observed in dynamic skin parameters such as vessel density and plexus depth following shaving ([Figure 6.22](#) and [Figure 6.23](#)) and the present chapter established significant correlations between such parameters ($r = -0.705$, $p < 0.001$). It is noted that the redness of the skin also yielded significant correlations with the dynamic skin parameters (redness and vessel density, $r = 0.567$, $p < 0.001$; redness and plexus depth, $r = -0.326$, $p < 0.001$). Visible redness of the skin is important in the evaluation of SS as consumers often regard an increase in surface redness with enhanced sensitivity. However, there is a missing link between increased redness and enhanced sensitivity. It may be that components of the epidermis responsible for the skins' sensory function are directly/indirectly activated by mechanical loads. Indeed, manipulation of hair while shaving reportedly leads to shearing of hair follicles and subsequent activation of mast cells (Cowley et al. 2012; Maurer et al. 2016; Rietzler et al. 2016). Additionally, others have hypothesized the role of keratinocytes and Merkel cells in SS (Ständer et al. 2009; Misery 2016; Sun et al. 2016), implicating abnormal activation of TRP channels present on these structures. Further research is needed to investigate this relationship and establish trends for mechanical stimulation of skin.

However, inter- and intra-subject variability is observed in the skin responses to shaving ([Section 6.3](#)). It is hypothesized that several intrinsic and extrinsic factors influence the tolerance thresholds for individuals (Sanders et al. 1995; Draelos 1997; Misery et al. 2006), implicating the subjective nature of perception of SS. Upon closer examination, no clear trends were revealed when exploring such associations ([Section 7.3.4](#)). This is believed to be a limitation of the results as the study included a small cohort of 10 participants only (Sawyer 1982). Thus, further analysis was restricted due to the low statistical power.

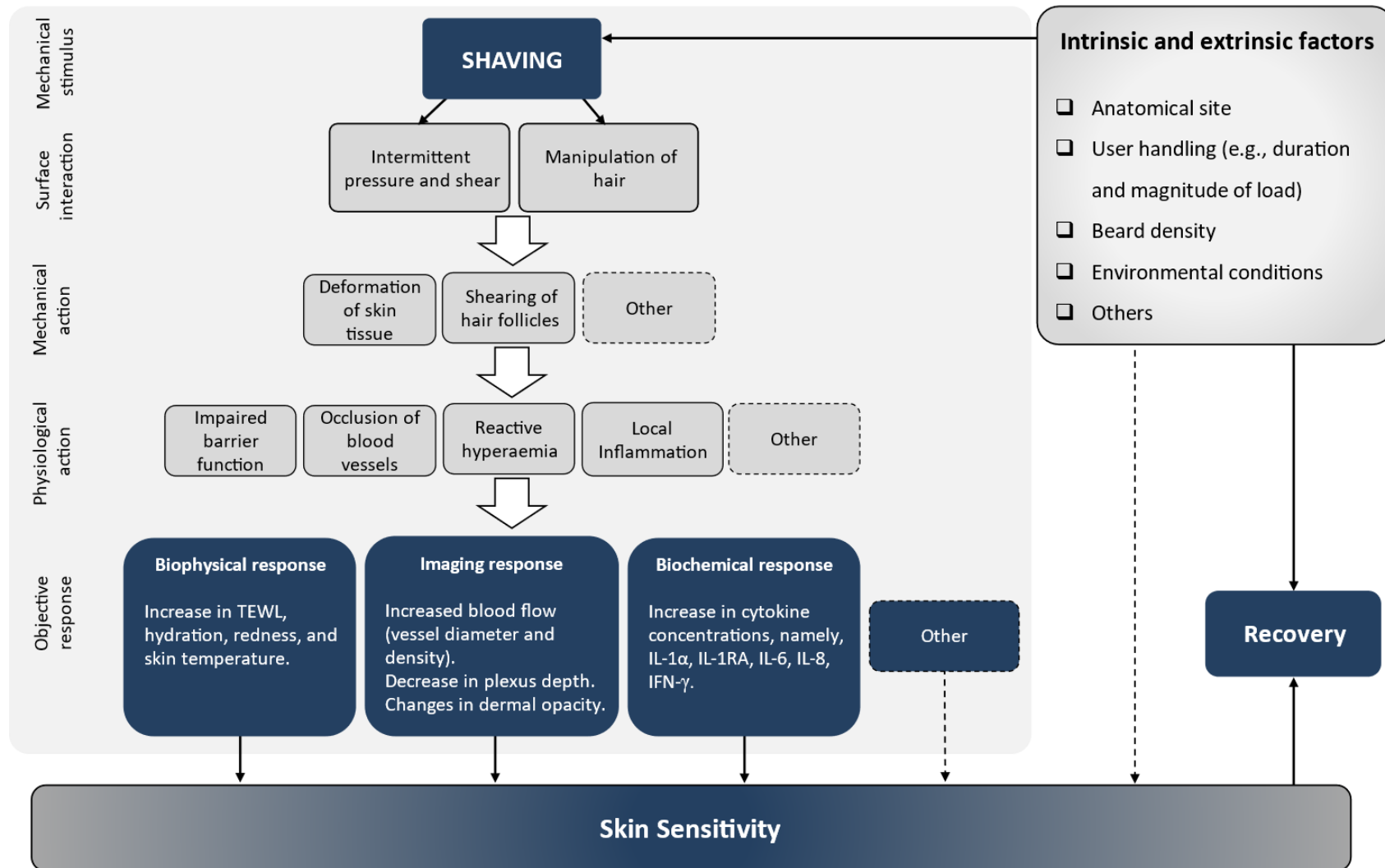


Figure 7.7 Conceptualization of the skin responses to shaving, and the intrinsic and extrinsic factors influencing skin sensitivity.

For device manufacturers hoping to develop skin-friendly products, it is important to also consider the self-reported comfort/discomfort associated with the product use. In the presented study, this parameter was recorded as the VAS where participants reported perceived sensitivity values on a scale from 0 to 10 following shaving. Indeed, intermediate efforts to improve product comfort should be aimed at reducing the VAS. However, objective skin parameters are still required as it is difficult to derive concepts for device improvements from subjective, perception-based data. Furthermore, there is a risk associated with extrapolating global device requirements from such datasets, where the expected improvement would need to be objectively quantified. As such, the authors believe that the approach highlighted in the presented thesis provides a suitable methodology to address the complexity underlying improving consumer comfort in response to interactions with skin contacting devices.

Conclusions

The shaving stimulus was characterised in the present chapter, defining extrinsic factors associated with the mechanical load. Furthermore, intrinsic factors were defined and specified for each participant. Results indicated that participants with higher self-reported mechanical sensitivity demonstrated higher force values while shaving and higher discomfort post shaving. Additionally, an increase in the perception of SS and the force of stimulus application correlated with a decrease in the SC integrity, decrease in optical density of the tissue, and a change in the skin reflectivity. An optimised array of skin responses was identified, including TEWL, SID, Vessel Density, SRR, IL-1 α , and IL-8.

Chapter 8 General Discussion and Future Work

8.1 Meeting the research objectives

This research project provides new insights into the effects of mechanical stimulus on the skin and its relationship with perception of skin sensitivity (SS). It is reported that more than 50% of the population identify as individuals with enhanced SS ([Section 1.3](#)), driving interest from industry and academia to define it objectively, and thus, support innovation in personalised strategies to maintain skin health. Previous research in this area has been limited by the lack of quantifiable skin responses associated with the multifactorial nature of SS, particularly with regards to mechanical stimuli ([Section 1.2](#)) caused by commonly used consumer devices such as shavers. Thus, a review of the state-of-the-art objective methods for characterizing skin tissue was conducted ([Section 2.3](#)), identifying several parameters with potential to provide insights underlying SS. For example, parameters such as TEWL (Loffler et al. 2001; Pinto et al. 2011), SC hydration (Roussaki-Schulze et al. 2005), epidermal thickness (Berardesca et al. 2013), and interleukin protein composition (Raj et al. 2017) are implicated in the perception of enhanced SS. It is hypothesized that studies exploring the relationship between these numerous parameters would help create a holistic model of the skin response. Furthermore, OCT was identified as a potential research tool for dermatological applications ([Section 2.3.9](#)). Consequently, the present thesis evaluated the feasibility of a multi-model approach, combining biophysical, biochemical, and imaging techniques with subjective responses to give a broad understanding regarding the factors associated with SS following mechanical insults.

The specific aims of this PhD project have been listed in [Section 2.5](#) and are repeated below with comments. Study I refers to the protocol executed in [Section 4.2.4](#), while Study II refers to that in [Section 6.2.2](#).

Aim 1: Investigate the use of robust objective parameters from OCT and biophysical approaches to evaluate the status of skin pre- and post-mechanical insult.

Relevant OCT-derived skin parameters were identified ([Section 3.2](#)), namely, epidermal thickness (Qin et al. 2018), scaled intensity drop (Adegun et al. 2013), and RMS surface roughness (Welzel et al. 2003). Algorithms were developed to estimate the values for facial skin in a pilot study. Using a research OCT device (Thorlabs, USA), feasibility of these parameters to characterise the skin tissue

pre-insult was evaluated (Sections 3.3.3 – 3.3.5). However, restrictions in tasks due to the COVID-19 pandemic prevented further experiments and the post-insult parameters remained unexplored. This task was followed up in Study I, where it was revealed that epidermal thickness was not detected in several scans. Subsequently, a new parameter was defined, Area under the Curve (AuC; Section 5.2.1), replacing the epidermal thickness to quantify the superficial skin tissue. Additionally, a commercial OCT system (Vivosight, UK) with dynamic functions was used in Study II, expanding the array of skin parameters to include those derived from cutaneous blood flow (Table 6.2). Thus, a wider array of OCT-skin parameters have been investigated including plexus depth, vessel diameter, vessel density, and skin reflectivity ratio.

With respect to the biophysical parameters, a literature review was conducted critiquing objective methods of characterising skin specifically following mechanical insults (Section 2.3). Furthermore, retrospective analysis was conducted on a dataset collected by another researcher (Richters et al. 2016), where the biophysical parameters, namely TEWL, hydration, and redness were measured at baseline and post tape stripping (Section 2.4). The retrospective analysis included normalising skin responses to the number of tape strips used and evaluating the temporal effect to inform prospective protocols. It was revealed that the skin responded to tape stripping within 30 minutes of interaction, with the corresponding response retained up to 24 hours. Aiming to identify a time-frame suitable for consumer-based studies, a prospective study was designed to investigate the changes in skin parameters at several intervals up to 30 minutes post stimulation. Results revealed that TEWL demonstrated the largest changes from baseline at 20 minutes post stimulus (Figure 4.10 and Figure 4.11). Consequently, it was recommended that for complex mechanical loads such as electric shaving, prospective studies can be designed to measure post stimulus skin responses at an interval of 20 minutes.

Results presented in this thesis revealed that the selected skin parameters varied in their sensitivity to detect temporal changes following mechanical insults (Table 6.4). For example, TEWL, hydration, and redness demonstrated statistically significant temporal differences for the cheek and neck following shaving, while AuC revealed significant trends only on the neck, and Rq did not reveal significant temporal changes.

Aim 2: Study the link between perceived skin sensitivity and the variability of skin response to simple mechanical loading using objective skin parameters.

Tape stripping was identified as a suitable simple mechanical load when investigating SS (Section 2.4.3). Volunteers with varying degrees of perceived SS were recruited based on a modified version

of an existing SS Questionnaire ([Appendix A](#)), and S-scores and SS groups were defined ([Section 4.2.2](#)). Study I was designed to investigate the temporal effect of tape stripping on the facial skin and explore variability between participants from different SS groups ([Chapter 4](#) and [Chapter 5](#)). Results revealed that the High SS group demonstrated largest values for hydration on the cheek ([Figure 4.19](#)). Furthermore, an exploratory analysis was defined, involving ranking participants for each skin parameter and sorting based on the SS groups ([Section 5.3.5](#)). Subsequent results did not reveal any clusters visually between the perceived skin sensitivity and the objective skin parameters. Suggestions for future studies have been included in [Section 8.5](#).

In Study II, a repetitive stimulus model was designed ([Section 6.2.2](#)), involving two sessions of tape stripping and shaving on contralateral forearms. The objective of this part of the protocol was to compare the skin response following the two mechanical stimuli, where it was concluded that tape stripping is not a suitable surrogate for shaving on the forearm ([Section 6.4](#)). As the primary region of interest in the present research is defined as the cheek and neck skin, associations to sensitivity following tape stripping on the forearm were not explored.

Aim 3: Study the influence of perceived skin sensitivity and the variability of skin response to complex mechanical loading using objective skin parameters.

A complex mechanical stimulus was designed using a novel electric shaver, where the interaction of the device with the skin surface is a combination of loading and manipulation of hair (Cowley et al. 2012). The device used in the present study was equipped with load sensors to estimate the applied force ([Figure 4.5](#)). The protocol in Study I included different mounts on the handle such that one session involved rubbing the skin with a frictional surface, whereas the other involved a shaving stimulus for duration of 30 seconds ([Section 4.2.5](#)). For the different SS groups, remarkable results were observed for TEWL and hydration on the cheek, where the High SS group demonstrated low TEWL values and high hydration values following the frictional surface stimulus ([Figure 4.18](#) and [Figure 4.19](#)). This finding is in contrast with other studies where individuals with SS demonstrated higher TEWL and lower hydration values when compared to those without SS (Muizzuddin et al. 1998; Seidenari et al. 1998; Roussaki-Schulze et al. 2005; Farage et al. 2006; Richters et al. 2016). However, as the protocol presented some limitations ([Section 4.4](#)), these results are uncertain.

In Study II, the protocol included a complex mechanical stimulus in the form of shaving for a duration of 60 seconds ([Section 6.2.2](#)). The shaving stimulus was objectively characterised, defining extrinsic parameters contributing to the skin response ([Section 7.2.2](#)). Statistically significant correlations were found between several intrinsic and extrinsic factors ([Section 7.3.2](#)). For example,

for higher self-reports of sensitivity to mechanical stimuli, it was observed that the force applied by the participant during shaving was higher and the discomfort reported post shaving was also higher. Furthermore, analysis of the relationship between the perceived and observed skin responses ([Section 7.3.4](#)) revealed an increase in the perception of SS and the loading force with a decrease in the SC integrity (measured by TEWL), decrease in optical density of the tissue (measured by SID), and a change in the skin reflectivity (measured by SRR). The authors believe this is one of the first studies correlating skin tissue response to mechanical stimulation with intrinsic and extrinsic factors in the context of electric shaving, addressing the gap between subjective and objective parameters in perception of skin sensitivity.

Aim 4: Inform device design for optimal skin-device interaction, addressing personalized solutions.

Case studies were developed as an exemplar report investigating the influence of complex mechanical loading on the skin response for one participant ([Section 7.3.1](#)). Due to the small cohort size (n=10), the results have not been generalised, suggesting opportunities for future studies to continue the investigation ([Section 7.4](#)). Nevertheless, the case studies revealed an increase in the VAS reported by the participant post-stimulus, observed in conjunction with an increase in the skin tissue parameters. Optimal skin-device interaction aiming to ensure consumer comfort should consider minimising the VAS while maintaining the device functionality. Translation of the research findings to industrial applications has been discussed in [Section 8.4](#).

8.2 Research novelty

Sensitive skin (SS) is a topic that is growing in relevance in the consumer industry as well as academia. This is evidenced by the increasing number of studies attempting to quantify and define the skin characteristics typically associated with enhanced SS (Diogo and Papoila 2010; Kim et al. 2013; Misery et al. 2017), identify methods to prevent and mitigate the unpleasant skin responses (Yokota et al. 2003; Chan 2018; Hawkins and Foy 2019), and investigations into associated skin pathologies (Kobayashi and Tagami 2004; Farage and Maibach 2010; Yatagai et al. 2018). Most of the available research focuses on enhanced skin sensitivity in response to chemical triggers (Loffler et al. 2001; Diogo and Papoila 2010; Sun et al. 2016; Jiang et al. 2020). However, mechanical loads on the skin surface are known to compromise skin integrity (Bouten et al. 2003; Gefen 2020; Abiakam et al. 2021), and represent a gap in the literature. This project aimed to evaluate the skin

response to simple and complex mechanical loads in the form of tape stripping and shaving, and simplifications of shaving loads in the form of interaction with a frictional surface. Protocols were designed to characterise the skin status by combining a wide array of established and emerging technologies with cutaneous applications. While typically in literature only a subset of parameters are reported, the present thesis included measurement of biophysical parameters such as TEWL and hydration; structural parameters derived from OCT imaging such as surface roughness and vessel density; and inflammatory biomarkers such as IL-1 α and IL-1RA. The authors believe this study is a first of its kind, specifically in the investigation of skin responses to shaving. The findings from this research have been conceptualised in Figure 7.7 and repeated in [Figure 8.1](#).

Furthermore, the anatomical sites primarily investigated in this thesis included the skin on the cheek and neck for males. The results offer novel data, creating opportunities for future studies examining characteristics of hirsute skin. Indeed, results revealed that the forearm skin differed significantly from the cheek/neck at baseline and in response to shaving. Additionally, there is a paucity of studies reporting values for healthy males, specifically on facial skin sites (Elsner 2012). Thus, this data is considered crucial for the development of skin contacting devices as results from broader studies examining differences in skin parameters with reference to gender, race, and anatomical sites have reported conflicting results (Berardesca et al. 1991; Reed 1995; Wa and Maibach 2010; Kleesz et al. 2011; Firooz et al. 2012; Hadi et al. 2016; Mehta et al. 2018; Voegeli et al. 2019)

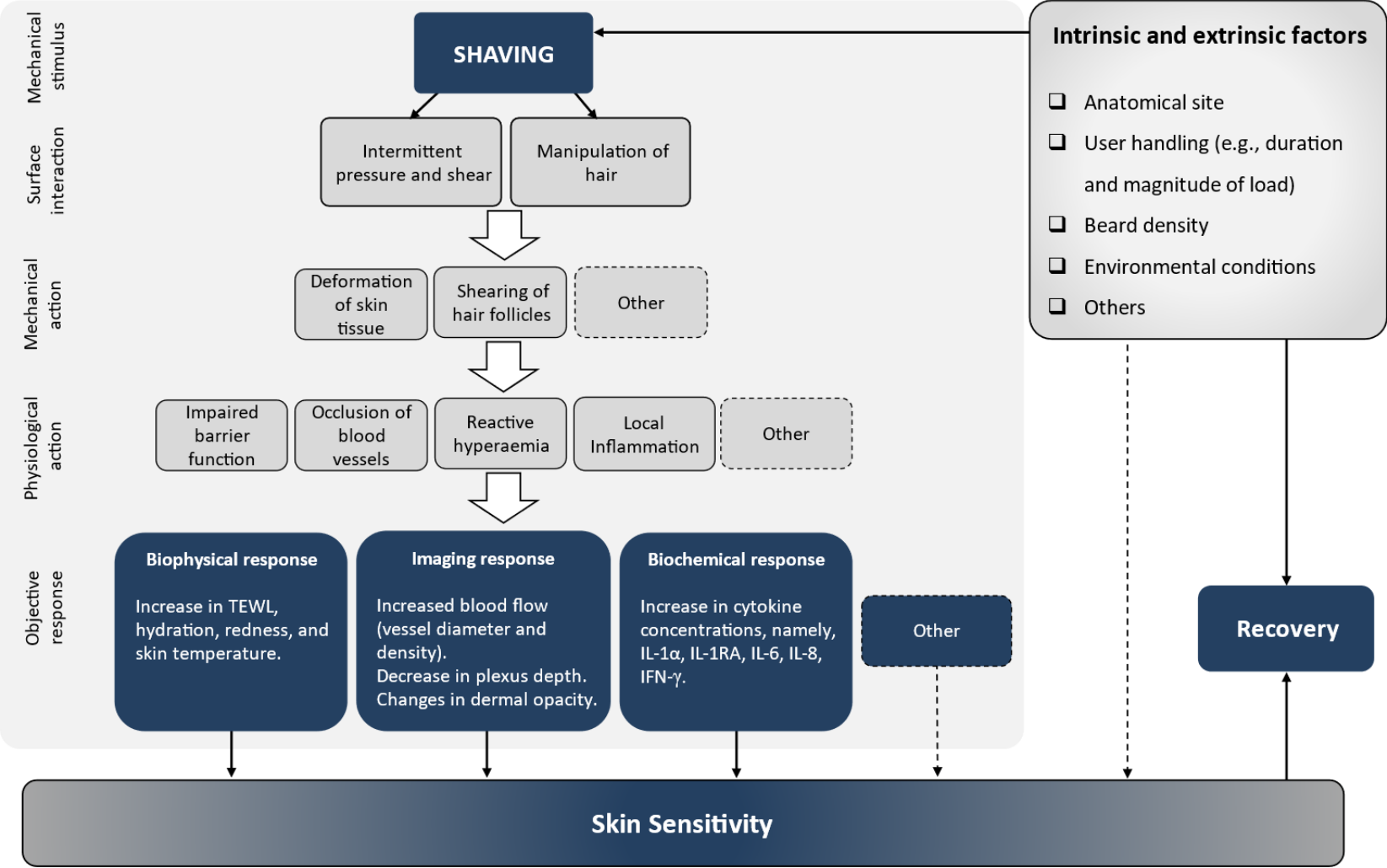


Figure 8.1 Revisiting the illustration of the conceptual relationship between shaving and skin sensitivity.

Thus, this thesis provides novel contributions to expanding the knowledge on sensitive skin and the inter- and intra- subject variability in facial skin responses to mechanical stimuli. In summary, key findings have been listed below:

- An increase in the perception of SS and the loading force correlated significantly with a decrease in the SC integrity, decrease in optical density of the tissue, and a change in the skin reflectivity. This highlights the complex nature of SS, implicating a multifactorial network of pathways.
- Participants with higher self-reported mechanical sensitivity demonstrated higher force values while shaving and higher discomfort post shaving. This suggests that comfort can be increased by pressing less hard while shaving.
- Significant differences between the basal skin on the cheek and neck were found. For example, the neck demonstrated higher TEWL, temperature, roughness, and IL-1 α concentrations, while the SID, AuC, and SRR was larger on the cheek.
- At baseline, the High SS group revealed lower TEWL values and higher hydration values when compared to the Low and Mild SS groups. These findings contradict previous studies and requires further investigation.
- Irrespective of SS, a harsh shaving stimulus resulted in statistically significant changes in the facial skin response followed by selective recovery characteristics.
- Inflammatory biomarkers such as IL-1 α and IL-1RA revealed >2-fold increases in the concentrations in response to shaving, with values approaching baseline after recovery. Strikingly, IL-8 demonstrated further increases in concentration after the recovery period as well. This is believed to be the first time an optimised tape based sebum biomarker analysis of shaving insults has been conducted to also analyse high and low abundance markers.
- Statistically significant associations between the array of skin parameters were found. For example, visible redness of the skin surface revealed correlations the other biophysical parameters (i.e., TEWL and hydration) and with the structural parameters (namely, blood vessel density and diameter). Indeed, TEWL and vessel density were correlated with majority of the other objective parameters. Additionally, most biochemical markers demonstrated significant correlations amongst themselves.
- Interestingly, epidermal thickness was not detectable with OCT in a majority of the facial scans. It is hypothesized that a distinct skin layers were not identified due to the digital smoothing of the wavy DEJ.
- At baseline and in response to shaving, the forearm was found to be an unsuitable proxy for the cheek/neck when investigating skin parameters.

- Damage mechanisms of tape stripping, frictional surface interaction, and electric shaving were studied. Tape stripping was revealed as an unsuitable surrogate of shaving, at least not with the device used.
- Suitable techniques were identified to characterise skin following mechanical loading, focusing on studies investigating SS. This led to the incorporation of OCT in skin status quantification, as suggested in the publication *Chaturvedi et al., (2021). Skin Res. & Techn. Quantifying skin sensitivity caused by mechanical insults: a review. Skin Research and Technology.*
- Following a novel test protocol to characterise skin response to mechanical insults, an optimised subset of parameters were identified that enabled skin characterisation with a limited set of variables.
- Algorithms were developed to estimate skin parameters derived from OCT images. These were optimized for the hirsute skin surfaces.
- Characteristics of bearded skin on the cheek and neck were established for healthy males.
- Guidelines for future protocols including a shaving load were developed. For instance, as skin tissue demonstrated largest changes from baseline at 20 minutes post stimulus, it is suggested to focus/design studies on that time point.

8.3 General limitations

One of the main limitations in this project included the restrictions of research activities due to COVID-19. In Study I, the institutional guidelines required a distance of 1.5 m between individuals. Consequently, the tape stripping stimulus was performed by the participants themselves, rather than the trained researcher. It is argued that an inappropriate technique may have been used due to the inevitable tendency to minimise pain ([Section 4.4](#)). Furthermore, measurement of the skin parameters was also performed by the participants, where it is likely that the handling of the instruments did not conform to the required standards. These factors are believed to have influenced the results, as comparison to literature suggested diminished skin responses were observed in [Chapter 4](#) and [Chapter 5](#).

In Study II, the results were limited due to a small cohort size. Participants were selected based on availability rather than responses to the SS Questionnaire. In addition, the protocol was executed as part of a secondment and the researcher had limited time at the institute, further complicating the scheduling efforts. The resulting cohort included 10 participants only. This limited the usability of certain statistical tests and generalizability of the findings. Additionally, this study aimed to investigate the influence of repetitive loading on the skin response. However, as the pilot test revealed a painful dermatitis response after the initial stimulus, the protocol was modified to

examine the skin on the contralateral side. Ideally, the skin characteristics would be measured from the same site for each individual under different test conditions to avoid potential influences of differing extrinsic factors.

Another considerable limitation in the present research was the lack of sufficient biochemical analysis. In Study I, the protocol did not include biofluid sampling due to inaccessibility to the required equipment and lack of facilities for analysis of the samples. In Study II, collaboration with another researcher allowed this analysis. However, the number of samples had to be reduced to accommodate the capacity of the ELISA plates. As this thesis propagates the use of a wide array of skin parameters for a comprehensive understanding of SS, the relationship of biochemical responses with respect to the biophysical and imaging parameters was not explored for all the test conditions.

8.4 Translation of research to industry

This project is motivated by the demands for personalised solutions and interventions to promote skin health in the consumer products industry ([Section 1.2](#)). For device manufacturers, the development criterion includes the usability of the product and the user experience. The usability of a product can be defined in terms of the efficiency and effectiveness in achieving the intended function, and is often objectively measured. For instance, a metric for a shaver is how *close* the device cuts the beard hair with respect to skin level. In contrast, the user experience is more subjective in nature, defined by the satisfaction of the consumer with the performance of the product. In the example of closeness of the shaver, a certain closeness may not be regarded as *close enough*. Consequently, mixed method studies recording qualitative and quantitative data regarding the products are considered important by the manufacturers. There is an opportunity to bridge the gap between academia and industry by introducing consumer products into academic experimental protocols to investigate the skin responses specific to those interventions. As such, the data presented in this thesis serves as an asset that device manufacturers developing skin contacting products can use to understand the skin responses to complex mechanical stimuli.

More specifically with respect to electrical shaving, results from the presented studies revealed significant spatial differences in the skin tissue. Indeed, as consumers often complain of more sensitivity on the neck than on the cheek (internal surveys), these findings can be further investigated towards developing site-specific skin-friendly devices. It is recommended to build solutions addressing localised heightened skin responses in individuals rather than considering

them as SS/non-SS individuals. Minimizing discomfort in response to shaving would thus be aimed at reducing the VAS post stimulus, improving the user experience related to the product.

As SS is largely driven by the perception of comfort rather than the objectively measurable stimulus-response relationship, monitoring the user experience remains an invaluable metric in the development of consumer products. The studies presented in thesis revealed associations between loading force, participant comfort, and skin tissue responses. Such findings address the difficulty in quantifying the skin-device interaction in a research environment and provides a direction for selection of suitable objective tools. The protocols executed in this research enabled the identification of core outcome sets such that an exclusively selected cohort may outweigh the need for larger, exploratory studies.

8.5 Future Work

An objective definition of Sensitive Skin remains to be established. Future studies researching the effects of mechanical stimuli on skin can expand the methodology presented in thesis with a clinically suitable number of participants to develop a quantifiable relationship between the various skin responses and factors influencing the trends. Due to the small cohort size, these results have been included only to provide an example of the analysis which may be considered in future studies.

For example, in Study II (n=10), a regression model identified the following relationship between perceived SS and observed skin parameters for the Short Beard session (Equation 8.1):

$$\begin{aligned} S \text{ Score} = & 0.433 + 0.1200 F_{rms} + 0.0044 VAS_{0.3} - 0.0319 TEWL \\ & - 1.522 SID + 0.1011 Vessel \text{ density} + 0.786 SRR \\ & + 0.0324 IL_{1\alpha} + 0.000120 IL_8 \end{aligned} \quad (\text{Equation 8.1})$$

where the skin tissue responses were normalised to baseline before modelling.

However, the R^2 value was estimated as 63.8%, revealing the percentage of variation in responses explained by the mathematical model. Interestingly, F_{rms} provided the largest influence in estimating the S-Score ($p = 0.007$; [Figure 8.2](#)), corroborating the findings presented in this thesis that identify loading force to be a critical factor in the perceived and observed changes associated with SS. In addition, SID also achieved statistical significance in estimating the S-Score ($p=0.032$), highlighting OCT as a promising tool in investigating SS. Furthermore, it is noted that two of the OCT-derived parameters (namely, SID and vessel density) and a high abundance biomarker (namely, IL-1 α) influenced the S-score to a greater extent than TEWL, which is popularly regarded as a key parameter underlying SS (Farage and Maibach 2010). Although some of the associations do not

achieve statistical significance in the present example, there may be opportunities for future studies to explore similar trends and subsequently improve the interventions affecting clinical outcomes.

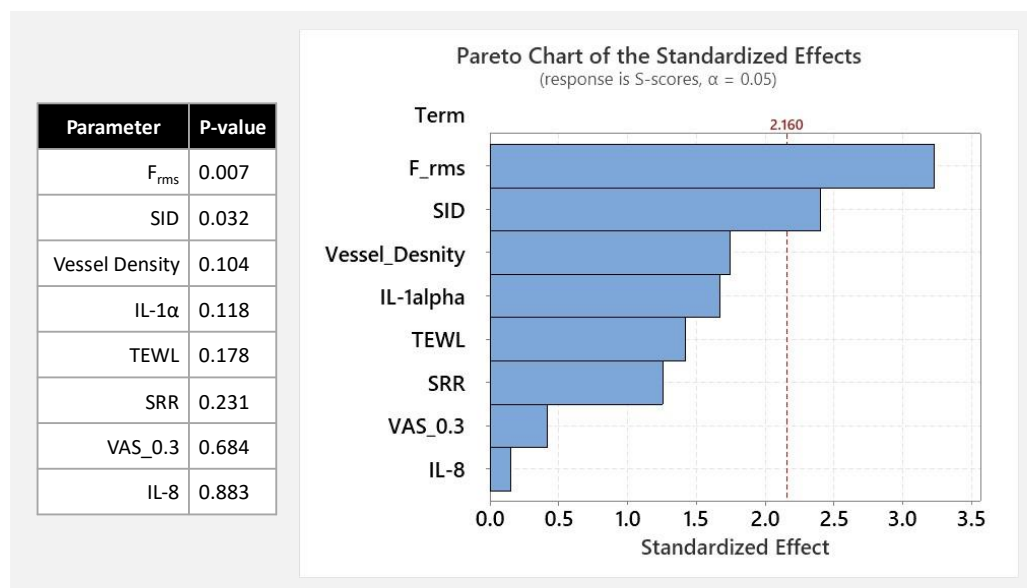


Figure 8.2 P-values and pareto chart of an exemplar regression model.

The combination of multimodal imaging techniques such as OCT, biophysical measures of SC function, and biomarkers of skin status provides a comprehensive overview of parameters critical in advancing our understanding of the skin. However, due to the highly subjective nature of SS, future studies should consider implementing psychosomatic models to explore the interplay between the observed and perceived factors. Indeed, some researchers claim SS is a psychological disorder (Misery 2017; Farage 2022) and have developed questionnaires to record self-reports of SS (Loffler et al. 2001; Misery et al. 2014; Richters et al. 2017). Furthermore, the role of biopsychosocial factors have also been investigated in chronic itch (Verhoeven et al. 2008), atopic dermatitis and psoriasis (Magin et al. 2008; Evers et al. 2005), and acne (Kenyon 1966), revealing greater levels of neuroticism in the patients. As such, further research is needed to better understand the complex interactions between psychological and physiological factors in SS, and to develop tools and interventions that can effectively address both aspects of the condition.

The feasibility of application of bioengineering tools in consumer settings should also be investigated. If key techniques are identified for suitably distinguishing SS responses, future steps would include advancing to in-store assessment of skin profiles. With improved understanding, personalised solutions could be adopted in the development of devices to accommodate the needs of varying skin types. Research in this direction could enable mitigation of adverse skin responses by identifying events where the skin is at risk of loss of integrity. The clinical impact of such interventions would support efforts to improve patients' quality of life.

Appendix A Skin Sensitivity Questionnaire

(Dutch version below)

Characteristics of enhanced skin sensitivity

1. How sensitive is your skin to the sun? Which skin type best describes you?
Skin colour refers to skin that has not been exposed to the sun.
 - Skin type I: I always burn and never tan (Characteristics: fair skin, often freckles, often red to light brown hair, often blue or green eyes)
 - Skin type II: I usually burn and sometimes tan (Characteristics: fair skin, often blond hair, often blue or green eyes)
 - Skin type III: I sometimes burn and usually tan (Characteristics: white to light brown skin, often dark blond or brown hair, often brown eyes)
 - Skin type IV: I seldom burn and tan easily (Characteristics: light brown skin, often brown hair and brown eyes)
 - Skin type V: I have naturally brown skin and tan easily (Characteristics: brown skin, often brown or black hair, often brown eyes)
 - Skin type VI: I have naturally black skin (Characteristics: dark brown or black skin, often black hair and often brown eyes)

2. How frequently does your skin breakout?
 - Often (e.g., because of presence of acne)
 - Sometimes (e.g., occasional red spots or bumps)
 - Never

3. What is your facial skin like in the morning (before washing)?
 - Tight
 - Comfortable
 - Oily

4. Do you think you have sensitive skin (e.g. in comparison to others)?
 - Yes
 - Sometimes
 - No

5. Does your skin react during or after shaving or contact with fabrics like clothes or towels?
 - 1 – never
 - 2
 - 3 –
 - 4
 - 5 – always

Kenmerken van verhoogde huidgevoeligheid

1. Hoe gevoelig is uw huid voor zonlicht?
Hieronder staan een aantal huidtypen genoemd. Kies het huidtype die het best bij u past.
Met de kleur van de huid wordt huid bedoeld die niet aan de zon is blootgesteld.
 - Huidtype I: Ik verbrand altijd en word niet bruin.
Kenmerken: zeer lichte huid, vaak sproeten, vaak rossig of lichtblond haar, vaak blauwe of groene ogen.
 - Huidtype II: Ik verbrand meestal en word soms bruin.
Kenmerken: lichte huid, vaak blond haar, vaak blauwe of groene ogen.
 - Huidtype III: Ik verbrand soms en word meestal bruin.
Kenmerken: lichte tot lichtbruine huid, vaak donkerblond of bruin haar, vaak bruine ogen.
 - Huidtype IV: Ik verbrand zeer zelden en word gemakkelijk bruin.
Kenmerken: lichtbruine huid, vaak bruin haar en bruine ogen.
 - Huidtype V: Ik heb een natuurlijk bruine huid en bruin gemakkelijk en snel.
Kenmerken: bruine huid, vaak bruin of zwart haar, vaak bruine ogen.
 - Huidtype VI: Ik heb een natuurlijk zwarte huid.
Kenmerken: zeer donker bruine of zwarte huid, vaak zwart haar en vaak bruine ogen.
2. Heeft u wel eens last van onregelmatige huid?
 - Vaak (bijv. door Acne)
 - Soms (Bijv wel eens last van rode plekjes/bultjes)
 - Nooit
3. Welk huidtype heeft u normaal gesproken in uw gezicht, wat betreft droogheid?
 - Droog (bijv. de huid kan schilferen en/of strak aanvoelen)
 - Normaal (voelt comfortabel)
 - Vettig (bijv. de huid kan glimmen)
4. Vindt u dat u een gevoelige huid heeft (bijv. in vergelijking met andere mensen)?
 - Ja
 - Een beetje
 - Nee
5. Reageert uw huid na/tijdens het scheren of contact met weefsels zoals kleding, handdoeken?
1 – 5 scale

Appendix B Study-II Participant Information Sheet

Study Title: Assessing the structural and functional response of skin to representative mechanical loads.

Researcher: Pakhi Chaturvedi

ERGO number: 71825

You are being invited to take part in the above research study. To help you decide whether you would like to take part or not, it is important that you understand why the research is being done and what it will involve. Please read the information below carefully and ask questions if anything is not clear or you would like more information before you decide to take part in this research. You may like to discuss it with others but it is up to you to decide whether or not to take part. If you are happy to participate you will be asked to sign a consent form.

What is the research about?

Skin sensitivity (SS) is a commonly occurring response to a range of stimuli, including environmental conditions, chemical irritants, and mechanical forces, e.g., shaving. More than 50% of the population are reported to present with varying degrees of sensitive skin, with an increasing number of individuals attending dermatology clinics with specific skin sensitivities. Furthermore, consumer products such as electrical shavers interact with the skin while exerting a combination of dynamic loading in the form of pressure and shear. Differences in individual tolerance to these devices has led to a demand for personalised products. The aim of this study is to use measurement tools to assess parameters of skin health before and after the application of a commercial shaver which incorporates a special sensor which depicts how hard you are pushing.

This work is carried out as part of the project “Skin Tissue Integrity under Shear” (STINTS) that is funded from the European Union’s Horizon 2020 research and innovation programme under the Marie Skłodowska-Curie Actions (MSCA) grant agreement no. 811965.

Why have I been asked to participate?

We are recruiting participants from the local university population. The sample we are looking for are males aged between 18 - 65 year. We are afraid if you have Eczema, Psoriasis, any facial trauma or malignancy you will be unable to take part, as the research process may cause further irritation to your skin. We also need to feel confident that you can give informed consent to take part in this study. We hope to use the data as part of preliminary research, as there is little information on objective markers of enhanced skin sensitivity.

What will happen to me if I take part?

This experiment will take place over three sessions of two hours for each participant based on the time interval from the last clean shave, i.e., 24 hours post shaving, 48 hours post shaving, 72 hours post shaving.

Each session will involve shaving on a patch of skin on your forearm, cheek, and neck using an electric shaver. The electric shaver may feel a little uncomfortable during the testing procedure. However, if this causes too much discomfort the testing will be stopped immediately.

On arrival to the lab, participants will be offered the chance to ask any questions. They will be asked to wear comfortable clothing including a short-sleeved tee-shirt. Their height and weight will be taken once consented. To allow the skin to acclimatize to the room temperature, the participant will be requested to wait for 20 minutes before the measurements can be initiated. During this time, the participant will be requested to complete a “Skin Sensitivity Questionnaire”. Furthermore, a square will be drawn on the left and right forearms (volar side), and only on one side of the face for the cheek and neck. This is done to standardize the location of the skin sample across multiple visits. A non-permanent eye-liner pencil will be used, and marks will be removed on completion of the testing. Then, a photograph will be taken of the skin sample highlighted. There will be no personal identifying features will be included in the image.

Before shaving, we will establish your baseline skin health using a range of tools. These include Optical Coherence Tomography imaging (OCT; for characterising skin layer thickness, pore count, and redness), Sebutapes (for collecting and analysing the biomarkers in the sebum), Tewameter (for characterizing TEWL and temperature), and Corneometer (for characterising surface hydration). These series of test procedures have been detailed below:

1. OCT Imaging –

- a. Participants will be seated with their forearm/cheek/neck in front of the OCT imaging probe such that the top layers of the skin are focused within the corresponding software (Figure 1a).
- b. The researcher will record 2D/3D OCT scans using the software. The scan will take approximately one minute (Figure 1b).

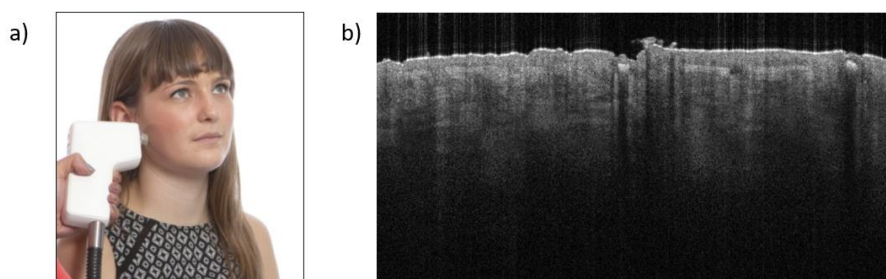


Figure 1 OCT measurement. a) Example of probe placement on the cheek from Vivosight catalogue, b) The outcome of the measurement as presented by the manufacturer’s software.

2. Sebutape sampling –

- a. The researcher will apply commercially available Sebutapes on the participant’s skin at a predefined site using gloved hands to avoid cross contamination of skin proteins.
- b. The adhesive side of the tape will be placed directly on the skin surface for 2 minutes.
- c. After the 2 minutes collection interval, the researcher will remove the tapes from the skin site using tweezers. Taking care not to crumple or fold the samples, each tape will be placed flat into individually labelled glass vials and immediately transferred to an Ultra-Low Temperature Freezer. The tape samples will be stored in the freezer until analysis of biomarkers can be performed.



Figure 2 Example of placement of Sebutape on a participant's forearm

3. TEWL measurement –

- a. The researcher will gently press the Tewameter probe (Figure 3a) on the skin area to be measured. The button on the side of the probe will be pressed to start the recording. The computer will show a signal and stores it while it plays a tone every second to indicate the signal was recorded.
- b. TEWL and temperature will be continuously recorded for a period of 1 minute.
- c. After 60 seconds, the researcher will press the button again to end the measurement.
- d. This will be repeated 2 times.

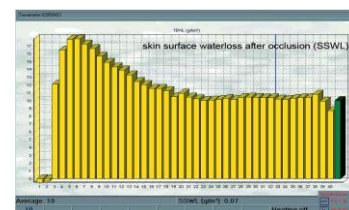
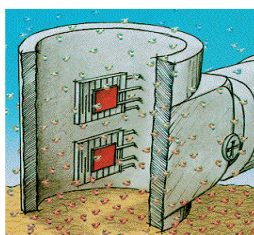


Figure 3 TEWL measurement. a) Open-chamber method, b) Temperature and humidity sensors inside the probe and c) The outcome of the measurement as presented by the manufacturer's software.

4. Hydration measurement –

- a. The researcher will gently press the Corneometer probe on the skin area to be measured (Figure 4a). The computer shows a signal and stores it while it plays a tone to indicate the signal was recorded.
- b. This will be repeated 5 times.

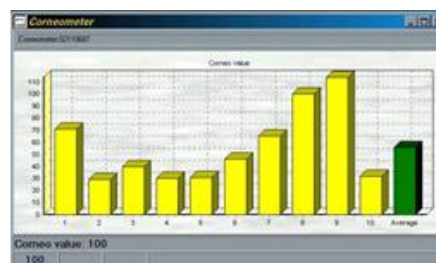


Figure 4 Hydration measurement. a) The Corneometer probe and b) the outcome of the measurement as presented by the manufacturer's software

Following this, the mechanical stimulus will be applied. For the left forearm, cheek, and neck, you will be asked to shave at the specified skin site on the using the electric shaver for 60 seconds. For the right forearm, the researcher will conduct tape stripping at the specified site. We will then ask you to rate the level of skin sensitivity you feel on a scale from 1 to 10. After 20 minutes, the measurements methods from before shaving will be repeated to record the post-stimulus skin parameters.

Are there any benefits in my taking part?

A £25 John Lewis voucher will be available on completion of the research project.

Additionally, your participation will contribute to establishing individual thresholds of tolerance to external mechanical stimuli. This will benefit the development skin friendly consumer products.

Are there any risks involved?

To minimise risks associated with cross contamination of biological substances, the shaving unit will be cleaned as per manufacturer guidelines. Furthermore, to minimise risks associated with COVID-19, the shaver will be disinfected as well.

Additionally, all researchers and participants will be provided personal protective equipment (face masks, hand washing/gloves, and aprons). Facilities to wash hands and to maximise social distancing will also be available. All research will be conducted under the Clinical Academic Facility Method Statement for keeping researchers and participants safe during COVID-19.

What data will be collected?

Personal data including your name and signature (consent forms) will be kept in a locked cabinet in the lead researchers office (card access only). This will only be accessible to the lead researcher. Thereafter, you will be given an anonymised reference number, which will be linked to all subsequent data we collect from you during this study.

During the study we will collect data regarding your age, gender, height, and weight. In addition, we will collect data regarding your shaving habits (that is, frequency of shaving facial hair and type of tool used). We will also collect data to characterise the skin parameters at the forearm, cheek, and neck, at baseline and after shaving. Furthermore, we will place a small tape on your skin to collect sebum, which is a natural oil released from the skin surface. We will use this sebum to analyse whether your skin has reacted to the external mechanical stimuli.

To monitor the growth of hair between the sessions, we will capture close-up photographs of the skin surface. There will be no personal identification factors included in this photograph. This will be an optional element to the consent form, i.e., you may opt out of photos being taken.

Physical study forms will be kept in a study file, stored in the Clinical Academic Laboratories (AA80) in a locked cabinet. Electronic files will be stored on a password protected laboratory computer. Anonymised files from the data collection will be shared between researchers (only those named in the above application) using an encrypted data stick.

Will my participation be confidential?

Your participation and the information we collect about you during the course of the research will be kept strictly confidential.

Only members of the research team and responsible members of the University of Southampton may be given access to data about you for monitoring purposes and/or to carry out an audit of the study to ensure that the research is complying with applicable regulations. Individuals from regulatory authorities (people who check that we are carrying out the study correctly) may

require access to your data. All of these people have a duty to keep your information, as a research participant, strictly confidential.

In accordance with data protection policy of the University of Southampton and the Data Protection Act 2018, your data will be kept anonymously (coded), and stored in a filing cabinet in the locked office of Dr Peter Worsley. Anonymous data will also be stored on computers and coded with an unidentifiable identification number in the laboratory, which is also locked. Only the investigators will have access to the data. Data will be stored securely for 10 years.

Do I have to take part?

No, it is entirely up to you to decide whether or not to take part. If you decide you want to take part, you will need to sign a consent form to show you have agreed to take part.

What happens if I change my mind?

You have the right to change your mind and withdraw at any time without giving a reason and without your participant rights being affected. If you withdraw from the study, we will keep the information about you that we have already obtained for the purposes of achieving the objectives of the study only.

What will happen to the results of the research?

Your personal details will remain strictly confidential. The data will be stored on an electronic database as per EU open access agreement. Research findings made available in any reports or publications will not include information that can directly identify you without your specific consent. After we have finished the study, we will write the findings up for publication in scientific journals and conference abstracts. These will present anonymised data from the study, where no personal information will be disclosed.

Where can I get more information?

If you would like further information before deciding if you would like to take part in our study, please contact the lead research, Dr Peter Worsley using the following email:
p.r.worsley@soton.ac.uk
p.chaturvedi@soton.ac.uk

What happens if there is a problem?

If you have a concern about any aspect of this study, you should speak to the researchers who will do their best to answer your questions.

If you remain unhappy or have a complaint about any aspect of this study, please contact the University of Southampton Research Integrity and Governance Manager (023 8059 5058, rgoinfo@soton.ac.uk).

For enquiries to the research team please contact

Dr Peter Worsley

Tel: 02381 208287

Email: P.R.Worsley@soton.ac.uk

Data Protection Privacy Notice

The University of Southampton conducts research to the highest standards of research integrity. As a publicly-funded organisation, the University has to ensure that it is in the public interest

when we use personally-identifiable information about people who have agreed to take part in research. This means that when you agree to take part in a research study, we will use information about you in the ways needed, and for the purposes specified, to conduct and complete the research project. Under data protection law, 'Personal data' means any information that relates to and is capable of identifying a living individual. The University's data protection policy governing the use of personal data by the University can be found on its website (<https://www.southampton.ac.uk/legalservices/what-we-do/data-protection-and-foi.page>).

This Participant Information Sheet tells you what data will be collected for this project and whether this includes any personal data. Please ask the research team if you have any questions or are unclear what data is being collected about you.

Our privacy notice for research participants provides more information on how the University of Southampton collects and uses your personal data when you take part in one of our research projects and can be found at <http://www.southampton.ac.uk/assets/sharepoint/intranet/Is/Public/Research%20and%20Integrity%20Privacy%20Notice/Privacy%20Notice%20for%20Research%20Participants.pdf>

Any personal data we collect in this study will be used only for the purposes of carrying out our research and will be handled according to the University's policies in line with data protection law. If any personal data is used from which you can be identified directly, it will not be disclosed to anyone else without your consent unless the University of Southampton is required by law to disclose it.

Data protection law requires us to have a valid legal reason ('lawful basis') to process and use your Personal data. The lawful basis for processing personal information in this research study is for the performance of a task carried out in the public interest. Personal data collected for research will not be used for any other purpose.

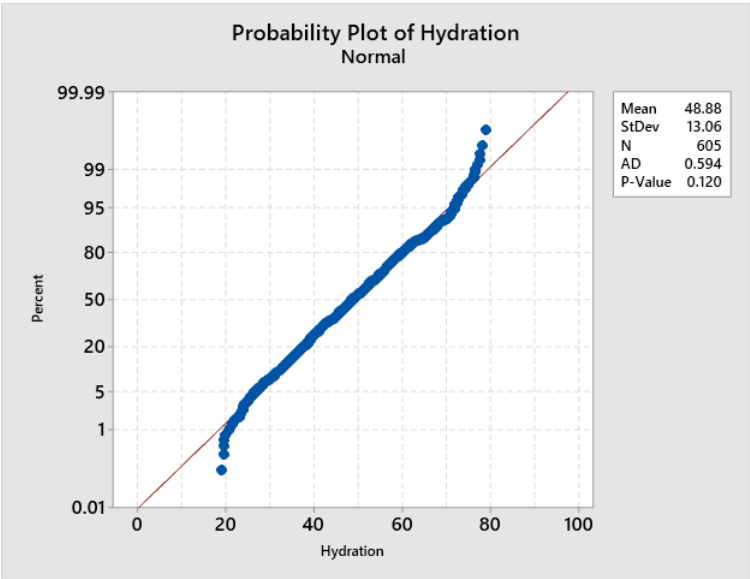
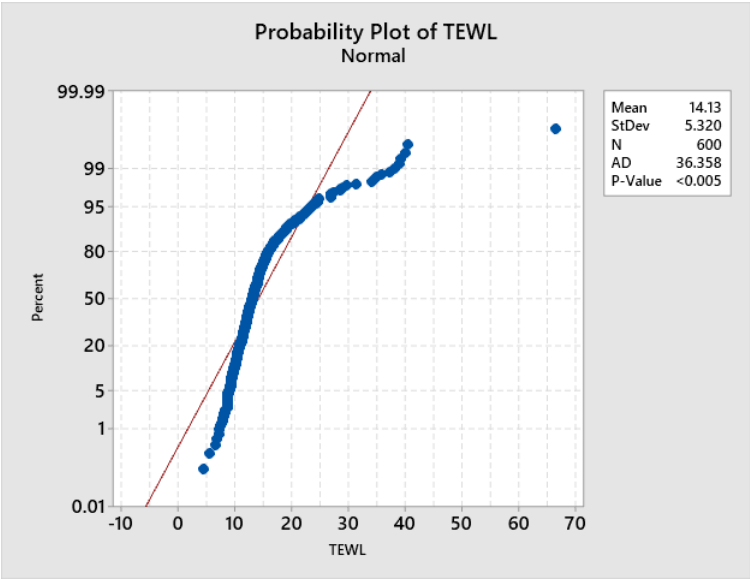
For the purposes of data protection law, the University of Southampton is the 'Data Controller' for this study, which means that we are responsible for looking after your information and using it properly. The University of Southampton will keep identifiable information about you for 10 years after the study has finished after which time any link between you and your information will be removed.

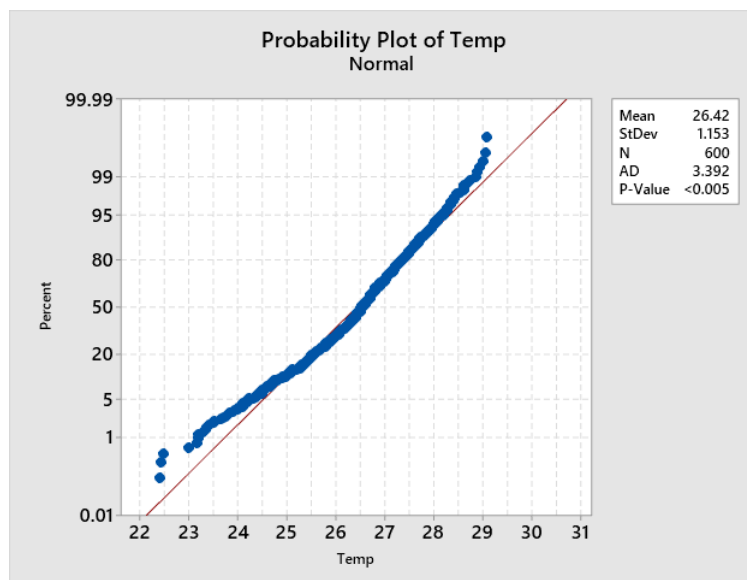
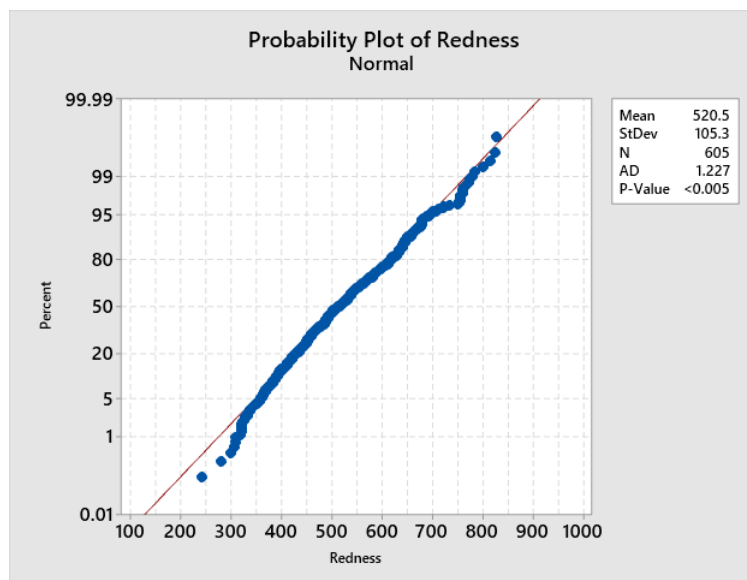
To safeguard your rights, we will use the minimum personal data necessary to achieve our research study objectives. Your data protection rights – such as to access, change, or transfer such information - may be limited, however, in order for the research output to be reliable and accurate. The University will not do anything with your personal data that you would not reasonably expect.

If you have any questions about how your personal data is used, or wish to exercise any of your rights, please consult the University's data protection webpage (<https://www.southampton.ac.uk/legalservices/what-we-do/data-protection-and-foi.page>) where you can make a request using our online form. If you need further assistance, please contact the University's Data Protection Officer (data.protection@soton.ac.uk).

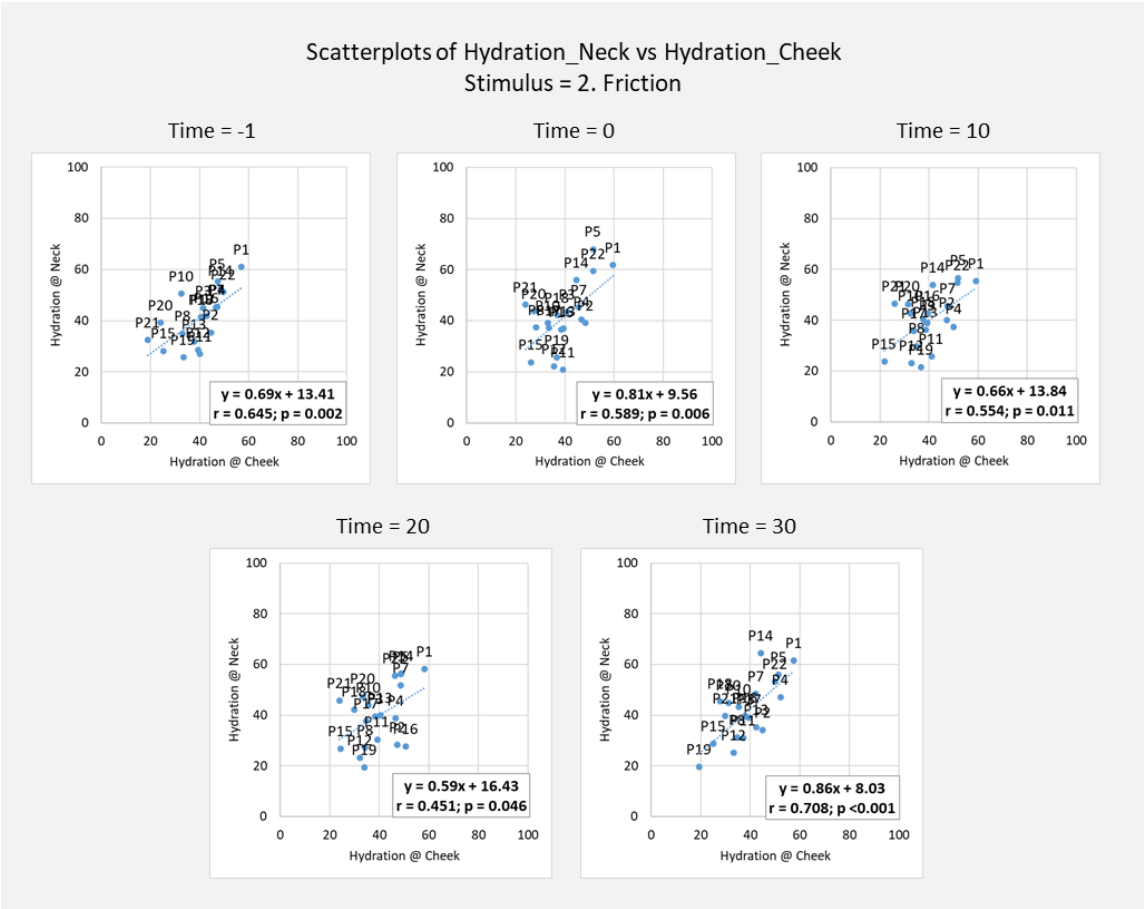
Appendix C Additional figures from Chapter 4

Normality test

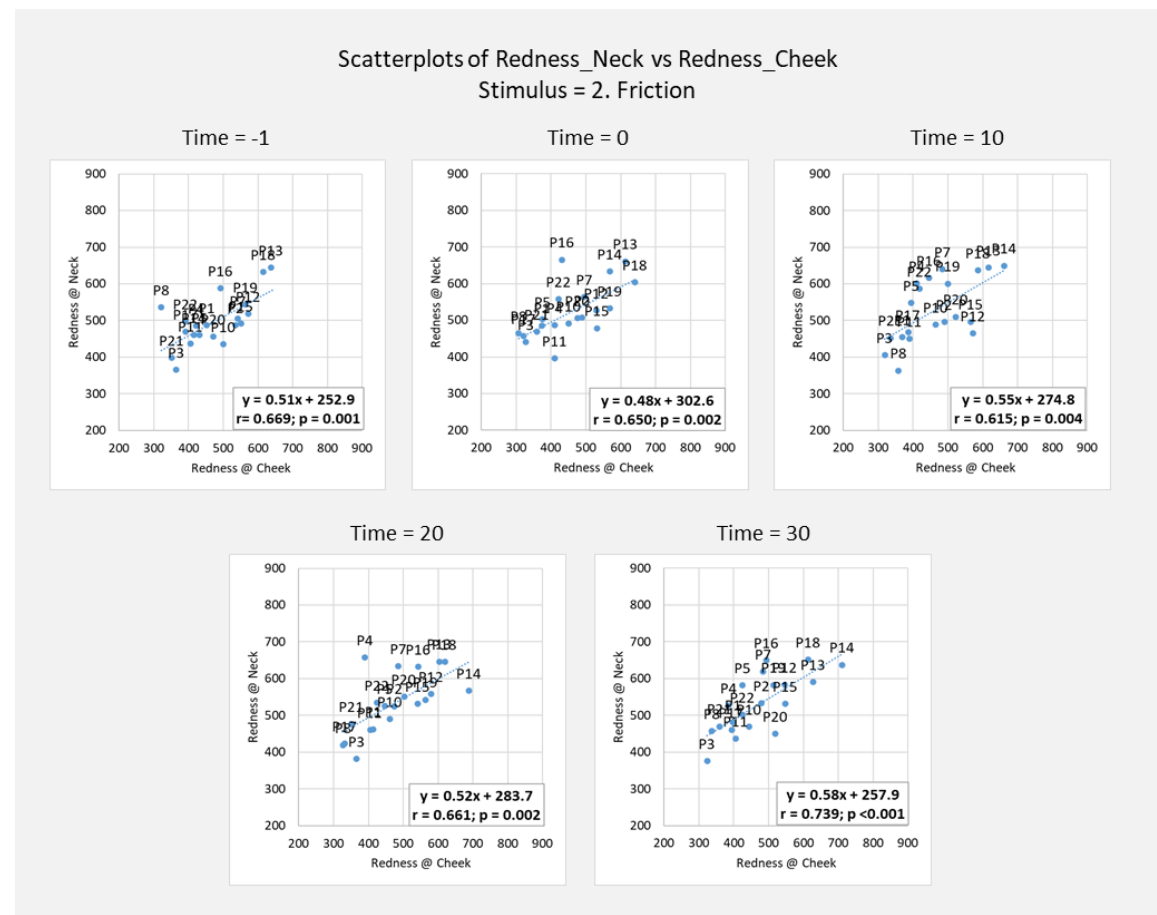




Cheek vs Neck Scatterplots

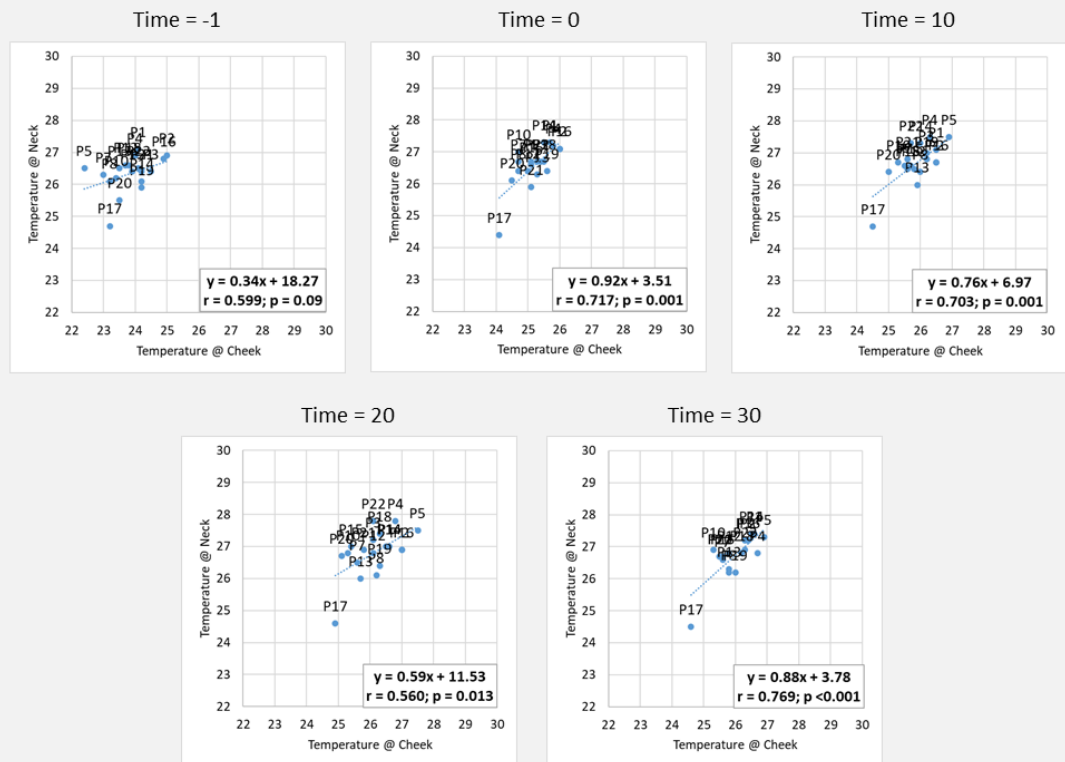


Relationship between the skin hydration on the cheek and the neck for session 2

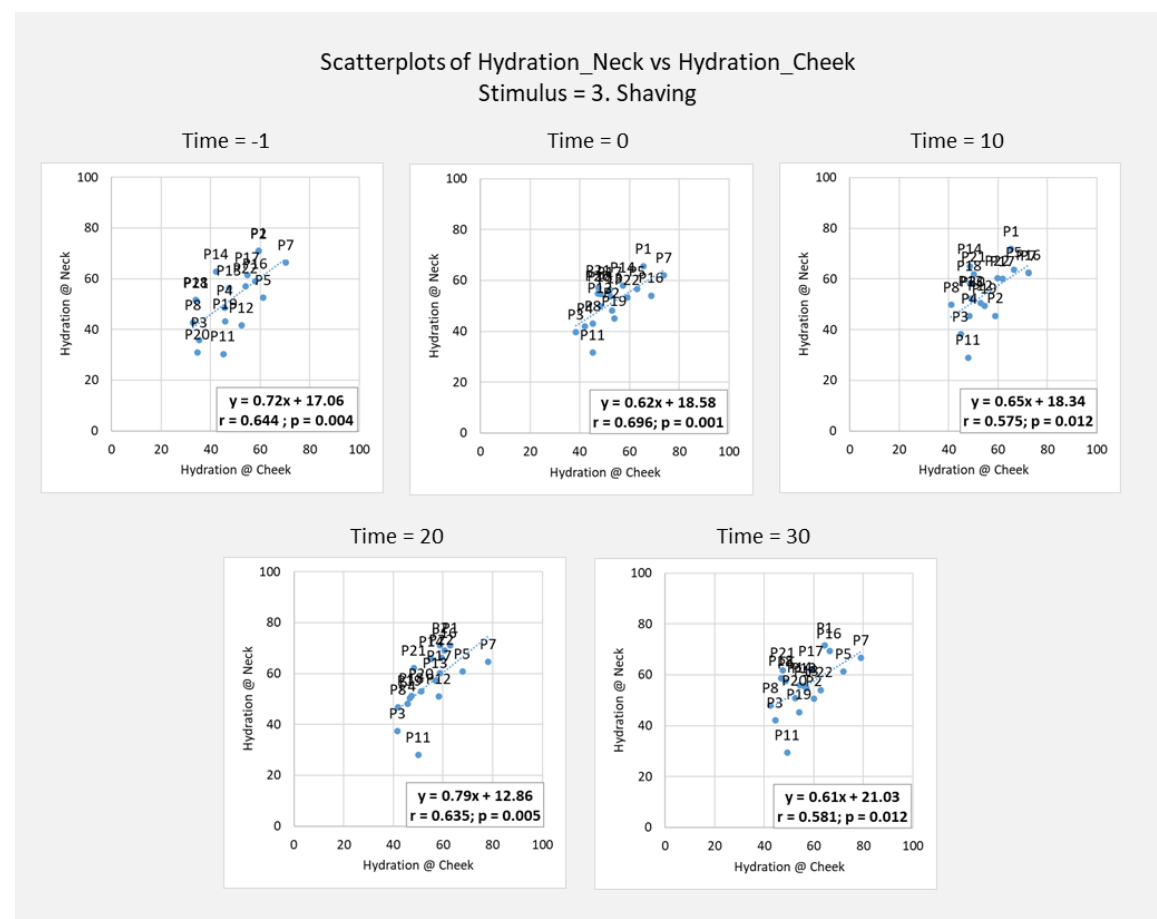


Relationship between the redness on the cheek and the neck for session 2

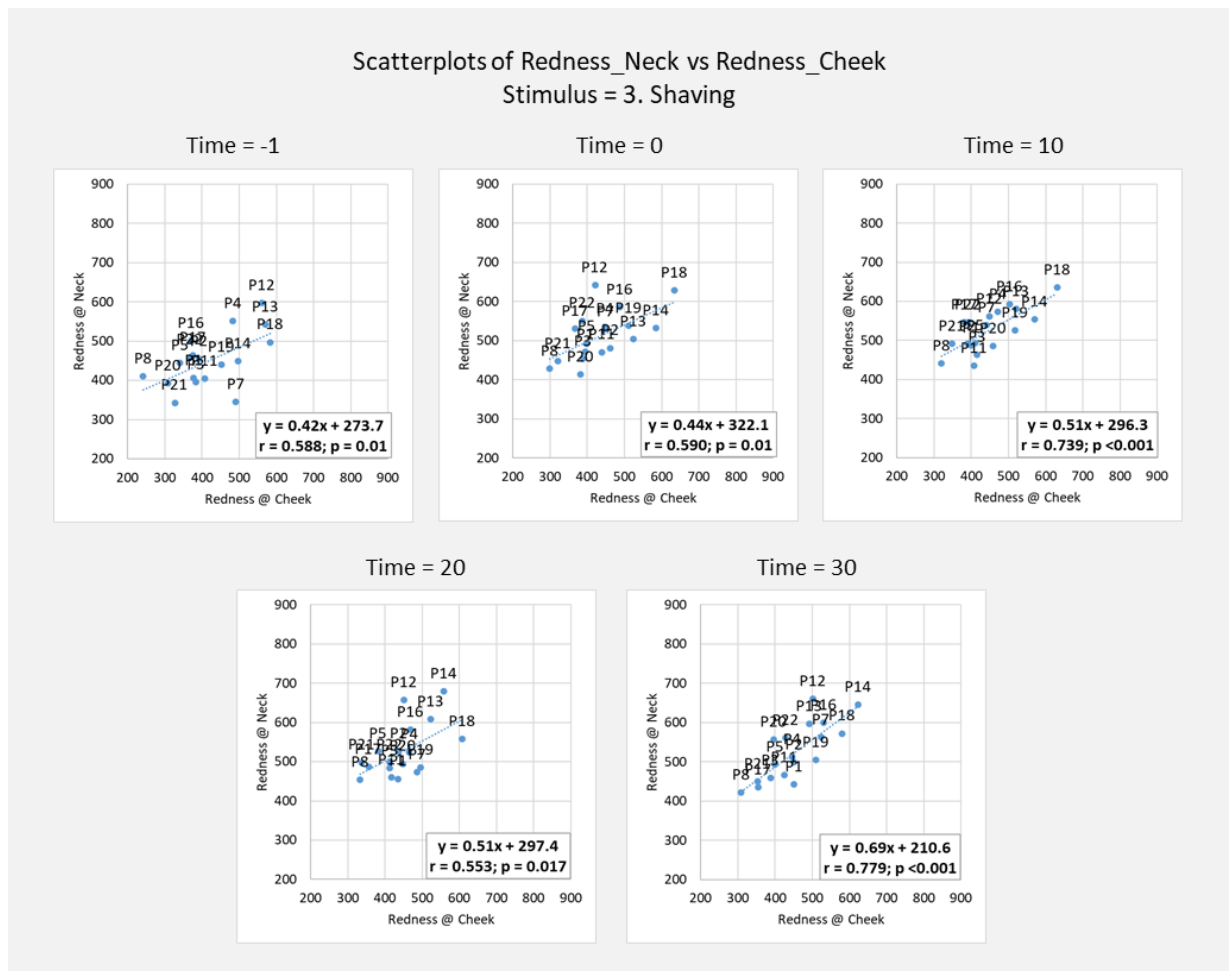
Scatterplots of Temperature_Neck vs Temperature_Cheek
Stimulus = 2. Friction



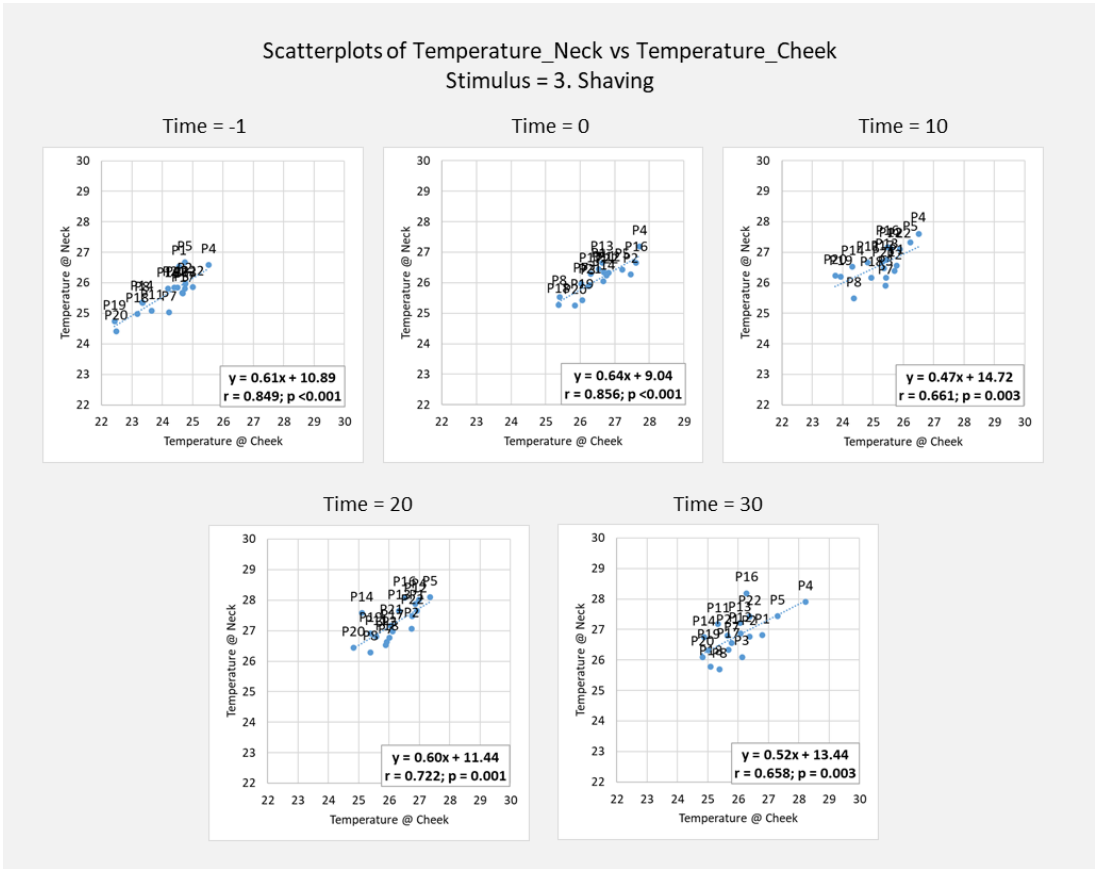
Relationship between the skin temperature on the cheek and the neck for session 2



Relationship between the skin hydration on the cheek and the neck for session 3



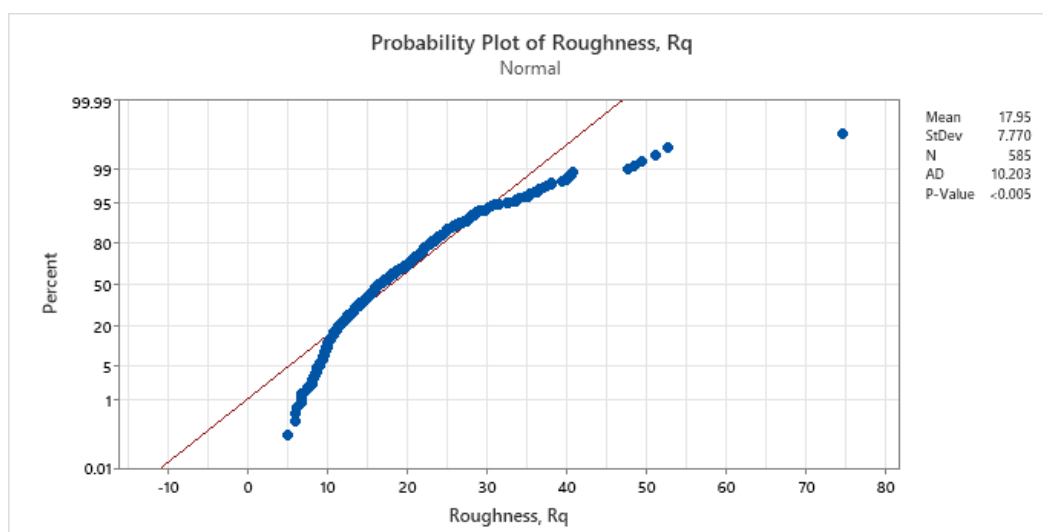
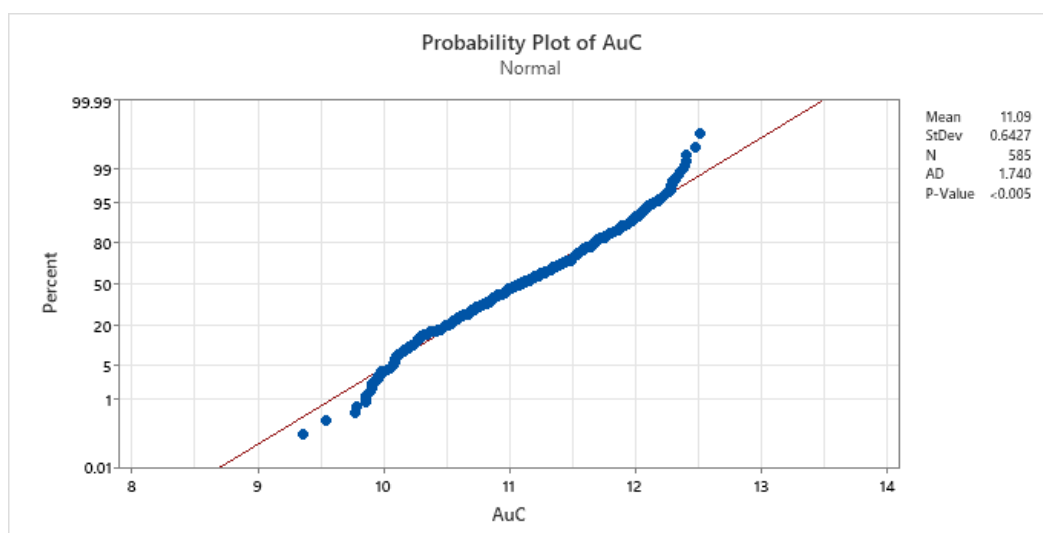
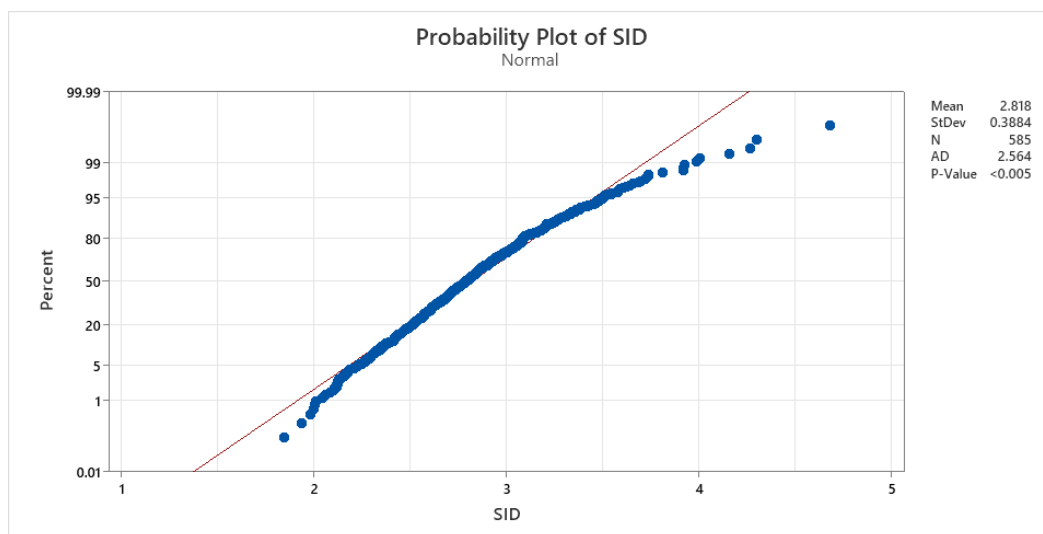
Relationship between the redness on the cheek and the neck for session 3



Relationship between the skin temperature on the cheek and the neck for session 3

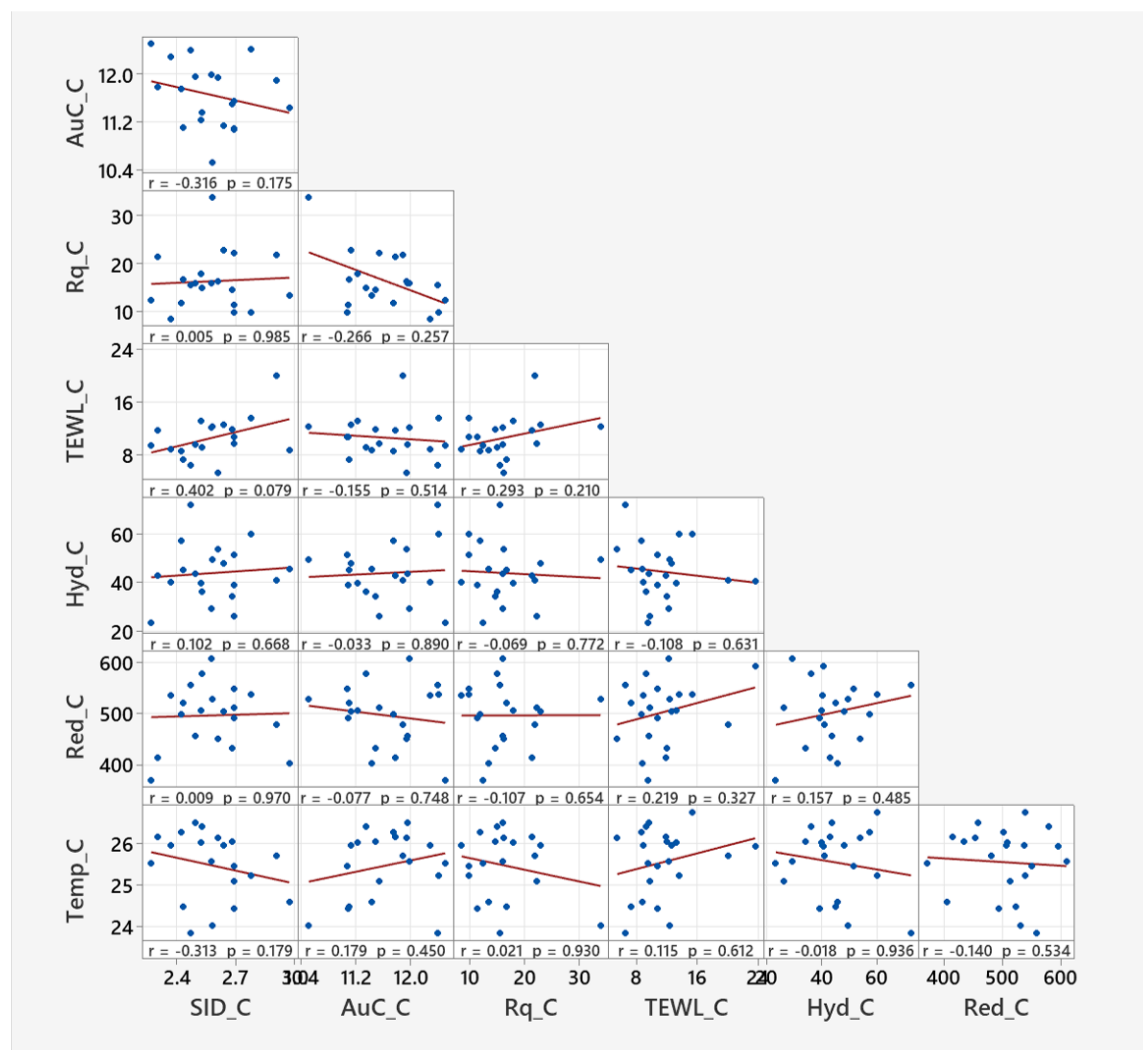
Appendix D Additional figures from Chapter 5

Normality test

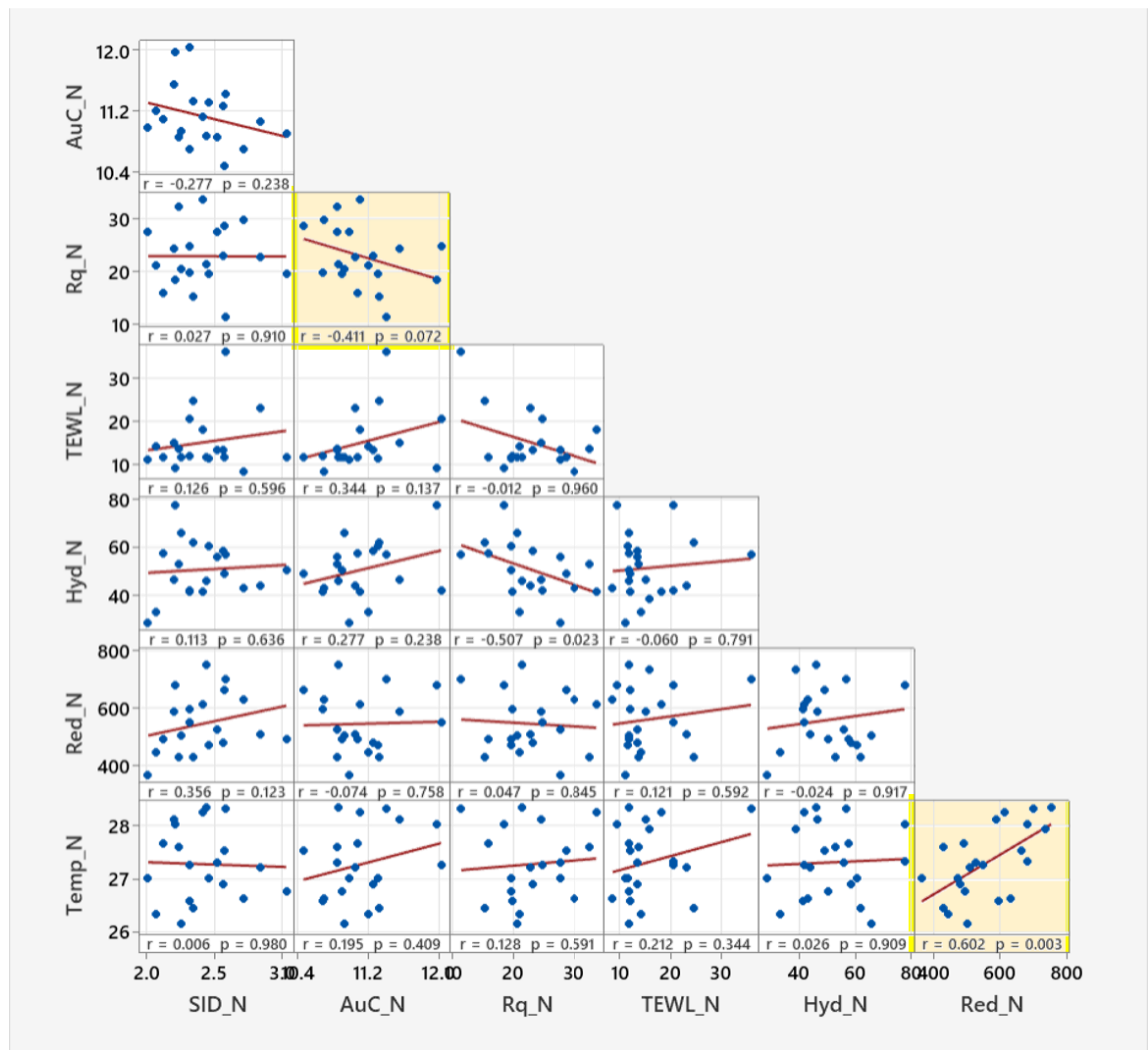


Scatterplots for OCT-skin parameters and biophysical parameters at baseline

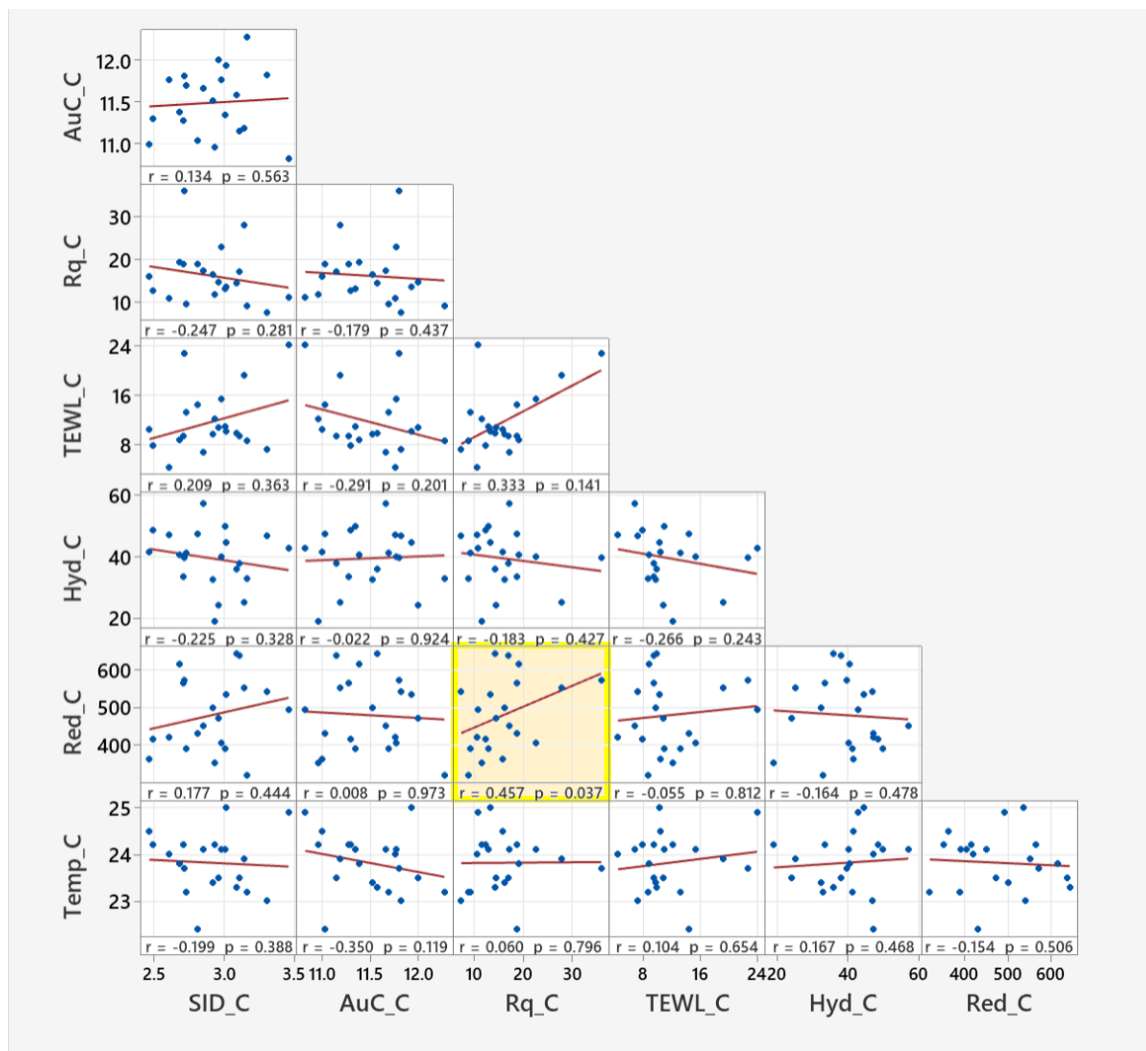
Session 1 - Cheek



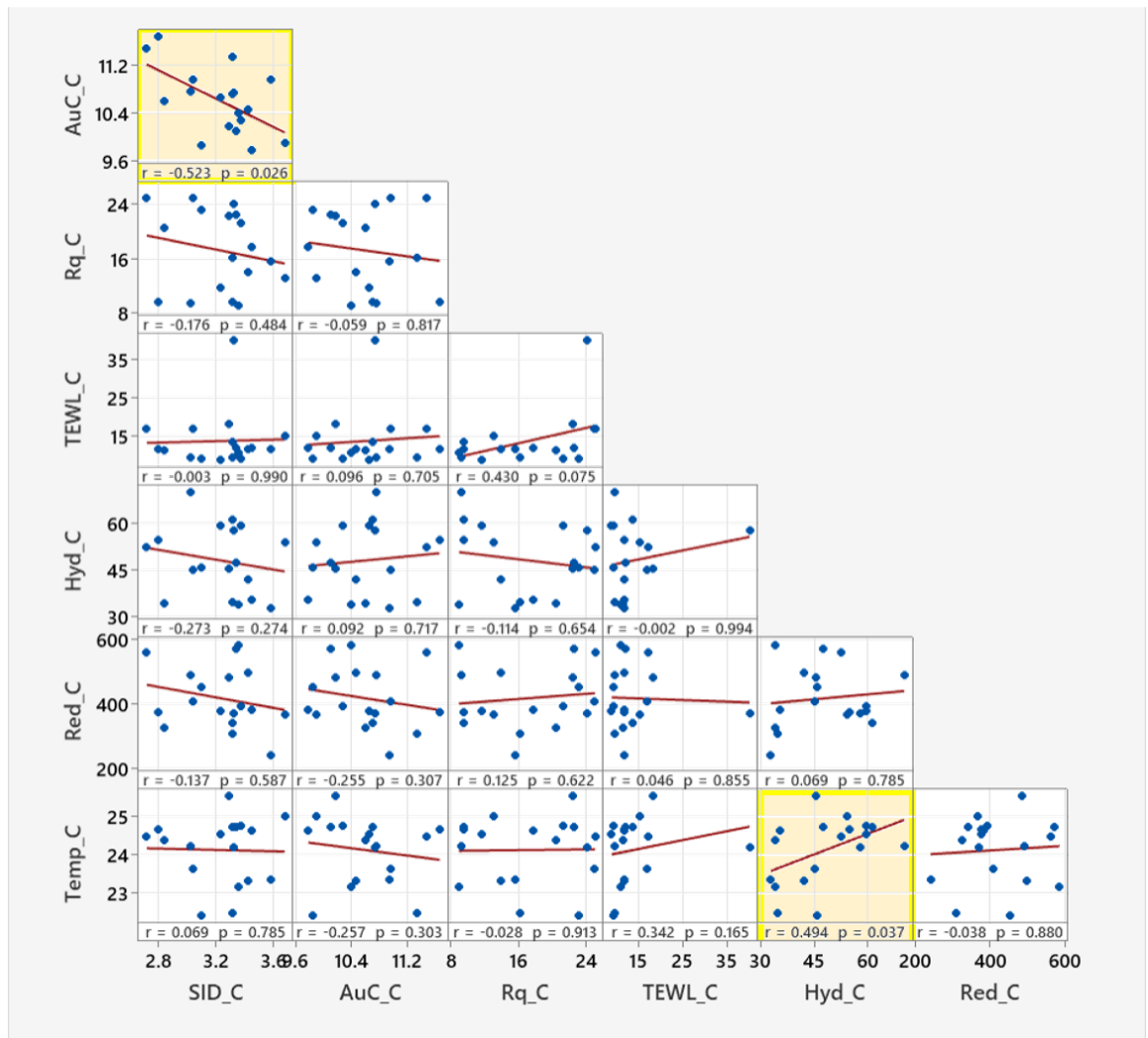
Session 1 - Neck



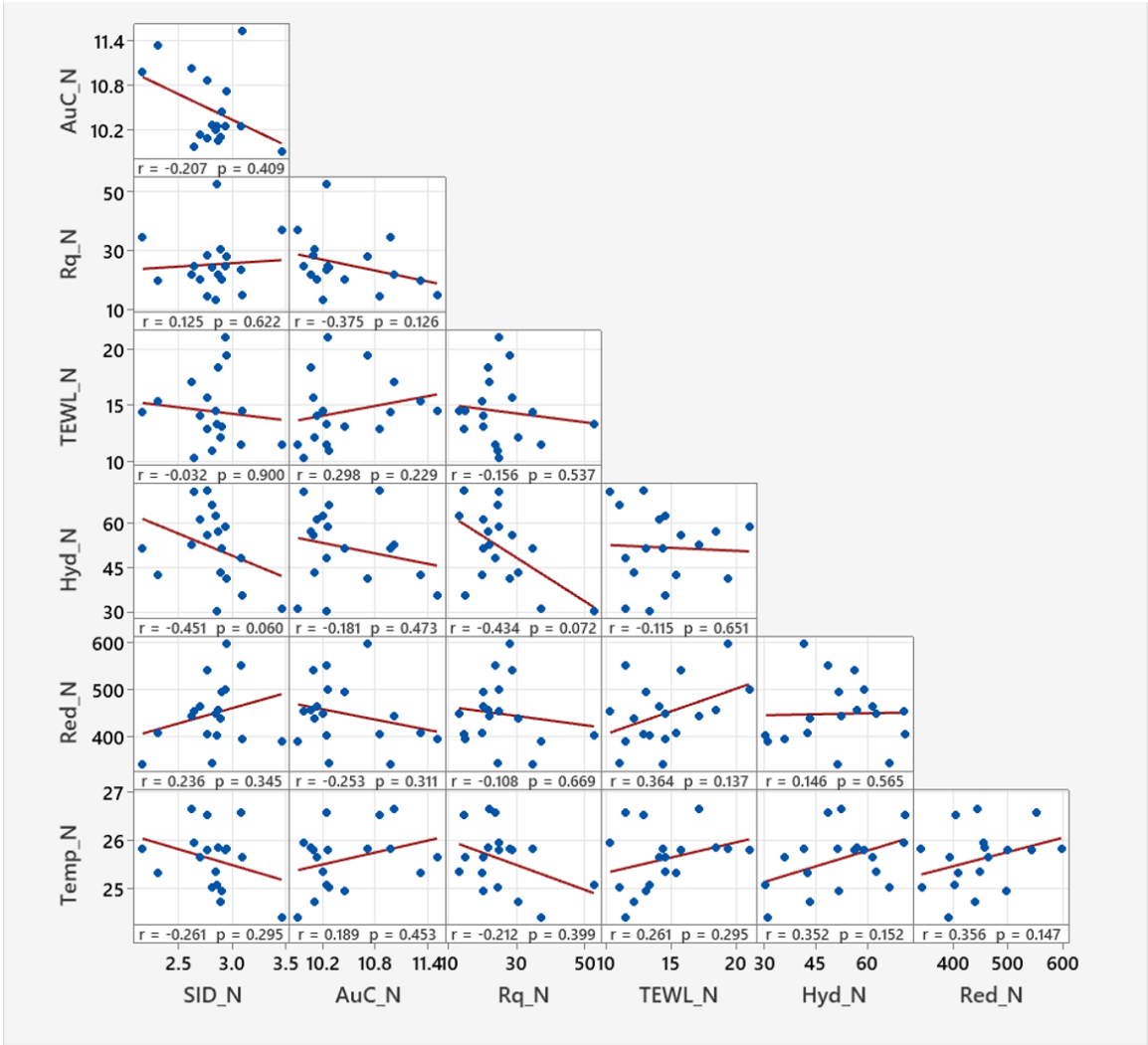
Session 2 - Cheek



Session 3 - Cheek



Session 3 - Neck



Relationship between OCT-skin parameters and extrinsic factors

Ranks for participants from Session 2 at baseline for the all the skin parameters, sorted by the SS category.

	Participant	SS Category	Shaving method	Shaving Frequency	Rank SID	Rank AuC	Rank Rq	Rank TEWL	Rank Hyd.	Rank Red.	Rank Temp.
Cheek	P11	Low SS	Rota	>5	11	5	1	2	12	12	7
	P18	Low SS	Blade	3, 4	4	9	2	12	11	2	11
	P22	Low SS	Blade	3, 4	12	10	10	6	2	13	7
	P5	Mild SS	Combination	>5	7	14	3	3	4	9	17
	P8	Mild SS	Combination	<2	15	1	16	13	15	17	14
	P13	Mild SS	Combination	3, 4	14	13	6	10	13	1	12
	P14	Mild SS	Combination	3, 4	2	11	11	14	3	11	4
	P16	Mild SS	Combination	>5	17	17	13	1	8	6	2
	P17	Mild SS	Combination	>5	6	7	15	4	10	14	14
	P19	Mild SS	Combination	>5	5	12	4	10	14	3	4
	P20	Mild SS	Rota	>5	10	2	8	7	16	7	12
	P21	Mild SS	Combination	3, 4	9	16	12	5	17	16	4
	P1	High SS	Combination	<2	8	8	5	16	1	8	7
	P2	High SS	Blade	<2	13	3	9	9	7	5	1
	P3	High SS	Rota	<2	1	15	7	8	9	15	3
Neck	P4	High SS	Blade	>5	3	6	14	17	5	10	10
	P7	High SS	Combination	3, 4	16	4	17	15	6	4	16
	P11	Low SS	Rota	>5	4	4	4	#N/A	16	15	#N/A
	P18	Low SS	Blade	3, 4	15	15	5	6	9	2	5
	P22	Low SS	Blade	3, 4	10	5	13	1	4	7	6
	P5	Mild SS	Combination	>5	1	3	16	10	2	13	6
	P8	Mild SS	Combination	<2	14	6	11	11	13	5	12
	P13	Mild SS	Combination	3, 4	8	12	2	5	15	1	6
	P14	Mild SS	Combination	3, 4	16	16	17	14	3	12	12
	P16	Mild SS	Combination	>5	5	10	6	3	8	3	4
	P17	Mild SS	Combination	>5	7	9	14	2	10	11	16
	P19	Mild SS	Combination	>5	12	14	1	8	17	4	14
	P20	Mild SS	Rota	>5	17	17	10	4	11	14	15
	P21	Mild SS	Combination	3, 4	9	13	9	9	14	16	9
	P1	High SS	Combination	<2	2	2	12	14	1	8	1
	P2	High SS	Blade	<2	3	1	8	12	12	8	2
	P3	High SS	Rota	<2	11	8	7	7	7	17	9
	P4	High SS	Blade	>5	6	7	3	16	5	10	2
	P7	High SS	Combination	3, 4	13	11	15	13	6	6	11

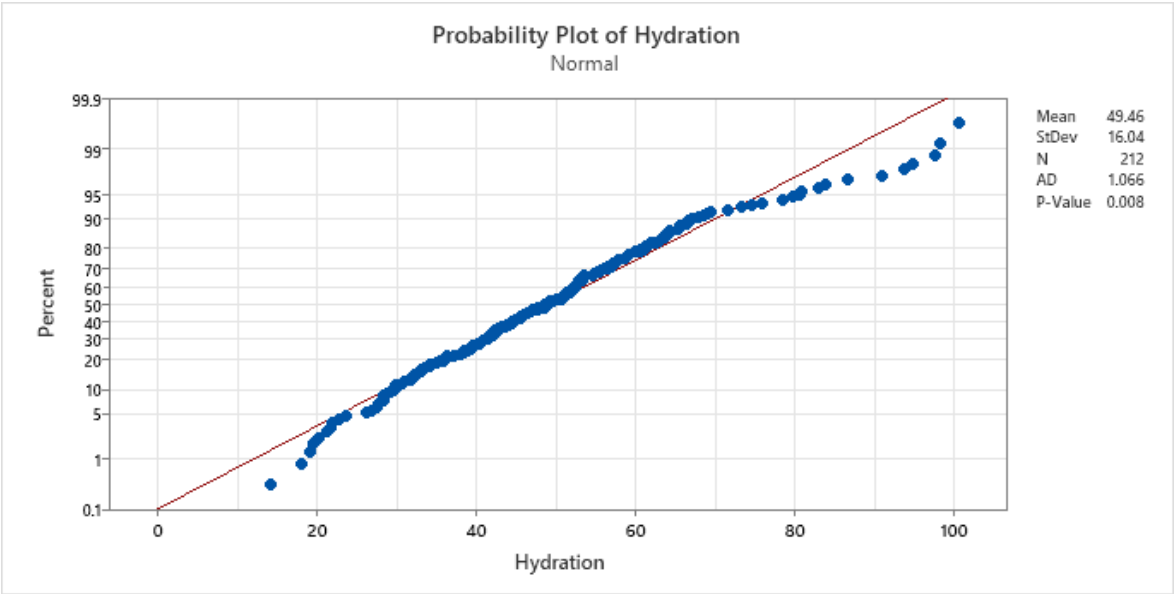
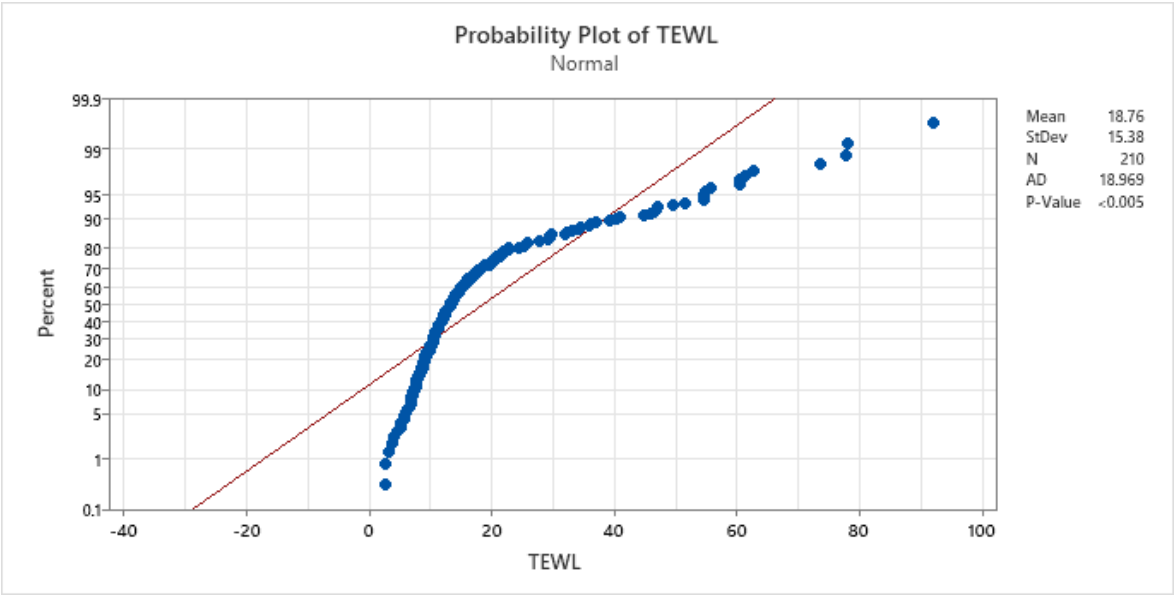
Appendix D

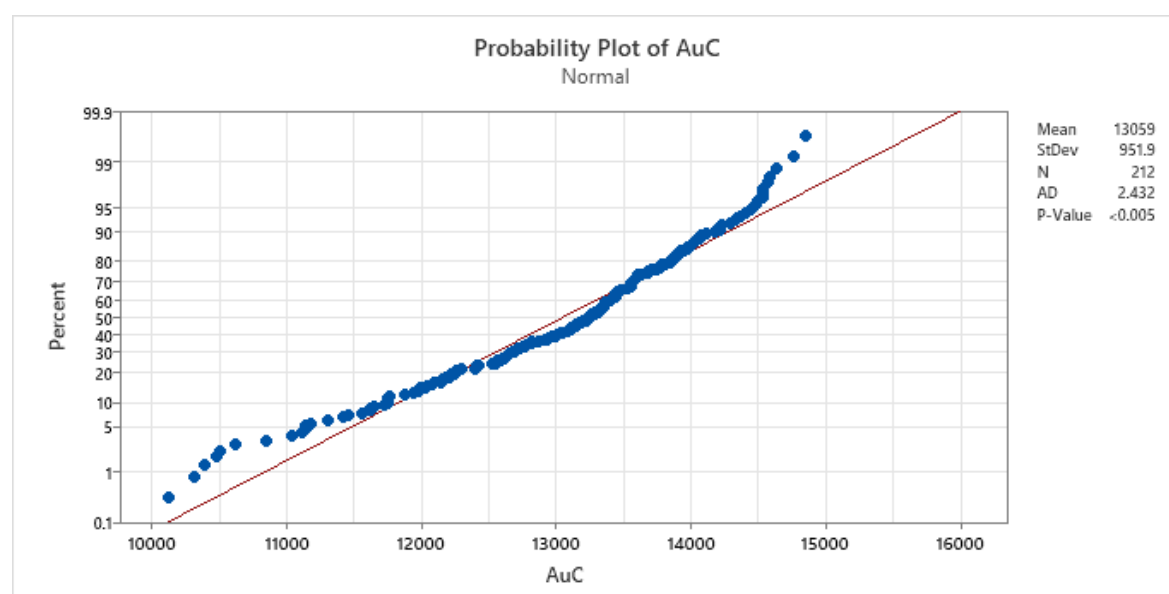
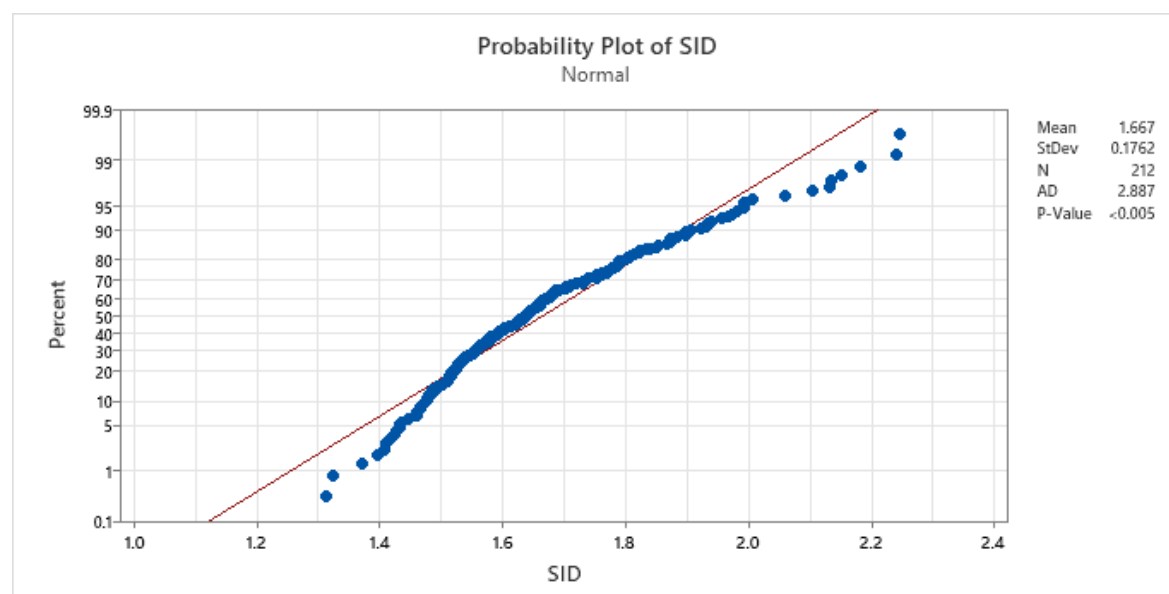
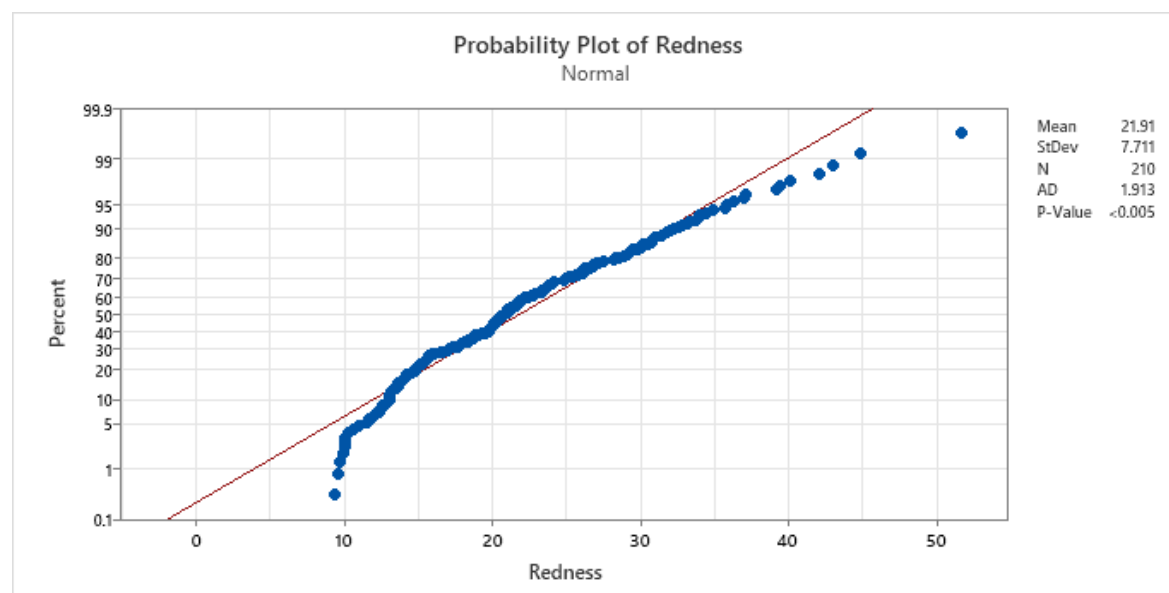
Ranks for participants from Session 3 at baseline for the all the skin parameters, sorted by the SS category.

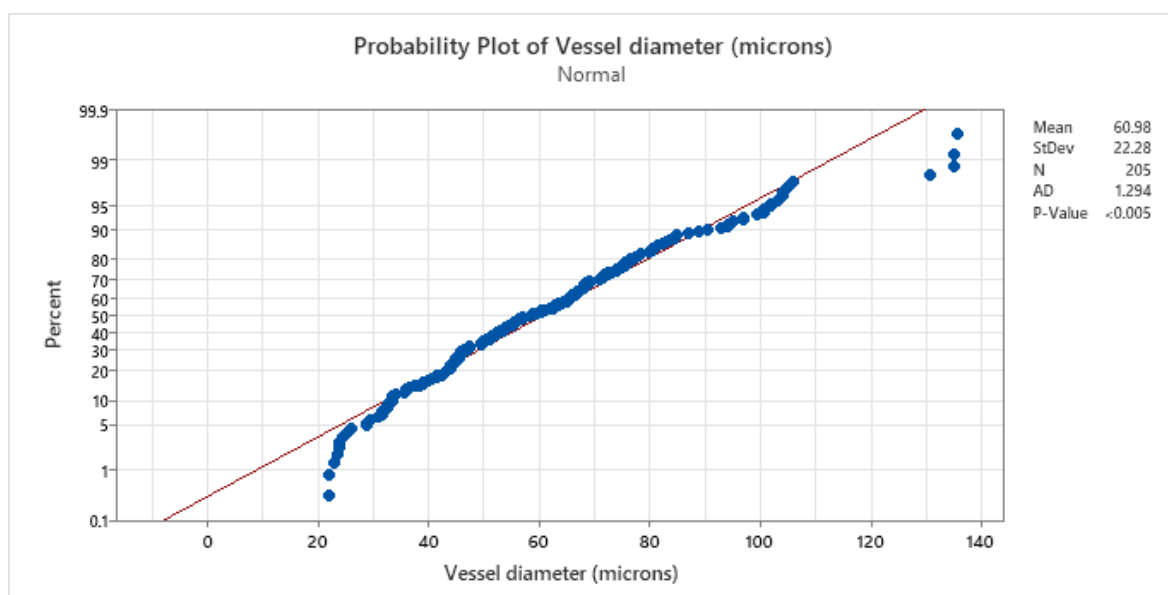
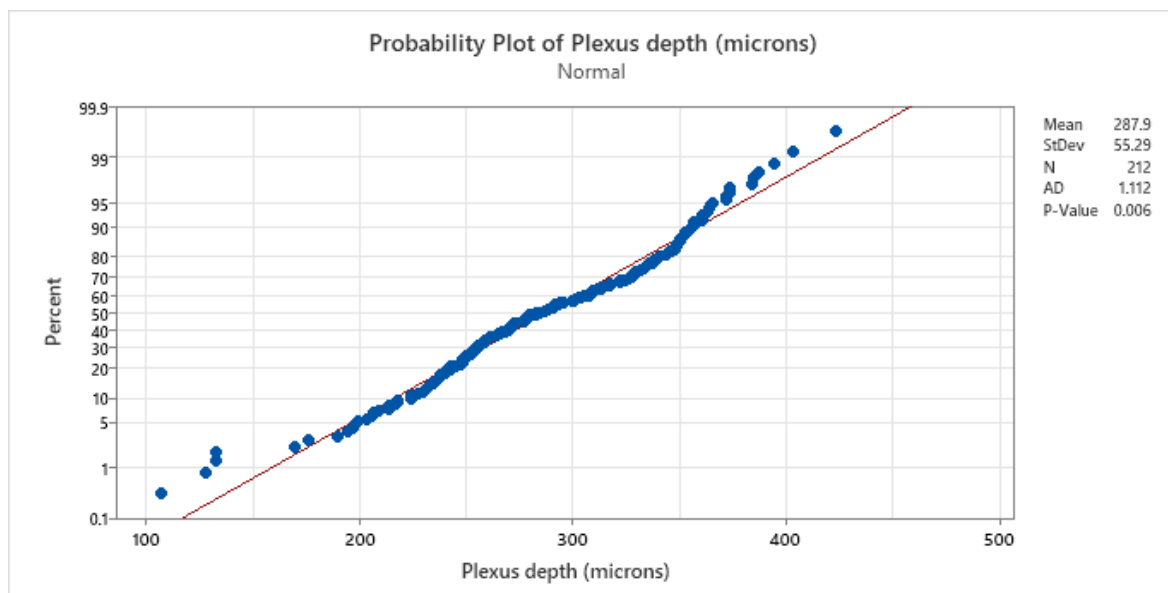
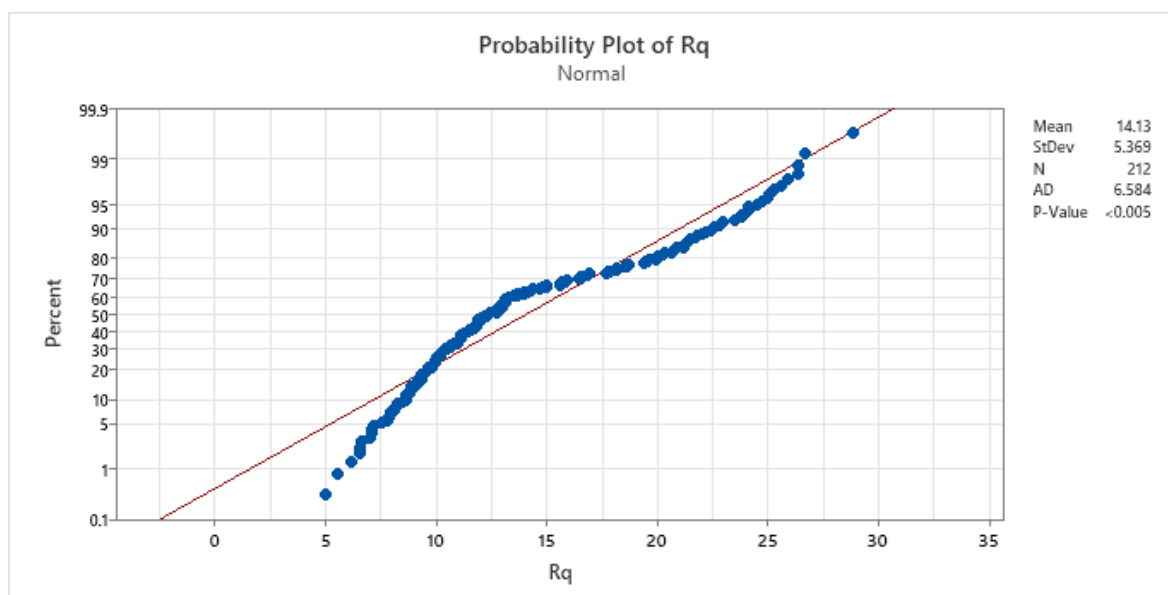
	Participant	SS Category	Shaving method	Shaving Frequency	Rank SID	Rank AuC	Rank Rq	Rank TEWL	Rank Hyd.	Rank Red.	Rank Temp.
Cheek	P11	Low SS	Rota	>5	4	3	1	3	11	7	12
	P18	Low SS	Blade	3, 4	12	11	17	12	16	1	15
	P22	Low SS	Blade	3, 4	17	15	12	4	7	13	2
	P5	Mild SS	Combination	>5	8	7	14	5	2	14	4
	P8	Mild SS	Combination	<2	16	4	10	10	17	17	13
	P13	Mild SS	Combination	3, 4	11	14	4	6	8	2	5
	P14	Mild SS	Combination	3, 4	14	10	11	9	12	3	14
	P16	Mild SS	Combination	>5	10	6	2	1	5	12	11
	P17	Mild SS	Combination	>5	1	1	15	8	6	11	6
	P19	Mild SS	Combination	>5	5	16	3	15	9	6	17
	P20	Mild SS	Rota	>5	9	2	9	13	14	16	16
	P21	Mild SS	Combination	3, 4	2	9	7	11	15	15	9
	P1	High SS	Combination	<2	6	8	13	17	3	10	8
	P2	High SS	Blade	<2	13	12	6	16	3	8	3
	P3	High SS	Rota	<2	15	17	8	7	13	9	7
	P4	High SS	Blade	>5	7	13	5	2	10	5	1
	P7	High SS	Combination	3, 4	3	5	16	14	1	4	10
Neck	P11	Low SS	Rota	>5	10	9	1	10	17	13	13
	P18	Low SS	Blade	3, 4	13	6	12	11	10	4	15
	P22	Low SS	Blade	3, 4	11	15	11	2	7	6	5
	P5	Mild SS	Combination	>5	3	3	10	3	9	9	1
	P8	Mild SS	Combination	<2	2	2	14	5	14	11	12
	P13	Mild SS	Combination	3, 4	7	14	5	4	8	2	8
	P14	Mild SS	Combination	3, 4	9	11	17	6	4	8	11
	P16	Mild SS	Combination	>5	14	8	7	1	6	3	7
	P17	Mild SS	Combination	>5	5	12	13	9	5	5	10
	P19	Mild SS	Combination	>5	12	13	4	13	13	10	16
	P20	Mild SS	Rota	>5	17	17	2	14	16	15	17
	P21	Mild SS	Combination	3, 4	1	4	3	8	11	17	6
	P1	High SS	Combination	<2	6	5	16	12	1	12	3
	P2	High SS	Blade	<2	4	16	6	17	2	7	4
	P3	High SS	Rota	<2	16	1	15	7	15	14	9
	P4	High SS	Blade	>5	15	10	9	15	12	1	2
	P7	High SS	Combination	3, 4	8	7	8	16	3	16	14

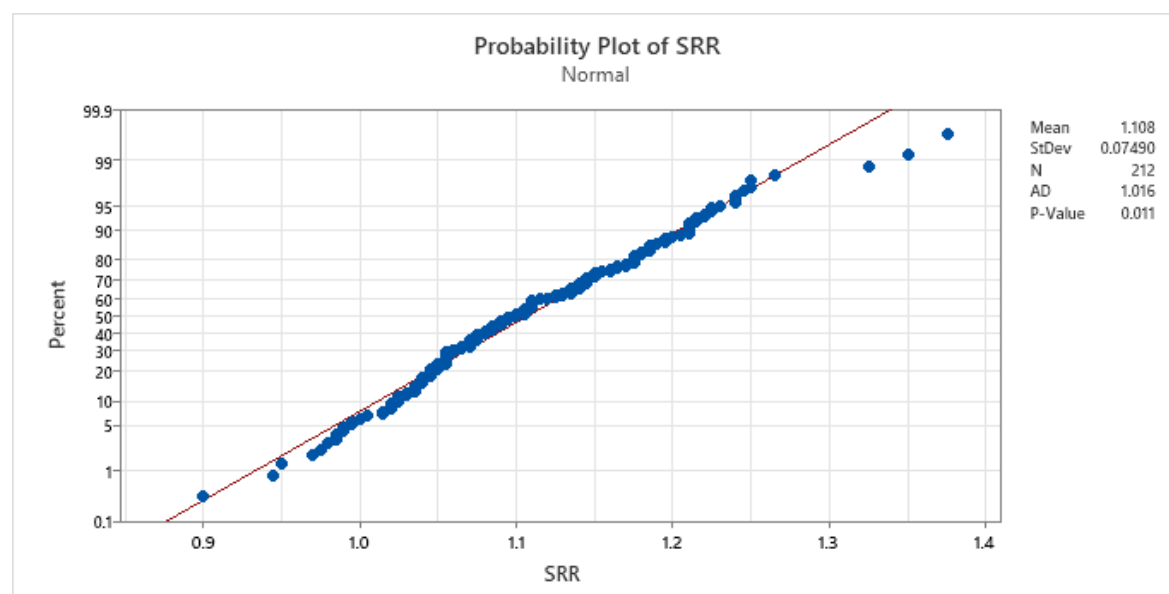
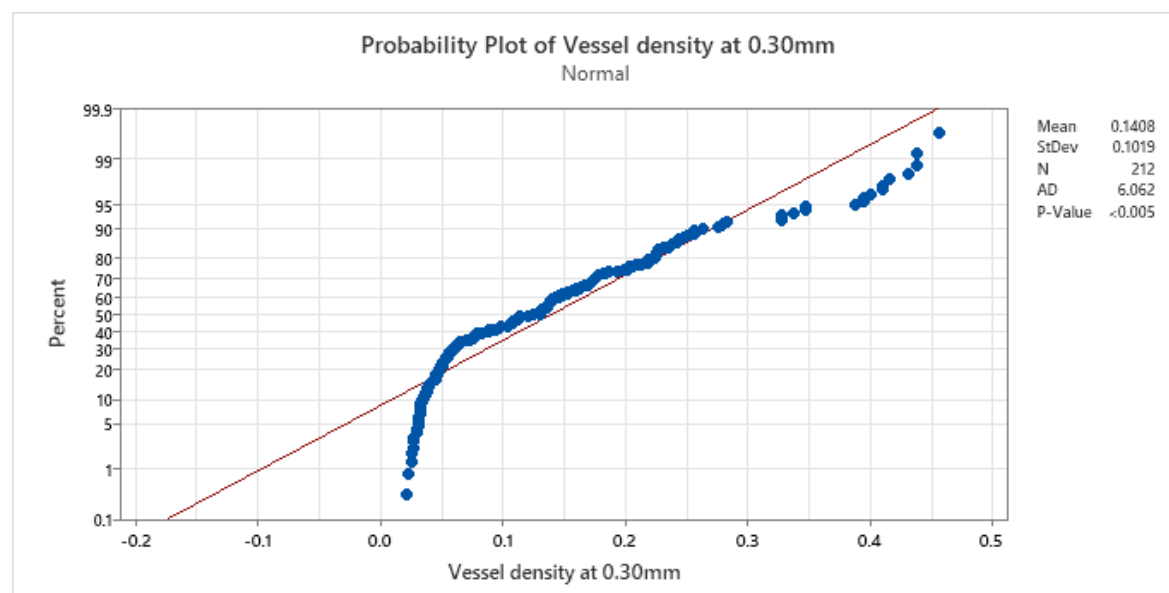
Appendix E Additional figures from Chapter 6

Normality test



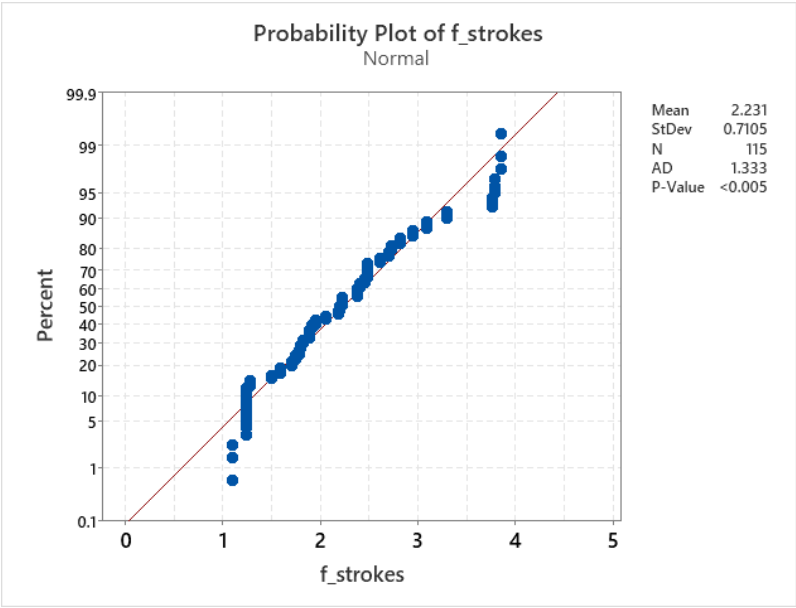
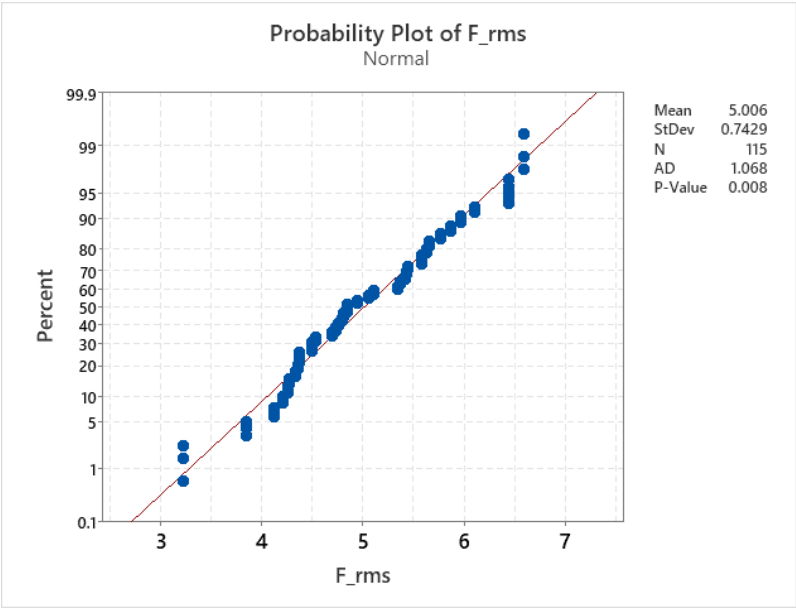


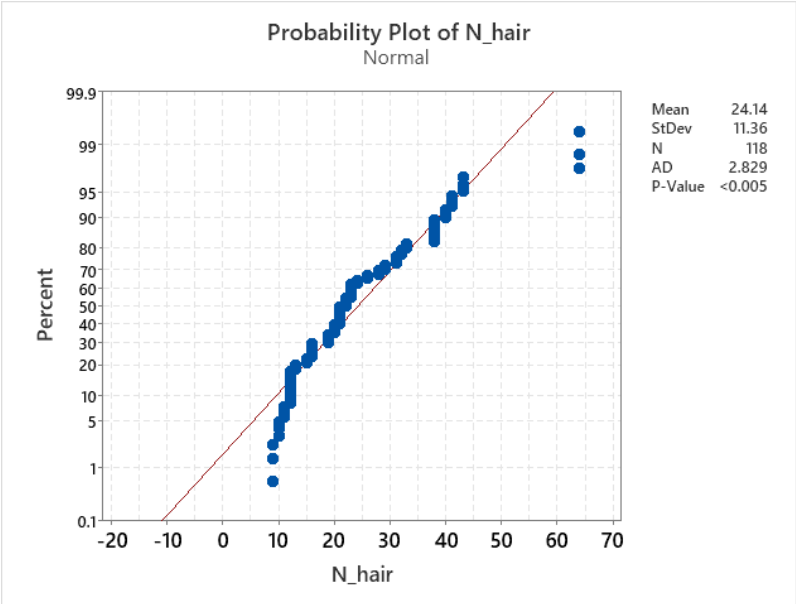
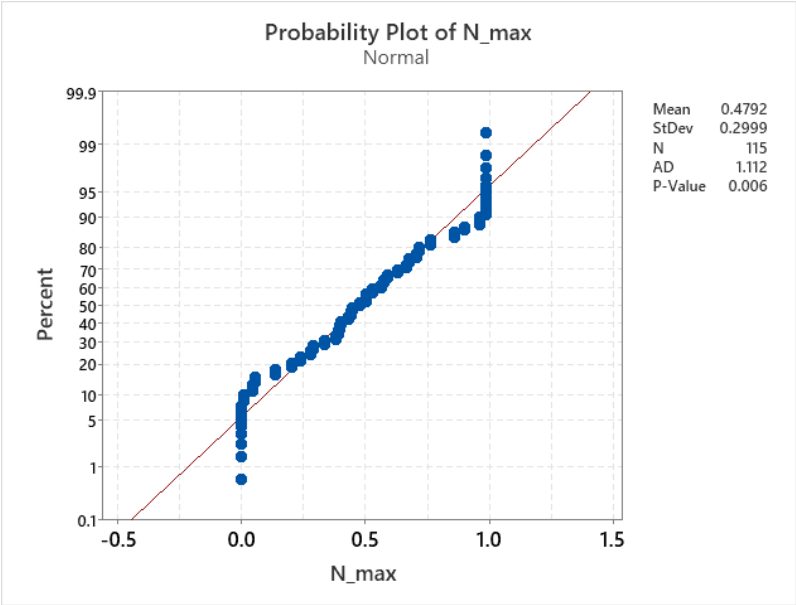




Appendix F Additional figures from Chapter 7

Normality test





Bibliography

- Abiakam, Nkemjika, Hemalatha Jayabal, Kay Mitchell, Dan Bader, and Peter Worsley. 2023. "Biophysical and Biochemical Changes in Skin Health of Healthcare Professionals Using Respirators during COVID-19 Pandemic." *Skin Research and Technology* 29 (1): 1–11. <https://doi.org/10.1111/srt.13239>.
- Abiakam, Nkemjika, Peter Worsley, Hemalatha Jayabal, Kay Mitchell, Michaela Jones, Jacqui Fletcher, Fran Spratt, and Dan Bader. 2021. "Personal Protective Equipment Related Skin Reactions in Healthcare Professionals during COVID-19." *International Wound Journal* 18 (3): 312–22. <https://doi.org/10.1111/IWJ.13534>.
- Abignano, Giuseppina, Sibel Zehra Aydin, Concepción Castillo-gallego, Vasiliki Liakouli, Daniel Woods, Adam Meekings, Richard J Wake, et al. 2013. "Virtual Skin Biopsy by Optical Coherence Tomography: The First Quantitative Imaging Biomarker for Scleroderma." *Annals of the Rheumatic Diseases* 72 (11): 1845–51. <https://doi.org/10.1136/annrheumdis-2012-202682>.
- Adegun, Oluyori Kutulola, Pete H. Tomlins, E. Hagi-Pavli, Dan L. Bader, and Farida Fortune. 2013. "Quantitative Optical Coherence Tomography of Fluid-Filled Oral Mucosal Lesions." *Lasers in Medical Science* 28 (5): 1249–55. <https://doi.org/10.1007/s10103-012-1208-y>.
- Agner, T., and J. Serup. 1989. "Quantification of the DMSO-response—a Test for Assessment of Sensitive Skin." *Clinical and Experimental Dermatology* 14 (3): 214–17. <https://doi.org/10.1111/j.1365-2230.1989.tb00935.x>.
- Andreassi, Marco, and Lucio Andreassi. 2007. "Utility and Limits of Noninvasive Methods in Dermatology." *Expert Review of Dermatology* 2 (3): 249–55. <https://doi.org/10.1586/17469872.2.3.249>.
- Antonov, Dimitar, Sibylle Schliemann, and Peter Elsner. 2016. "Methods for the Assessment of Barrier Function." *Current Problems in Dermatology (Switzerland)* 49: 61–70. <https://doi.org/10.1159/000441546>.
- Arx, Thomas von Arx von, Kaori Tamura, Oba Yukiya, and Scott Lozanoff. 2018. "The Face – A Vascular Perspective. A Literature Review." *Swiss Dental Journal* 128 (5): 382–92.
- Askaruly, Sanzhar, Yujin Ahn, Hyeongeun Kim, Andrey Vavilin, Sungbea Ban, Pil Un Kim, Seunghun Kim, Haekwang Lee, and Woonggyu Jung. 2019. "Quantitative Evaluation of Skin Surface Roughness Using Optical Coherence Tomography in Vivo." *IEEE Journal of Selected Topics in*

Bibliography

- Quantum Electronics* 25 (1). <https://doi.org/10.1109/JSTQE.2018.2873489>.
- Bader, Dan L., and Peter R. Worsley. 2018. "Technologies to Monitor the Health of Loaded Skin Tissues." *BioMedical Engineering Online*. BioMed Central Ltd. <https://doi.org/10.1186/s12938-018-0470-z>.
- Balsam, MS, and Sagarin E. 2009. *Cosmetic Science and Technology*. <https://doi.org/10.1016/B978-1-85617-943-0.10041-3>.
- Bangert, Christine, Patrick M. Brunner, and Georg Stingl. 2011. "Immune Functions of the Skin." *Clinics in Dermatology* 29 (4): 360–76. <https://doi.org/10.1016/j.clindermatol.2011.01.006>.
- Barber, Cara, and Susan Boiko. 2022. "Tape Stripping: Investigational, Diagnostic, and Therapeutic Uses in Dermatology." *Clinics in Dermatology* 40 (4): 355–62. <https://doi.org/10.1016/J.CLINDERMATOL.2022.02.008>.
- Bashir, S. J., A. L. Chew, A. Anigbogu, F. Dreher, and Howard I. Maibach. 2001. "Physical and Physiological Effects of Stratum Corneum Tape Stripping." *Skin Research and Technology* 7 (1): 40–48. <https://doi.org/10.1034/j.1600-0846.2001.007001040.x>.
- Bentov, Itay, and May J. Reed. 2015. "The Effect of Aging on the Cutaneous Microvasculature." *Microvascular Research* 100: 25–31. <https://doi.org/10.1016/j.mvr.2015.04.004>.
- Berardesca, E., P. Masson, L. Rodrigues, C. L. Gummer, J. L. L  v  que, M. Loden, G. Pi  rard, et al. 1997. "EEMCO Guidance for the Assessment of Stratum Corneum Hydration: Electrical Methods." *Skin Research and Technology* 3 (2): 126–32. <https://doi.org/10.1111/j.1600-0846.1997.tb00174.x>.
- Berardesca, Enzo, Maddalena Cespa, Nadia Farinelli, Giacomo Rallbiosi, Howard I. Maibach, Policlinico S Matteo, Giacomo Rabbiosi, and Howard I. Maibach. 1991. "In Vivo Transcutaneous Penetration of Nicotines and Sensitive Skin." *Contact Dermatitis* 25 (1): 35–38. <https://doi.org/10.1111/j.1600-0536.1991.tb01770.x>.
- Berardesca, Enzo, Miranda A. Farage, and Howard Maibach. 2013. "Sensitive Skin: An Overview." *International Journal of Cosmetic Science* 35 (1): 2–8. <https://doi.org/10.1111/j.1468-2494.2012.00754.x>.
- Berardesca, Enzo, Jean Luc L  v  que, Philippe Masson, G. E. Pi  rard, L. Rodrigues, V. Rogiers, P. Elsner, et al. 2002. "EEMCO Guidance for the Measurement of Skin Microcirculation." *Skin Pharmacology and Applied Skin Physiology* 15 (6): 442–56. <https://doi.org/10.1159/000066451>.

- Berardesca, Enzo, Howard L. Maibach, and Joachim W. Fluhr, eds. 2006. *Sensitive Skin Syndrome*. *Sensitive Skin Syndrome*. 1st ed. CRC Press. <https://doi.org/10.3109/9781420004601>.
- Berardesca, Enzo, J. De Rigal, J. L. Leveque, and H. L. Maibach. 1991. "In Vivo Biophysical Characterization of Skin Physiological Differences in Races." *Dermatology* 182 (2): 89–93. <https://doi.org/10.1159/000247752>.
- Bertuglia, Silvia, Antonio Colantuoni, and Marcos Intaglietta. 2000. "Regulation of Vascular Tone and Capillary Perfusion." *Textbook of Angiology*, 439–54. https://doi.org/10.1007/978-1-4612-1190-7_35.
- Bhaktaviziam, Chetty, Herbert Mescon, and Alexander G. Matoltsy. 1963. "Shaving: I. Study of Skin and Shavings." *Archives of Dermatology* 88 (6): 874–79. <https://doi.org/10.1001/ARCHDERM.1963.01590240198033>.
- Black, D., A. Del Pozo, J. M. Lagarde, and Y. Gall. 2000. "Seasonal Variability in the Biophysical Properties of Stratum Corneum from Different Anatomical Sites." *Skin Research and Technology* 6 (2): 70–76. <https://doi.org/10.1034/j.1600-0846.2000.006002070.x>.
- Bostan, Luciana E., Peter R. Worsley, Shabira Abbas, and Dan L. Bader. 2019. "The Influence of Incontinence Pads Moisture at the Loaded Skin Interface." *Journal of Tissue Viability* 28 (3): 125–32. <https://doi.org/10.1016/j.jtv.2019.05.002>.
- Bouten, Carlijn V., Cees W. Oomens, Frank P.T. Baaijens, and Dan L. Bader. 2003. "The Etiology of Pressure Ulcers: Skin Deep or Muscle Bound?" *Archives of Physical Medicine and Rehabilitation* 84 (4): 616–19. <https://doi.org/10.1053/apmr.2003.50038>.
- Breternitz, M., M. Flach, J. Präßler, P. Elsner, and J. W. Fluhr. 2007. "Acute Barrier Disruption by Adhesive Tapes Is Influenced by Pressure, Time and Anatomical Location: Integrity and Cohesion Assessed by Sequential Tape Stripping; A Randomized, Controlled Study." *British Journal of Dermatology* 156 (2): 231–40. <https://doi.org/10.1111/j.1365-2133.2006.07632.x>.
- Bronneberg, Debbie, Sander W. Spiekstra, Lisette H. Cornelissen, Cees W. Oomens, Susan Gibbs, Frank P.T. Baaijens, and Catlijn V.C. Bouten. 2007. "Cytokine and Chemokine Release upon Prolonged Mechanical Loading of the Epidermis." *Experimental Dermatology* 16 (7): 567–73. <https://doi.org/10.1111/j.1600-0625.2007.00566.x>.
- Chan, Kam Tim Michael. 2018. "Clinical Review on Sensitive Skin: History, Epidemiology, Pathogenesis and Management." *Journal of Clinical & Experimental Dermatology Research* 09 (04): 1–6. <https://doi.org/10.4172/2155-9554.1000453>.

Bibliography

- Chaturvedi, Pakhi, Peter R. Worsley, Giulia Zanelli, Wilco Kroon, and Dan L. Bader. 2021. "Quantifying Skin Sensitivity Caused by Mechanical Insults: A Review." *Skin Research and Technology*, October. <https://doi.org/10.1111/SRT.13104>.
- Chopra, Karan, Daniel Calva, Michael Sosin, ; Kashyap, Komarraju Tadisina, Bs ; Abhishake Banda, Carla De, et al. 2015. "A Comprehensive Examination of Topographic Thickness of Skin in the Human Face Cosmetic Medicine." *Aesthetic Surgery Journal* 35 (8): 1007–13. <https://doi.org/10.1093/asj/sjv079>.
- Clarys, P., K. Alewaeters, R. Lambrecht, and A. O. Barel. 2000. "Skin Color Measurements: Comparison between Three Instruments: The Chromameter®, the DermaSpectrometer® and the Mexameter®." *Skin Research and Technology* 6 (4): 230–38. <https://doi.org/10.1034/j.1600-0846.2000.006004230.x>.
- Cowley, K, K. Vanoosthuyze, Gillette Reading, and Innovation Centre. 2012. "Insights into Shaving and Its Impact on Skin" 166: 6–12. <https://doi.org/10.1111/j.1365-2133.2011.10783.x>.
- Dąbrowska, Agnieszka K., Christian Adlhart, Fabrizio Spano, Gelu-Marius Rotaru, Siegfried Derler, Lina Zhai, Nicholas D. Spencer, and René M. Rossi. 2016. "In Vivo Confirmation of Hydration-Induced Changes in Human-Skin Thickness, Roughness and Interaction with the Environment." *Biointerphases* 11 (3): 031015. <https://doi.org/10.1116/1.4962547>.
- Darlenski, R., S. Sassning, N. Tsankov, and J. W. Fluhr. 2009. "Non-Invasive in Vivo Methods for Investigation of the Skin Barrier Physical Properties." *European Journal of Pharmaceutics and Biopharmaceutics* 72 (2): 295–303. <https://doi.org/10.1016/j.ejpb.2008.11.013>.
- Deegan, Anthony J., and Ruikang K. Wang. 2019. "Microvascular Imaging of the Skin." *Physics in Medicine and Biology* 64 (7). <https://doi.org/10.1088/1361-6560/ab03f1>.
- Diogo, Lucília, and Ana Luísa Papoila. 2010. "Is It Possible to Characterize Objectively Sensitive Skin?" *Skin Research and Technology* 16 (1): 30–37. <https://doi.org/10.1111/j.1600-0846.2009.00404.x>.
- Do, Le Hanh Dung, Nazanin Azizi, and Howard Maibach. 2020. "Sensitive Skin Syndrome: An Update." *American Journal of Clinical Dermatology* 21 (3): 401–9. <https://doi.org/10.1007/s40257-019-00499-7>.
- Dolečková, Iva, Aneta Čápková, Lenka Machková, Soňa Moravčíková, Markéta Marešová, and Vladimír Velebný. 2021. "Seasonal Variations in the Skin Parameters of Caucasian Women from Central Europe." *Skin Research and Technology* 27 (3): 358–69.

<https://doi.org/10.1111/srt.12951>.

- Draelos, Zoe Diana. 1997. "Sensitive Skin: Perceptions, Evaluation, and Treatment." *Contact Dermatitis* 8 (2): 67–78. [https://doi.org/10.1016/S1046-199X\(97\)90000-2](https://doi.org/10.1016/S1046-199X(97)90000-2).
- Duarte, Ida, Jéssica Eleonora, P. S. Silveira, Mariana De Figueiredo, Silva Hafner, Raquel Toyota, Debora Midori, and M Pedroso. 2017. "Sensitive Skin: Review of an Ascending Concept." *An Bras Dermatol* 92 (4): 521–26. <https://doi.org/10.1590/abd1806-4841.201756111>.
- Eberlein-Konig, B., T. Schafer, J. Huss-Marp, U. Darsow, M. Mohrenschlager, O. Herbert, D. Abeck, U. Kramer, H. Behrendt, and J. Ring. 2000. "Skin Surface PH, Stratum Corneum Hydration, Trans-Epidermal Water Loss and Skin Roughness Related to Atopic Eczema and Skin Dryness in a Population of Primary School Children." *Acta Dermato-Venereologica* 80 (3): 188–91. <https://doi.org/10.1080/000155500750042943>.
- Elsner, P. 2012. "Overview and Trends in Male Grooming." *British Journal of Dermatology* 166 (SUPPL.1): 2–5. <https://doi.org/10.1111/j.1365-2133.2011.10782.x>.
- Erp, P.E J., Y. K. Seo, J. H. Baek, A. R. Choi, M. K. Shin, and J. S. Koh. 2016. "Facial Skin Physiology Recovery Kinetics during 180 Min Post-Washing with a Cleanser." *Skin Research and Technology* 22 (2): 148–51. <https://doi.org/10.1111/srt.12241>.
- Erp, Piet E. J. van, M. Peppelman, and Denise Falcone. 2018. "Noninvasive Analysis and Minimally Invasive in Vivo Experimental Challenges of the Skin Barrier." *Experimental Dermatology* 27 (8): 867–75. <https://doi.org/10.1111/exd.13743>.
- Evers, Andrea W.M., Y. Lu, P. Duller, P. G.M. Van Der Valk, F. W. Kraaimaat, and P. C.M. Van De Kerkhoft. 2005. "Common Burden of Chronic Skin Diseases? Contributors to Psychological Distress in Adults with Psoriasis and Atopic Dermatitis." *British Journal of Dermatology* 152 (6): 1275–81. <https://doi.org/10.1111/j.1365-2133.2005.06565.x>.
- Falcone, Denise, Renee J.H. Richters, Natallia E. Uzunbajakava, Piet E. J. van Erp, and Peter C. M. van de Kerkhof. 2017. "Sensitive Skin and the Influence of Female Hormone Fluctuations: Results from a Cross-Sectional Digital Survey in the Dutch Population." *European Journal of Dermatology* 27 (1). <https://doi.org/10.1684/ejd.2016.2913>.
- Farage, Miranda A. 2008. "Perceptions of Sensitive Skin: Changes in Perceived Severity and Associations with Environmental Causes." *Contact Dermatitis* 59 (4): 226–32. <https://doi.org/10.1111/j.1600-0536.2008.01398.x>.
- . 2019. "The Prevalence of Sensitive Skin." *Frontiers in Medicine* 6 (May): 98.

Bibliography

- <https://doi.org/10.3389/fmed.2019.00098>.
- . 2022. "Psychological Aspects of Sensitive Skin: A Vicious Cycle." *Cosmetics* 9 (4). <https://doi.org/10.3390/cosmetics9040078>.
- Farage, Miranda A., Alexandra Katsarou, and Howard I. Maibach. 2006. "Sensory, Clinical and Physiological Factors in Sensitive Skin: A Review." *Contact Dermatitis* 55 (1): 1–14. <https://doi.org/10.1111/j.0105-1873.2006.00886.x>.
- Farage, Miranda A., and Howard Maibach. 2010. "Sensitive Skin: Closing in on a Physiological Cause." *Contact Dermatitis* 62 (3): 137–49. <https://doi.org/10.1111/j.1600-0536.2009.01697.x>.
- Feingold, Kenneth R., and Peter M. Elias. 2014. "Role of Lipids in the Formation and Maintenance of the Cutaneous Permeability Barrier." *Biochimica et Biophysica Acta - Molecular and Cell Biology of Lipids* 1841 (3): 280–94. <https://doi.org/10.1016/j.bbalip.2013.11.007>.
- Feldmeyer, Laurence, Sabine Werner, Lars E. French, and Hans Dietmar Beer. 2010. "Interleukin-1, Inflammasomes and the Skin." *European Journal of Cell Biology* 89 (9): 638–44. <https://doi.org/10.1016/j.ejcb.2010.04.008>.
- Firooz, A, A Rajabi-Estarabadi, H Zartab, N Pazhohi, F Fanian, and L Janani. 2016. "The Influence of Gender and Age on the Thickness and Echo-Density of Skin." <https://doi.org/10.1111/srt.12294>.
- Firooz, Alireza, Bardia Sadr, Shahab Babakoohi, Maryam Sarraf-Yazdy, Ferial Fanian, Ali Kazerouni-Timsar, Mansour Nassiri-Kashani, Mohammad Mehdi Naghizadeh, and Yahya Dowlati. 2012. "Variation of Biophysical Parameters of the Skin with Age, Gender, and Body Region." *The Scientific World Journal* 2012. <https://doi.org/10.1100/2012/386936>.
- Fluhr, Joachim W., R Darlenski, N Tsankov, and David A. Basketter. 2008. "Skin Irritation and Sensitization: Mechanisms and New Approaches for Risk Assessment." *Skin Pharmacol Physiol* 21: 124–35. <https://doi.org/10.1159/000131077>.
- Fluhr, Joachim W., Kenneth R. Feingold, and Peter M. Elias. 2006. "Transepidermal Water Loss Reflects Permeability Barrier Status: Validation in Human and Rodent in Vivo and Ex Vivo Models." *Experimental Dermatology* 15 (7): 483–92. <https://doi.org/10.1111/j.1600-0625.2006.00437.x>.
- Fullerton, A., T. Fischer, A. Lahti, K. P. Wilhelm, H. Takiwaki, and J. Serup. 1996. "Guidelines for Measurement Skin Colour and Erythema A Report from the Standardization Group of the

- European Society of Contact Dermatitis *." *Contact Dermatitis* 35 (1): 1–10. <https://doi.org/10.1111/j.1600-0536.1996.tb02258.x>.
- Galzote, C., R. Estanislao, M. O. Suero, A. Khaiat, M. I. Mangubat, R. Moideen, H. Tagami, and X. Wang. 2014. "Characterization of Facial Skin of Various Asian Populations through Visual and Non-Invasive Instrumental Evaluations: Influence of Seasons." *Skin Research and Technology* 20 (4): 453–62. <https://doi.org/10.1111/srt.12140>.
- Gambichler, T, G Moussa, P Regeniter, C Kasseck, M R Hofmann, F G Bechara, M Sand, P Altmeyer, and K Hoffmann. 2007. "Physics in Medicine & Biology Validation of Optical Coherence Tomography in Vivo Using Cryostat Histology Related Content." *Physics in Medicine & Biology* 52. <https://doi.org/10.1088/0031-9155/52/5/N01>.
- Gambichler, Thilo, Volker Jaedicke, and Sarah Terras. 2011. "Optical Coherence Tomography in Dermatology: Technical and Clinical Aspects." *Archives of Dermatological Research* 303 (7): 457–73. <https://doi.org/10.1007/s00403-011-1152-x>.
- Gambichler, Thilo, Rebecca Matip, Georg Moussa, Peter Altmeyer, and Klaus Hoffmann. 2006. "In Vivo Data of Epidermal Thickness Evaluated by Optical Coherence Tomography: Effects of Age, Gender, Skin Type, and Anatomic Site." *Journal of Dermatological Science* 44 (3): 145–52. <https://doi.org/10.1016/j.jdermsci.2006.09.008>.
- Gao, Yanrui, Xuemin Wang, Shuangyu Chen, Shuyuan Li, and Xiaoping Liu. 2013. "Acute Skin Barrier Disruption with Repeated Tape Stripping: An in Vivo Model for Damage Skin Barrier." *Skin Research and Technology* 19 (2): 162–68. <https://doi.org/10.1111/srt.12028>.
- Geerligs, Marion. 2009. "Skin Layer Mechanics." <https://doi.org/10.6100/IR657803>.
- Gefen, Amit. 2020. "Device-Related Pressure Ulcers : SECURE Prevention." *Journal of Wound Care* 29 (2).
- Gerhardt, L. C., V. Strässle, A. Lenz, N. D. Spencer, and S. Derler. 2008. "Influence of Epidermal Hydration on the Friction of Human Skin against Textiles." *Journal of the Royal Society Interface* 5 (28): 1317–28. <https://doi.org/10.1098/rsif.2008.0034>.
- Gorcea, M., M. E. Lane, and D. J. Moore. 2019. "A Proof-of-Principle Study Comparing Barrier Function and Cell Morphology in Face and Body Skin." *International Journal of Cosmetic Science* 41 (6): 613–16. <https://doi.org/10.1111/ics.12568>.
- Gorcea, Mihaela, Jonathan Hadgraft, David J. Moore, and Majella E. Lane. 2013. "In Vivo Barrier Challenge and Initial Recovery in Human Facial Skin." *Skin Research and Technology* 19 (1):

- 14–16. <https://doi.org/10.1111/j.1600-0846.2012.00654.x>.
- Graham, Helen K, Alexander Eckersley, Matiss Ozols, Kieran T Mellody, and Michael J Sherratt. 2019. *Skin Biophysics: From Experimental Characterisation to Advanced Modelling*. *Skin Biophysics From Experimental Characterisation to Advanced Modelling*.
- Guerra-Tapia, A. 2019. "Diagnosis and Treatment of Sensitive Skin Syndrome: An Algorithm for Clinical Practice." *Actas Dermo-Sifiliográficas (English Edition)* 110 (10): 800–808. <https://doi.org/10.1016/j.adengl.2019.10.004>.
- Hachem, Jean Pierre, Mao Quiang Man, Debra Crumrine, Yoshikazu Uchida, Barbara E. Brown, Vera Regiers, Diane Roseeuw, Kenneth R. Feingold, and Peter M. Elias. 2005. "Sustained Serine Proteases Activity by Prolonged Increase in PH Leads to Degradation of Lipid Processing Enzymes and Profound Alterations of Barrier Function and Stratum Corneum Integrity." *Journal of Investigative Dermatology* 125 (3): 510–20. <https://doi.org/10.1111/j.0022-202X.2005.23838.x>.
- Hadi, H., A. I. Awadh, N. M. Hanif, N. F.A. Md Sidik, M. R.N. Mohd Rani, and M. S.M. Suhaimi. 2016. "The Investigation of the Skin Biophysical Measurements Focusing on Daily Activities, Skin Care Habits, and Gender Differences." *Skin Research and Technology: Official Journal of International Society for Bioengineering and the Skin (ISBS) [and] International Society for Digital Imaging of Skin (ISDIS) [and] International Society for Skin Imaging (ISSI)* 22 (2): 247–54. <https://doi.org/10.1111/SRT.12257>.
- Halvorsen, Jon Anders, Anne Braae Olesen, Magne Thoresen, Jan Øyvind Holm, Espen Bjertness, and Florence Dalgard. 2008. "Comparison of Self-Reported Skin Complaints with Objective Skin Signs among Adolescents." *Acta Dermato-Venereologica* 88 (6): 573–77. <https://doi.org/10.2340/00015555-0505>.
- Hawkins, Stacy S., and Vickie Foy. 2019. "The Spectrum of Sensitive Skin: Considerations for Skin Care in Vulnerable Populations." *Journal of Drugs in Dermatology: JDD* 18 (1): s68–74.
- Hu, X., Raman Maiti, X. Liu, Lutz Christian Gerhardt, Zing S. Lee, Robert A. Byers, Steve E. Franklin, Roger Lewis, Stephen J. Matcher, and Matthew J. Carré. 2016. "Skin Surface and Sub-Surface Strain and Deformation Imaging Using Optical Coherence Tomography and Digital Image Correlation." *Optical Elastography and Tissue Biomechanics III* 9710 (March 2016): 971016. <https://doi.org/10.1117/12.2212361>.
- Huang, Adam, Chung Wei Lee, and Hon Man Liu. 2016. "Rolling Ball Sifting Algorithm for the Augmented Visual Inspection of Carotid Bruit Auscultation." *Scientific Reports* 2016 6:1 6 (1):

1–9. <https://doi.org/10.1038/srep30179>.

- Hughes, A. J., S. S. Tawfik, K. P. Baruah, E. A. O'Toole, and R. F.L. O'Shaughnessy. 2021. "Tape Strips in Dermatology Research*." *British Journal of Dermatology* 185 (1): 26–35. <https://doi.org/10.1111/bjd.19760>.
- Inamadar, Arun C., and Aparna Palit. 2013. "Sensitive Skin: An Overview." *Indian Journal of Dermatology, Venereology and Leprology* 79 (1): 9–16. <https://doi.org/10.4103/0378-6323.104664>.
- Issachar, N., Y. Gall, M. T. Borrel, and M. C. Poelman. 1998. "Correlation between Percutaneous Penetration of Methyl Nicotinate and Sensitive Skin, Using Laser Doppler Imaging." *Contact Dermatitis* 39 (4): 182–86. <https://doi.org/10.1111/j.1600-0536.1998.tb05890.x>.
- Jan, Yih Kuen, Bernard Lee, Fuyuan Liao, and Robert D. Foreman. 2012. "Local Cooling Reduces Skin Ischemia under Surface Pressure in Rats: An Assessment by Wavelet Analysis of Laser Doppler Blood Flow Oscillations." *Physiological Measurement* 33 (10): 1733–45. <https://doi.org/10.1088/0967-3334/33/10/1733>.
- Jayabal, Hemalatha, Dan L. Bader, and Peter Worsley. 2022. "Development of an Efficient Extraction Methodology to Analyse Potential Inflammatory Biomarkers from Sebum." *Skin Pharmacology and Physiology*, December. <https://doi.org/10.1159/000528653>.
- Jayabal, Hemalatha, Barbara M. Bates-Jensen, Nkemjika S. Abiakam, Peter R. Worsley, and Dan L. Bader. 2021. "The Identification of Biophysical Parameters Which Reflect Skin Status Following Mechanical and Chemical Insults." *Clinical Physiology and Functional Imaging* 41 (4): 366–75. <https://doi.org/10.1111/CPF.12707>.
- Jiang, Wen-cai, Hui Zhang, Yafei Yingying Yafei Yingying Yafei Yingying Xu, Changqing Jiang, Yafei Yingying Yafei Yingying Yafei Yingying Xu, Wei Liu, and Yimei Tan. 2020. "Cutaneous Vessel Features of Sensitive Skin and Its Underlying Functions." *Skin Research and Technology* 26 (November 2019): 431–37. <https://doi.org/10.1111/srt.12819>.
- Jiang, Xiaoqiong, Xiangqing Hou, Ning Dong, Haisong Deng, Yu Wang, Xiangwei Ling, Hailei Guo, Liping Zhang, and Fuman Cai. 2020. "Skin Temperature and Vascular Attributes as Early Warning Signs of Pressure Injury." *Journal of Tissue Viability* 29 (4): 258–63. <https://doi.org/10.1016/j.jtv.2020.08.001>.
- Jongh, Cindy M. de, René Lutter, Maarten M. Verberk, and Sanja Kezic. 2007. "Differential Cytokine Expression in Skin after Single and Repeated Irritation by Sodium Lauryl Sulphate."

Bibliography

- Experimental Dermatology* 16 (12): 1032–40. <https://doi.org/10.1111/j.1600-0625.2007.00628.x>.
- Josse, G., J. George, and D. Black. 2011. "Automatic Measurement of Epidermal Thickness from Optical Coherence Tomography Images Using a New Algorithm." *Skin Research and Technology* 17 (3): 314–19. <https://doi.org/10.1111/j.1600-0846.2011.00499.x>.
- Kanazawa, Toshiki, Aya Kitamura, Gojiro Nakagami, Taichi Goto, Tomomitsu Miyagaki, Akitatsu Hayashi, Sanae Sasaki, Yuko Mugita, Shinji Iizaka, and Hiromi Sanada. 2016. "Lower Temperature at the Wound Edge Detected by Thermography Predicts Undermining Development in Pressure Ulcers: A Pilot Study." *International Wound Journal* 13 (4): 454–60. <https://doi.org/10.1111/iwj.12454>.
- Kennedy, Brendan F., Xing Liang, Steven G. Adie, Derek K. Gerstmann, Bryden C. Quirk, Stephen A. Boppart, and David D. Sampson. 2011. "In Vivo Three-Dimensional Optical Coherence Elastography." *Optics Express* 19 (7): 6623. <https://doi.org/10.1364/oe.19.006623>.
- Kenyon, F. E. 1966. "Psychosomatic Aspects of Acne: A Controlled Study." *Transactions of the St. John's Hospital Dermatological Society* 52 (1): 71–78. <https://europepmc.org/article/med/4223404>.
- Kim, E, Y Kim, D Lee, J Kim, M Kim, H Eun, K Kim, and J Chung. 2013. "Sensitive Skin: Why Is It Sensitive?" *Journal of Investigative Dermatology* 133: S135. <http://www.embase.com/search/results?subaction=viewrecord&from=export&id=L71083264%5Cnhttp://dx.doi.org/10.1038/jid.2013.100%5Cnhttps://www.mobilelibrary.com/vlib/order/OpenURLReceive.aspx?clientid=11412&sid=EMBASE&issn=0022202X&id=doi:10.1038%2Fjid.2013>.
- Kim, Eunjoo, Gayoung Cho, Nam Gae Won, and Juncheol Cho. 2013. "Age-Related Changes in Skin Bio-Mechanical Properties: The Neck Skin Compared with the Cheek and Forearm Skin in Korean Females." *Skin Research and Technology* 19 (3): 236–41. <https://doi.org/10.1111/srt.12020>.
- Kleesz, P., R. Darlenski, and Joachim W. Fluhr. 2011. "Full-Body Skin Mapping for Six Biophysical Parameters: Baseline Values at 16 Anatomical Sites in 125 Human Subjects." *Skin Pharmacology and Physiology* 25 (1): 25–33. <https://doi.org/10.1159/000330721>.
- Kobayashi, H., and H. Tagami. 2004. "Distinct Locational Differences Observable in Biophysical Functions of the Facial Skin: With Special Emphasis on the Poor Functional Properties of the Stratum Corneum of the Perioral Region." *International Journal of Cosmetic Science* 26 (2):

91–101. <https://doi.org/10.1111/j.0412-5463.2004.00208.x>.

- Kolbe, Ludger, Jeannine Immeyer, Jan Batzer, Ursula Wensorra, Karen Tom Dieck, Claudia Mundt, Rainer Wolber, et al. 2006. "Anti-Inflammatory Efficacy of Licochalcone A: Correlation of Clinical Potency and in Vitro Effects." *Archives of Dermatological Research* 298 (1): 23–30. <https://doi.org/10.1007/s00403-006-0654-4>.
- Kottner, Jan, G. Dobos, A. Andruck, C. Trojahn, J. Apelt, H. Wehrmeyer, C. Richter, and Ulrike Blume-Peytavi. 2015. "Skin Response to Sustained Loading: A Clinical Explorative Study." *Journal of Tissue Viability* 24 (3): 114–22. <https://doi.org/10.1016/j.jtv.2015.04.002>.
- Kottner, Jan, Laine Ludriksone, Natalie Garcia Bartels, and Ulrike Blume-Peytavi. 2014. "Do Repeated Skin Barrier Measurements Influence Each Other's Results? An Explorative Study." *Skin Pharmacology and Physiology* 27 (2): 90–96. <https://doi.org/10.1159/000351882>.
- Lademann, J., U. Jacobi, C. Surber, H. J. Weigmann, and J. W. Fluhr. 2009. "The Tape Stripping Procedure - Evaluation of Some Critical Parameters." *European Journal of Pharmaceutics and Biopharmaceutics* 72 (2): 317–23. <https://doi.org/10.1016/j.ejpb.2008.08.008>.
- Lambers, H., S. Piessens, A. Bloem, H. Pronk, and P. Finkel. 2006. "Natural Skin Surface PH Is on Average below 5, Which Is Beneficial for Its Resident Flora." *International Journal of Cosmetic Science* 28 (5): 359–70. <https://doi.org/10.1111/j.1467-2494.2006.00344.x>.
- Lammintausta, K., Howard Maibach, and D. Wilson. 1988. "Mechanisms of Subjective (Sensory) Irritation. Propensity to Non-Immunologic Contact Urticaria and Objective Irritation in Stingers." *Dermatosen in Beruf Und Umwelt* 36 (2): 45–49.
- Loffler, Harald, Heinrich Dickel, Oliver Kuss, Thomas L. Diepgen, and Issak Effendy. 2001. "Characteristics of Self-Estimated Enhanced Skin Susceptibility." *Acta Dermato-Venereologica* 81.
- Loffler, Harald, F. Dreher, and Howard Maibach. 2004. "Stratum Corneum Adhesive Tape Stripping: Influence of Anatomical Site, Application Pressure, Duration and Removal." *British Journal of Dermatology* 151 (4): 746–52. <https://doi.org/10.1111/j.1365-2133.2004.06084.x>.
- Luebberding, S., N. Krueger, and M. Kerscher. 2014. "Mechanical Properties of Human Skin in Vivo: A Comparative Evaluation in 300 Men and Women." *Skin Research and Technology* 20 (2): 127–35. <https://doi.org/10.1111/srt.12094>.
- Ly, Bao Chau K., Ethan B. Dyer, Jessica L. Feig, Anna L. Chien, and Sandra Del Bino. 2020. "Research Techniques Made Simple: Cutaneous Colorimetry: A Reliable Technique for Objective Skin

Bibliography

- Color Measurement." *Journal of Investigative Dermatology* 140 (1): 3-12.e1. <https://doi.org/10.1016/J.JID.2019.11.003>.
- Ma, Y. F., C. Yuan, W. C. Jiang, X. L. Wang, and P. Humbert. 2017. "Reflectance Confocal Microscopy for the Evaluation of Sensitive Skin." *Skin Research and Technology* 23 (2): 227–34. <https://doi.org/10.1111/srt.12327>.
- Magin, P. J., C. D. Pond, W. T. Smith, A. B. Watson, and S. M. Goode. 2008. "A Cross-Sectional Study of Psychological Morbidity in Patients with Acne, Psoriasis and Atopic Dermatitis in Specialist Dermatology and General Practices." *Journal of the European Academy of Dermatology and Venereology* 22 (12): 1435–44. <https://doi.org/10.1111/j.1468-3083.2008.02890.x>.
- Maiti, Raman, Mengqui Duan, Simon G. Danby, Roger Lewis, Stephen J. Matcher, and Matthew J. Carré. 2020. "Morphological Parametric Mapping of 21 Skin Sites throughout the Body Using Optical Coherence Tomography." *Journal of the Mechanical Behavior of Biomedical Materials* 102 (October 2019). <https://doi.org/10.1016/j.jmbbm.2019.103501>.
- Maiti, Raman, Lutz Christian Gerhardt, Zing S. Lee, Robert A. Byers, Daniel Woods, José A. Sanz-Herrera, Steve E. Franklin, Roger Lewis, Stephen J. Matcher, and Matthew J. Carré. 2016. "In Vivo Measurement of Skin Surface Strain and Sub-Surface Layer Deformation Induced by Natural Tissue Stretching." *Journal of the Mechanical Behavior of Biomedical Materials* 62 (September): 556–69. <https://doi.org/10.1016/j.jmbbm.2016.05.035>.
- Marrakchi, Slaheddine, and Howard I. Maibach. 2007. "Biophysical Parameters of Skin: Map of Human Face, Regional, and Age-Related Differences." *Contact Dermatitis* 57 (1): 28–34. <https://doi.org/10.1111/j.1600-0536.2007.01138.x>.
- Maurer, M., M. Rietzler, R. Burghardt, and F. Siebenhaar. 2016. "The Male Beard Hair and Facial Skin - Challenges for Shaving." *International Journal of Cosmetic Science* 38 (June 2015): 3–9. <https://doi.org/10.1111/ics.12328>.
- Mayrovitz, H. N., and S. G. Carta. 1996. "Laser-Doppler Imaging Assessment of Skin Hyperemia as an Indicator of Trauma after Adhesive Strip Removal." *Advances in Wound Care* 9 (4): 38–42.
- Mehta, Hita H., Vivek V. Nikam, Chandrashekher R. Jaiswal, and Hemant B. Mehta. 2018. "A Cross-Sectional Study of Variations in the Biophysical Parameters of Skin among Healthy Volunteers." *Indian Journal of Dermatology, Venereology and Leprology* 84 (4): 521. https://doi.org/10.4103/IJDVL.IJDVL_1151_15.
- Meijer, Jan H., Piet H. Germs, Hans Schneider, and Miel W. Ribbe. 1994. "Susceptibility to Decubitus

- Ulcer Formation." *Archives of Physical Medicine and Rehabilitation* 75 (3): 318–23. [https://doi.org/10.1016/0003-9993\(94\)90036-1](https://doi.org/10.1016/0003-9993(94)90036-1).
- Metz, Martin, Frank Siebenhaar, and Marcus Maurer. 2008. "Mast Cell Functions in the Innate Skin Immune System." *Immunobiology* 213 (3–4): 251–60. <https://doi.org/10.1016/J.IMBIO.2007.10.017>.
- Misery, L, E Myon, N Martin, S Consoli, S Boussetta, T Nocera, and C. Taieb. 2006. "Sensitive Skin: Psychological Effects and Seasonal Changes." *Journal of the European Academy of Dermatology and Venereology*. <https://doi.org/10.1111/j.1468-3083.2006.02027.x>.
- Misery, Laurent. 2017. "Neuropsychiatric Factors in Sensitive Skin." *Clinics in Dermatology* 35 (3): 281–84. <https://doi.org/10.1016/j.clindermatol.2017.01.011>.
- Misery, Laurent, Henri Duboc, Benoit Coffin, Emilie Brenaut, Flavien Huet, and Charles Taieb. 2019. "Association between Two Painful and Poorly Understood Conditions: Irritable Bowel and Sensitive Skin Syndromes." *European Journal of Pain (United Kingdom)* 23 (1): 160–66. <https://doi.org/10.1002/ejp.1296>.
- Misery, Laurent, Catherine Jean-Decoster, Sophie Mery, Victor Georgescu, and Vincent Sibaud. 2014. "A New Ten-Item Questionnaire For Assessing Sensitive Skin: The Sensitive Scale-10." *Acta Derm Venereol* 94: 635–39. <https://doi.org/10.2340/00015555-1870>.
- Misery, Laurent, K. Loser, and Sonja Ständer. 2016. "Sensitive Skin." *Journal of the European Academy of Dermatology and Venereology* 30: 2–8. <https://doi.org/10.1111/jdv.13532>.
- Misery, Laurent, Sonja Ständer, Jacek C. Szepietowski, Adam Reich, Joanna Wallengren, Andrea W.M. Evers, Kenji Takamori, et al. 2017. "Definition of Sensitive Skin: An Expert Position Paper from the Special Interest Group on Sensitive Skin of the International Forum for the Study of Itch." *Acta Dermato-Venereologica* 97 (1): 4–6. <https://doi.org/10.2340/00015555-2397>.
- Mogensen, Mette, Hanan A Morsy, Lars Thrane, and Gregor B E Jemec. 2008. "Morphology and Epidermal Thickness of Normal Skin Imaged by Optical Coherence Tomography." *Dermatology*. <https://doi.org/10.1159/000118508>.
- Monnier, J., L. Tognetti, M. Miyamoto, M. Suppa, E. Cinotti, M. Fontaine, J. Perez, et al. 2020. "In Vivo Characterization of Healthy Human Skin with a Novel, Non-Invasive Imaging Technique: Line-Field Confocal Optical Coherence Tomography." *Journal of the European Academy of Dermatology and Venereology* 34 (12): 2914–21. <https://doi.org/10.1111/JDV.16857>.
- Muizzuddin, Neelam, Kenneth D. Marenus, and Daniel H. Maes. 1998. "Factors Defining Sensitive

Bibliography

- Skin and Its Treatment.” *Contact Dermatitis* 9 (3): 170–75. [https://doi.org/10.1016/S1046-199X\(98\)90020-3](https://doi.org/10.1016/S1046-199X(98)90020-3).
- Nickoloff, Brian J., and Yathi Naidu. 1994. “Perturbation of Epidermal Barrier Function Correlates with Initiation of Cytokine Cascade in Human Skin.” *Journal of the American Academy of Dermatology* 30 (4): 535–46. [https://doi.org/10.1016/S0190-9622\(94\)70059-1](https://doi.org/10.1016/S0190-9622(94)70059-1).
- Nurulain T. Zaveri. 2016. “Potential Use of OCT-Based Microangiography in Clinical Dermatology.” *Physiology & Behavior* 176 (10): 139–48. <https://doi.org/10.1111/srt.12255>.Potential.
- Olsen, Jonas, Jon Holmes, and Gregor B. E. Jemec. 2018. “Advances in Optical Coherence Tomography in Dermatology—a Review.” *Journal of Biomedical Optics* 23 (04): 1. <https://doi.org/10.1117/1.jbo.23.4.040901>.
- Ota, Naoko. 2002. “Identification of Skin Sensitivity through Corneocytes Measurements.”
- Paepe, K. De, E. Houben, R. Adam, J. P. Hachem, D. Roseeuw, and V. Rogiers. 2009. “Seasonal Effects on the Nasolabial Skin Condition.” *Skin Pharmacology and Physiology* 22 (1): 8–14. <https://doi.org/10.1159/000159772>.
- Paul, Dereck W, Pejhman Ghassemi, Jessica C Ramella-Roman, Nicholas J Prindeze, Lauren T Moffatt, Abdulnaser Alkhalil, and Jeffrey W Shupp. 2015. “Noninvasive Imaging Technologies for Cutaneous Wound Assessment: A Review.” *Wound Repair and Regeneration*. <https://doi.org/10.1111/wrr.12262>.
- Pena Ferreira, M. Rosa, P. C. Costa, and Fernanda M. Bahia. 2010. “Efficacy of Anti-Wrinkle Products in Skin Surface Appearance: A Comparative Study Using Non-Invasive Methods.” *Skin Research and Technology : Official Journal of International Society for Bioengineering and the Skin (ISBS) [and] International Society for Digital Imaging of Skin (ISDIS) [and] International Society for Skin Imaging (ISSI)* 16 (4): 444–49. <https://doi.org/10.1111/J.1600-0846.2010.00458.X>.
- Perkins, Mary A., Marcia A. Osterhues, Miranda A. Farage, and Michael K. Robinson. 2001. “A Noninvasive Method to Assess Skin Irritation and Compromised Skin Conditions Using Simple Tape Adsorption of Molecular Markers of Inflammation.” *Skin Research and Technology* 7 (4): 227–37. <https://doi.org/10.1034/j.1600-0846.2001.70405.x>.
- Pinto, Pedro, Catarina Rosado, Catarina Parreirão, and Luis Monteiro Rodrigues. 2011. “Is There Any Barrier Impairment in Sensitive Skin?: A Quantitative Analysis of Sensitive Skin by Mathematical Modeling of Transepidermal Water Loss Desorption Curves.” *Skin Research and Technology* 17 (2): 181–85. <https://doi.org/10.1111/j.1600-0846.2010.00478.x>.

- Primavera, G., and Enzo Berardesca. 2005. "Sensitive Skin: Mechanisms and Diagnosis." *International Journal of Cosmetic Science* 27 (1): 1–10. <https://doi.org/10.1111/j.1467-2494.2004.00243.x>.
- Proksch, Ehrhardt, Johanna M. Brandner, and Jens Michael Jensen. 2008. "The Skin: An Indispensable Barrier." *Experimental Dermatology* 17 (12): 1063–72. <https://doi.org/10.1111/j.1600-0625.2008.00786.x>.
- Qin, Ou, Yimei Tan, Wencai Jiang, Qin Fu, Yafei Xu, and Changqing Jiang. 2018. "Non-Invasive Assessment of Changes and Repair Dynamics Post Irritant Intervention in Skin Barrier" 11 (5): 4490–99.
- Raj, N., R. Voegeli, A. V. Rawlings, S. Doppler, D. Imfeld, M. R. Munday, and M. E. Lane. 2017. "A Fundamental Investigation into Aspects of the Physiology and Biochemistry of the Stratum Corneum in Subjects with Sensitive Skin." *International Journal of Cosmetic Science* 39 (1): 2–10. <https://doi.org/10.1111/ics.12334>.
- Rawlings, A. V., and Clive R. Harding. 2004. "Moisturization and Skin Barrier Function." *Dermatologic Therapy* 17 (1): 43–48. <https://doi.org/10.1111/j.1396-0296.2004.04s1005.x>.
- Re, Á, M. Baverel, L. Reiche, R. Jourdain, C. M. Willis, S. Shaw, O D E Lacharrie, et al. 2001. "Sensitive Skin : An Epidemiological Study." *British Journal of Dermatology* 145 (2): 258–63. <https://doi.org/10.1046/j.1365-2133.2001.04343.x>.
- Reed, J. T. 1995. "Skin Type, but Neither Race nor Gender, Influence Epidermal Permeability Barrier Function." *Archives of Dermatology* 131 (10): 1134–38. <https://doi.org/10.1001/ARCHDERM.131.10.1134>.
- Richters, Renee J.H., Denise Falcone, Natallia E. Uzunbajakava, Babu Varghese, Peter J. Caspers, Gerwin J. Puppels, Piet E. J. van Erp, and Peter C. M. van de Kerkhof. 2017. "Sensitive Skin: Assessment of the Skin Barrier Using Confocal Raman Microspectroscopy." *Skin Pharmacology and Physiology* 30 (1): 1–12. <https://doi.org/10.1159/000452152>.
- Richters, Renee J.H., Denise Falcone, Natallia E. Uzunbajakava, Willem Verkruysse, Piet E. J. van Erp, and Peter C. M. van de Kerkhof. 2015. "What Is Sensitive Skin? A Systematic Literature Review of Objective Measurements." *Skin Pharmacology and Physiology* 28 (2): 75–83. <https://doi.org/10.1159/000363149>.
- Richters, Renee J.H., Natallia E. Uzunbajakava, Denise Falcone, J. C.M. M. Hendriks, E. J. Jaspers, Peter C.M. M. van de Kerkhof, and Piet E.J. J. van Erp. 2016. "Clinical, Biophysical and

Bibliography

- Immunohistochemical Analysis of Skin Reactions to Acute Skin Barrier Disruption - A Comparative Trial between Participants with Sensitive Skin and Those with Nonsensitive Skin." *British Journal of Dermatology* 174 (5): 1126–33. <https://doi.org/10.1111/bjd.14307>.
- Richters, Renee J.H., Natallia E. Uzunbajakava, J. C. M. Hendriks, J. W. Bikker, Piet E. J. van Erp, and Peter C. M. van de Kerkhof. 2017. "A Model for Perception-Based Identification of Sensitive Skin." *Journal of the European Academy of Dermatology and Venereology* 31 (2): 267–73. <https://doi.org/10.1111/jdv.13829>.
- Rietzler, M, M Maurer, F Siebenhaar, S Angelino, J Handt, R. Burghardt, and H Smetana. 2016. "Innovative Approaches to Avoid Electric Shaving-Induced Skin Irritation." *International Journal of Cosmetic Science* 38 (June 2015): 10–16. <https://doi.org/10.1111/ics.12329>.
- Rimm-Kaufman, Sara E., and Jerome Kagan. 1996. "The Psychological Significance of Changes in Skin Temperature." *Motivation and Emotion* 20 (1): 63–78. <https://doi.org/10.1007/BF02251007>.
- Rodijk, Floor M.W., Giulia Zanelli, M. Geerligs, Piet E.J. J. van Erp, and M. Peppelman. 2016. "The Influence of Different Shavers on the Skin Quantified by Non-Invasive Reflectance Confocal Microscopy." *Skin Research and Technology* 22 (3): 311–17. <https://doi.org/10.1111/srt.12263>.
- Rossi, M, and A Carpi. 2004. "Skin Microcirculation in Peripheral Arterial Obliterative Disease" 58: 427–31. <https://doi.org/10.1016/j.biopha.2004.08.004>.
- Roussaki-Schulze, A V, E Zafiriou, D Nikoulis, E Klimi, E Rallis, and E Zintzaras. 2005a. "Objective Biophysical Findings in Patients with Sensitive Skin." *Drugs under Experimental and Clinical Research*. <https://pubmed.ncbi.nlm.nih.gov/16444908/>.
- . 2005b. "Objective Biophysical Findings in Patients with Sensitive Skin - PubMed." *Drugs under Experimental and Clinical Research*. <https://pubmed.ncbi.nlm.nih.gov/16444908/>.
- Rubinstein, Eduardo H., and Daniel I. Sessler. 1990. "Skin-Surface Temperature Gradients Correlate with Fingertip Blood Flow in Humans." *Anesthesiology*.
- Sanders, J. E., B. S. Goldstein, and D. F. Leotta. 1995. "Skin Response to Mechanical Stress: Adaptation Rather than Breakdown - A Review of the Literature." *Journal of Rehabilitation Research and Development* 32 (3): 214–26.
- Sawyer, Alan G. 1982. "Statistical Power and Effect Size in Consumer Research." *ACR North American Advances* NA-09. <https://www.acrwebsite.org/volumes/5890/volumes/v09/NA-09/full>.

- Schmid-Wendtner, M.-H., and H.C. Korting. 2006. "The PH of the Skin Surface and Its Impact on the Barrier Function." *Skin Pharmacology and Physiology* 19 (6): 296–302. <https://doi.org/10.1159/000094670>.
- Schmitz, Lutz, Uwe Reinhold, Erhard Bierhoff, and Thomas Dirschka. 2013. "Optical Coherence Tomography: Its Role in Daily Dermatological Practice." *JDDG - Journal of the German Society of Dermatology* 11 (6): 499–507. <https://doi.org/10.1111/ddg.12073>.
- Seidenari, Stefania, Mariangela Francomano, and Lucia Mantovani. 1998. "Baseline Biophysical Parameters in Subjects with Sensitive Skin." *Contact Dermatitis* 38 (6): 311–15. <https://doi.org/10.1111/j.1600-0536.1998.tb05764.x>.
- Shellow, Harold. 1938. "DERMATITIS FROM THE USE OF DRY SHAVERS." *Journal of the American Medical Association* 110 (21): 1748. <https://doi.org/10.1001/jama.1938.62790210005008d>.
- Shriner, David L., and Howard I. Maibach. 1996. "Regional Variation of Nonimmunologic Contact Urticaria." *Skin Pharmacology and Physiology* 9 (5): 312–21. <https://doi.org/10.1159/000211433>.
- Sklar, Lindsay R, Fahad Almutawa, Henry W Lim, and Iltefat Hamzavi. 2013. "Effects of Ultraviolet Radiation, Visible Light, and Infrared Radiation on Erythema and Pigmentation: A Review." *Photochem. Photobiol. Sci* 12: 54. <https://doi.org/10.1039/c2pp25152c>.
- Slodownik, Dan, Jason Williams, Adriene Lee, Bruce Tate, and Rosemary Nixon. 2007. "Controversies Regarding the Sensitive Skin Syndrome." *Expert Review of Dermatology* 2 (5): 579–84. <https://doi.org/10.1586/17469872.2.5.579>.
- Soetens, Jibbe Frits Jack, Peter R. Worsley, Dan L. Bader, and Cees W. Oomens. 2019. "Investigating the Influence of Intermittent and Continuous Mechanical Loading on Skin through Non-Invasive Sampling of IL-1 α ." *Journal of Tissue Viability* 28 (1): 1–6. <https://doi.org/10.1016/j.jtv.2018.12.003>.
- Song, E. J., J. A. Lee, J. J. Park, H. J. Kim, N. S. Kim, K. S. Byun, G. S. Choi, and T. K. Moon. 2015. "A Study on Seasonal Variation of Skin Parameters in Korean Males." *International Journal of Cosmetic Science* 37 (1): 92–97. <https://doi.org/10.1111/ics.12174>.
- Sparavigna, Adele, Michele Setaro, and Antonino Di Pietro. 2006. "'Heathy Skin 2005': Results of an Italian Study on Healthy Population with Particular Regard to the Aging Phenomenon." *Journal of Plastic Dermatology* 2 (1): 23–29.
- Ständer, Sonja, Stefan W. Schneider, Carsten Weishaupt, Thomas A. Luger, and Laurent Misery.

Bibliography

2009. "Putative Neuronal Mechanisms of Sensitive Skin." *Experimental Dermatology* 18 (5): 417–23. <https://doi.org/10.1111/j.1600-0625.2009.00861.x>.
- Sun, L., X. Wang, Y. Zhang, T. Wang, X. Li, and Y. Ma. 2016. "The Evaluation of Neural and Vascular Hyper-Reactivity for Sensitive Skin." *Skin Research and Technology* 22 (3): 381–87. <https://doi.org/10.1111/srt.12278>.
- Surber, Christian, Fabian P. Schwarb, and Eric W. Smith. 2001. "Tape-Stripping Technique." *Journal of Toxicology - Cutaneous and Ocular Toxicology* 20 (4): 461–74. <https://doi.org/10.1081/CUS-120001870>.
- Swanson, Eric C., Janna L. Friedly, Ruikang K. Wang, and Joan E. Sanders. 2020. "Optical Coherence Tomography for the Investigation of Skin Adaptation to Mechanical Stress." *Skin Research and Technology*, no. February (March): 1–12. <https://doi.org/10.1111/srt.12843>.
- Tagami, H. 2008. "Location-Related Differences in Structure and Function of the Stratum Corneum with Special Emphasis on Those of the Facial Skin." *International Journal of Cosmetic Science* 30 (6): 413–34. <https://doi.org/10.1111/j.1468-2494.2008.00459.x>.
- Tagami, H., M. Ohi, K. Iwatsuki, Y. Kanamaru, M. Yamada, and B. Ichijo. 1980. "Evaluation of the Skin Surface Hydration in Vivo by Electrical Measurement." *Journal of Investigative Dermatology* 75 (6): 500–507. <https://doi.org/10.1111/1523-1747.ep12524316>.
- Taghavikhalilbad, Adeleh, Saba Adabi, Anne Clayton, Hadi Soltanizadeh, Darius Mehregan, and Mohammad R. N. Avanaki. 2017. "Semi-Automated Localization of Dermal Epidermal Junction in Optical Coherence Tomography Images of Skin." *Applied Optics* 56 (11): 3116. <https://doi.org/10.1364/ao.56.003116>.
- Tang, Yayuan, Weixi Cai, and Baojun Xu. 2015. "Profiles of Phenolics, Carotenoids and Antioxidative Capacities of Thermal Processed White, Yellow, Orange and Purple Sweet Potatoes Grown in Guilin, China." *Food Science and Human Wellness* 4 (3): 123–32. <https://doi.org/10.1016/j.fshw.2015.07.003>.
- Terui, T., T. Hirao, Y. Sato, T. Uesugi, M. Honda, M. Iguchi, N. Matsumura, K. Kudoh, S. Aiba, and H. Tagami. 1998. "An Increased Ratio of Interleukin-1 Receptor Antagonist to Interleukin-1 α in Inflammatory Skin Diseases." *Experimental Dermatology*, no. 6: 327–34. <https://doi.org/10.1111/J.1600-0625.1998.TB00332.X>.
- Trojahn, C., G. Dobos, M. Schario, L. Ludriksone, U. Blume-Peytavi, and J. Kottner. 2015. "Relation between Skin Micro-Topography, Roughness, and Skin Age." *Skin Research and Technology* 21

- (1): 69–75. <https://doi.org/10.1111/srt.12158>.
- Tsugita, Tetsuya, Takafumi Nishijima, Takashi Kitahara, and Yoshinori Takema. 2013. “Positional Differences and Aging Changes in Japanese Woman Epidermal Thickness and Corneous Thickness Determined by OCT (Optical Coherence Tomography).” *Skin Research and Technology* 19 (3): 242–50. <https://doi.org/10.1111/SRT.12021>.
- Tupker, R. A., J. Pinnagoda, P. J. Coenraads, and J. P. Nater. 1990. “Susceptibility to Irritants: Role of Barrier Function, Skin Dryness and History of Atopic Dermatitis.” *British Journal of Dermatology* 123 (2): 199–205. <https://doi.org/10.1111/j.1365-2133.1990.tb01847.x>.
- Turner, G A, A E Moore, V P J Marti, S E Paterson, and A G James. 2006. “Impact of Shaving and Anti-Perspirant Use on the Axillary Vault.” *International Journal of Cosmetic Science* 29: 31–38.
- Tzen, Yi-Ting, David M Brienza, Patricia Karg, and Patrick Loughlin. 2010. “Effects of Local Cooling on Sacral Skin Perfusion Response to Pressure: Implications for Pressure Ulcer Prevention.” *Journal of Tissue Viability* 19: 86–97. <https://doi.org/10.1016/j.jtv.2009.12.003>.
- Ulfgren, A. K., L. Klareskog, and M. Lindberg. 2000. “An Immunohistochemical Analysis of Cytokine Expression in Allergic and Irritant Contact Dermatitis.” *Acta Dermato-Venereologica* 80 (3): 167–70. <https://doi.org/10.1080/000155500750042899>.
- Verdier-Sévrain, Sylvie, and Frederic Bonté. 2007. “Skin Hydration: A Review on Its Molecular Mechanisms.” *Journal of Cosmetic Dermatology* 6 (2): 75–82. <https://doi.org/10.1111/j.1473-2165.2007.00300.x>.
- Verhoeven, Elisabeth W.M., Suzanne De Klerk, Floris W. Kraaijaat, Peter C. M. van de Kerkhof, Elke M.G.J. De Jong, and Andrea W.M. Evers. 2008. “Biopsychosocial Mechanisms of Chronic Itch in Patients with Skin Diseases: A Review.” *Acta Dermato-Venereologica* 88 (3): 211–18. <https://doi.org/10.2340/00015555-0452>.
- Vingan, Nicole R, Ennifer Barillas, Abby Culver, and Jeffrey M Kenkel. 2023. “Evaluation and Characterization of Facial Skin Aging Using Optical Coherence Tomography,” no. September 2022: 22–34. <https://doi.org/10.1002/lsm.23611>.
- Voegeli, R., J. Gierschendorf, B. Summers, and A. V. Rawlings. 2019. “Facial Skin Mapping: From Single Point Bio-Instrumental Evaluation to Continuous Visualization of Skin Hydration, Barrier Function, Skin Surface PH, and Sebum in Different Ethnic Skin Types.” *International Journal of Cosmetic Science* 41 (5): 411–24. <https://doi.org/10.1111/ics.12562>.
- Wa, Chrystal V., and Howard Maibach. 2010. “Mapping the Human Face: Biophysical Properties.”

Bibliography

- Skin Research and Technology* 16 (1): 38–54. <https://doi.org/10.1111/j.1600-0846.2009.00400.x>.
- Wang, Hequn, Utku Baran, and Ruikang K. Wang. 2015. “In Vivo Blood Flow Imaging of Inflammatory Human Skin Induced by Tape Stripping Using Optical Microangiography.” *Journal of Biophotonics* 8 (3): 265–72. <https://doi.org/10.1002/jbio.201400012>.
- Wang, Shang, and Kirill V. Larin. 2016. “Optical Coherence Elastography for Tissue Characterization: A Review.” *Journal of Biophotonics* 344 (6188): 1173–78. <https://doi.org/10.1126/science.1249098.Sleep>.
- Wang, Y. N., and J. E. Sanders. 2003. “How Does Skin Adapt to Repetitive Mechanical Stress to Become Load Tolerant?” *Medical Hypotheses* 61 (1): 29–35. [https://doi.org/10.1016/S0306-9877\(03\)00100-2](https://doi.org/10.1016/S0306-9877(03)00100-2).
- Weatherall, Ian L., and Bernard D. Coombs. 1992. “Skin Color Measurements in Terms of CIELAB Color Space Values.” *Journal of Investigative Dermatology* 99 (4): 468–73. <https://doi.org/10.1111/1523-1747.EP12616156>.
- Welzel, Julia. 2001. “Optical Coherence Tomography in Dermatology.” *Skin Research and Technology* 100 (3): 163–66. <https://doi.org/10.3109/9781420003307-38>.
- Welzel, Julia, Maike Bruhns, and Helmut H. Wolff. 2003. “Optical Coherence Tomography in Contact Dermatitis and Psoriasis.” *Archives of Dermatological Research* 295 (2): 50–55. <https://doi.org/10.1007/s00403-003-0390-y>.
- Welzel, Julia, C. Reinhardt, E. Lankenau, C. Winter, and H. H. Wolff. 2004. “Changes in Function and Morphology of Normal Human Skin: Evaluation Using Optical Coherence Tomography.” *British Journal of Dermatology* 150 (2): 220–25. <https://doi.org/10.1111/j.1365-2133.2004.05810.x>.
- Wert, Luuk A. De, Dan L. Bader, Cees W.J. Oomens, Lisette Schoonhoven, Martijn Poeze, and Nicole D. Bouvy. 2015. “A New Method to Evaluate the Effects of Shear on the Skin.” *Wound Repair and Regeneration* 23 (6): 885–90. <https://doi.org/10.1111/wrr.12368>.
- Wert, Luuk A. De, Margot Geerts, Sander Van Der Brug, Laura Adriaansen, Martijn Poeze, Nicolaas Schaper, and Nicole D. Bouvy. 2019. “The Effect of Shear Force on Skin Viability in Patients with Type 2 Diabetes.” *Journal of Diabetes Research* 2019. <https://doi.org/10.1155/2019/1973704>.
- Witkin, Andrew P. 1984. “SCALE-SPACE FILTERING: A New Approach To Multi-Scale Description Andrew,” 1–4.

- Yatagai, Tsuyoshi, Takatoshi Shimauchi, Hayato Yamaguchi, Jun ichi Sakabe, Masahiro Aoshima, Shigeki Ikeya, Kazuki Tatsuno, et al. 2018. "Sensitive Skin Is Highly Frequent in Extrinsic Atopic Dermatitis and Correlates with Disease Severity Markers but Not Necessarily with Skin Barrier Impairment." *Journal of Dermatological Science* 89 (1): 33–39. <https://doi.org/10.1016/j.jdermsci.2017.10.011>.
- Yokota, T, M Matsumoto, T Sakamaki, R Hikima, S Hayashi, M Yanagisawa, H Kuwahara, S Yamazaki, and T Ogawa. 2003. "Classification of Sensitive Skin and Development of a Treatment System Appropriate for Each Group." *IFSCC Magazine* 6 (4): 303–7. https://jglobal.jst.go.jp/en/detail?JGLOBAL_ID=200902208956747599.
- Zhang, Ming, and V. C. Roberts. 1993. "The Effect of Shear Forces Externally Applied to Skin Surface on Underlying Tissues." *Journal of Biomedical Engineering* 15 (6): 451–56. [https://doi.org/10.1016/0141-5425\(93\)90057-6](https://doi.org/10.1016/0141-5425(93)90057-6).